ADVANCED D-PARTITIONING ANALYSIS AND DESIGN OF ROBUST CONTROL SYSTEMS

A Thesis Submitted to the School of Graduate Studies in Conformity with the Requirements for the Degree of Doctor of Philosophy in Engineering

Prof. Kamen Yanev

Department of Electrical Engineering
Faculty of Engineering and Technology

University of Botswana
January 2015

Approval

This thesis has been examined and approved as meeting the requirements for fulfillment of the Doctor of Philosophy Degree in Engineering.

Supervisor: . . . . . Date: . . . . . .

/ Prof. Shedden Masupe /

Declaration:

I, Prof. Kamen Yanev, declare that this thesis is my work, except where due references are made and it has never been submitted for a degree at this or any other University or Institution of higher learning.

Signature: . . . . . Date: . . . . . .

/ Prof. Kamen Yanev /

Abstract

There is a need for control systems to be robust or insensitive to parameter variations, disturbances and noise. In the process of design and analysis of a robust control system, it is essential to determine the regions of stability, corresponding to the variation of one or more system parameters. Most of the research and development efforts on stability analysis of systems with variable parameters and robust control design have focused on very specific and limited cases. There is a shortage of a user friendly universal analysis tool or procedure that can show the variable parameters margins, their interaction and the robust assessment for different types of control systems. Also, there is a growing need for a comprehensive technique of a robust controller design that can lead to system insensitivity for any of the parameters variations, disturbances and noise within specific limits.

An innovative broad-spectrum analysis tool that can determine the regions of stability, defined by the variations of the system's parameters and their interaction in the n-dimensional parameter space, is presented in this thesis. The analysis of the interaction between the uncertain system parameters is bringing a new light in the solution of the problem of stability. The developed analysis tool is applied for stability and robust assessment of linear as well as digital and nonlinear control systems with variable parameters. The robust analysis of digital control systems is performed in the discrete time-domain. In cases of nonlinear control systems, the system's stability and robust assessment is based on the interaction between their nonlinear and linear sections. The evaluation of robustness is also accomplished by examining the system's sensitivity in terms of parameters uncertainties, external disturbances and noise.

This thesis also proposes **a strategy for designing a robust controller, capable of preventing the effects of the simultaneous variations of multiple parameters in control systems.** The implementation of the designed robust controller results in targeted system's performance, robustness and stability and proves that it is effective for linear as well as for digital and nonlinear control systems. It is capable of suppressing the effects of plant's parameters uncertainties, external disturbances and noise within specific limits. The robust controller, build by microcontrollers based on the difference equations of its sections, can be applied to any complex control system.

Acknowledgments

There are several people who have in one way or another involved in the research resulting in this thesis and to whom I whish to express my gratitude. First, I would like to thank my former Head of Department Prof. Shedden Masupe for initially convincing and inspiring me to start the research resulting in my PhD study and for serving as my thesis supervisor. I would like to thank him for being co-author in some of my publications related to this research and also to thank him for his great supervision, support, confidence and encouragement throughout my thesis work.

I would also like to thank Professor George Anderson, Dean of School of Graduate Studies, for his support, for being my co-author of a number of papers related to this thesis and for the fruitful discussions during my work.

My gratitude is extended to all members of the Department of Electrical Engineering and Faculty of Engineering and Technology for their support. The innumerable discussions, regarding not only research but everything under the sun have created a stimulating and enjoyable atmosphere to work in.

Finally, I would like to thank my family for their continued support throughout the years. I would like to express my deepest gratitude to my wife Jeny and my daughter Karolina for their encouragement and understanding during the extent of this work.

January 2015

Prof. Kamen Yanev

Dedication

To my beloved family…….

Statement of Originality

The main contribution of this research is the achievement of further **advancement of the method of the D-partitioning** and the development of a user friendly stability analysis tool. **The analysis tool is designed as a universal interactive procedure** that can be applied to linear, digital and nonlinear control systems with variable parameters. **The innovation is in terms of results that represent a transparent picture of stability regions in the parameter space** and the way the dimensions of these regions are affected by the variation and interaction of the system's parameters.

Further contribution of this research is the **suggested method for design of a universal robust controller,** achieved by applying forward-series compensation with two degrees of freedom. The controller can suppress the influence of parameters variations, disturbances and noise and is effectively applied to complex linear, digital and nonlinear control systems. **Innovation is demonstrated in the unique property of the designed robust controller that can operate effectively for variations of any one of the system's parameters within prescribed limits. It rejects the impact of the simultaneous parameters uncertainties, disturbances and noise,** making the system insensitive to these effects.

By applying the advanced D-partitioning analysis tool before and after the robust compensation, the system is evaluated for stability. **The results demonstrate that the designed robust controller also improves considerably the system's stability and performance.** In addition, **the analysis of the system's robustness is accomplished by graphical assessment of its sensitivity in terms of any parameters uncertainties, external disturbances and noise.**

The novelties of the **contributions are supported by thirteen journal papers, published in a wide spectrum of international journals of Automatic Control and System Engineering.** In addition, **the novelties of the contributions are supported by four published and presented conference papers at international conferences on Control, Modelling and Simulation and Systems Engineering.** All these publications are done during the period of the PhD research and are as follows:

Published Refereed Journal Papers:

[1] **Yanev K.M.**, Anderson G.O., Masupe S., *Multivariable System's Parameters Interaction and Robust Control Design*, Journal of International Review of Automatic Control, Vol. 4, N. 2., ISSN: 1974-6059, pp. 180-190, **March 2011**.

[2] **Yanev K.M**, Anderson G.O., Masupe S., *Stability and Robustness of a Control System for Precise Speed Control*, International Journal of Energy Systems, Computers and Control, Vol. 2, N. 1, ISSN: 0976-6782, pp. 11– 24, **June 2011**.

[3] **Yanev, K.M.**, Anderson G.O., Masupe S., *Application of the D-partitioning for Analysis and Design of a Robust Photovoltaic Solar Tracker System*, International Journal of Energy Systems, Computers and Control, Vol. 2, N. 1, ISSN: 0976-6782, pp. 43–54, **October 2011**.

[4] Masupe S., **Yanev K.M.,** *Design and D-Partitioning Analysis of Optimal Control System Compensation*, International Review of Automatic Control, Vol. 4, N. 6, ISSN: 1974-6059, pp. 838-845**, November 2011**.

[5] **Yanev K.M.**, Anderson G.O., Masupe S., *Strategy for Design and Analysis of a Robust Controller for Linear Control Systems,* International Journal of Energy Systems, Computers and Control, Vol. 2, No. 1, ISSN: 0976-6782, pp. 55–66, **December 2011**.

[6] **Yanev K.M.*,** Anderson G.O., Masupe S., *Strategy for Analysis and Design of Digital Robust Control Systems,* ICGST-ACSE International Journal on Automatic Control and System Engineering, Volume 12, Issue 1, ISSN: 1687-4811, pp. 37–44, **June 2012.**

[7] **Yanev K.M.,** Masupe S., *Robust Design and Efficiency in Case of Parameters Uncertainties, Disturbances and Noise,* International Review of Automatic Control, Vol. 5, N. 6, ISSN: 1974-6059, pp. 860-867, **November 2012**.

[8] **Yanev K.M.,** *Advanced D-Partitioning Stability Analysis in the 3-Dimensional Parameter Space,* International Review of Automatic Control, ISSN: 1974-6059, Vol. 6, N. 3, pp. 236-240, **May 2013**.

Yanev K.M.* - Based on this publication, accepted as a Member of (ICGST) International Congress for Global Science and Technology:
http://www.icgst-amc.com/institute/Community.aspx?InstId=3&aid=3461
http://www.icgst.com/

[9] Kiravu C., **Yanev K.M.,** M.T. Oladiran M.T., *Visualizing Power Frequency Dynamics Using D-Partitioning,* International Review of Automatic Control, ISSN: 1974-6059, Vol. 6, N. 5, pp. 626-630, **September 2013.**

[10] **Yanev K.M.,** *Advanced Interactive Tools for Analysis and Design of Nonlinear Robust Control Systems,* International Review of Automatic Control, ISSN: 1974-6059, Vol. 6, N. 5, pp. 720-727, **November 2013.**

[11] **Yanev K.M.,** *Analysis and Design of a Servo Robust Control System,* International Review of Automatic Control, ISSN: 1974-6059, Vol. 7, N. 2, pp. 217-224, **March 2014.**

[12] **Yanev K.M., November 2014,** "D-Partitioning Analysis of Digital Control Systems by Applying the Bilinear Tustin Approximation", International Review of Automatic Control, ISSN: 1974-6059, Vol. 7, N. 6, pp. 517-523, **November 2014.**

[13] **Yanev K.M., January 2015,** "Advanced D-Partitioning Analysis and its Comparison with the Kharitonov's Theorem Assessment", Journal of Multidisciplinary Engineering Science and Technology, ISSN: 3159-0040, Vol. 2, Issue 1, pp. 338-344, **January 2015.**

Published and Presented Refereed Conference Papers:

[1] **Yanev, K.M.,** Anderson G.O., Masupe S., *D-partitioning Analysis and Design of a Robust Photovoltaic Light Tracker System*, Botswana Institution of Engineers (BIE) 12th Annual Conference, Paper 6001, ISBN: 97899912-0-731-5, **October 2011.**

[2] **Yanev K.M,** Anderson G.O., Masupe S., *Strategy for Analysis and Design of a Digital Robust Controller for Nonlinear Control Systems,* 4th IASTED Africa Conference on Modeling and Simulation, Gaborone, ISBN 978-0-88986-929-5, pp. 213-220, **September 2012.**

[3] **Yanev, K.M.,** *D-Partitioning Analysis and Robust Control Design of Systems with Multivariable Parameters*, Botswana Institution of Engineers (BIE) 13th Conference, Paper C13-135, ISBN: 97899912-0-731-5, **October 2013.**

[4] **Yanev, K.M.,** *System Robustness and Sensitivity in Case of Parameter Uncertainties, Disturbances and Noise,* 5th IASTED Africa Conference on Modeling and Simulation, Gaborone, ISBN 978-0-88986-929-5, pp. 213-220, **September 2014**.

Contents

List of Figures

List of Tables

List of Abbreviations and Acronyms

PI	Proportional-Integral
PD	Proportional- Derivative
PID	Proportional-Integral-Derivative
FLC	Fuzzy Logic Control
ADC	Analogue-to-Digital Converter
DAC	Digital-to-Analogue Converter
ZOH	Zero-Order Hold
SISO	Single-Input single-output
LTI	Linear Time-Invariant
QFT	Quantitative feedback theory
DC	Direct Current
IP	Performance Index
MIMO	Multi-Input Multi-Output
LMI	Linear Matrix Inequalities
ITAE	Integral of Time multiplied by the Absolute value of Error
PMO	Percentage Maximum Overshoot
RC	Resistive-Capacitive
CPU	Central Processing Unit
2-D	Two-Dimensional
3-D	Three-Dimensional
AGC	Automatic Generation Control
PV	Photo-Voltaic
AWB	Active Wheatstone Bridge
RCU	Reference and Comparison Unit
VPPG	Variable-Phase Pulse Generator
BC	Bridge Converter

Nomenclature

$G(s)$	Characteristic Equation of a Control System
s	Laplace Operator
ω	Variable Frequency
$D(0)$	D-Partitioning Regions of Stability
$D(m)$	D-Partitioning Regions of Instability
m	Number of the Roots in the Right-Hand Side of the s-Plane
ν	Single System Variable Parameter
μ, γ	Two System Variable Parameters
K	System Gain
T	Time-Constant
$A_0(s)$	Transfer Function of the Original System Type 0, variable gain
$G_0(s)$	Forward Transfer Function of System Type 0
$A_{1T}(s)$	Transfer Function of the Original System Type 1, variable time-constant
$e(t)$	System Error
t	Time
ζ	Relative Damping Ratio
t_s	Settling Time of the System's Step Response
t_m	Time to Maximum Overshoot of the System's Step Response
$G_{P1}(s)$	Plant Transfer Function, System Type 1
$G_{OL}(s)$	Open-Loop Transfer Function
$G_{CL}(s)$	Closed-Loop Transfer function
$G_S(s)$	Transfer Function of the Series Robust Controller Stage
$G_F(s)$	Transfer Function of the Forward Robust Controller Stage
$G_T(s)$	Transfer Function of the Total Robust System
$W(s)$	Unity-Feedback Plant Transfer Function
$E(s)$	Input of a Control System
$C(s)$	Output of a Control System
$S_G^W(s)$	Sensitivity of $W(s)$ with Respect to any Variations of $G_P(s)$
$Q_{Robust\ D}(s)$	Disturbance-to-Output Sensitivity

$Q_{Robust\ N}(s)$	Disturbance-to-Output Sensitivity
T_s	Sampling Period
T_{min}	Minimum Time-Constant of the of the Continuous System
ω_c	Sampling Frequency
$G_d(z)$	Open-Loop Transfer Function in the Discrete-Time Domain
$G_{dfb}(z)$	Closed-Loop Transfer Function in the Discrete-Time Domain
$E(z)$	Input Signal of a Digital Filter
$M(z)$	Output Signal of a Digital Filter
$N(M)$	Describing Transfer Function
$Z(M)$	Negative Reciprocal Value of the Describing Function
M	Input Magnitude to a Nonlinear Element
m	Instantaneous Input to a Nonlinear Element
n	Instantaneous Output from a Nonlinear Element
h	Hysteresis Factor
S	Saturation Factor
D	Dead Zone

Chapter 1

INTRODUCTION

1.1 Background of the Problem

Modern control techniques have allowed optimization of control systems for better performance. However, optimal control algorithms are not always tolerant to changes in the control system or the environment. **Robust control** is a branch of control theory that has a purpose to obtain a system that performs adequately over a large range of uncertain parameters, disturbances and noise [1]. Application of the robust technique is important to building dependable systems. The goal is to allow exploration of the design space for alternative methods that will make the systems insensitive to changes in their parameters, external noise and disturbances and can maintain their stability and performance.

The problem of **robust stability** has its origins back in 19^{th} century. Recently this problem has received a lot of attention as evidenced by large number of publications. Controllers that are designed using robust control methods tend to be able to cope with differences between the true system and the nominal model. Robust methods aim to achieve robust performance and stability in the presence of system variable parameters, disturbances and noise [1], [2]. A control system is robust when it has low sensitivities and is stable over the range of uncertainties. As a result the system's performance continues to meet its specifications.

The key issue with robust control systems is uncertainty and how the control system can deal with this problem. The block diagram at Figure 1.1 shows an expanded view of a simple feedback control loop where disturbing factors are entering the system at three different locations. Mainly, there is parameters uncertainty in the model of the plant. Further, even if considering that the disturbances may occur in the plant, usually it is assumed that they are additive to the system's output signal. Also there is external noise which is read on the sensor inputs. Each of these different types of disturbing factors can have an additive component.

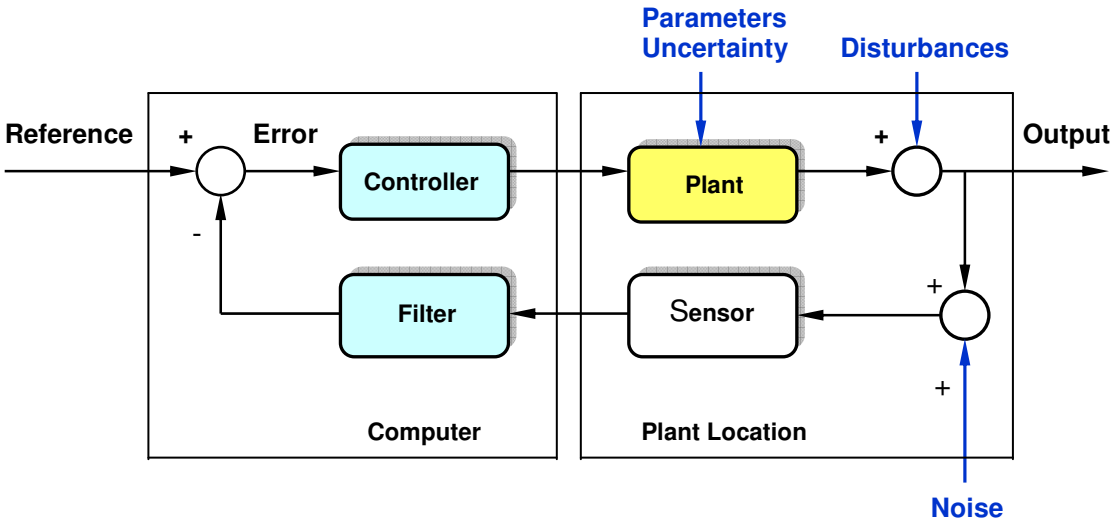

Figure 1.1: *General Robust Control System Involving a Computer*

This chapter will show the motivation for the suggested research, the thesis objectives, the research approach, the expected contributions and the thesis outline.

1.2 Motivation

Control systems must yield performance that is robust or insensitive to parameter variations, disturbances and noise. In the process of design of a robust control system, it is important to determine the regions of stability, corresponding to the variation of one or more system parameters. By applying any one of the known stability criterions like, Nyquist, Bode, Nichols, Hurwitz, Routh or Raus the stability can be determined only if all system's parameters are defined and constant. Although a high volume of research in robust analysis and control over the past 15 years has lead to a growth in procedures, the techniques for robust control have been criticized for their accessibility, the tediousness of the methods, the general application to conventional systems and the conservatism that they often present [3]. To bring the robust control techniques to be used by broad industry, a variety of tools have been developed. However, there is always an issue of the correctness of the tools especially when they are used to simplify a very complex technique. Even with the research devoted to robust analysis and control, the gap between the robust control theory and its practical application still exist. Many of the techniques for robust analysis and control are developed with the aid of applied mathematics. It is

acknowledged by the control engineering community that it is sometimes problematical even to comprehend the basic concept that is being exploited. **All these factors, challenging some aspects of the practical application of robust analysis and control are an indicator of lack of maturity of the subject** [3], [4].

Most of the research on the matter of stability analysis of systems with variable parameters and robust control design is limited to very specific cases like the criterion of Vishegradsky, the Root Locus method and the Neimark's D-partitioning method used for particular design of PI or PID controllers. Implementation of others, like the criterion of Mikhailov and the criterion of Ackermann are more theoretically related than associated to practical applications. The main challenge of the H_2 and H-Infinity (H_∞) methods is the necessity of a very strict problem formulation, since applying it to a wrong system, with inaccurately defined parameters, often makes performance worse rather than better. All the authors acknowledge that it is challenging to create an acceptable lookup table in order to implement the Fuzzy Logic Control (FLC)**.**

An extensive literature review reveals that there is a shortage of universal analysis tool, procedure or algorithm that can show the variable parameter margins and their interaction for different type of control systems. Also, there is a lack of universal design techniques of a robust controller that can make a system insensitive for any one of the parameters variations, disturbances and noise within specific limits. All these shortcomings of a user friendly universal robust analysis tool and a universal method for robust controller design are motivating a research on a new approach that is having the intention of bring a number of new contributions in these subjects.

1.3 Thesis Statement (Objectives)

1.3.1 Development of Stability Analysis Tool for Systems with Variable Parameters

The main objective of this research is to achieve a general stability analysis tool, rather than one attached to just few specific control systems, or systems with specific limitations. The aim of this research is to develop a broad-spectrum analysis tool that can determine graphically the regions of stability defined by the variation of the system's parameters and their interaction in the n-dimensional parameter space. Cases of n-parameter variation systems of Type 0

and Type 1 will be explored. The developed analysis tool will be applied to linear as well as to digital and nonlinear control systems with variable parameters. The shortcoming of the existing methods dealing with these problems is the lack of a universal analysis tool that can show the variable parameter limitations and their interaction for different type of control systems.

1.3.2 Robust Controller Design

In addition to the developed analysis tool, the second objective is to suggest a method for design of an optimal robust controller that could be implemented to systems with variable parameters and subjected to disturbances and noise within specific limits. ***The objective is to achieve a design procedure of a universal robust controller that can be applicable generally, rather than one to be associated to specific control systems, or systems with specific limitations***. The controller, applicable for unlimited number of parameter uncertainties, disturbances and noise, will be an alternative solution to the problem of robustness. The designed robust controller could be efficiently applied to linear as well as to digital and nonlinear control systems. The shortcoming of the existing controllers dealing with these problems is the lack of a general robust controller that is applicable for different system types.

1.4. Research Approach (Methodology)

1.4.1 Development of Stability Analysis Tool for Linear, Digital and Nonlinear Control Systems

The approach to develop an analysis tool for linear control systems is ***transforming the Laplace s-plane into an n-dimensional parameter space with the aid of interactive MATLAB procedures. This will introduce a clear graphical display of the system's parameters variation and their interaction. As a result, this will determine regions of stability and instability in the parameter space.***

The suggested research will achieve further advancement of the initial ideas of Neimark's D-partitioning method which was not sufficiently implemented for broader practical systems with multivariable parameters [5], [6].

The advancement of the method will be demonstrated in a number of successive steps, for the cases of one, two or more variable system parameters. Also its application will be repeatedly verified for linear, digital and nonlinear control systems.

A digital control system can be accurately represented by the combination of an ideal sampler, a digital filter, solving the controller difference equation, and a zero-order hold (ZOH). This gives the unique opportunity for further advancement of the D-partitioning analysis for its application in the discrete-time domain, observing a proper ratio between the system sampling period and the plant's minimum time constant, considering the Euler's approximation. Introducing discretization by employing the Bilinear Transform, known also as the Tustin's Method [7], [8], the continuous-time system prototype is converted into its discrete-time equivalent and further the D-partitioning analysis can be applied in the discrete-time domain.

Since nonlinear control systems consist of linear and nonlinear components, their stability can be determined by the Goldfarb stability criterion [8], [9]. It is founded on the interaction between the linear and nonlinear sections of the system, based on the Describing Function analysis. That also gives the unique opportunity for further advancement in the D-partitioning analysis for its application for nonlinear control systems with an approach similarly used for linear and digital control systems. If a digital controller is to be applied, the analysis is done in the discrete-time domain.

1.4.2 Approach of Robust Control Design

In cases of systems with variable parameters, subjected to noise and disturbances, a system becomes robust if a specialized optimal controller is applied. ***The method intended for the controller design is compensation with two degrees of freedom enforcing a desired system relative damping and therefore a desired margin of stability [10]. The designed controller will suppress the simultaneous effects of the parameters uncertainties, noise and disturbances within specific limits***, so that they would affect insignificantly the final system performance. The unique properties of the designed robust controller and its application will be repeatedly demonstrated for linear, digital and nonlinear control systems of Type 0 and Type 1. The transfer functions of the robust controller stages can be presented in the discrete-time domain. Then, the design will be based on the application of

microcontrollers, programmed to solve the difference equations of the controller stages.

The methodology tools to achieve both research objectives will be the application of interactive MATLAB procedures.

1.5 Expected Contributions

The main contribution of this research is to achieve further advancement of the method of the D-partitioning and to develop an analysis tool that can examine in great detail the effects of multi-parameters variation on system's stability. The analysis tool is intended to be designed as a universal interactive procedure that can be applied for linear, digital and nonlinear control systems with variable parameters. The procedure will define graphically regions of stability in the space of the system's parameters. ***The contribution will be in terms of results that represent a transparent picture of stability regions and the way the dimensions of these regions are affected by the variation and interaction of the system's parameters.*** The analysis tool will be helpful in evaluating the system's stability, robustness and performance before and after implementing the robust controller. The efficiency of the developed analysis tool will further be tested to linear as well as to discrete and nonlinear control systems with different uncertain parameters, contributing further to the theory of control systems stability. ***The developed analysis tool will have the advantage of a clear graphical display of the variation of each parameter and interaction between parameters, determining regions of stability.*** As a result proper parameter values can be chosen for a desirable performance and stability of a system.

Further, ***the proposed research is to contribute in suggesting a strategy for design of a robust control system or a system, insensitive to the changes of its parameters, noise and disturbances.*** The design will be focused on a specialized optimal robust controller. This approach is preferable as an alternative to adaptive control in cases of variable and disturbing factors within specific limits and presence of unstructured system uncertainties [10]. Also it is strongly preferable to robustness achieved with the conventional feedback configuration accomplished with a very high loop gain, since normally this is detrimental to stability [11], [12].

The contribution will be in terms of the unique property of the designed robust controller that can operate effectively for any of the system's parameter variations or simultaneous variation of a number of parameters, external disturbances and noise and can be applied successfully for linear, digital and nonlinear control systems. If the transfer functions of the robust controller stages are presented in the discrete-time domain, microcontrollers programmed to solve the corresponding difference equations, can serve as digital robust controller. In the process of the robust controller analysis and design, a consideration on real-life industrial control systems with multivariable parameters will be taken into account.

The achievements in this study are believed to lead to the advancement of the knowledge in the field of stability analysis of systems with variable parameters and robust controller design.

The project is worth researching not only because it advances knowledge. It has a considerable practical aspect as well. It can improve the performance of a lot of industrial control systems that have unstable and variable parameters due to different ambient conditions or are subjected to noise and disturbance. The models that will be suggested in this research are reflection of complex real-time plants.

1.6 Thesis Outline

Chapter 2 introduces a detailed literature review of all known and published methods related to stability of systems with variable parameters. The literature review also captures all known and published design procedures of robust systems. Following the literature review and based on the existing known methods, conclusive assessment is done on the motivation, research approach and the expected contributions of the research presented in the thesis.

Chapter 3 discloses the development and application of a stability analysis tool for linear control systems with variable parameters, based on the further expansion and maturity of the method of the D-partitioning. A modification of the analysis tool for control systems with simultaneous multiple variable parameters is a further innovative contribution. Interaction between two or more simultaneously varying control system

parameters brings a new light in the graphical determination of stability regions and limitations in proper choice of the parameters.

Chapter 4 presents the suggested strategy for design of a robust controller for linear control systems with variable parameters. To enforce a desired system damping and therefore a desired margin of stability, a controller of two degrees of freedom is designed and applied to linear control systems. In cases of one or more simultaneously varying plant's parameters, a system becomes insensitive to the effects of the parameters uncertainties, as well as to the effects of external disturbances and noise and its final performance is unaffected.

Based on the developed stability analysis tool for linear control systems, Chapter 5 illustrates further advancement of the stability analysis tool for discrete control systems. The method of the D-partitioning is applied on the condition of a proper relationship between the system's sampling period and its minimum time-constant.

A digital robust controller is designed and introduced in Chapter 6. It is based on microcontrollers that are programmed to solve the difference equations of the controller's sections. The controller implementation results in system's robustness.

Founded on the developed stability analysis tool for linear control systems and the Goldfarb stability criterion based on the Describing Function analysis, Chapter 7 shows further advancement of the stability analysis tool for nonlinear control systems.

Chapter 8 demonstrates the design and application of a robust controller to nonlinear control systems. The controller is also based on microcontrollers, programmed to solve the difference equations of the controller's sections. It suppresses the effects of the system's parameters variations and the overall system becomes robust.

In Chapter 9, a two-stage flow chart diagram describes the sequence of steps to analyse and design a robust control system based on the advanced in this research method of the D-partitioning and implementation of the optimal robust controller.

Finally, Chapter 10 concludes the thesis by stating the achievements in this research. It summarises the novelties on control system analysis and robust design strategies and identifies potential directions for future research.

Chapter 2

LITERATURE REVIEW

Due to the nature of the research presented in the thesis, the literature review in this chapter will consider the concepts related to analysis of stability of systems with variable parameters and robust controller design.

2.1 Sources Describing Stability Analysis of Systems with Variable Parameters

2.1.1 Stability Analysis based on the Method of D-Partitioning and other Related Graphical Methods

In his work “Determination of the values of parameters for which an automatic system is stable” Neimark [13], [14] suggested for the first time a method of evaluation of linear system stability, when the system’s parameters are variable. The method was categorized as the method of D-partitioning. The method is considering the division of the space of the *n* order system’s characteristic equation coefficients into a number of regions corresponding to different number of the roots in the right-hand side of the s-plane. The theoretical significance of the problem is that it constitutes a development of a stability theory closely related to the problem of robustness of dynamical systems. The method involves determination of constrains of the system parameters, defined by regions at which the system remains stable. At its initial steps the method was stating rather its theoretical possibilities and its applications were quite limited. The method was further developed by Neimark in few new directions published in 1978, 1992, 2006 [15], [16], [17], [18]. Although, the initial ideas of the method involve determination of constrains of the system parameters, defined by regions at which the system remains stable, at its initial steps the method was stating rather its theoretical possibilities and its applications were quite limited. Although, Neimark expanded his initial ideas, they were rarely implemented because of their obscurity.

The criterion of Vishegradsky [5], [19] is limited to third order linear systems and is restricted to variation of only one parameter. Its mathematical interpretation is defined from the coefficients of a third order differential equation describing a system with variable parameters. The criterion states that the system will be stable if all the coefficients are positive and the difference between the products of the middle and the products of the border coefficients is also positive. A curve is plotted in the space of two of the coefficients that defines regions of stability and instability. The disadvantage of the method is that it deals in a hidden mode with the system parameters and is not defining the stability regions directly in terms of the real system parameters, like gain or time-constants. The method is not applicable for discrete and nonlinear systems.

Jakub O. and Vojtech V. in their research “Modification of Neimark D-Partition Method for Desired Phase Margin” [20], describe a method used for controller design which ensures closed loop stability with desired stability degree. The aim is to design PID controller for a plant, so that not only stability will be ensured but performance in term of phase margin too. By introducing the equation of the PID controlled in the characteristic equation of the closed loop system, the D-partitioning curve for the controller parameters can be plotted. Although useful, this analysis is limited to systems stabilized with PID controllers.

Liu Jinggong and Xue Yali in their research “Calculation of PI Controller Stable Region Based on D-Partition Method” [21] provide a calculation method based on the D-partitioning. The method is useful but limited to systems that can be stabilized with PI controller.

Lanzkron and Higgins, in their research “D-decomposition Analysis of Automatic Control Systems” [22], establish a direct correlation of the points between the polar-plane and the parameter space of a controller. By mapping the boundaries of the asymptotic stability domain of the polar-plane onto the parameter space the stable region of the controller can be confirmed. The method is a modification of the Neimark’s D-partitioning and is limited to controller design only.

Considering the criterion of Mikhailov [23], based on the polynomial of the characteristic equation of an n-order closed loop system, a special curve is plotted,

known as the Mikhailov curve. The criterion states that the phase angle of the rotating vector plotting the Mikhailov curve should correspond to the order of the characteristic equation. The Mikhailov curve representing an n-order stable system is a smooth spiral running forward to the infinity. The analysis and the method of plotting the curve are represented by a sequence of equations and procedures. This method needs specialized software and can be applied only to linear systems.

In recent years, there were a number of successive publications made by Yanev, [24], [25], [26], [27] that were published before the initiation of the current thesis and related to systems with uncertain parameters. They bring further development of the method of the D-partitioning and robust control design.

From the extensive literature review, it was concluded that most of the graphical analysis of systems with variable parameters are based on the initial ideas of Neimark's D-partitioning. Altogether the publications on the matter are few and they treat only some specific applications of the method. The conclusion is that up to now there is no generalized stability analysis tool applicable for control systems of different nature which is based on the D-partitioning. It is an intention such tool to be developed in the progress of the research presented in this thesis.

2.1.2 Stability Analysis of Systems with Variable Parameters based on the H-Infinity (H_∞) Method

The H-infinity (H_∞) method, advocated by Doyle and Glover [28], is used in control theory to synthesize controllers achieving robust performance or stabilization. The H_∞ method is a mathematical optimization problem that results in determining an optimal controller. The process is represented by a configuration with a plant and a controller. The plant is considered with two inputs, a reference signal and a manipulated variable. The plant has also two outputs, an error signal that is to be minimized and a measured variable used to control the system. The input/output signals are considered as vectors, whereas plant and the controller are represented by matrices. A special function involving the vectors and the matrices is defined. The objective of the control design is to find a controller such that the defined function is minimized according to the H_∞ norm.

In the paper of Guan and his co-authors: “Observer-Based Robust H-Infinity Control for Uncertain Time-Delay Systems” [29], suggest a method to construct a robust H_∞ controller for uncertain time-delay systems. The parameter uncertainties are time-varying. Observer and controller are designed so that the uncertain system to be maintained stable. The suggested method is only theoretically based.

The paper of Juma and Werner: “Robust H_∞ Output Feedback Sliding Mode Control with Applications,” [30] presents an output feedback sliding mode control scheme for uncertain dynamical systems. In the presented research, an implementation of an output feedback controller based H_∞ minimization is considered. The controller shows that sliding mode control gives less overshoot, better steady state error and faster rising time. Limitation in this technique is that only state feedback is considered.

The only advantage of the H_∞ technique over the classical control techniques is that it is applicable to multivariable systems. A disadvantage is the need for a reasonably good model of the system to be controlled. If the robust problem formulation is not absolutely correct, this may result in a worse rather than better system performance. Non-linear systems are not well-handled. The results of the H_∞ design can not be graphically presented. Up to now, more attention has been paid to the development of the H_∞ theory than to its practical application.

2.1.3 Stability Analysis of Systems with Variable Parameters based on the Root-Locus Technique

The Root-Locus technique developed by Evans [31], [32], displays linear system poles trajectories if a system parameter varies. The Root-Locus method of Evans is one of the most popular and powerful tools for both analysis and design of single-input single-output (SISO) linear time-invariant (LTI) systems. There are two main application areas for this method. Stability: to obtain conditions of a real parameter under which the closed-loop system remains stable. Design: the method offers a tool for design of lead-lag compensators, PI, PD and PID controllers. As the system gain is changed, the system poles and zeros move around in the s-plane. Root-Locus allows graphically locating of the poles and zeros for every value of the gain. In addition, the Root-Locus can be used to design a feedback system for a specific relative damping ratio and natural frequency. Along with many advantages and

simplicity of application, the Root-Locus technique is limited to a single parameter variation and cannot be applied to systems with multivariable parameters.

The paper “Robust Root Locus Application in Design and Analysis of Typical Industrial Control System Model” published by Kostov and Karlova [33] is an approach to controller design in the complex plain, satisfying some performance specifications. The Root-Loci, plotted for the variable system gain, shows the values of this parameter, causing instability. The design example is based on a specific plant model and a PID controller. This research is demonstrating again the limitations in application of the Root-Locus technique.

In the paper of Merrikh and Afshar “Extending the Root-Locus Method to Fractional-Order Systems” [34], is an approach for constructing the root-loci plot for fractional-order systems. Important features of the Root-Loci are studied and a comprehensive algorithm is presented.

In his work “Simple technique for Root-Locus Plotting”, Cywiak [35] suggests a technique for calculating and plotting the Root-Locus of a linear control system. The characteristic equation of the system is analyzed as a polynomial, which is a function of the gain parameter of the system. The Root-Locus is found by varying and sampling the gain in the range of interest. For each value of the gain, a complete set of roots is obtained.

Although the Root-Locus technique is very popular for stability analysis, it is limited to cases of variation of one system parameter and cannot reflect any interaction of simultaneous variation of a number of parameters.

2.1.4 Stability Analysis of Systems with Variable Parameters based on the Routh-Hurwitz Stability Criterion

Routh, E. J. (1877) and Hurwitz, A. (1895) independently suggested the ideas of a stability criterion, known as the Routh-Hurwitz stability criterion, or the Routh-Hurwitz test [36]. This stability analysis method is very popular and it is described in detail in almost all textbooks of control engineering, for instance: “Modern Control Systems” by Dorf R.C., and Bishop R.H., [10], “Automatic Control Systems” by Kuo B.C [11] and many others. The Routh-Hurwitz stability criterion can be useful for determining

the marginal values of system variable parameters of different nature. Its disadvantage is that it cannot be used in case of systems with multivariable parameters, since it cannot determine the marginal values of more than one system variable parameter. The Routh-Hurwitz stability criterion does not offer any graphical display visualizing its results.

2.1.5 Stability Analysis of Systems with Variable Parameters based on the Kharitonov's Theorem

The Kharitonov's Theorem assessment [37] is applicable in the cases when the variation of the system's parameters is defined within specific limits. It provides a test of stability for a so-called interval polynomial. Based on the interval polynomial and the limits of the variable parameters, four so-called Kharitonov polynomials are created. The interval polynomial is stable, if all four Kharitonov polynomials are stable. The stability of each one of them is determined with the aid of the Routh-Hurwitz stability croterion.

The Kharitonov's Theorem assessment is useful for determining system's stability in the cases of variation of large number of the system's parameters with defined specific limits. The disadvantage of the method is that it cannot determine the parameter marginal values of stability. Also, there is lack of any graphical display visualizing its results. Another disadvantage of the Kharitonov's assessment is that the Kharitonov polynomials deal with the variations of the Kharitonov characteristic interval polynomial coefficients, rather than with the system's parameter variations. The parameter variations cannot be directly observed from the four Kharitonov polynomials.

2.1.6 Stability Analysis of Nonlinear Control Systems with Variable Parameters

The paper "Order Formation in Learning Nonlinear Robust Control Systems by Use of Neural Networks", by Nakanishi and Inoue [38], suggests an application of neural networks for achieving robustness in nonlinear systems by competition between a neural network, acting as a robust controller, and uncertainties of the plant.

Rohr, Pereira, and Coutinho, in their research "Robustness Analysis of Nonlinear Systems Subject to State Feedback Linearization" [39], presented a methodology to

the robust stability analysis of SISO nonlinear systems subjected to state feedback linearization. The stability conditions are described in terms of linear matrix inequalities, which are known to have a numerical solution.

In further related research [40], the authors are having different specific approach in dealing with uncertainty in non-linear control systems. The proposed combination of dynamics projection and online estimation is to relax the robust control design and to make robust control less conservative while being effective.

Following the literature review on the analysis of nonlinear control systems with variable parameters, the conclusion is that all the suggested analysis methods are related only to very specific cases. They are implemented with the aid of considerable computation and can be realized by means of specialized programming.

2.1.7 Stability Analysis of Discrete Control Systems with Variable Parameters

The paper of Egupov and Ivanov “Analysis of Discrete Automatic Control Systems with Varying Parameters Using the Method of Orthogonal Expansions” [41] is based on an algorithm for analysis of discrete control systems with variable parameters, expanding the output signal in a specially formulated normalized system of functions.

The review of the published research on analysis of discrete-time control systems with variable parameters demonstrates mainly theoretical and mostly specialized cases that are accomplished by programming procedures.

2.1.8 Stability Analysis of Systems with Variable Parameters Based on Fuzzy Control and Fuzzy-Neural Control Technique

In their book “Fuzzy Control” by Kevin Passino and Stephen Yurkovich [42] discuss some advantages of the Fuzzy Logic Control (FLC) compared with conventional control. It is shown that FLC provides a methodology for implementing human’s philosophy to arrive to a solution by a process of trial and error and self-organizing learning, an alternative to setting rules of knowledge about how to control a system.

The paper “Robust Position Control in DC Motor by Fuzzy Sliding Mode Control” of Zadeh, Yazdian, and Mohamadian [43], suggests solutions to solve the problem of

DC motor control by implementing sliding mode of control. However, this control would not have the sufficient flexibility in accordance to changes of the inputs.

In the presented paper of Theodoridis and Christodoulou, “Direct Adaptive Control of Unknown Multi-variable Nonlinear Systems with Robustness Analysis using a new Neuro-Fuzzy Representation and a Novel Approach of Parameter Hopping” [44], the authors suggest a method based on a new neuro-fuzzy dynamical system definition. The combination of these two different technologies has given rise to fuzzy-neural or neuro-fuzzy approaches. They are intended to capture the advantages of both methods. The complexity of the suggested method is limiting its applications.

All the approaches of analysis and design of control systems with uncertain parameters by means of Fuzzy Control and Fuzzy-Neural Control Technique can be realized by means of specialized programming. The main advantage of FLC is introduction of parallel multiple fuzzy rules, human knowledge and robust control. The components of a fuzzy controller are the fuzzification interface that transforms input values into fuzzy values, the knowledge base that contains knowledge of the application, the decision-making logic that performs inference for fuzzy control actions and the defuzzification interface. A lookup table, related to the FLC shows the relationships between the input and output variables. All authors acknowledge that it is extremely complex to create an acceptable lookup table and to implement FLC.

2.2 Robust Control Design

In his research Geromel [45] reflect on the problem of robust stability based on the topological structure of systems and systems subject to parametric uncertainties. The use of Lyapunov functions for robust controller synthesis is then considered. The method is restricted to linear systems.

In the paper of Guo and Zhang “Robust Reliability Method for Quadratic Stability Analysis and Stabilization of Dynamic Interval Systems” [46], a new robust reliability method has been presented. The method is based on the linear matrix inequality approach. Implementation of the method requires advanced programming.

An optimization algorithm, proposed by Halikias and Zolotas [47] in their published paper “Design of Optimal Robust Fixed-Structure Controllers using the Quantitative Feedback Theory Approach”, is applied to design fixed-structure controllers for highly uncertain systems. Quantitative feedback theory is used for robust control design.

In their paper “Robust Adaptive Control of Manipulators in the Task Space by Dynamical Partitioning Approach”, Shafiei and Soltanpour [48], based on the physical properties of the robot manipulator, describe the design of the adaptive control for compensation of parameter uncertainties. Since the robot dynamics have structured and unstructured uncertainties therefore adaptive control cannot succeed in presence of unstructured uncertainties. In addition to the adaptive control, a robust control for compensation of unstructured uncertainties is designed.

Blizorukova, Kappel and Maksimov, in their research “A problem of Robust Control of a System with Time Delay” [49] consider a problem of robust control of a system with time delay. An algorithm for solving this problem based on the methods of the theories of dynamical reconstruction and guaranteed control has been designed.

In his research “Robust Parameter Design with Feed-Forward Control”, Joseph [50] formulated and developed a methodology for robust parameter design by means of feed-forward control. The approach can be used to obtain the optimal control law. The focus is on reducing the signal variation in the response after compensating for the effect of noise.

In his work “Multivariable Control systems” Megretski [51] examines a common effect, usually associated with unstable zeroes and poles of the open loop plant. This effect, called the waterbed effect, can be explained mathematically in terms of integral inequalities imposed on the closed loop transfer functions.

The adaptive control appeared first in 1958 in relation to the use of an adaptive system for aircraft control and digital process control. In his book “Adaptive Control Algorithms, Analysis and Applications” Landau [52] explains the concepts of the adaptive control, defines and gives practical examples and applications the different adaptive control types. **Adaptive control** is a control method that **uses a controller which must adapt** to a controlled system with variable or uncertain parameters. For example, as an aircraft flies, its mass will slowly decrease as a result of fuel consumption. A control law is needed that adapts itself to such changing conditions.

Adaptive control covers a set of techniques which provide a systematic approach for automatic adjustment of controllers in real time. When the parameters of a plant change considerably in time, an adaptive control approach is considered in order to achieve and maintain an acceptable level of control system performance [53]. Then

the type of control is characterized as a continuous adaptation. An adaptive control system can be interpreted as a feedback system where the controlled variable is the performance index (IP). For instance the relative damping for a closed-loop system is an IP which allows quantifying a desired performance. The measured IP will be compared to the desired IP and their difference will be fed into an adaptation mechanism. From their comparison, the adaptation mechanism modifies the parameters of the adjustable controller to generate a control signal in order to maintain the IP of the control system close to the reference one [54]. The control system under consideration is an adjustable dynamic system in the sense that its performance can be adjusted by modifying the parameters of the controller.

A detailed classification of adaptive control techniques is given by Loannou [52] in his book “Robust Adaptive Control” and can be displayed in 27 groups based on numerous different factors. Although adaptive control improves the robust performance, **it cannot succeed in the presence of unstructured uncertainties**. Also it is recognized that it is complex and expensive. Adaptive control is mainly recommended for control systems with considerable structured uncertainties and/or requirement of very precise maintenance of desired level of control system performance. [52], [53], [54].

Quantitative feedback theory (QFT) developed by Horowitz, I. [55] in 1963 and further developed by Horowitz and Sidi, M. [39] in1972 is a frequency domain technique utilising the Nichols chart in order to achieve a desired robust design over a specified region of plant uncertainty. The (QFT) was finalized by Horowitz, I. [56] in his paper “Survey of Quantitative Feedback Theory (QFT)”. At the QFT every parameter of the transfer function is included into an interval of possible values.

The system is represented by a family of plants rather than by a standalone expression. The open loop system is not allowed to have frequencies below the constraint, and at high frequencies it should not cross the *Ultra High Frequency Boundary*. The designer introduces Controller functions and tunes their parameters, a process called Loop Shaping, until the best possible controller is reached without violation of the frequency constraints.

The experience of the designer is an important factor in finding a satisfactory controller. Finally, the QFT design may be completed with a Pre-Filter design. A

shaping on the Bode diagram may be used. Post design analysis is then performed to ensure the system response is satisfactory according with the problem requirements. The design of the Controller and the Pre-Filter is a 12-step procedure.

The following disadvantages of the QFT are acknowledged by Constantine Houpis from the Air Force Institute of Technology, Ohaio, USA [57]: The Loop Shaping depends on CAD (*Computer Aided Design*) packages and on the experience of the designer for the tuning of the Controller. For pre-filter design, shaping on Bode diagrams is used. Post design analysis and tuning is required. QFT is applicable for limited range of parameters uncertainties. QFT is applicable only for plants with structured parametric uncertainty. The QFT design procedure can be accomplished by a very large number of 12 design steps that are repeated for adjustments.

The Robust Control Toolbox product is a *collection of functions and tools* that help to analyze and design multi-input multi-output (MIMO) control systems with uncertain elements. This software provides assortment of *robustness analysis* commands that let to direct calculation of the bounds on worst-case performance without random sampling. Robust Control Toolbox software offers an assortment of model-order *reduction commands* that helps to find less complex low-order approximations to plant and controller models. As a summary, the MATLAB Robust Control Toolbox provides tools for implementing advanced robust control optimization methods like $H\infty$, H_2, linear matrix inequalities (LMI), and μ-Analysis and Synthesis robust control [52], [53], [58].

2.3 Conclusions, Limitations and Delimitations based on the Literature Review

2.3.1 Conclusions

The conclusion based on the extensive literature review is that up to now there is not any published generalized stability analysis tool and robust control design method applicable for different type of control systems with variable parameters. **It is an intention such analysis tool based on further evolution of the D-partitioning to be developed and a specialized optimal robust controller to be designed in the progress of the research presented in this thesis.**

2.3.2 Limitations

The developed analysis tool will be based on advancement of the D-partitioning analysis. Although **limited to a three-dimensional space**, if more than three system parameters are variable, **they can be grouped for the application of the analysis**.

The optimal robust controller will be operating successfully even if the system parameters **increase or decrease in the range of 10 times with respect to their original values**. At the same time, the designed robust controller can be **applicable for unlimited number of unpredictable and random parameter variations**. All physical systems are subject to some types of irrelevant signals or noise and disturbances during their operation. Some of these signals, like change in ambient temperature, may affect directly the parameters of the system. Others, like variation of motor torque, affect directly the system output signal that is the load angular velocity. Although this research will mainly concentrate to the design of robust controllers for systems with variable parameters, it will be proved that the designed robust controller **is effective also for variations of external noise and disturbance of a rate of at least ten fold that affect directly the system output signals**.

2.3.3 Delimitations

PI, PD, PID and compensation controllers will not be discussed, since this subject has been resolved in already published research. Control systems contain elements that drift or vary with time. Correct determination of the exact parameter values is often quite challenging and problematic. For this reasons, **optimization methods like $H\infty$, $H2$ and linear matrix inequalities (LMI) will not be applied in this research, since they require a very accurate model of the system to be controlled**. **Optimizing a system with wrongly determined parameters often makes its performance worse rather than better.** At the same time, the suggested in this research analysis and design methods are to a certain degree insensitive to the accuracy and parameters drift. The application of robust control is considered quite sufficient in case of limited uncertainties. For this reason, as well as for the reason that **adaptive control cannot succeed in presence of unstructured and unpredictable uncertainties** and also due to the industrial **cost implications**, **adaptive control will not be considered at this stage of the research.**

The Routh-Hurwitz Stability Criterion can be very useful for confirming the marginal values of a variable system parameter. Its disadvantage is that it is inapplicable for systems with multivariable parameters. Comparison will be done between the Routh-Hurwitz Stability Criterion and the developed in this research analysis method.

Also, **comparison between the Kharitonov's interval polynomial having defined limits of the variable parameters** and the developed in this research analysis method will prove the advantages of the latest.

Due to substantial disadvantages of the Quantitative feedback theory (QFT), as acknowledged by Constantine Houpis from the Air Force Institute of Technology, Ohaio, USA, it will not be considered in this research.

Since adaptive control is essential for robotics, aircrafts and space ships systems and other complex plants with considerable parameter variation uncertainties, the designed robust control system can be **further upgraded in a further research** to an adaptive control system by applying the most suitable for the case adaptive control technique.

Chapter 3

ADVANCED STABILITY ANALYSIS OF LINEAR CONTROL SYSTEMS WITH VARIABLE PARAMETERS

As already seen from the literature review there are a number of known methods and criterions dealing with the problem of stability of systems with variable parameters. As disclosed, most of them have limitations in their application of unrelated character. It is found out that up to now there is no generalized stability analysis tool or procedure applicable for control systems of different nature. **It is an intention, such tool to be suggested and developed in the progress of this chapter. Initially it will be applied for linear control systems with uncertain parameters.**

3.1 Choice and Nature of the Method Used for the Development of the Stability Analysis Tool

The method of the D-partitioning, if well clarified and further advanced, has advantages compared with all other mentioned methods in terms of an opportunity of a transparent graphical display of all variable parameters regions for which the system remains stable. The purpose of the current research is to advance further the D-partitioning method and emphasize on its practical application. It has the objective to clarify it in a user friendly manner in order to simplify its implementation. By applying the basic initial ideas of the method, the main line of the research is the development of a generalized stability analysis tool and demonstrating its application. With the aid of the tool, proper parameter values can be chosen for a desirable performance and stability of a system. **The analysis tool can be practically used when one, two or more system's parameters are varied independently or simultaneously.** Basically it defines regions of stability in the space of the system's parameters. The tool can be essential and very useful for the design and analysis of robust control systems.

3.2 D-Partitioning as Suggested by Neimark

3.2.1 The Space of Characteristic Equation Coefficients

The roots of the characteristic equation of a control system depend on the coefficients of this equation and therefore depend on the system's parameters. Generally, for an *n*-order characteristic equation, *m* roots may be positioned in the right-hand side and (*n* - *m*) in the left-hand side of the s-plane. To implement the method of the D-partitioning, the *n*-order characteristic equation of a control system is presented in the format:

$$G(s) = a_0 s^n + a_1 s^{n-1} + ... + a_n = 0 \tag{3.1}$$

where s is the Laplace operator

$a_0, a_1, \ldots, a_n$ - are parameter-dependent coefficients

If $a_0 = 1$ and the position of one of the roots is at the origin of the coordinate system, or a pair of roots is at the imaginary axis, the system has a marginal stability.

By substituting $s = j\omega$*, equation (3.1) can be transformed to equation (3.2):

$$G(j\omega) = (j\omega)^n + a_1 (j\omega)^{n-1} + ... + a_n = 0 \tag{3.2}$$

If the frequency varies within the range of $-\infty \le \omega \le +\infty$ in the space of the characteristic equation coefficients $a_1, a_2, ..., a_{n-1}, a_n$, then equation (3.2) will represent a plane in an *n*-dimensional space.

When the characteristic equation is of a third order, it can be described as:

$$G(s) = s^3 + a_1 s^2 + a_2 s + a_3 = 0 \tag{3.3}$$

* The Laplace Transform is a general form of the Fourier Transform, $s = \sigma + j\omega$ that displays frequency spectrum with a decay ($\sigma \neq 0$). A special case of Laplace transform is $s = j\omega$. It displays frequency spectrum without a decay ($\sigma = 0$). When the Laplace transform variable $s = \sigma + j\omega$ is reduced to $s = j\omega$, the attenuation component (σ) is ignored and only the frequency response (ω) is taken into consideration, implying that the signal is sinusoidal. This is the case of Nyquist and Bode plots and the D-partitioning that provide insight into the response of a system after the transient effects have died out, or ($\sigma = 0$).

There is always such a correlation between the coefficients of equation (3.3), at which either the position of one of the roots is at the origin of the coordinate system, or a pair of roots is placed on the imaginary axis of the s-plane. By substituting $s = j\omega$, (3.3) is transformed to equation (3.4), defining a plane *N* in the *3*-dimensional space of the coefficients: a_1, a_2, a_3 , as shown in Figure 3.1.

$$G(j\omega) = (j\omega)^3 + a_1(j\omega)^2 + a_2(j\omega) + a_3 = 0 \tag{3.4}$$

As seen in Figure 3.1, only specific values of the coefficients: a_{10}, a_{20}, a_{30} define a point *M* that is positioned on the surface of the plain *N*. This occurs only when the roots of the characteristic equation are on the imaginary axis (case of marginal stability). Therefore, the plane *N*, defined by equation (3.4), divides the space of the coefficients into a number of regions. The regions are labeled as *D(m)*, where *m* represents the number of the roots in the right-hand side of the s-plane.

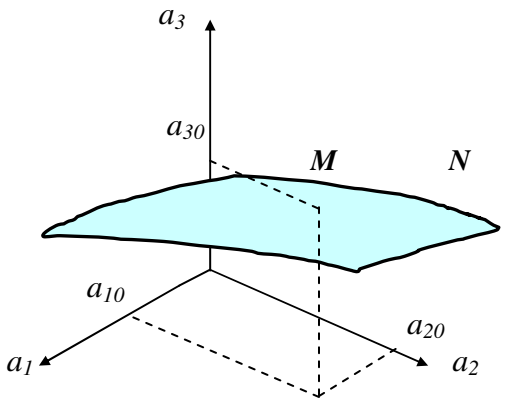

Figure 3.1: *Three-Dimensional Space of the Characteristic Equation Coefficients*

3.2.2 Neimark's Definition and Additional Considerations on the D-Partitioning

The term D-Partitioning was used for the first time by the famous Russian professor Yurii Isaakovich Neimark (1920–2011) from the Lobachevski State University of Nizhni Novgorod (established in 1916 and considered as one of the best classical universities in Russia). Professor Neimark was a member of the Russian Academy of Science – one of the highest scientific institutions in the world.

The D-Partitioning initial ideas were suggested by Prof. Neimark in 1948 and are available only in Russian sources. Prof. Neimark suggested for the first time a method of evaluation of linear system stability, when the system's parameters are variable. **Then the method was categorized as the method of D-Partitioning. The initial ideas of the method of D-Partitioning were formulated by Prof. Neimark in the following definition:**

The division of the space of the characteristic equation coefficients $a_1, a_2, \ldots, a_{n-1}, a_n$ *, into a number of regions corresponding to different number of the roots* ***m*** *in the right-hand side of the s-plane is considered as the D-Partitioning* [14], [16], [24], [62].

At its initial steps the method was stating rather its theoretical possibilities and its applications were quite limited. The method was further extended by Prof. Neimark in few new directions published in 1978, 1992, 2006 – available mainly in Russian sources***** [15], [16], [17], [18].

By applying the basic initial ideas of Prof. Neimark, the main line of this research is to do further advancement of the D-Partitioning method, developing a generalized stability analysis tool and demonstrating its application. The advancement of the analysis developed in this research is in terms of its practical application in case one, two or more system's parameters are varied independently or simultaneously.

By implementing an interactive MATLAB procedure methodology, the advancement of the D-Partitioning represented in this research is based on the innovative transparent graphical display of the simultaneous interaction between n-variable parameters, as well as the determination of the simultaneous marginal values of n-variable parameters.

In case of a third order system, described by the characteristic equation (3.3), there will be four regions: *D(3), D(2), D(1), D(0)*. Only the region *D(0)* will be a region of stability, since it corresponds to such a correlation of the coefficients, respectively of the system's parameters, for which the characteristic equation has no roots in the right hand-side of the s-plane. Therefore, the condition for stability is met only for region *D(0)*.

*****http://www.mathnet.ru/links/ca771bf661cdf8ba6204339c749e626e/at3334.pdf

http://www.mathnet.ru/php/archive.phtml?wshow=paper&jrnid=at&paperid=3334&option_lang=eng#forwardlinks

3.3. Advanced D-Partitioning: Case of One Variable Parameter

3.3.1 General Consideration

The further advancement of the original Neimark's D-Partitioning will be presented in this research in a number of successive steps for the cases of one, two or more variable system parameters. Its application will be repeatedly demonstrated for linear, discrete and nonlinear control systems. In case of one variable parameter, the D-partitioning will be implemented in the complex plane of this parameter.

Initially, it is suggested in this research, that the hypothetical system characteristic equation (3.1) is introduced in the following format to expose the variable parameter:

$$G(s) = P(s) + vQ(s) = 0 \tag{3.5}$$

where $P(s)$ and $Q(s)$ are polynomials of the Laplace operator s

ν is the single variable system parameter

The borders of the D-partitioning can be determined by substituting $s = j\omega$ in the characteristic equation (3.5) and varying the frequency within the range $-\infty \le \omega \le +\infty$. Accordingly, the equation (3.5) is transformed to equation (3.6) as follows:

$$G(j\omega) = P(j\omega) + vQ(j\omega) = 0 \tag{3.6}$$

Further, v can be presented also as a complex number as follows:

$$v = -\frac{P(j\omega)}{Q(j\omega)} = X(\omega) + jY(\omega) \tag{3.7}$$

where the real part $X(\omega)$ of this complex number corresponds in reality to the value of the variable parameter of the control system.

Then, the D-partitioning regions can be obtained graphically in the complex plane $v = X(\omega) + Y(\omega)$, by varying the frequency within the range $-\infty \le \omega \le +\infty$. Suppose a root of the system's characteristic equation, is moved from the left-hand side to the right-hand side of the s-plane, crossing the imaginary axis, as shown in Figure 3.2.

This movement of the root from the stable into the unstable region of the s-plane corresponds to a crossing of the border of the D-partitioning region in the specified direction, seen in Figure 3.3.

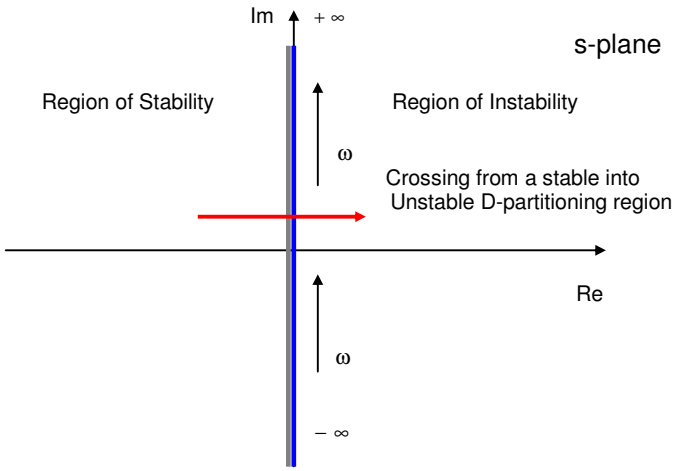

Figure 3.2: *Root Movement from Stable into Instable Region of the s-Plane*

If a root is moved along the imaginary axis of the s-plane when the frequency ω changes from $-\infty$ to $+\infty$, the region of stability remains always on the left-hand side of the plane (Fig. 3.2). Similarly, in the complex plane $\nu = X(\omega) + jY(\omega)$, the region of stability is always on the left-hand side of the D-partitioning curve for frequency variation from $-\infty$ to $+\infty$ (Figure 3.3).

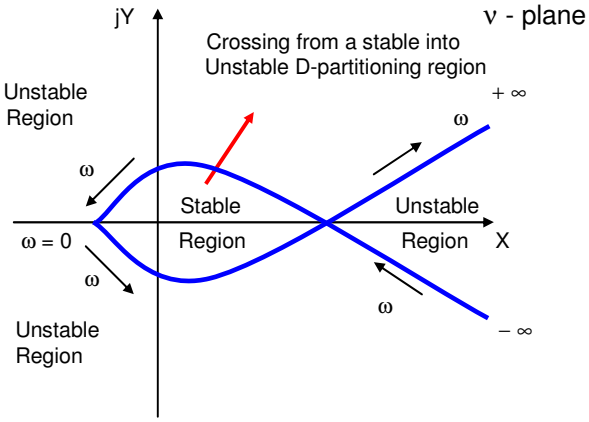

Figure 3.3: *D-Partitioning in the ν - Plane for a Frequency Variation from $-\infty$ to $+\infty$*

3.3.2 Advancement of the D-Partitioning by Variable Gain

3.3.2.1 D-Partitioning by Variable Gain (System Type 0)

In this research, a number of original examples of practical implementation of the method will be shown. As initial example, a real-life **cruise control system** is reduced to a third order system of Type 0 [24], [62]. Cruise control is a system that automatically controls the speed of a motor vehicle. The system takes over the throttle of the car to maintain a steady speed as set by the driver. The flow of a fluid and the engine's power is managed automatically. The basic block diagram of a cruise control system [56] is shown in Figure 3.4.

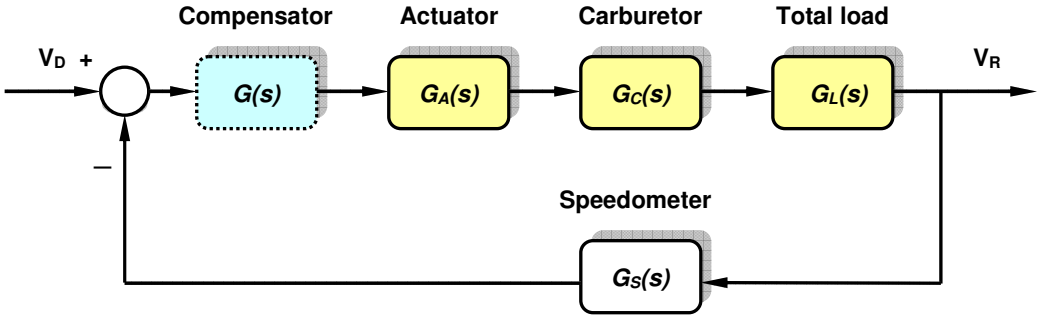

Figure 3.4: *Cruise Control System*

The following assumptions are considered:

V_D is the desired speed of the motor vehicle

V_R is the real speed of a motor vehicle

$$G(s) = G_S(s) = 1;\ G_A(s) = \frac{1}{0.1s+1};\ G_C(s) = \frac{1}{0.02s+1};\ G_L(s) = \frac{0.02K}{0.01s+1}; \quad (3.8)$$

The open loop linear transfer function of the system with variable parameter K is:

$$G_O(s) = G_A(s) \times G_C(s) \times G_L(s) =$$
$$= \frac{1000K}{(s+10)(s+50)(s+100)} = \frac{1000K}{s^3 + 160s^2 + 6500s + 50000} \quad (3.9)$$

The transfer function of the feedback system can be represented as:

$$G_{CL}(s) = \frac{Go(s)}{1+Go(s)} = \frac{1000K}{(s+10)(s+50)(s+100)+1000K} \quad (3.10)$$

It is suggested that the original **gain factor *K*** of the system is a variable parameter due to some temperature effects within the environment of its operation. The characteristic equation of the feedback system is:

$$G(s) = (s+10)(s+50)(s+100) + 1000K = 0 \tag{3.11}$$

To expose the variable parameter equation (3.11) is presented as:

$$G(s) = P(s) + KQ(s) = 0 \tag{3.12}$$

Where the polynomials of equation (3.12) are as follows:

$$P(s) = (s+10)(s+50)(s+100) \tag{3.13}$$

$$Q(s) = 1000 \tag{3.14}$$

The variable parameter is presented as:

$$K(s) = -\frac{P(s)}{Q(s)} = -\frac{(s+10)(s+50)(s+100)}{1000} = -\frac{s^3 + 160s^2 + 6500s + 50000}{1000} \tag{3.15}$$

The D-partitioning curve in terms of one variable parameter can be plotted in the complex plane within the frequency range –∞ ≤ ω ≤ +∞, facilitated by MATLAB the "nyquist" m-code, This is illustrated for the case of the variable gain factor *K* in Figure 3.5a. The procedure can work on any computer where the MATLAB program is installed.

```
>> K=tf([1 160 6500 50000],[1000])
 Transfer function:
-s^3 - 160 s^2 - 6500 s - 50000
-------------------------------
1000
>> nyquist(K)
```

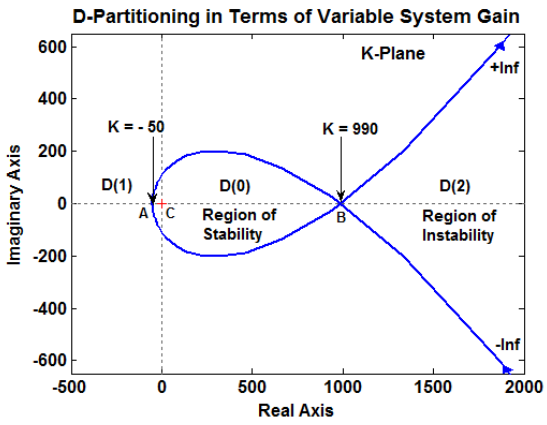

Figure 3.5a: *D-Partitioning Facilitated by the "nyquist" m-code*

To avoid any misunderstanding or misinterpretation of the D-Partitioning procedure, the "nyquist" m-code is modified into a "dpartition" m-code with the aid of the MATLAB Editor and a proper formatting. The "dpartition" m-code will plot the curve of a specific system parameter in terms of the frequency variation from $-\infty$ to $+\infty$.

```
>>  K=tf([-1 -160 -6500 -50000],[1000])
 Transfer function:
-s^3 - 160 s^2 - 6500 s - 50000
------------------------------
1000
>> dpartition(K)
```

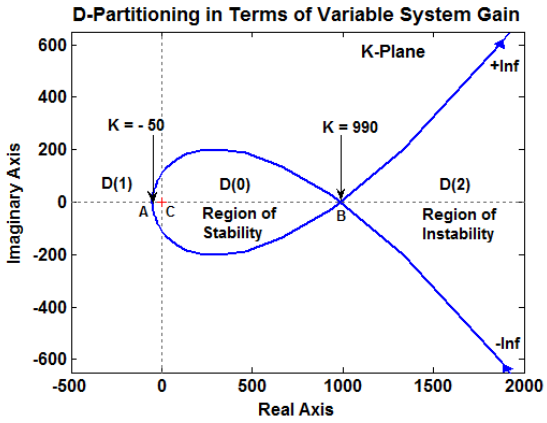

Figure 3.5b: *D-Partitioning Facilitated by the newly developed "dpartition" m-code*

It is obvious that the results obtained by the "dpartition" m-code are the same as those achieved by the "nyquist" m-code. This D-Partitioning procedure can work only on a computer where the new developed "dpartition" m-code is included in the MATLAB program.

In order to benefit from the D-partitioning analysis shown in this research, the wider engineering community can still use the "nyquist" m-code for the purpose of plotting the D-partitioning curve.

It is seen that the D-partitioning determines three regions on the *K*-plane: D(0), D(1) and D(2). **Only D(0) is the region of stability, being the one, always on the left-hand side of the curve for a frequency variation from $-\infty$ to $+\infty$.**

The Cauchy principle of argument is very well observed and the path in the variable parameter is actually closed, since to plot it the MATLAB code "nyquist" or "dpartition" is used. Here **only a limited part of the D-Partitioning curve is shown – this part that is of interest of determining the regions of stability.**

From the equations (3.8) and (3.9), it is seen that **the system gain is 0.02*K***, while ***K* is considered as a gain factor**. The gain factor range related to the segment *AB*, corresponds to a stable system since it is within the stable region D(0).

The results, obtained from the D-partitioning are compared and confirmed with the outcome from the Nyquist analysis for the cases of negative gain factors $K \in [-80, -30]$, corresponding to system gains $0.02K \in [-1.6, -0.6]$ accordingly, shown in Figure 3.6. The case of ***K* = -50, or a system gain 0.02*K* = -1 corresponds to a marginal case**, while $K = -80$, corresponding to $0.02K = -1.6$ corresponds to an unstable state of the system.

The results, obtained from the D-partitioning are also compared and confirmed with the outcome from the Nyquist analysis for the cases of the positive gain factors $K \in [400,1200]$ corresponding to gains $0.02K \in [8,24]$ accordingly, as shown in Figure 3.7a and zoomed in Figure 3.7b. The case of ***K* = 990, or a system gain 0.02*K* = 19.8 corresponds to a marginal case**, while $K = 1200$, corresponding to $0.02K = 24$ corresponds again to an unstable state of the system.

The results from the Nyquist analysis prove the outcome of the D-Partitioning and confirm that the system's region of stability is within the range of $-50 < K < 990$, **corresponding to the range of the system gain $-1 < 0.02K < 19.8$.**

```
>> K=[-30:-5:-80];
>> for n=1:length(K)
Ao_array(:,:,n)=tf([1000*K(n)],
[1 160 6500 50000]);
end
>> nyquist(Ao_array)
```

To examine the effect of the variable gain factor *K* on the system's stability, an LTI array of *Ao* is created. The results from the LTI array, for negative gain factors *K*, confirm the results from the D-Partitioning analysis.

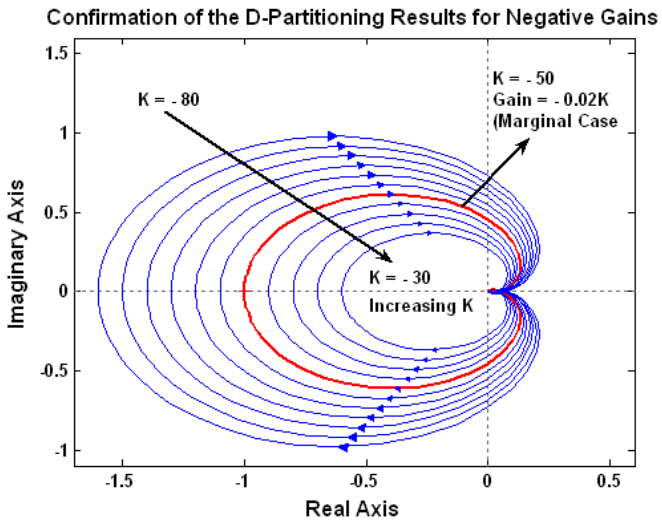

Figure 3.6: *Confirmation of the D-Partitioning with the Aid of the Nyquist Criterion (Cases of Negative Gains)*

The effects of the variable gain factor *K* on the system's stability are again examined with, an LTI array model of Ao. It is created for several values of *K* around its expected value that brings the control system to its marginal performance.

<u>The results from the LTI array model, for positive gain factors *K*, confirm the results from the D-Partitioning analysis.</u>

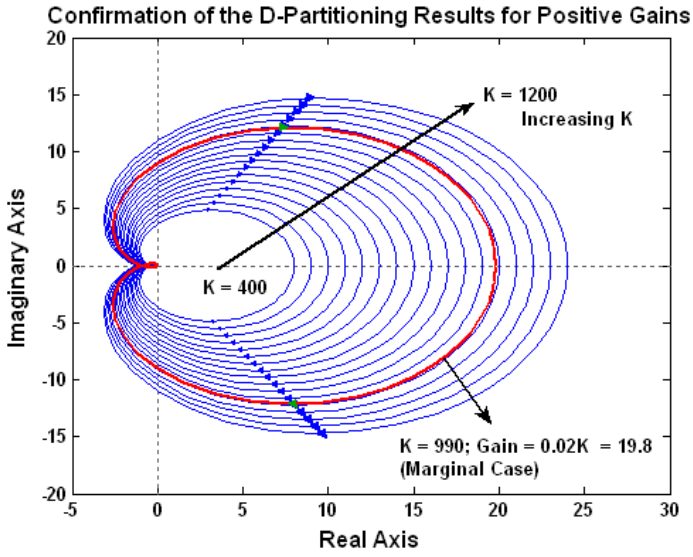

Figure 3.7a: *Confirmation of the D-Partitioning with the Aid of the Nyquist Criterion (Cases of Positive Gains)*

```
>> K=[400:50:1200];
>> for n=1:length(K)
Ao_array(:,:,n)=tf([1000*K(n)],
[1 160 6500 50000]);
   end
>> Ao1=tf([990000],
[1 160 6500 50000])
   Transfer function:
          990000
-----------------------------
s^3 + 160 s^2 + 6500 s + 50000
nyquist(Ao_array,Ao1)
>> nyquist(Ao_array,Ao1)
```

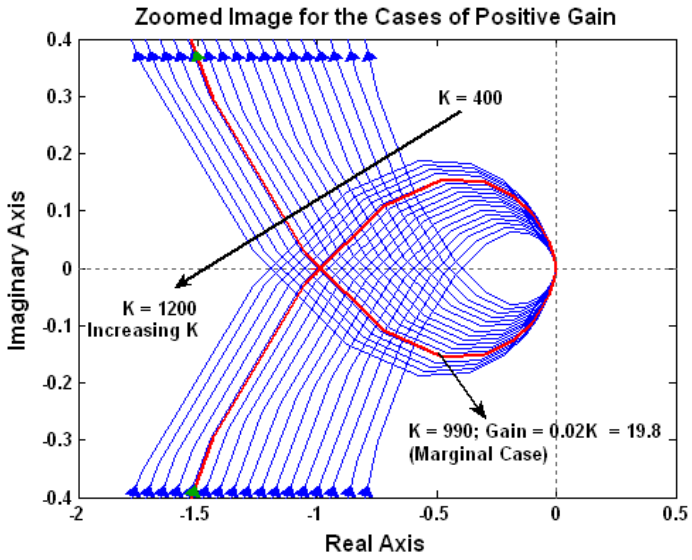

Figure 3.7b: *Zoomed Image of the Marginal Gain, Confirmed with the Aid of the Nyquist Stability Criterion (Cases of Positive Gains)*

3.3.2.2 D-Partitioning by Variable Gain (System Type 1)

The objective of a **solar-tracker control system** is to point the PV modules to the brightest point in the sky [63], [64], [65], [66]. The schematic diagram of the system is

shown in Figure 3.8. The tracking sensor is an error discriminator, consisting of two photovoltaic cells mounted behind a rectangular slit in a cylinder enclosure. The cells are mounted in such a way that when the sensor is pointed at the brightest point in the sky, a beam of light from the slit overlaps both cells. The sensor itself is mounted at 90° to the surface of the PV panels. The photovoltaic cells are used as current sources and are connected in opposite polarity to the input of an operational amplifier. Any difference in the currents of the two sells is sensed and amplified by the operational amplifier. Since the current of each cell is proportional to the illumination on the cell, an error signal will be present at the output of the amplifier when the light from the slit is not precisely centered on the cells. This error voltage when fed to the servo-amplifier will cause the motor to drive the system back into alignment.

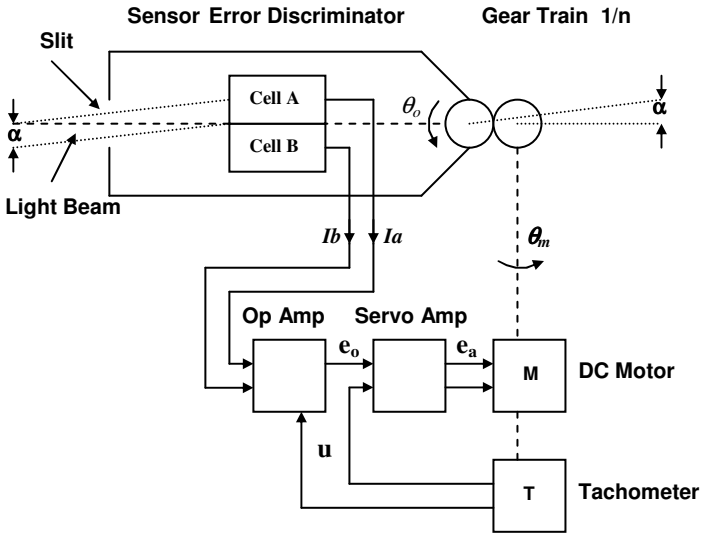

Figure 3.8: *Schematic Diagram of the Light Tracking System*

The block diagram of the light tracking system is shown in Figure 3.9. The input variable θ_r represents the reference angle of the bright light beam, while θ_o matches the sensor axis. The difference between these two angles depicts the error α. The objective of the light tracking system is to maintain the error α between θ_r and θ_o near zero. The parameters of the system are chosen as follows:

Sensor constant K_s = 0.01 A/rad; OP constant R_F = 1000; **Servo amplifier constant K = Variable**; DC motor gain constant K_i = 0.0125 Nm/A; Armature resistance

R_a = 6.25Ω; Armature inductance L_a = 0.01H; Inertia J = 10^{-6} kg.m^2; Damping B = 0; Motor constant K_b = 0.0125V/rad/sec; Motor speed n = 800;

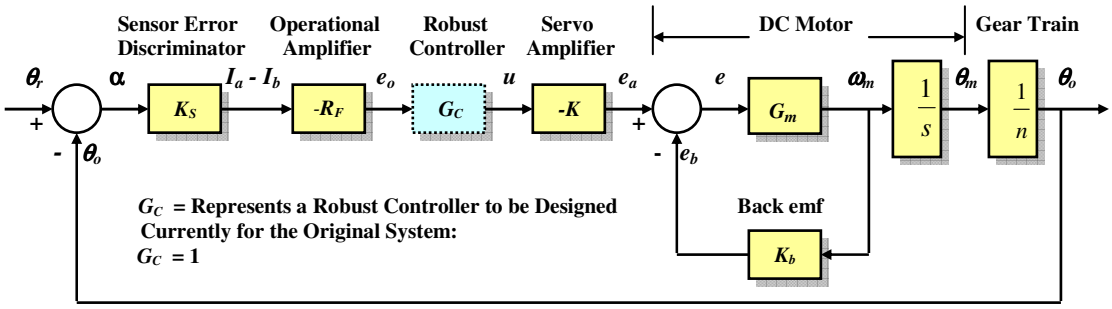

Fig. 3.9: *Block Diagram of the Light Tracking System*

Initially, the transfer function of the robust controller is assumed to be $G_C(s)$ = 1. The transfer function of the DC motor can be represented as:

$$\frac{\theta_m}{e_a} = \frac{K_i}{JL_a s^3 + (R_a J + L_a B)s^2 + (R_a B + K_b K_i)s} \tag{3.16}$$

By substituting the system parameters values, the transfer function of the complete open-loop system:

$$A_1(s) = \frac{K_S R_F K K_i / n}{JL_a s^3 + (R_a J + L_a B)s^2 + (R_a B + K_b K_i)s} = \frac{K}{s(1+0.02s)(1+0.005s)} \tag{3.17}$$

Initially, the system is discussed for the case of an uncertain gain K. Further, a case of an uncertain time-constant T is considered and the system is examined if both the gain K and the time-constant T are variable.

Considering a unity feedback control system, the closed-loop transfer function is:

$$A_{CL}(s) = \frac{A_1(s)}{1 + A_1(s)} = \frac{K}{s(1+0{,}02s)(1+0{,}005s) + K} \tag{3.18}$$

Then the characteristic equation of the closed-loop system is determined as:

$$G(s) = s(1+0.02s)(1+0.005s) + K = 0 \tag{3.19}$$

An equation in terms of the variable parameter K can be obtained from the characteristic equation as follows:

$$G(s) = P(s) + KQ(s) = 0 \tag{3.20}$$

$$P(s) = s(1+0.02s)(1+0.005s) \tag{3.21}$$

$$Q(s) = 1 \tag{3.22}$$

$$K(s) = -\frac{P(s)}{Q(s)} = -\frac{s(1+0.02s)(1+0.005s)}{1} = -\frac{0.0001s^3 + 0.025s^2 + s}{1} \tag{3.23}$$

The D-partitioning in terms of the variable parameter *K*, as seen from Figure 3.10, is obtained with the aid of the MATLAB code as shown below, considering $s = j\omega$ and varying the frequency within the range $-\infty \leq \omega \leq +\infty$.

```
>> K=tf([0.0001 0.025 1 0],[0 1])
Transfer function:
-0.0001 s^3 - 0.025 s^2 – s
>>dpartition(K)
```

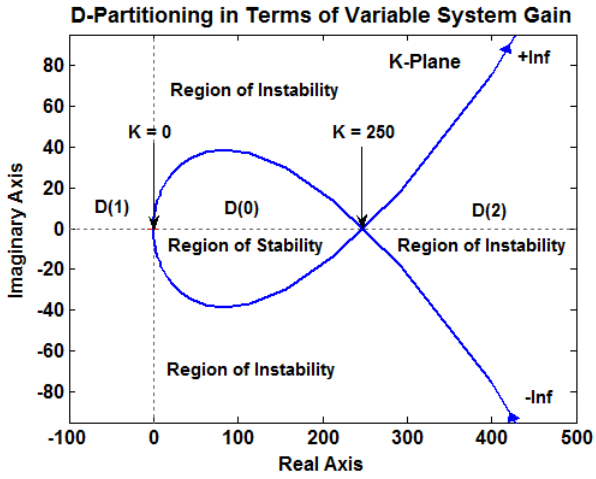

Figure 3.10: *D-Partitioning in Terms of the Variable System Gain (System Type 1)*

As seen from Figure 3.10, the D-partitioning determines three regions on the *K*-plane: D(0), D(1) and D(2). Only D(0) is the region of stability, being the one, always on the left-hand side of the curve for a frequency variation from $-\infty$ to $+\infty$. The system is stable within the range of the servo amplifier gain $0 \leq K \leq 250$ that can be proven in a similar way like for the systems of Type 0.

3.3.3 Advancement the of D-Partitioning in Terms of Variable Time-constant

It is suggested that a third order hypothetical control system is considered where one of the time-constants $T_3 = \nu$ is the variable, while all other system parameters are known and constant. The objective is to determine the regions of stability if the

system parameter T_3 varies. The characteristic equation is presented as follows, now exposing the variable parameter T_3:

$$G(s) = P(s) + vQ(s) = P(s) + T_3 Q(s) = 0 \tag{3.24}$$

The D-partitioning curve can be plotted by substituting $s = j\omega$ and allocating frequency values within the range $-\infty \leq \omega \leq +\infty$.

$$v = T_3 = -\frac{P(j\omega)}{Q(j\omega)} = X(\omega) + jY(\omega) \tag{3.25}$$

To find out the ranges of the time-constant T_3 for which the control system is stable, a similar procedure like the one used for the case of variable gain is applied.

3.3.3.1 D-partitioning by Variable Time-constant (System Type 0)

The following system is suggested to illustrate the application of the D-partitioning in case of variable time-constant consisting of an **armature-controlled dc motor and a type-driving mechanism** [63], [67]. The variation of the load causes variation of the mechanism time-constant.

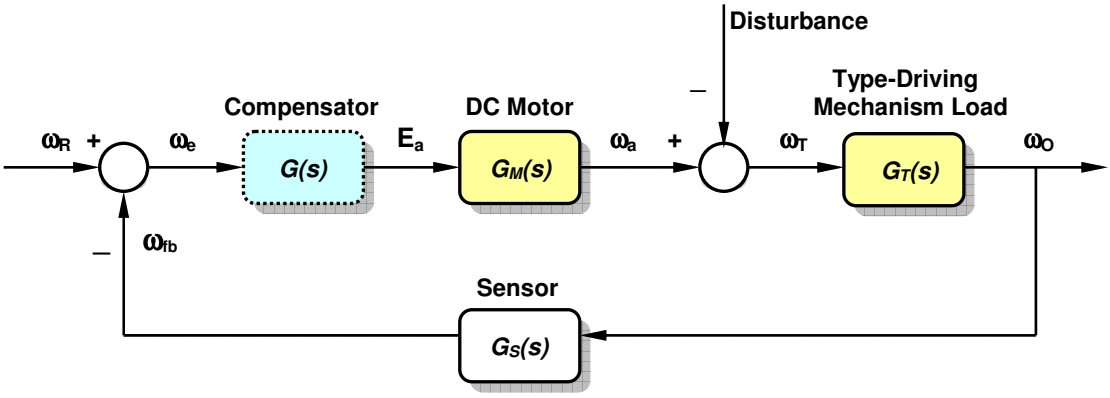

Figure 3.11: *Armature-Controlled DC Motor and a Type-Driving Mechanism*

Initially, the transfer function of the controller is considered $G(s) = 1$. The transfer function of the DC motor can be represented as:

$$G_M(s) = \frac{\omega_a}{E_a} = \frac{K_T}{JL_a s^2 + (R_a J + L_a B)s + (R_a B + K_e K_T)} = \frac{10}{(1+0.5s)(1+0.8s)} \tag{3.26}$$

Where	J = 0.01 kg.m^2	is the load inertia
	B = 0 (negligible)	is the load damping
	R_a = 0.5Ω	is the armature resistance
	L_a = 0.4H;	is the armature inductance
	K_e = 0.1V/rad/sec	is the voltage constant of the motor
	K_T = 10 Nm/A	is the DC motor gain constant

The gain K = 10 and the two motor time-constants T_1 = 0.5 sec and T_2 = 0.8 sec are known and constant values. The time-constant of the type-driving mechanism, T_3 is unstable and variable parameter due to the variation of the mechanical load. The dynamics of the type-driving mechanism is described by the following transfer function with a variable time-constant:

$$G_T(s) = \frac{1}{(1 + T_3 s)} \tag{3.27}$$

Finally, the transfer function of the open loop system is presented as:

$$G_o(s) = \frac{\omega_o}{\omega_e} = \frac{K}{(1+T_1 s)(1+T_2 s)(1+T_3 s)} = \frac{10}{(1+0.5s)(1+0.8s)(1+T_3 s)} \tag{3.28}$$

$$G_o(s) = \frac{\omega_o}{\omega_e} = \frac{10}{0.4T_3 s^3 + (1.3T_3 + 0.4)s^2 + (T_3 + 1.3)s + 1} \tag{3.29}$$

From equation (3.28), the characteristic equation of the unity feedback control system is determined as:

$$G(s) = 0.4T_3 s^3 + (1.3T_3 + 0.4)s^2 + (T_3 + 1.3)s + 11 \tag{3.30}$$

The regions of stability reflecting the variation of the system parameter T_3 are determined by implementing the method of the D-Partitioning. The time-constant T_3 is presented from equation (3.30) as follows:

$$T_3 = -\frac{T_1 T_2 s^2 + (T_1 + T_2)s + K + 1}{T_1 T_2 s^3 + (T_1 + T_2)s^2 + s} = -\frac{0.4s^2 + 1.3s + 11}{0.4s^3 + 1.3s^2 + s} \tag{3.31}$$

Considering equation (3.30), the D-Partitioning curve, is plotted for the frequency variation within the range $-\infty \le \omega \le +\infty$. As seen from Figure 3.12, the D-Partitioning

determines four regions in the complex T3-Plane: D1(0), D2(0), D(1) and D(2). Only D1(0) and D2(0) are regions of stability, since they are always on the left-hand side of the D-Partitioning curve for the frequency variation within the range $-\infty \leq \omega \leq +\infty$.

```
>> T3=tf([-0.4 -1.3 -11],
         [0.4 1.3 1 0])
Transfer function:
-0.4 s^2 - 1.3 s - 11
---------------------
0.4 s^3 + 1.3 s^2 + s
>> dpartition(T3)
```

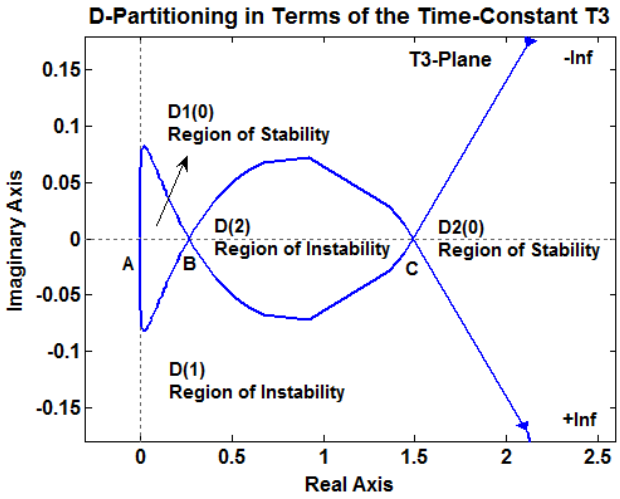

Figure 3.12: *D-Partitioning in Terms of the Time-Constant T_3 (System Type 0)*

Even when the time-constant T_3 is the variable parameter, the pattern of the D-Partitioning depends also on the system gain and may change significantly for different values of the system gain. To determine the range of the time-constant T_3 for which the system is stable, it is required to consider only the real values of T_3. Then the regions of stability are reduced to lines of stability. **If T_3 is varied within a range of 0 sec to 0.265 sec, corresponding to the segment AB, the system will be stable**, since AB is within the region of stability D1(0). **If T_3 is varied within a range of 0.265 sec to 1.5 sec, corresponding to the segment BC, the system will be unstable**, since BC is within the region of instability D(2). **If $T_3 > 1.5$ sec, the system becomes stable and is operating in the region of stability D2(0).** At points B and C the system becomes marginal. Three cases are considered, each one corresponding to one of the defined by the D-Partitioning regions. If the time-constant is $T_3 = 0.1$ sec, the system operates within the region of stability D1(0) according to the D-Partitioning. Then both the system gain and phase margins are positive, being $G_m = 4.89$ dB and $P_m = 4.48$ rad/sec accordingly, confirming the results obtained from the D-Partitioning analysis that the closed-loop system is stable. The region D1(0) is too small to find a point remote enough from the marginal points A and B. Therefore oscillations are expected throughout the sector AB.

```
>> T3=0.1
>> Go01=tf([10],[0.04 0.53 1.4 1])
>> margin(Go01)
GM=4.89, PM=4.48
```

There are continuous oscillations with constant amplitude at the marginal points A and B. Both gain and phase margins are equal to zero, G_m = 0 dB, P_m = 0 rad/sec.

```
>> T3=0.25
>> Go02=tf([10],[0.1 0.725 1.55 1])
>> margin(Go02)
GM=0, PM=0
```

```
>> T3=1.5
>> Go03=tf([10],[0.6 2.35 2.8 1])
 >> margin(Go03)
GM=0, PM=0
```

Further, variable time-constant is set to T_3 = 0.7 sec, close to the middle of the region of instability D(2). Then both the system gain and phase margins are negative, being G_m = −1.56 dB and P_m = −5.65 rad/sec accordingly, confirming the results obtained from the D-Partitioning analysis that the closed-loop system is unstable. The step response of the closed-loop system consists of oscillations with continuously rising amplitude, indicating instability of the system in the region of D(2).

```
>> T3=0.7
>> Go04=tf([10],[0.28 1.31 2 1])
>> margin(Go04)
GM=-1.56, PM=-5.65
```

If the time-constant is set to T_3 = 10 sec, the operation of the system is within the region of stability D2(0). Both the system gain and phase margins are positive, being G_m = 11.3 dB and P_m = 43.9 rad/sec and again confirming the D-Partitioning analysis results that the closed-loop system is stable.

```
>> T3=10
>> Go05=tf([10],[4 13.4 11.3 1])
>> margin(Go05)
GM=11.3, PM=43.9
```

3.3.3.2 D-Partitioning by Variable Time-constant (System Type 1)

The **sun-tracker control system** of Type 1, described in section 3.3.2.2, is taken again into account. Assuming a constant system gain of K = 300, now one of the system's time-constants, T_1, is considered as variable. The D-Partitioning analysis is applied in a similar sequence. The forward transfer function is:

$$A_{1T}(s) = \frac{300}{s(1+T_1 s)(1+0.005s)} \tag{3.32}$$

The closed-loop transfer function of the unity feedback system is obtained as:

$$A_{CLT}(s) = \frac{A_{1T}(s)}{1+A_{1T}(s)} = \frac{300}{s(1+T_1 s)(1+0.005s)+300} \tag{3.33}$$

Then the characteristic equation of the closed-loop system is determined as:

$$G(s) = s(1+T_1 s)(1+0.005s)+300 = 0 \tag{3.34}$$

The regions of stability of the system can be determined in terms of the variable time-constant T_1. From equation (3.34), the variable parameter is presented as follows:

$$T_1 = -\frac{0{,}005s^2 + s + 300}{0{,}005s^3 + s^2} \tag{3.35}$$

```
>> T1 = tf([-0.005 -1 -300],
[0.005 1 0 0])
Transfer function:
-0.005 s^2 - s - 300
--------------------
0.005 s^3 + s^2
>> dpartition(T1)
```

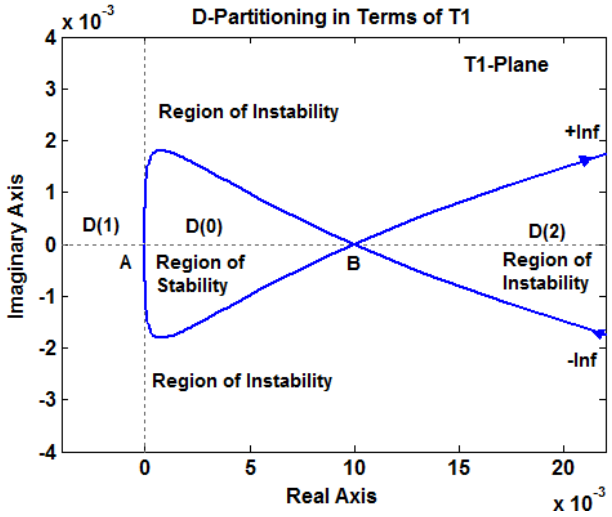

Figure 3.13: *D-Partitioning in Terms of the Time-Constant T_1 (System Type 1)*

As seen from Figure 3.13, the D-Partitioning determines three different regions on the complex T1-Plane: D(0), D(1) and D(2). Only D(0) is the region of stability, since its position is always on the left-hand side of the D-partitioning curve for the frequency variation within the range $-\infty \leq \omega \leq +\infty$. The pattern of the D-Partitioning in case of systems Type 1 is different from the one of systems Type 0. Again, the D-Partitioning pattern of systems Type 1 depends also on the system's gain and may change considerably for different values of the gain. To determine the range of the time-constant T_1 for which the system is stable, it is required to consider only the real

values of *T1*. **If the parameter T_1 is varied within a range of 0 sec to 0.01 sec, corresponding to the segment AB, the system will be stable,** since AB is within the region of stability D(0). **If T_1 becomes larger than 0.01 sec the system will be unstable,** being within the region of instability D(2). It is also obvious that the time-constant T_1 cannot be negative.

Time-constant T_1 = 0.004 sec corresponds to a point within the region of stability D(0). The system Gain margin is G_m = 3.52 dB and the Phase margin is P_m = 12.1 rad/sec are both positive, confirming the conclusion from the D-Partitioning analysis that the closed-loop system is stable. The step response of the closed-loop system for this case represents oscillations with decreasing amplitude, confirming as well the D-Partitioning analysis results for a closed-loop stable system.

```
>>T1=0.004
>> A1T1 = tf([300],[0.00002 0.009 1 0])
>> margin(A1T)
GM=3.52, PM=12.1
```

The case T_1 = 0.01 sec corresponds to point B, being the border between the region of stability D(0) and region of instability D(2). For the case the system Gain margin is G_m = 0 dB and the Phase margin is P_m = 0 rad/sec, confirming the results from the D-partitioning analysis.

```
>>T1=0.01
>> A1T2 = tf([300],[0.00005 0.015 1 0])
>> margin(A1T)
GM=0, PM=0
```

A time-constant T_1 = 0.02 sec corresponds to a point within the region of instability D(2). Both the system Gain and Phase margins are negative, being G_m = -1.58 dB and P_m = -4.12 rad/sec.

```
>>T1=0.02
>> A1T = tf([300],[0.0001 0.025 1 0])
>> margin(A1T)
GM=-1.58, PM=-4.12
```

This further confirms the results obtained by the D-Partitioning analysis and the instability within the D(2) region.

If the gain is reduced, the region D(0) will be enlarged and the system will be stable even with larger variations of the time-constant T_1.

3.4. Advanced D-Partitioning: A Case of Multivariable Parameters

3.4.1 Advanced D-Partitioning by Two Variable Parameters

If two of the system parameters are variable simultaneously [24], [67], [68] the system general characteristic equation (3.1) can be presented as:

$$G(s) = \mu P(s) + \gamma Q(s) + R(s) = 0 \tag{3.36}$$

where $P(s)$, $Q(s)$, and $R(s)$ are polynomials of s

μ and γ are variables equal to the system's variable parameters

The border of the D-Partitioning in the plain (μ, γ) is determined by:

$$G(j\omega) = \mu P(j\omega) + \gamma Q(j\omega) + R(j\omega) = 0 \tag{3.37}$$

If

$$\left.\begin{aligned} P(j\omega) &= P_1(\omega) + jP_2(\omega) \\ Q(j\omega) &= Q_1(\omega) + jQ_2(\omega) \\ R(j\omega) &= R_1(\omega) + jR_2(\omega) \end{aligned}\right\} \tag{3.38}$$

Equation (3.38) is presented by a set of two equations:

$$\left.\begin{aligned} \mu P_1(\omega) + \gamma Q_1(\omega) + R_1(\omega) = 0 \\ \mu P_2(\omega) + \gamma Q_2(\omega) + R_2(\omega) = 0 \end{aligned}\right\} \tag{3.39}$$

By solving the set of equations (3.39) with respect to μ and γ the following results are achieved:

$$\left.\begin{aligned} \mu &= \frac{\Delta_1}{\Delta} \\ \gamma &= \frac{\Delta_2}{\Delta} \end{aligned}\right\} \tag{3.40}$$

where

$$\left.\begin{aligned}\Delta &= \begin{bmatrix} P_1(\omega) & Q_1(\omega) \\ P_2(\omega) & Q_2(\omega) \end{bmatrix} \\ \Delta_1 &= \begin{bmatrix} -R_1(\omega) & Q_1(\omega) \\ -R_2(\omega) & Q_2(\omega) \end{bmatrix} \\ \Delta_2 &= \begin{bmatrix} P_1(\omega) & -R_1(\omega) \\ P_2(\omega) & -R_2(\omega) \end{bmatrix}\end{aligned}\right\} \qquad (3.41)$$

It is obvious from equations (3.41) that the determinants Δ, Δ_1 and Δ_2 represent odd functions. Therefore, considering equation (3.40), the variable parameters μ and γ are considered as even functions. It follows that each one of the parameters μ and γ has over-tracing values within the frequency region $-\infty \leq \omega \leq +\infty$, as seen from equation (3.42):

$$\left.\begin{aligned}\mu(+\omega) &= \mu(-\omega) \\ \gamma(+\omega) &= \gamma(-\omega)\end{aligned}\right\} \qquad (3.42)$$

Then, if in the plain (μ, γ), the D-Partitioning curve is plotted following the frequency increment from $-\infty$ to 0, the rest part of the curve, plotted for frequency increment from 0 to $+\infty$ is over-tracing the already plotted curve in reverse order as seen in Figure 3.14. As stability region border is taken this part of the curve that corresponds to the realistic parameter values.

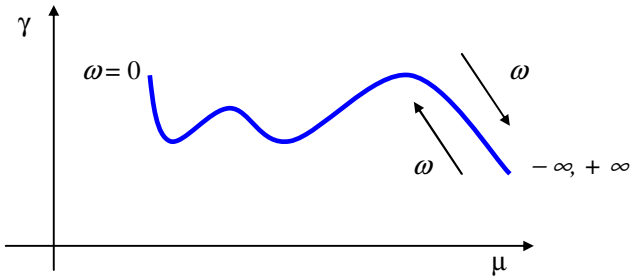

Figure 3.14: *Over-Tracing Curves*

The regions of the D-Partitioning also depend on straight lines in the (μ ,γ) plane, known as *special lines*. The special lines are plotted for two border frequencies $\omega = 0$ and $\omega = +\infty$. Then the coefficients a_n and a_o of the equation (1) depend directly on the parameters μ and γ and the equations of the special lines are obtained by:

$$a_n = 0, \qquad a_o = 0 \tag{3.43}$$

The coefficient a_n determines a special line when $\omega = 0$, while the coefficient a_o determines a special line when $\omega = +\infty$.

The D-Partitioning regions could be determined by plotting the main D-Partitioning curve, together with the special lines on the (μ, γ) plane. The locked regions between these parts of the curve, corresponding to realistic physically realized system parameters and the special lines are identified as the regions of stability. The realistic stable regions are also always located on the left-hand side of the D-Partitioning curve, following the frequency increment.

3.4.2 D-Partitioning by Two Variable Parameters (System Type 0)

The characteristic equation (3.44) of a **hypothetical third order unity feedback system** of Type 0 is considered as follows:

$$G(s) = (T_1 s + 1)(T_2 s + 1)(T_3 s + 1) + K = 0 \tag{3.44}$$

It is suggested that simultaneously two of the system's parameters are variable:

$$T_1 = \mu \ , \qquad K = \gamma. \tag{3.45}$$

The objective is to determine the regions of variation of these two parameters, for which the system will be stable.

Equations (3.44) are substituted in (3.45), from where:

$$\mu[T_2 T_3 s^3 + (T_2 + T_3)s^2 + s] + \gamma + T_2 T_3 s^2 + (T_2 + T_3)s + 1 = 0 \tag{3.46}$$

By substituting $s = j\omega$ in equation (3.46) and taking into account (3.36), the set of equations (3.46) could be presented in the detailed form:

$$\left.\begin{aligned} P(j\omega) &= [T_2 T_3 (j\omega)^3 + (T_2 + T_3)(j\omega)^2 + j\omega] \\ Q(j\omega) &= 1 \\ R(j\omega) &= T_2 T_3 (j\omega)^2 + (T_2 + T_3) j\omega + 1 \end{aligned}\right\} \tag{3.47}$$

Considering equations (3.38), (3.39) and (3.40) the variable system's parameters can be determined as:

$$\left.\begin{aligned} \mu &= \frac{T_2 + T_3}{T_2 T_3 \omega^2 - 1} \\ \gamma &= \frac{(T_2 T_3 \omega^2 - 1)^2 + (T_2 + T_3)^2 \omega^2 + 1}{T_2 T_3 \omega^2 - 1} \end{aligned}\right\} \tag{3.48}$$

Comparing the equation sets (3.40) and (3.48), it is obvious that:

$$\Delta = T_2 T_3 \omega^2 - 1 \tag{3.49}$$

The determinant Δ becomes $\Delta = 0$ at a specific frequency $\omega = \omega_\infty$ that can be found out from equation (3.49) as:

$$\omega = \omega_\infty = \sqrt{\frac{1}{T_2 T_3}} \tag{3.50}$$

It is clear from equations (3.40) that at $\omega = \omega_\infty$, when $\Delta = 0$, both system parameters are approaching infinity:

$$\mu(\omega_\infty) \to \infty, \quad \gamma(\omega_\infty) \to \infty, \tag{3.51}$$

This implies that the main D-Partitioning curve has an interruption, or a breakdown, at a frequency $\omega = \omega_\infty$. It consists of two parts, the first one is plotted within the frequency range $0 < \omega < \omega_\infty$, while the second one is obtained for $\omega_\infty < \omega < \infty$.

The special lines are determined by comparing the equations (3.1) and (3.46) identifying the coefficients a_n and a_o and equalizing them to zero:

$$\left.\begin{aligned} &a_n = \mu T_2 T_3 = 0, \qquad a_o = \gamma + 1 = 0 \\ &\text{or} \\ &\mu = 0 = Const. \qquad \gamma = -1 = Const. \end{aligned}\right\} \tag{3.52}$$

The regions of stability are determined by the D-Partitioning curve, defined by equations (3.48) and the special lines, defined by equations (3.52). For a better clarification and simplicity, first the functions $\mu(\omega)$ and $\gamma(\omega)$ are plotted, as shown in Figure 3.15(a) and Figure 3.15(b).

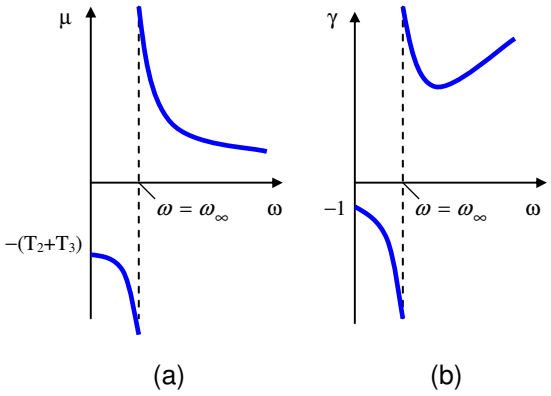

Figure 3.15: *The graphical presentations of $\mu(\omega)$ and $\gamma(\omega)$ showing the interruption of the curves at a frequency $\omega = \omega_\infty$*

Finally, by combining the curves $\mu(\omega)$, $\gamma(\omega)$ and the special lines, the D-Partitioning is obtained in the (μ, γ) plane as seen in Figure 3.16.

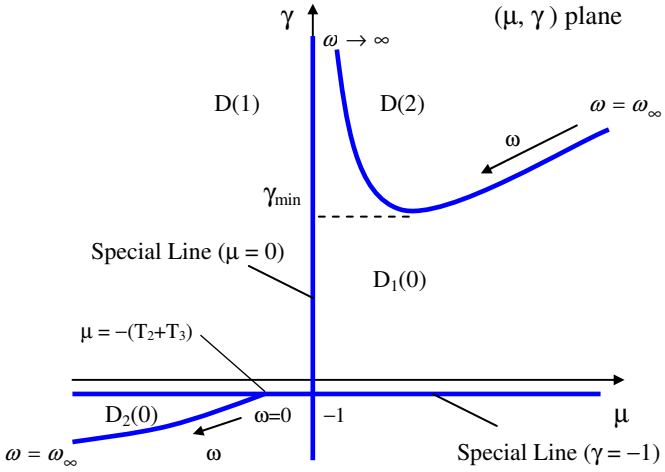

Figure 3.16: *The regions of stability $D_1(0)$ and $D_2(0)$ locked between the D-Partitioning curves and the special lines*

Taking into account that $\mu = T_1$ is a time-constant and it can adopt only positive values, practically only the stable region $D_1(0)$ should be considered. The region of stability $D_1(0)$ is locked within the left-hand side of the D-Partitioning curve, corresponding to frequency rise from $\omega = \omega_\infty$ to $\omega \to \infty$ and the special line $\gamma = -1$. Since the gain $K = \gamma$ may also adopt only positive values, the realistic border of the stable region $D_1(0)$ should be considered $K = \gamma = 0$.

Further, the conclusion is that for small values of the gain $K < \gamma_{min}$, the system is stable for any values of the time-constant $\mu = T_1$. The value of γ_{min} can be easily determined by taking the first derivative of the second equation of the set (3.48). Large gain values $K > \gamma_{min}$ could be employed only for very small or very large values of the time-constant $\mu = T_1$.

3.4.3 D-Partitioning in Case of Two Simultaneously Variable Parameters - System Gain and a System Time-Constant (System Type 0)

The analysis shown above can be demonstrated for the control system of Type 0 of an **armature-controlled dc motor and a type-driving mechanism** described in section 3.3.3.1. In this case the gain and one of the time-constants are uncertain and variable. The open-loop transfer function of the system is presented as:

$$G(s) = \frac{K}{(1+Ts)(1+0.5s)(1+0.8s)} \tag{3.53}$$

Then the characteristic equation of the unity feedback system is:

$$K + (1+Ts)(1+0.5s)(1+0.8s) = 0 \tag{3.54}$$

By substituting $s = j\omega$ equation (3.66) is modified to:

$$K = -1 + (1.3T + 0.4)\omega^2 + j\omega(0.4T\omega^2 - 1.3 - T) \tag{3.55}$$

Since the gain may obtain only real values, the imaginary term of equation (3.55) is set to zero, from where:

$$\omega^2 = \frac{1.3 + T}{0.4T} \tag{3.56}$$

The result of (3.56) is substituted into the real part of equation (3.55), from where:

$$K = \frac{1.3T^2 + 1.69T + 0.52}{0.4T} = 3.25T + 4.225 + \frac{1.3}{T} \tag{3.57}$$

The D-Partitioning curve $K = f(T)$ is plotted with the aid of the following code:

```
>> T = 0:0.1:5;
>> K = 3.25.*T+4.225+1.3./T
    K =
   Columns 1 through 10
   Inf   17.5500   11.3750    9.5333    8.7750    8.4500    8.3417    8.3571    8.4500    8.5944
   Columns 11 through 20
   8.7750    8.9818    9.2083    9.4500    9.7036    9.9667   10.2375   10.5147   10.7972   11.0842
   Columns 21 through 30
   11.3750   11.6690   11.9659   12.2652   12.5667   12.8700   13.1750   13.4815   13.7893   14.0983
   Columns 31 through 40
   14.4083   14.7194   15.0313   15.3439   15.6574   15.9714   16.2861   16.6014   16.9171   17.2333
   Columns 41 through 50
   17.5500   17.8671   18.1845   18.5023   18.8205   19.1389   19.4576   19.7766   20.0958   20.4153
   Column 51
   20.7350
>> plot(T,K)
```

The D-Partitioning curve $K = f(T)$ defines the border between the region of stability D(0) and instability D(1) for the case of simultaneous variation of the two system parameters. Each point of the D-Partitioning curve represents also the marginal values of the two simultaneously variable parameters. This is a unique advancement and an innovation in the theory of control systems stability analysis.

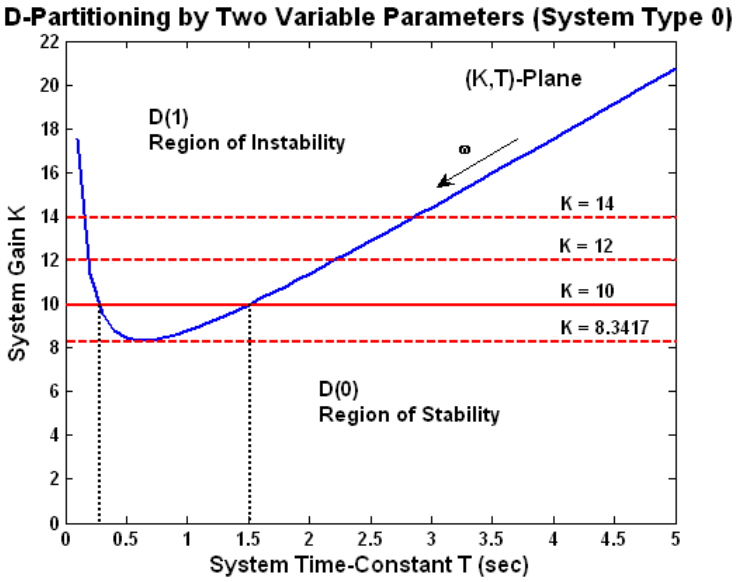

Figure 3.17: *D-Partitioning in terms of Two Variable Parameters (System Type 0)*

The demonstration of the system performance in case of variation of the time-constant T is done at gain set to $K = 10$. **When $0 < T < 0.25$ sec and $T > 1.5$ sec the system is stable.** But it becomes **unstable in the range 0.25 sec $< T <$ 1.5 sec.** The system performance can also be investigated for any other values of the variable gain K, like $K = 12$, $K = 14$, etc. It is obvious that if K is varied, this affects the values of T at which the system may become unstable. Higher values of K, enlarges the range of T at which the system will fall into instability. But if $K < 8.3417$, a limit determined with the aid of MATLAB interface procedure, the system is stable for any value of the T. It is obvious that the system performance and stability depends on the interaction between the two simultaneously varying parameters.

3.4.4 D-Partitioning in the 3-D Space for the Case of Three Simultaneously Variable System Parameters (System Type 0)

If the system has three uncertain and variable parameters, their interaction can be presented in the 3-Dimensional (3-D) space of these parameters. It is demonstrated for the control system of Type 0 of the armature-controlled dc motor and a type-driving mechanism described in section 3.3.3.1. In this case it is suggested that the system gain K and two of the time-constants T_1 and T_2 are variable [68]. Then the equation (3.53) can be modified to:

$$G(s) = \frac{K}{(1+T_1 s)(1+T_2 s)(1+0.8s)} \tag{3.58}$$

The characteristic equation of the corresponding unity feedback system is:

$$K + (1+T_1 s)(1+T_2 s)(1+0.8s) = 0 \tag{3.59}$$

By substituting $s = j\omega$ equation (3.71) is modified to:

$$K = -1 + 0.8(T_1 + T_2)\omega^2 + j\omega(-T_1 - T_2 - 0.8 + 0.8T_1T_2\omega^2) \tag{3.60}$$

The imaginary term of equation (3.60) is set to zero, since the gain may obtain only real values, from where:

$$\omega^2 = \frac{T_1 + T_2 + 0.8}{0.8T_1T_2} \tag{3.61}$$

When the result of (3.61) is substituted into the real part of equation (3.60), the relationship between the three variable parameters of the system is presented as:

$$K = -1 + 0.8(T_1 + T_2) + \frac{T_1 + T_2 + 0.8}{0.8 T_1 T_2} \tag{3.62}$$

The D-Partitioning plane is plotted in the (K, T_1, T_2)-Space of the variable parameters. It is plotted with the aid of the following code (the code is only partly presented, due to its considerable length):

```
>> [X,Y] = meshgrid([0:.15:3])
X =
Columns 1 through 10
    0   0.1500   0.3000   0.4500   0.6000   0.7500   0.9000   1.0500   1.2000   1.3500
    0   0.1500   0.3000   0.4500   0.6000   0.7500   0.9000   1.0500   1.2000   1.3500
   ---------------------------------------------------------------------------------------------------------------
    0   0.1500   0.3000   0.4500   0.6000   0.7500   0.9000   1.0500   1.2000   1.3500
Columns 11 through 20
  1.5000   1.6500   1.8000   1.9500   2.1000   2.2500   2.4000   2.5500   2.7000   2.8500
  1.5000   1.6500   1.8000   1.9500   2.1000   2.2500   2.4000   2.5500   2.7000   2.8500
 ---------------------------------------------------------------------------------------------------------------
  1.5000   1.6500   1.8000   1.9500   2.1000   2.2500   2.4000   2.5500   2.7000   2.8500
Column 21
  3.0000
  3.0000
 --------
  3.0000
Y =
Columns 1 through 10
    0       0       0       0       0       0       0       0       0       0
  0.1500   0.1500   0.1500   0.1500   0.1500   0.1500   0.1500   0.1500   0.1500   0.1500
  0.3000   0.3000   0.3000   0.3000   0.3000   0.3000   0.3000   0.3000   0.3000   0.3000
 ---------------------------------------------------------------------------------------------------------------
  3.0000   3.0000   3.0000   3.0000   3.0000   3.0000   3.0000   3.0000   3.0000   3.0000
Columns 11 through 20
    0       0       0       0       0       0       0       0       0       0
  0.1500   0.1500   0.1500   0.1500   0.1500   0.1500   0.1500   0.1500   0.1500   0.1500
  0.3000   0.3000   0.3000   0.3000   0.3000   0.3000   0.3000   0.3000   0.3000   0.3000
 ---------------------------------------------------------------------------------------------------------------
  3.0000   3.0000   3.0000   3.0000   3.0000   3.0000   3.0000   3.0000   3.0000   3.0000
Column 21
    0
  0.1500
  0.3000
 ---------
  3.0000
>> Z = -1+0.8.*(X+Y).*(X+Y+0.8)./(0.8.*X.*Y)
Warning: Divide by zero.
Z =
Columns 1 through 10
    NaN      Inf      Inf      Inf      Inf      Inf      Inf      Inf      Inf      Inf
    Inf   13.6667   11.5000   11.4444   11.9167   12.6000   13.3889   14.2381   15.1250   16.0370
    Inf   11.5000    8.3333    7.6111    7.5000    7.6333    7.8889    8.2143    8.5833    8.9815
   ---------------------------------------------------------------------------------------------------------------
    Inf   26.6500   14.0333    9.8611    7.8000    6.5833    5.7889    5.2357    4.8333    4.5315
Columns 11 through 20
    Inf      Inf      Inf      Inf      Inf      Inf      Inf      Inf      Inf      Inf
 16.9667   17.9091   18.8611   19.8205   20.7857   21.7556   22.7292   23.7059   24.6852   25.6667
  9.4000    9.8333   10.2778   10.7308   11.1905   11.6556   12.1250   12.5980   13.0741   13.5526
 ---------------------------------------------------------------------------------------------------------------
  4.3000   4.1197   3.9778   3.8654   3.7762   3.7056   3.6500   3.6069   3.5741   3.5500
Column 21
    Inf
 26.6500
 14.0333
------------
  3.5333
>> surf(X,Y,Z,gradient(Z))
```

The D-Partitioning plane, as seen in Figure 3.18, is **defining the border between the space of stability D(0), below the plane, and the space of instability D(1), above the plane, for the case of simultaneous variation of three system's parameters.**

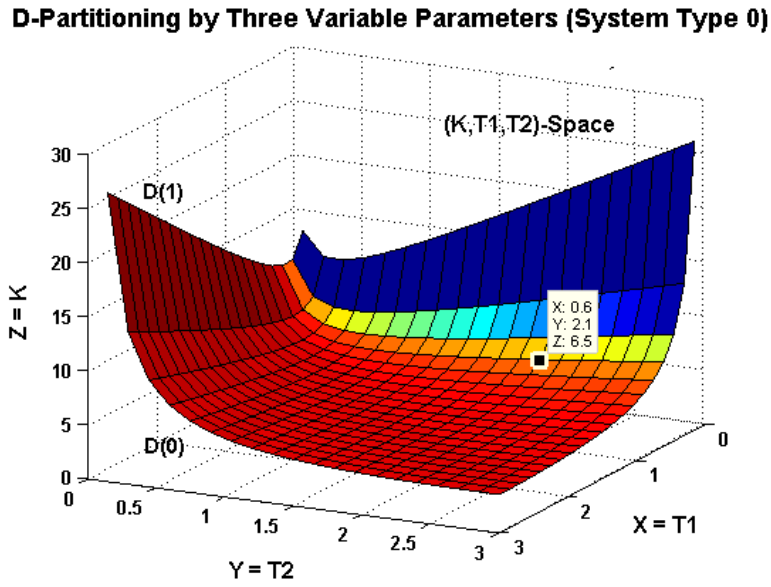

Figure 3.18: *D-Partitioning in terms of Three Variable Parameters (System Type 0)*

Any point of the D-Partitioning plane represents the marginal values of the three simultaneously variable parameters, this being a unique advancement and an innovation in the theory of control systems stability analysis. As seen in Figure 3.18, if the marginal gain is $K = Z = 6.5$, the marginal values of the two time-constants are $T_1 = X = 0.6$ sec and $T_2 = Y = 2.1$ sec accordingly. These results can be confirmed, if substituted in equation (3.62). When the system gain is $K = Z = 6.5$, if any of the time-constants marginal values is exceeded, as $T_1 > 0.6$ sec or $T_2 > 2.1$ sec, the control system will become unstable. Similar consideration can be done for any other combination of the three uncertain system parameters.

3.4.5 D-Partitioning in Case of Two Simultaneously Variable Parameters - System Gain and System Time-Constant (System Type 1)

The analysis of a system with two variable parameters is demonstrated for the control **photovoltaic solar-tracker control system** of Type 1 that is described in section 3.3.2.2. The gain and one of the time-constants are considered variable. The open-loop transfer function of the system is presented as:

$$A_1(s) = \frac{K}{s(1+Ts)(1+0{,}005s)} \tag{3.63}$$

The characteristic equation of the closed-loop transfer function is:

$$K + s(1+Ts)(1+0{,}005s) = 0 \tag{3.64}$$

By substituting $s = j\omega$ equation (3.64) is modified to:

$$K = (T + 0.005)\omega^2 + j\omega(0.005\,T\omega^2 - 1) \tag{3.65}$$

The imaginary term of equation (3.65) is set to zero, from where:

$$\omega^2 = \frac{1}{0.005\,T} \tag{3.66}$$

The result of (3.66) is substituted into the real part of equation (3.65), from where:

$$K = \frac{T + 0.005}{0.005T} = 200 + \frac{1}{T} \tag{3.67}$$

The D-Partitioning curve $K = f(T)$ can be plotted with the aid of the following code:

```
>> T = 0:0.001:0.1;
>> K = 200+1./T

K =
 1.0e+003 *
  Columns 1 through 10
 Inf   1.2000   0.7000   0.5333   0.4500   0.4000   0.3667   0.3429   0.3250   0.3111
 Columns 11 through 20
  0.3000   0.2909   0.2833   0.2769   0.2714   0.2667   0.2625   0.2588   0.2556   0.2526
 Columns 21 through 30
    0.2500   0.2476   0.2455   0.2435   0.2417   0.2400   0.2385   0.2370   0.2357   0.2345
  Columns 31 through 40
  0.2333   0.2323   0.2313   0.2303   0.2294   0.2286   0.2278   0.2270   0.2263   0.2256
 Columns 41 through 50
  0.2250   0.2244   0.2238   0.2233   0.2227   0.2222   0.2217   0.2213   0.2208   0.2204
 Columns 51 through 60
   0.2200   0.2196   0.2192   0.2189   0.2185   0.2182   0.2179   0.2175   0.2172   0.2169
 Columns 61 through 70
   0.2167   0.2164   0.2161   0.2159   0.2156   0.2154   0.2152   0.2149   0.2147   0.2145
 Columns 71 through 80
   0.2143   0.2141   0.2139   0.2137   0.2135   0.2133   0.2132   0.2130   0.2128   0.2127
 Columns 81 through 90
   0.2125   0.2123   0.2122   0.2120   0.2119   0.2118   0.2116   0.2115   0.2114   0.2112
 Columns 91 through 100
   0.2111   0.2110   0.2109   0.2108   0.2106   0.2105   0.2104   0.2103   0.2102   0.2101
 Column 101
 0.2100

>> plot(T,K)
```

The D-Partitioning curve $K = f(T)$, shown in Figure 3.19, defines the border between the region of stability D(0) and instability D(1) for the simultaneous variation of the two system's parameters.

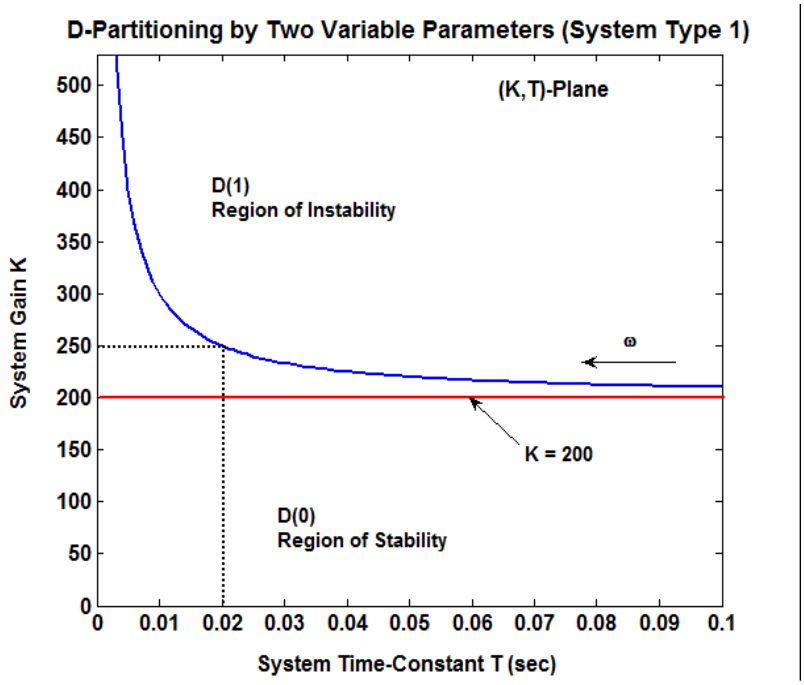

Figure 3.19: *D-Partitioning in terms of Two Variable Parameters (System Type 1)*

As seen from Figure 3.19, for gains $K < 200$, the system is stable for any value of T. **If the gain is $K > 200$ the system stability becomes dependable on the value of the gain K and may become unstable for large values of the time-constant T.** This is demonstrating the interaction between the two variable parameters. For instance, it is shown that If the system gain is $K = 250$, the system becomes unstable for any time-constant $T > 0.02$ sec.

Again, each point of the D-Partitioning curve represents the marginal values of the two simultaneously variable parameters, being a unique advancement and innovation in the theory of control systems stability analysis.

3.4.6 D-Partitioning in the 3-D Space for the Case of Three Simultaneously Variable System Parameters (System Type 1)

The case of three variable parameters can be demonstrated for the control system of Type 1, described in section 3.3.3.2. The system gain K and two of the time-constants T_1 and T_2 are variable. In this case, equation (3.63) is modified to:

$$A_1(s) = \frac{K}{s(1+T_1 s)(1+T_2 s)} \tag{3.68}$$

The characteristic equation of the unity closed-loop system is defined as:

$$K + s(1+T_1 s)(1+T_2 s) = 0 \tag{3.69}$$

By substituting $s = j\omega$ equation (3.81) becomes:

$$K = (T_1 + T_2)\omega^2 + j\omega(T_1 T_2 \omega^2 - 1) \tag{3.70}$$

The imaginary term of equation (3.82) is set to zero, from where:

$$\omega^2 = \frac{1}{T_1 T_2} \tag{3.71}$$

The result of (3.71) is substituted into the real part of equation (3.70), from where:

$$K = \frac{T_1 + T_2}{T_1 T_2} \tag{3.72}$$

The D-Partitioning plane is drawn in the (K,T_1,T_2)-Space of the system variable parameters by implementing the following code(the code is only partly presented, due to its considerable length):

```
>> [X,Y] = meshgrid([0:.1:2])
X =
  Columns 1 through 10
       0   0.1000   0.2000   0.3000   0.4000   0.5000   0.6000   0.7000   0.8000   0.9000
       0   0.1000   0.2000   0.3000   0.4000   0.5000   0.6000   0.7000   0.8000   0.9000
      ---------------------------------------------------------------------------------------------------------------
  Columns 11 through 20
      1.0000   1.1000   1.2000   1.3000   1.4000   1.5000   1.6000   1.7000   1.8000   1.9000
      1.0000   1.1000   1.2000   1.3000   1.4000   1.5000   1.6000   1.7000   1.8000   1.9000
     ---------------------------------------------------------------------------------------------------------------
    Column 21
    2.0000
    2.0000
     ---------
Y =
  Columns 1 through 10
       0       0       0       0       0       0       0       0       0       0
    0.1000   0.1000   0.1000   0.1000   0.1000   0.1000   0.1000   0.1000   0.1000   0.1000
    0.2000   0.2000   0.2000   0.2000   0.2000   0.2000   0.2000   0.2000   0.2000   0.2000
    ---------------------------------------------------------------------------------------------------------------
    2.0000   2.0000   2.0000   2.0000   2.0000   2.0000   2.0000   2.0000   2.0000   2.0000
  Columns 11 through 20
       0       0       0       0       0       0       0       0       0       0
    0.1000   0.1000   0.1000   0.1000   0.1000   0.1000   0.1000   0.1000   0.1000   0.1000
    0.2000   0.2000   0.2000   0.2000   0.2000   0.2000   0.2000   0.2000   0.2000   0.2000
    ---------------------------------------------------------------------------------------------------------------
    2.0000   2.0000   2.0000   2.0000   2.0000   2.0000   2.0000   2.0000   2.0000   2.0000
  Column 21
       0
    0.1000
    0.2000
   ----------
    2.0000
```

```
>> Z = (X+Y)./(X.*Y)
Warning: Divide by zero.
Z =
  Columns 1 through 10
     NaN     Inf     Inf     Inf     Inf     Inf     Inf     Inf     Inf     Inf
     Inf  20.0000  15.0000  13.3333  12.5000  12.0000  11.6667  11.4286  11.2500  11.1111
     Inf  15.0000  10.0000   8.3333   7.5000   7.0000   6.6667   6.4286   6.2500   6.1111
     Inf  13.3333   8.3333   6.6667   5.8333   5.3333   5.0000   4.7619   4.5833   4.4444
    ---------------------------------------------------------------------------------------------------------------
     Inf  10.5000   5.5000   3.8333   3.0000   2.5000   2.1667   1.9286   1.7500   1.6111
  Columns 11 through 20
     Inf     Inf     Inf     Inf     Inf     Inf     Inf     Inf     Inf     Inf
  11.0000  10.9091  10.8333  10.7692  10.7143  10.6667  10.6250  10.5882  10.5556  10.5263
   6.0000   5.9091   5.8333   5.7692   5.7143   5.6667   5.6250   5.5882   5.5556   5.5263
   4.3333   4.2424   4.1667   4.1026   4.0476   4.0000   3.9583   3.9216   3.8889   3.8596
  ---------------------------------------------------------------------------------------------------------------
   1.5000   1.4091   1.3333   1.2692   1.2143   1.1667   1.1250   1.0882   1.0556   1.0263
  Column 21
     Inf
  10.5000
   5.5000
   3.8333
   ----------
   1.0000
>> surf(X,Y,Z,gradient(Z))
```

Similarly, to the case already discussed, as seen in Figure 3.20, **the D-Partitioning plane divides the entire space for the case of simultaneous variation of three system's parameters into a stability space D(0), and an instability space D(1).**

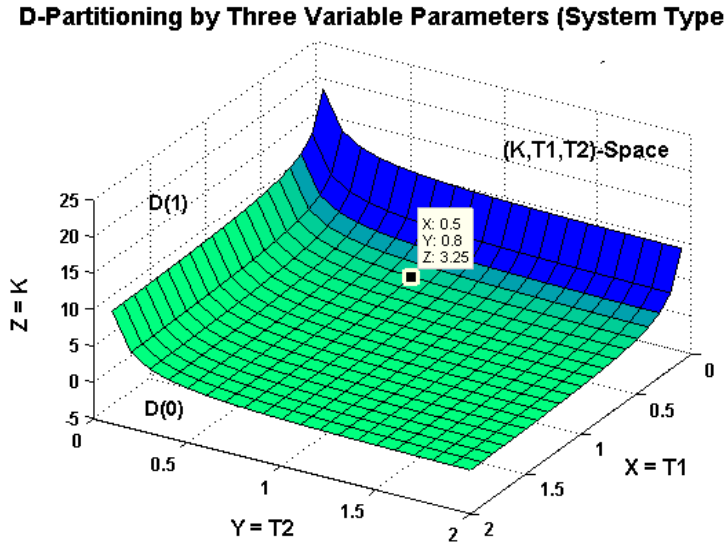

Figure 3.20: *D-Partitioning in terms of Three Variable Parameters (System Type 1)*

From the data corresponding to the point, chosen on the D-Partitioning plane, the interpretation is that if the system gain is $K = Z = 3.25$, the marginal values of two variable time-constants are correspondingly $T_1 = X = 0.5$ sec and $T_2 = Y = 0.8$ sec. These results are confirmed, if substituted in equation (3.72). When the gain is set to

$K = Z = 3.25$ and if any of the time-constants values are exceeded, like $T_1 > 0.5$ sec, or $T_2 > 0.8$ sec, the system becomes unstable. This interaction will be reflected for any other combination of the three variable system parameters. It is also acknowledged that again **any point of the D-Partitioning plane represents the marginal values of the three simultaneously variable parameters, considered as advancement and innovation in the theory of control systems stability analysis.**

3.5. Advanced D-Partitioning: A Case of Higher Order Minimum Phase System with Variable Parameters

The D-Partitioning analysis can be introduced as a direct method for visualizing the performance of power systems subjected to load changes. In Automatic Generation Control (AGC) schemes [69], D-Partitioning provides visually clearer stability limits. The method assumes a test power system of known parameters embedding distributed solar power generation. For the purposes of illustrating the D-Partitioning method, a functional (AGC) test power system is adopted. Its transfer function is shown in equation (73), based on the test AGC system parameters' values:

$B = 7$	Integral controller gain
$K = 20$ (variable)	System's controller gain
$D = 0.8$	Frequency-dependent load coefficient
$H = 5$ sec	System's inertia constant
$\Delta N_L(s)$	Change in system disturbance
$\tau_g = 0.2$ sec	Generator time constant
$\tau_T = 0.5$ sec	Turbine time constant
$\Delta\Omega(s)$	Change in frequency
$Q(s)$	Disturbance rejection

The test AGC system is a higher order minimum phase system with zeros [62]. Its transfer function is presented by equation (73). In this case, the system's controller gain K is variable parameter.

$$Q(s) = \frac{\Delta\Omega(s)}{-\Delta N_L(s)} = \frac{s(1+\tau_g s)(1+\tau_T s)}{s(D+2Hs)(1+\tau_g s)(1+\tau_T s) + B + Ks}$$
$$= \frac{0.1s^3 + 0.7s^2 + s}{s^4 + 7.08s^3 + 10.56s^2 + (K+0.8)s + 7} \quad (3.73)$$

Equations (3.74) and (3.75) represent the closed loop system transfer function and the system's characteristic equation accordingly

$$W(s)=\frac{Q(s)}{1+Q(s)}=\frac{\dfrac{0.1s^3+0.7s^2+s}{s^4+7.08s^3+10.56s^2+(K+0.8)s+7}}{1+\dfrac{0.1s^3+0.7s^2+s}{s^4+7.08s^3+10.56s^2+(K+0.8)s+7}}= \tag{3.74}$$

$$=\frac{0.1s^3+0.7s^2+s}{s^4+7.18s^3+11.26s^2+1.8s+Ks+7}$$

$$G(s)=s^4+7.18s^3+11.26s^2+1.8s+Ks+7=0 \tag{3.75}$$

From the characteristic equation of the system, an equation in terms of the variable *K* is derived as follows:

$$K(s)=-\frac{s^4+7.18s^3+11.26s^2+1.8s+7}{s} \tag{3.76}$$

The D-Partitioning in terms of the variable parameter *K*, as seen from Figure 3.10, is obtained with the aid of the MATLAB code as shown below:

```
>> K=tf([1 7.18 11.26 1.8 7],[1 0])

Transfer function:
s^4 + 7.18 s^3 + 11.26 s^2 + 1.8 s + 7
---------------------------------------
                S

>> dpartition(K)
```

The system will be stable only within the *Region of Stability.* It is always on the left-hand side of the D-Partitioning curve that is obtained by increasing the frequency and observing the Cauchy principle. Since *K* may obtain only real values, the system will be stable only within the range 2.81 < K < 73.7.

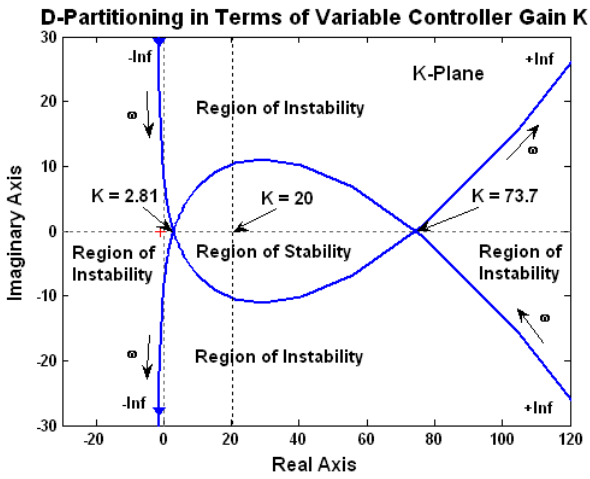

Figure 3.21: *D-Partitioning in terms of Variable K (Higher Order Minimum Phase System with zeros)*

As seen from the initial statement, the system's controller gain is to be set at $K = 20$ that is within the region of stability established by the D-Partitioning analysis. The system's marginal performance is tested at $K = 73.7$.

```
>> Q=tf([0.1 0.7 1],
        [1 7.08 10.26 74.5 7])

Transfer function:
     0.1 s^2 + 0.7 s + 1
-----------------------------------------
s^4 + 7.08 s^3 + 10.26 s^2 + 74.5 s + 7

>> margin(Q)
GM=0.00742, PM=-0.00558
```

It is seen from the test that both the Gain margin (Gm) and the Phase margin (Pm) are very low values at *K* = 73.7, proving the outcome of the D-Partitioning analysis.

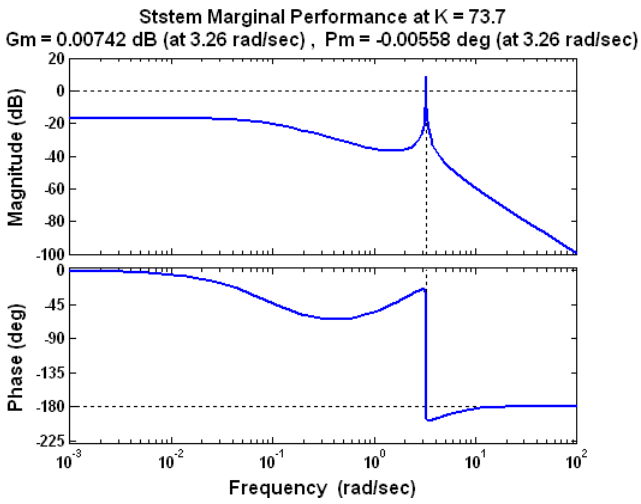

Figure 3.22: *Marginal Performance at K = 73.7*

3.6. Comparison of the Achieved Advanced D-Partitioning Analysis with other well-known Methods

3.6.1 Comparison of the D-Partitioning with the Routh-Hurwitz Stability Criterion

The results from the achieved advanced D-Partitioning analysis can be compared with results obtained by applying the Routh-Hurwitz stability criterion [36].

As an example, the case of the **cruise control system** can be examined for stability. From the equations (3.8) and (3.9), it is seen that **the system gain is 0.02*K***, while ***K* is considered as the variable gain factor**. Its open loop transfer function is:

$$G_O(s) = \frac{1000K}{s^3 + 160s^2 + 6500s + 50000} \tag{3.77}$$

The characteristic equation of the system is:

$$G(s) = s^3 + 160\,s^2 + 6500\,s + 50000 + 1000\,K \qquad (3.78)$$

To apply the Routh-Hurwitz stability criterion, the following table is created:

Table 3.1

Routh-Hurwitz Stability Criterion (Variable Gain *K*)

s^3	1	6500	0
s^2	160	$50000 + 1000K$	0
s^1	b_1	0	…
s^0	c_1	…	…

From where: $b_1 = \dfrac{160 \times 6500 - 1 \times (50000 + 1000K)}{160} \rangle 0$ or $K < 990$

Also: $c_1 = \dfrac{b_1 \times (50000 + 1000K) - 160 \times 0}{b_1} \rangle 0$ or $K > -50$

Finally, it is obvious that **the system is stable if the gain factor is within the limits –50 < *K* < 990, or the system's gain is within the limits –1 < 0.02*K* < 19.8.** These results confirm the results from the achieved advanced D-Partitioning analysis as shown in Figure 3.5b, presented for confirmation in Figure 3.23.

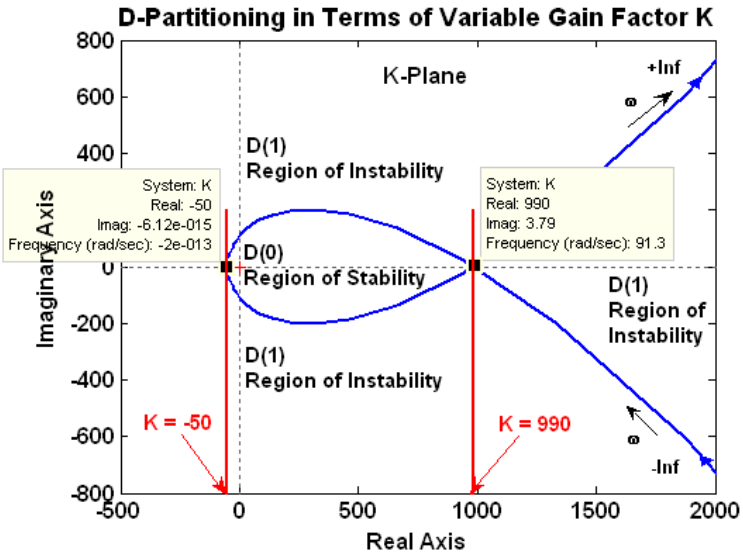

Figure 3.23: *D-Partitioning Analysis Confirming the Routh-Hurwitz Stability Criterion (Variable Gain Factor K)*

Further, the **armature-controlled dc motor with a type-driving mechanism** is taken into account, having **a variable time-constant *T.*** Its transfer function is:

$$G_o(s) = \frac{\omega_o}{\omega_e} = \frac{10}{0.4T_3 s^3 + (1.3T_3 + 0.4)s^2 + (T_3 + 1.3)s + 1} \tag{3.79}$$

Its characteristic equation is:

$$G(s) = 0.4T_3 s^3 + (1.3T_3 + 0.4)s^2 + (T_3 + 1.3)s + 11 \tag{3.80}$$

To apply the Routh-Hurwitz stability criterion, the following table is created:

Table 3.2

Routh-Hurwitz Stability Criterion (Time-Constant *T*)

s^3	$0.4T_3$	$T_3 + 1.3$	0
s^2	$1.3T_3 + 0.4$	11	0
s^1	b_1	0	…
s^0	c_1	…	…

where

$$b_1 = \frac{(1.3T_3 + 0.4) \times (T_3 + 1.3) - 0.4T_3 \times 11}{(1.3T_3 + 0.4)} \rangle 0 \quad \text{or } T_3 > 1.5 \text{ and } T_3 < 0.265$$

$$c_1 = \frac{b_1 \times 11 - (1.3T_3 + 0.4) \times 0}{b_1} \rangle 0$$

It is evident that the system is stable if $T_3 <$ 0.265 sec and $T_3 >$ 1.5 sec. These results verify the results from the advanced D-Partitioning analysis as revealed in Figure 3.12, shown for confirmation in Figure 3.24.

Although the **Routh-Hurwitz stability criterion** can be useful for determining the marginal values of system variable parameters of different nature, **it has considerable disadvantages**, especially in cases of higher order systems. It is also **inconclusive** in the case of the system with variable time-constant since it is not confirming that the system will be actually stable within the range 0 sec < T_3 < 0.265 sec.

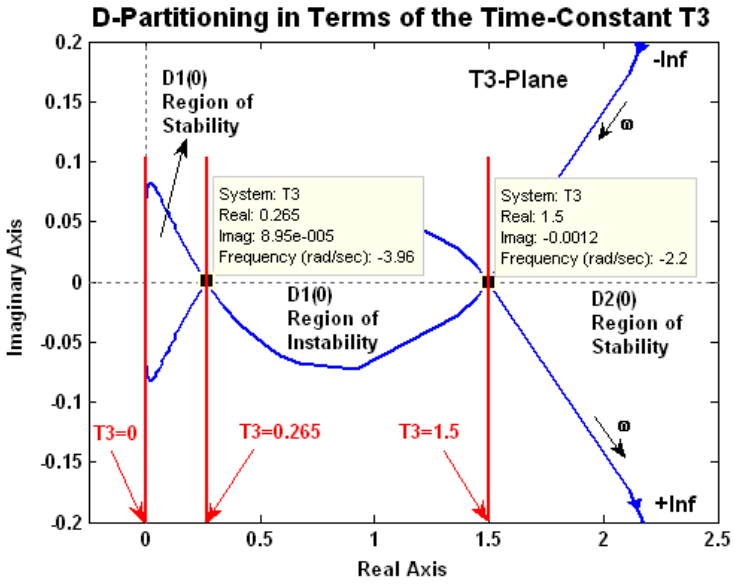

Figure 3.24: *D-Partitioning Analysis Confirming the Routh-Hurwitz Stability Criterion (Variable Time-Constant T)*

Further, the **Routh-Hurwitz stability test cannot be used in case of systems with multivariable parameters,** since **it cannot determine the marginal values of more than one system variable parameter. The Routh-Hurwitz stability criterion does not offer any graphical display visualizing its results.**

Alternatively, the achieved in this research advanced **D-Partitioning analysis has considerable advantages**, compared with the Routh-Hurwitz stability criterion. Due to the methodology of applying an interactive MATLAB procedure, **the D-Partitioning analysis can be applied successfully for higher order systems, obtaining the results of the marginal values of more than one system variable parameter with insignificant effort.** The **transparent graphical display** of the regions of stability is considered **as another significant advantage** of the D-Partitioning. **The exact marginal values of the multivariable parameters can be easily obtained** with the aid of an interactive MATLAB procedure on the D-Partitioning curve.

3.6.2 Comparison of the Achieved Advanced D-Partitioning Analysis with the Kharitonov's Theorem Assessment

The Kharitonov's Theorem assessment is applicable in the cases when **the variation of the system's uncertain parameters is defined within specific limits** [37].

If again the system of the **armature-controlled dc motor with a type-driving mechanism** is examined, its characteristic equation is considered as an interval polynomial, while its variable parameters K and T_3 are defined within specific limits of variation. To demonstrate the application of the Kharitonov's Theorem assessment of the system's stability, two cases are presented as follows:

Case 1: The characteristic interval polynomial, shown in equation (3.81) is the family of all polynomials:

$$P_1(s) = K + 1 + (T_3 + 1.3)s + (1.3T_3 + 0.4)s^2 + 0.4T_3 s^3 \qquad (3.81)$$

$K \in [8,10]$, or $8 < K < 10$ and $T_3 \in [1,2]$, or $1 \text{ sec} < T_3 < 2 \text{ sec}$

The interval polynomial $P_1(s)$ is stable, (i.e. all members of the family are stable) if and only if the four so-called **Kharitonov polynomials** are stable:

$$\left.\begin{aligned} k_1(s) &= 10 + 1 + (1 + 1.3)s + (1.3 + 0.4)s^2 + 0.4s^3 \\ k_2(s) &= 10 + 1 + (2 + 1.3)s + (1.3 \times 2 + 0.4)s^2 + 0.4 \times 2s^3 \\ k_3(s) &= 8 + 1 + (2 + 1.3)s + (1.3 \times 2 + 0.4)s^2 + 0.4 \times 2s^3 \\ k_4(s) &= 8 + 1 + (1 + 1.3)s + (1.3 + 0.4)s^2 + 0.4s^3 \end{aligned}\right\} \qquad (3.82)$$

After calculation, the Kharitonov polynomials are in the proper state for assessment:

$$\left.\begin{aligned} k_1(s) &= 27.5 + 5.75s + 4.25s^2 + s^3 \\ k_2(s) &= 13.75 + 4.125s + 3.75s^2 + s^3 \\ k_3(s) &= 11.25 + 4.125s + 3.75s^2 + s^3 \\ k_4(s) &= 22.5 + 5.75s + 4.25s^2 + s^3 \end{aligned}\right\} \qquad (3.83)$$

The **Routh-Hurwitz stability criterion** is applied to all these polynomials $k_i(s)$, $(i = 1, 2, 3, 4)$.

Table 3.3

Results from the Four Kharitonov Polynomials (Case 1)

$k_1(s)$		$k_2(s)$		$k_3(s)$		$k_4(s)$	
1	5.75	1	4.125	1	4.125	1	5.75
4.25	27.5	3.75	13.75	3.75	11.25	4.25	22.5
–0.7206		0.4583		1.125		0.4559	
27.5		13.75		11.25		22.5	

In this particular case, the first column of the Routh array for the three polynomials $k_2(s)$, $k_3(s)$ and $k_4(s)$ are all positive (that is, there is no change of sign in the first column). But **the polynomial $k_1(s)$ has change of sign in the first column of the Routh array.** This means that **the closed-loop system will be unstable for the given set of coefficients variations.**

Case 2: Even though the polynomial $k_1(s)$ in Table 3.3 have change of sign in the first column and one of the components of the Routh array is negative, its value is close to zero. This means that **the closed-loop system** is close to the state of **margin of stability**. If the set of parameter variations is changed, the closed-loop system may become stable. This is demonstrated with the following changes in the characteristic interval polynomial, shown in equation (3.84):

$$P_2(s) = K + 1 + (T_3 + 1.3)s + (1.3T_3 + 0.4)s^2 + 0.4T_3 s^3 \qquad (3.84)$$

$K \in [4,6]$, or $4 < K < 6$ and $T_3 \in [2,4]$, or $2 \text{ sec} < T_3 < 4 \text{ sec}$

The interval polynomial $P_2(s)$ is stable if and only if the four so-called **Kharitonov polynomials** are stable:

$$\left.\begin{aligned} k_1(s) &= 6 + 1 + (2 + 1.3)s + (1.3 \times 2 + 0.4)s^2 + 0.4 \times 2s^3 \\ k_2(s) &= 6 + 1 + (4 + 1.3)s + (1.3 \times 4 + 0.4)s^2 + 0.4 \times 4s^3 \\ k_3(s) &= 4 + 1 + (4 + 1.3)s + (1.3 \times 4 + 0.4)s^2 + 0.4 \times 4s^3 \\ k_4(s) &= 4 + 1 + (2 + 1.3)s + (1.3 \times 2 + 0.4)s^2 + 0.4 \times 2s^3 \end{aligned}\right\} \qquad (3.85)$$

After calculation, the Kharitonov polynomials are in the proper state for assessment:

$$\left.\begin{aligned} k_1(s) &= 8.75 + 2.875s + 3.75s^2 + s^3 \\ k_2(s) &= 4.375 + 3.3125s + 3.5s^2 + s^3 \\ k_3(s) &= 3.125 + 3.3125s + 3.5s^2 + s^3 \\ k_4(s) &= 6.25 + 2.875s + 3.75s^2 + s^3 \end{aligned}\right\} \quad (3.86)$$

Again the **Routh-Hurwitz stability criterion** is applied to all these polynomials $k_i(s)$, $(i = 1, 2, 3, 4)$, as follows in Table 3.4:

Table 3.4

Results from the Four Kharitonov Polynomials (Case 2)

$k_1(s)$		$k_2(s)$		$k_3(s)$		$k_4(s)$	
1	2.875	1	3.3125	1	3.3125	1	2.875
3.75	8.75	3.5	4.375	3.5	3.125	3.75	6.25
0.5416		2.0625		2.4196		1.2083	
8.75		4.375		3.125		6.25	

Since the first column of **each Kharitonov Polynomial contains no change in sign** and all its components are positive, the conclusion is that all of the roots of each $k_i(s)$, $(i = 1, 2, 3, 4)$ polynomial have negative real parts. Therefore the closed-loop control system is stable for all coefficient values in the specific ranges. **That is, the feedback control system is guaranteed asymptotically stable.**

The Kharitonov's Theorem assessment can be useful for determining system's stability in the cases of **variation of large number of the system's parameters when defined within specific limits**. At the same time this method has substantial **disadvantages. The method is short of determination of the parameter marginal values of stability, the results are achieved after considerable calculations and there is lack of any graphical display visualizing its results.** Also, the Kharitonov's assessment is applicable only for **a prearranged and specified set of parameter variations.**

The major disadvantage of the Kharitonov's Theorem assessment is that the Kharitonov polynomials deal with the coefficients variations of the Kharitonov characteristic interval polynomial, rather than directly with the system's parameter variations. The variations of the system's parameters remain in a hidden mode. These variations cannot be directly observed from the four Kharitonov polynomials.

Alternatively, the advanced **D-Partitioning analysis,** achieved in this research, **has considerable advantages**, compared with the Kharitonov's assessment. The advanced **D-Partitioning analysis does not need a specified set of limits of parameter variations. It is applicable generally and can deliver results representing the exact marginal values of the multivariable parameters.** The D-Partitioning analysis results are obtained easily with the aid of the interactive MATLAB procedure. The D-Partitioning curve in terms of the two variable parameters is plotted by the simple MATLAB code:

```
>> T = 0:0.1:5;
>> K = 3.25.*T+4.225+1.3./T
>> plot(T,K)
```

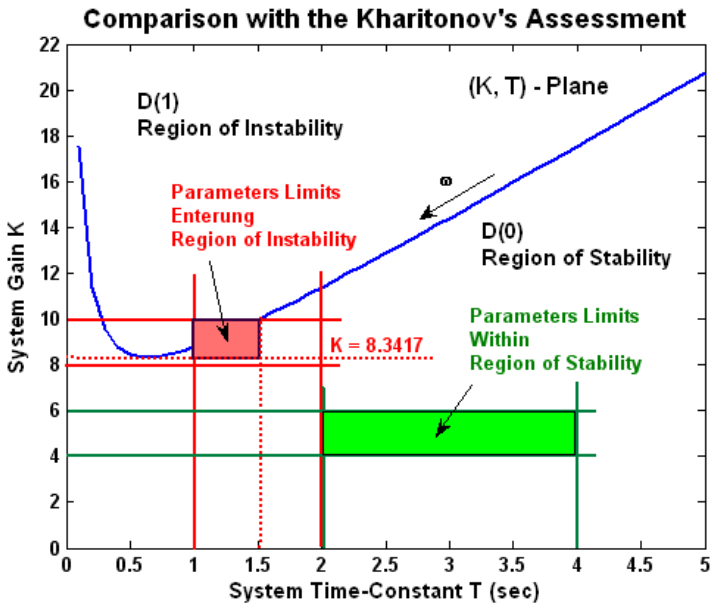

Figure 3.25: *Advanced D-Partitioning Analysis compared with the Kharitonov's Theorem Assessment in Terms of Two Simultaneously Variable Parameters (Demonstration of Stability Assessment for Case 1 and Case 2)*

The clear graphical display of the regions of stability is another significant advantage of the D-Partitioning. A graphical evaluation between the two methods of analysis is validating the considerable advantage of the achieved in this research D-Partitioning analysis compared with the Kharitonov's assessment. Both Case 1 and 2 of the Kharitonov's assessment are considered.

The graphical result is showing immediately the Region of Stability D(0) and the Region of Instability D(1) that can be used for the complete general assessment of the closed-loop system stability.

From Figure 3.25 it is obvious that if the two variables are within the limits $K \in$ [8,10], and $T_3 \in$ [1,2], **these parameter limits are entering the region of instability**. If the two variable parameters are within the limits $K \in$ [4,6] and $T_3 \in$ [2,4], **these parameters limits are entirely within the region of stability**.

This phenomenon is demonstrating the considerable advantage of the D-Partitioning analysis in comparison with the Kharitonov's assessment. By applying the D-Partitioning analysis and implementing a simple interactive MATLAB procedure, the system's **asymptotic stability** can be promptly determined and it can be graphically demonstrated, avoiding the significant calculations for the Kharitonov's assessment.

Each point on the D-Partitioning curve represents the marginal values of the two variable parameters, a property that is not offered by the Kharitonov's assessment. Also, by applying the D-Partitioning analysis, the system stability can be assessed immediately for any simultaneous variation of the two variable parameters without the need of determining the Kharitonov polynomials and calculating the values of the Routh array columns.

3.7. Summary on the Achieved Advanced D-Partitioning Method for Linear Control Systems

Founded on the D-Partitioning as suggested by the initial ideas of Neimark, presented in **Section 3.2**, further advancement of the method is achieved in terms of applying this analysis initially by one variable system parameter.

In **Section 3.3**, a new procedure is suggested aiming to obtain the D-Partitioning in terms of the variable system gain or time-constant. Based on the analysis of systems of Type 0 and Type 1 with a variable gain or a variable time-constant, the conclusion is that developed tool for obtaining the D-Partitioning curve can be used for both system types. The analysis is applicable for any continuous-time LTI system, represented by a transfer function having both poles and zeros [69,] [70], [71].

The D-Partitioning curve, plotted on the complex plane of the variable parameter, develops regions of stability and instability, showing a clear picture of the parameter limits of variation to keep the system stable.

In **Section 3.4,** the D-Partitioning analysis is further advanced for systems with multivariable parameters [67]. The system performance and stability for both system Type 0 and Type 1 is significantly dependent on the magnitude as well as the strong interaction between the variable parameters.

The pattern of the D-Partitioning in case two variable parameters of systems Type 0 is different from the one of systems Type 1. For a specific gain a system Type 0 may be stable for low and high time-constant values, but unstable for some mid-range time-constant values. The analysis of a system Type 1 is showing that the system may be stable for any value of the time-constant, below a specific border magnitude of the gain. Increasing the gain above this border magnitude, may still keep the system stability, but only for lower time-constant values.

The D-partitioning in case two variable parameters is demonstrating the strong interaction between the variable parameters. Also, each point of the D-Partitioning curve represents the marginal values of the two simultaneously variable parameters. This is a unique advancement and an innovation in the theory of control systems stability analysis.

The D-partitioning analysis by three variable parameters is achieved in the 3-D space and could be very useful for control system design [68]. For both systems, Type 0 and Type 1, the D-Partitioning plane divides the space of the variable parameters into a space of stability and a space of instability. The values of the three uncertain and interacting parameters can be determined by interactive MATLAB procedure, allowing moving a curser on the D-Partitioning plane.

The D-partitioning in case three variable parameters is indicative of the strong interaction between the variable parameters. Again, each point of the D-partitioning plane represents the marginal values of the three simultaneously variable parameters. This again is considered as a unique advancement and an innovation in the theory of control systems stability analysis.

For control systems with larger number of variable or uncertain parameters, the 3-D D-Partitioning analysis can be applied, if the parameters are grouped in essential sets of three and the interaction between the parameters and the groups is analysed.

Section 3.5 presents an advanced D-Partitioning for a case of higher order minimum phase system with variable parameters.

Finally, a comparison is suggested between the achieved in this research advanced D-Partitioning analysis and other well-known methods.

In Section 3.6.1, comparison with the Routh-Hurwitz Test is proving the advantages of the D-Partitioning analysis. The Routh-Hurwitz stability test is irrelevant for systems with multivariable parameters and it cannot determine the marginal values of more than one variable parameter. It does not offer graphical display its results.

In Section 3.6.2, comparison with the Kharitonov's Theorem Assessment is proving again the advantages of the D-Partitioning analysis. As discussed, the Kharitonov's assessment method cannot determine directly the parameter marginal values of stability. Also, the results for the stability assessment are achieved after considerable calculations and there is lack of any graphical display visualizing its outcome. The parameter variations cannot be directly observed from the four Kharitonov polynomials.

Chapter 4

DESIGN OF A ROBUST CONTROLLER

The approach to the controller design will be compensation with two degrees of freedom, enforcing the desired system performance. The design steps will be repeatedly demonstrated with some modifications for linear, digital and nonlinear control systems of Type 0 and Type 1. The controller will restrain the effects of parameters variations, disturbances and noise and improve system stability.

4.1 Meeting Specific Performance Criteria

Control systems usually require performance criteria that consider simultaneously the response error *e(t)* and the time *t* at which it occurs. A very useful criterion is the *Integral of Time multiplied by the Absolute value of Error (ITAE)** [8], [9], [69], [71]. As a decisive design factor, for the design strategy of a robust controller, the (ITAE) is considered as follows:

$$\mathrm{ITAE} = \int_0^\infty t\left|e(t)\right|dt \tag{4.1}$$

The minimum value of this integral is well definable as the system parameters are varied. Considering a second order system, **ITAE has a minimum if the damping ratio is $\zeta = 0.707$.** This value will be taken as a performance objective targeted by the proposed optimization design. **If a system is higher than the second order, a pair of dominant poles can represent the system dynamics. Then, ζ can still be used to indicate the location of these poles and the damping ratio is referred as the relative damping ratio of the system.**

* There are a number of known performances indices like: IAE, ISE, ITSE, ISTAE, ISTSE and ITAE. For a second order system, all of them are indicating that a damping ratio of $\zeta = 0.7$ corresponds to optimal or near optimal performance. Comparison between these performance indices reveals that the ITAE (*Integral of Time multiplied by the Absolute value of Error)* provides the best selectivity in the sense that the minimum value of the ITAE is apparent and most easily detectable as the system parameters are varied.

The relative damping is going to be considered as the required performance index (IP) of the system. Meeting the ITAE criterion, the following objectives should be targeted in the optimization design (ITAE) [67], [71]:

$$\left.\begin{array}{l} \zeta = 0.707 \\ PMO \leq 4\% \\ t_s / t_m \leq 2.5 \end{array}\right\} \tag{4.2}$$

where

PMO is Percentage Maximum Overshoot of the system's step response

t_s is settling time of the system's step response

t_m is the time to maximum overshoot of the system's step response

One of the solutions of meeting the ITAE is by implementing a robust controller consisting of several stages. With the aid of a series and a forward stage, the controller employs desired optimal dominant system poles, enforcing a desired system damping, stability and time response. For systems Type 0, additional integration ensures the system's steady-state error to become equal to zero.

4.2 Design of a Robust Controller for a System Type 1

4.2.1 Design of the Robust Controller Stages for a System Type 1

As an example for a design of a robust controller, the described in section 3.3.2.2 **solar-tracker control system** of Type 1 is considered. Taking into account equation (3.32), the open-loop transfer function of the suggested sun-tracker system is reflected as the plant transfer function G_{P1} (s) and is presented as:

$$G_{P1}(s) = \frac{K}{s(1+Ts)(1+0.005s)} = \frac{K}{0.005Ts^3 + (T+0.005)s^2 + s} \tag{4.3}$$

It is assumed that the system has two variable parameters which are the system's gain K and one of the system's time-constants T. To follow the design procedure, initially any one of the variables can be considered as a constant. At first the time-constant is set to its originally designed value of T = 0.02 sec, while K is let to be the variable. The robust controller, consisting of a series stage G_{S1}(s) and a forward

stage G_{F1}(s) is incorporated in the control system as shown in Figure 4.1. The following design steps are considered:

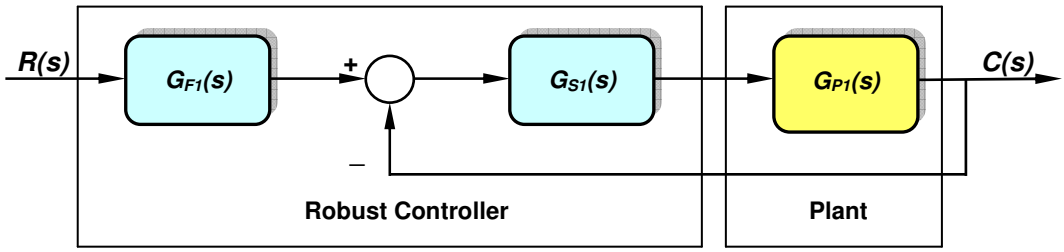

Figure 4.1: *Two-Step Robust Controller Incorporated in the Control System*

Step 1: The robust controller is going to be built on basis of the desired performance of the plant's closed-loop system. Then, initially the plant G_{P1} *(s)* as a stand-alone block, is involved in a unity feedback system. Its closed-loop transfer function $G_{CL1}(s)$ at T = 0.02 sec is presented as:

$$G_{CL1}(s) = \frac{K}{s(1+Ts)(1+0{,}005s)+K} = \\ = \frac{K}{0.005Ts^3+(T+0.005)s^2+s+K} = \frac{K}{0.0001s^3+0.025s^2+s+K} \tag{4.4}$$

Step 2: The strategy for constructing the series stage $G_{S1}(s)$ of the controller is to place its two zeros near the desired dominant closed-loop poles that satisfy the ITAE criterion. The reason for this is that **after applying the unity negative feedback to the cascade connection of $G_{S1}(s)$ and G_{P1} *(s)*, these zeros will appear as dominant poles of the closed-loop system** involving the plant and the series controller stage. In order to determine the optimal desired dominant closed-loop poles, it is important to establish the optimal value of the gain K corresponding to ζ = 0,707. This is established by plotting the relationship $\zeta = f(K)$ with the aid of the following code:

```
>>K=[15:0.01:25];
>> for n=1:length(K)
G_array(:,:,n)=tf([10000*K(n)],[1 250 10000 10000*K(n)]);
end
>> [y,z]=damp(G_array);
>> plot(K,z(1,:))
```

The optimal value of the gain that corresponds to relative damping ratio ζ = 0,707 is K = 19.82. It is determined with the aid of interactive MATLAB procedure, based on the plot $\zeta = f(K)$, as shown in Figure 4.2.

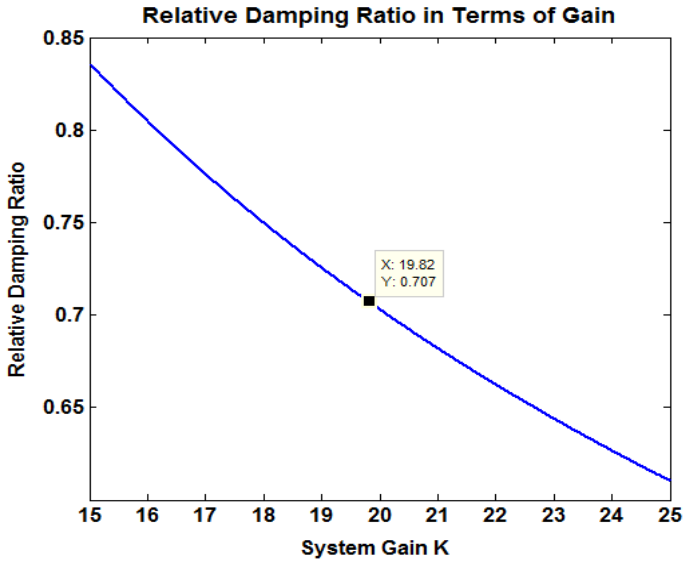

Figure 4.2: *Gain K = 19.82 Corresponding to Damping Ratio ζ = 0,707*

Step 3: If the optimal gain value *K* = 19.82 is substituted in equation (4.4), the transfer function of the closed-loop system is modified to:

$$G_{CL1}(s) = \frac{198200}{s^3 + 250s^2 + 10000s + 198200} \tag{4.5}$$

The following procedure is performed in order **to establish the desired closed-loop poles, corresponding to the optimal gain value *K* = 19.82.** It is determined from the code:

```
>> GCL1=tf([198200],[1 250 10000 198000])
>> damp(GCLo)
 Eigenvalue                  Damping      Freq. (rad/s)
 -2.19e+001 + 2.19e+001i     7.07e-001    3.10e+001
 -2.19e+001 - 2.19e+001i     7.07e-001    3.10e+001
 -2.06e+002                  1.00e+000    2.06e+002
```

Ii is seen from the code that the desired closed-loop poles are –21.9 ± j21.9.

Step 4: The desired closed-loop poles can be approximated to –22 ± j22 and are placed as zeros to the series controller stage $G_{S1}(s)$. **These zeros will appear as dominant poles of the closed-loop system** involving the plant and the series stage $G_{S1}(s)$.The transfer function of the series robust controller $G_{S1}(s)$ is presented as:

$$G_{S1}(s) = \frac{(s+22+j22)(s+22-j22)}{968} = \frac{s^2+44s+968}{968} \tag{4.6}$$

Step 5: To realize physically the $G_{S1}(s)$, two remote poles at $s_{1,2}$ = (–1250, j0) can be added with negligible effect on the system performance. To simplify the analysis, the transfer function of the cascade connection of the series controller stage and the plant will still be determined by implementing the equations (4.6) as follows:

$$\begin{aligned} G_{OL1}(s) = G_{S1}(s)G_{P1}(s) &= \frac{0.001K(s^2+44s+968)}{0.005Ts^3+(T+0.005)s^2+s} = \\ &= \frac{0.001K(s^2+44s+968)}{0.0001s^3+0.025s^2+s} \end{aligned} \tag{4.7}$$

Step 6: Then, if G_{OL1}(s) is involved in a unity feedback system, its closed-loop transfer function is determined as:

$$\begin{aligned} G_{CL1S}(s) &= \frac{0.001K(s^2+44s+968)}{0.005Ts^3+(T+0.005)s^2+s+0.001K(s^2+44s+968)} = \\ &= \frac{0.001K(s^2+44s+968)}{0.0001s^3+0.025s^2+s+0.001K(s^2+44s+968)} \end{aligned} \tag{4.8}$$

Step 7: As seen from the equation (4.8), the closed-loop zeros will attempt to cancel the closed loop poles of the system, being in their vicinity. To avoid this problem, a forward controller **G_{F1}(s) is added in cascade** to the closed-loop system G_{CL1S}, **with the purpose to cancel the zeros of G_{CL1S}.** Therefore, the transfer function of the forward controller is selected as follows:

$$G_{F1}(s) = \frac{968}{s^2+44s+968} \tag{4.9}$$

Step 8: Then, the transfer function of the total compensated system is determined as:

$$\left.\begin{aligned} G_{T1}(s) &= G_{F1}(s)G_{CL1S}(s) = \\ &= \frac{K}{0.005Ts^3+(T+0.005)s^2+s+0.001K(s^2+44s+968)} = \\ &= \frac{K}{0.0001s^3+0.025s^2+s+0.001K(s^2+44s+968)} \end{aligned}\right\} \tag{4.10}$$

4.2.3 D-Partitioning Analysis of the Robust Control System Type 1

To compare the system margin of stability before and after the robust compensation, the D-Partitioning in terms of the variable parameter *K* after the compensation can be determined from the characteristic equation of (4.10) based on the total system.

$$K = -\frac{0.0001s^3 + 0.025s^2 + s}{0.001s^2 + 0.044s + 1} \tag{4.11}$$

The D-Partitioning curve after the application of the robust compensation is plotted with aid of the code:

```
>> K = tf([-0.0001 -0.025 -1 0],[0.001 0.044 2])
>> dpartition(K)
```

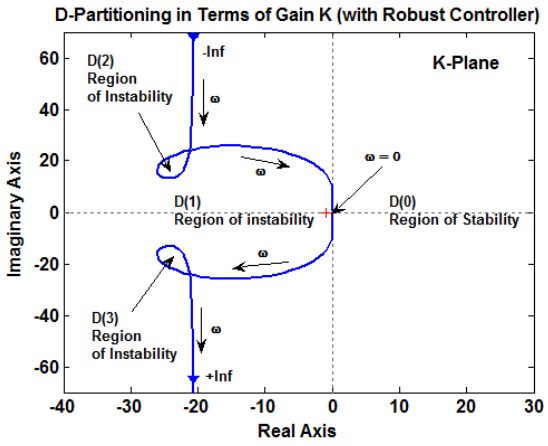

Figure 4.3: *D-Partitioning in Terms of the Gain K* ***after the Robust Compensation***

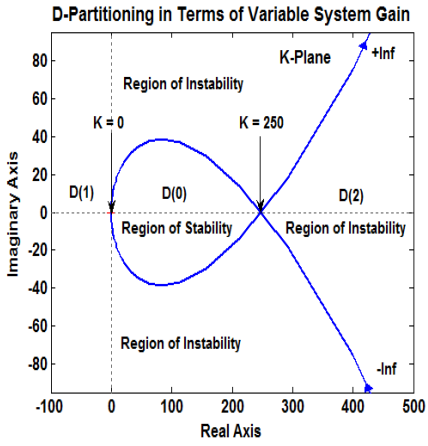

Figure 4.4: *D-Partitioning in Terms of the Gain K* ***before the Robust Compensation***

As seen from Figure 4.3, the D-Partitioning determines four regions of the *K*-plane: D(0), D(1), D(2) and D(3). Only D(0) is the region of stability, being always on the left-hand side of the D-Partitioning curve for a frequency variation from $-\infty$ to $+\infty$.

By comparing Figure 4.3 and Figure 4.4, it is seen that **the robust controller has improved considerably the margin of stability of the compensated system.** While the original system becomes marginal at K = 250, it is seen that after the robust compensation, the system will be stable for any positive values of the gain, or $K > 0$, all these positive values being in the region D(0).

4.2.3 Robust Performance Assessment of the Compensated System Type 1

Consideration of the system's transient responses is used for the analysis and comparison of the system robustness before and after the compensation. The system's transient responses before the robust compensation for different values of the gain within the region of the system's stability, K = 20, 50 and 100, are determined by taking into account the characteristic equation (4.3) of the original plant, where T = 0.02 sec. The following code is applied:

```
>> Gp120=tf([0 20],[0.0001 0.025 1 0])
>> Gp150=tf([0 50],[0.0001 0.025 1 0])
>> Gp1100=tf([0 100],[0.0001 0.025 1 0])
>> Gp1fb20=feedback(Gp120,1)
>> Gp1fb50=feedback(Gp150,1)
>> Gp1fb100=feedback(Gp1100,1)
>> step(Gp1fb20,Gp1fb50,Gp1fb100)
```

The compensated system is examined for robustness considering the system's transient responses, by substituting random even higher values for the system's gain, K = 100, K = 200, K = 500, in the equation of the transfer function (4.10), corresponding to the compensated robust system:

$$G_{T1}(s)_{K\,=\,100} = \frac{100}{0.0001\,s^3 + 0.125\,s^2 + 5.4s + 96.8} \tag{4.12}$$

$$G_{T1}(s)_{K\,=\,200} = \frac{200}{0.0001s^3 + 0.225s^2 + 9.8s + 193.6} \tag{4.13}$$

$$G_{T1}(s)_{K\,=\,500} = \frac{500}{0.0001s^3 + 0.525s^2 + 23s + 484} \tag{4.14}$$

The transient responses of the system Type 1 for the three different cases of the gain variation are determined by the code:

```
>> GT100 = tf([100], [0.0001 0.125 5.4 96.8])
>> GT200 = tf([200],[0.0001 0.225 9.8 193.6])
>> GT500 = tf([500], [0.0001 0.525 23 484])
 >> step(GT100,GT200,GT500)
```

Taking into account the codes shown above, the system's transient responses achieved after and before the robust compensation are reflected accordingly in Figure 4.5 and 4.6:

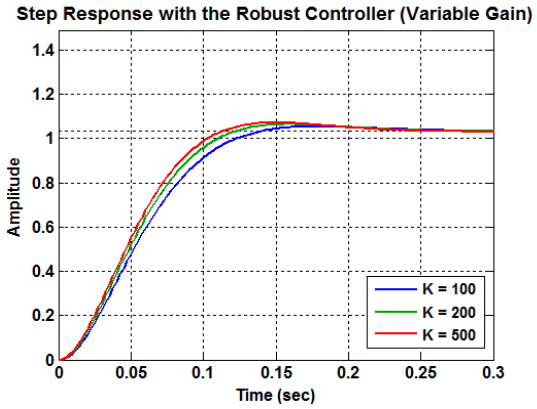

Figure 4.5*: Transient Responses of the* ***Robust*** *Control System of Type 1* ***after the Robust Compensation*** *(K = 100, K = 200, K = 500)*

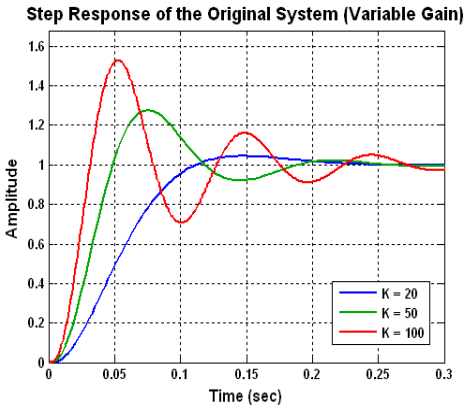

Figure 4.6: *Transient Responses of the* ***Original*** *Control System of Type 1* ***before the Robust Compensation*** *(K = 20, K = 50, K = 100)*

As seen from Figure 4.5, due to the effect of the applied robust controller, the system becomes quite insensitive to considerable variation of the gain *K*. Further experiments of the robust system with gain variation within the limits $0.5K < K < 5K$ prove that the system is still quite insensitive to variations of the gain *K*.

Since the considered system is with two variable parameters, now the time-constant is altered, as follows: T = 0.001 sec, T = 0.02 sec, T = 0.08 sec, while keeping the system's gain at K = 200. Initially these values are substituted in equation (4.3) that is the transfer function of the original system as follows:

```
>> Gp1001=tf([0 200],[0.000005 0.006 1 0])
>> Gp102=tf([0 200],[0.0001 0.025 1 0])
>> Gp108=tf([0 200],[0.0004 0.085 1 0])
>> Gp1fb001=feedback(Gp1001,1)
>> Gp1fb02=feedback(Gp102,1)
>> Gp1fb08=feedback(Gp108,1)
>> step(Gp1fb001,Gp1fb02,Gp1fb08)
```

Further, the values T = 0.001 sec, T = 0.02 sec, T = 0.08 sec and K = 100 are substituted in equation (4.10) of the robust compensated system:

$$G_{T1}(s)_{T\,=\,0.001} = \frac{200}{0.000005\ s^3 + 0.306\,s^2 + 14.2s + 193.6} \tag{4.15}$$

$$G_{T1}(s)_{T\,=\,0.02} = \frac{200}{0.0001\,s^3 + 0.325\,s^2 + 14.2s + 193.6} \tag{4.16}$$

$$G_{T1}(s)_{T\,=\,0.08} = \frac{200}{0.0004\,s^3 + 0.385\,s^2 + 14.2s + 193.6} \tag{4.17}$$

The transient responses of the compensated robust control system of Type 1 for the three different cases representing the time constant variation are determined by the code:

```
>> GT0001 = tf([200],[0.000005 0.306 14.2 193.6])
>> GT002 = tf([200], [0.0001 0.325 14.2 193.6])
>> GT008 = tf([200],[0.0004 0.385 14.2 193.6])
>> step(GT0001,GT002,GT008)
```

The comparison of the system robustness after and before the compensation is reflected in Figure 4.7 and 4.8:

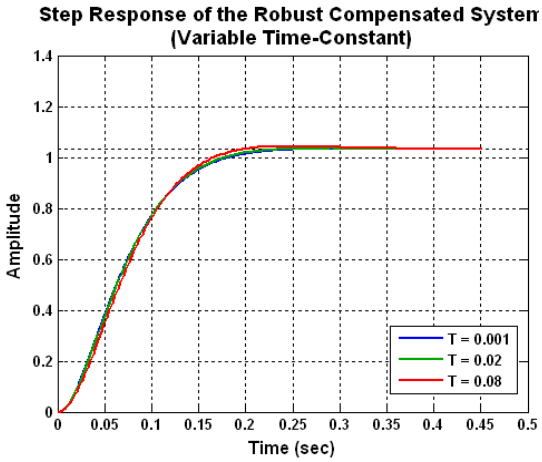

Figure 4.7: *Transient Responses of the System Type 1* ***after*** ***the Robust Compensation*** *(T = 0.001 sec, T = 0.02 sec, T = 0.08 sec at K = 200)*

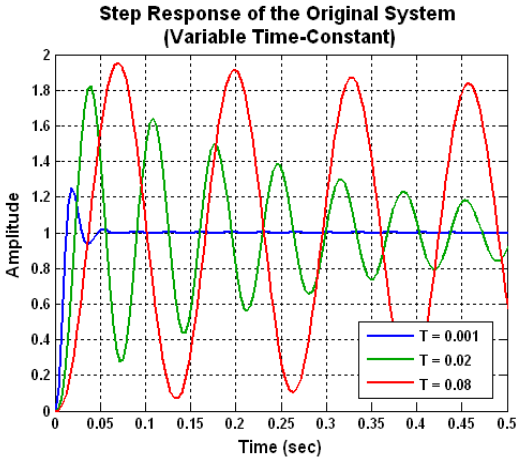

Figure 4.8: *Step Responses of the Original System Type 1* ***before*** ***the Robust Compensation*** *(T = 0.001 sec, T = 0.02 sec, T = 0.08 sec at K = 200)*

As seen from Figure 4.7, the compensated robust control system is quite insensitive to considerable variation of the time constant *T*. Experiments with the time constant

variation within the limits $0.1T < T < 10T$, after the application of the robust controller, demonstrate that the system is still quite insensitive to variations of the time constant.

To assess the system's performance after the application of the robust controller, an average system case is chosen with K = 300 and T = 0.02 sec. This case will differ insignificantly from the other cases of the discussed variable K and T. The performance evaluation is accomplished by the following code:

```
>> GT002 = tf([300],[0.0001 0.325 14.2 290.4])
>> damp(GT002)
```

Eigenvalue	Damping	Freq. (rad/s)
-2.20e+001 + 2.05e+001i	7.31e-001	3.01e+001
-2.20e+001 - 2.05e+001i	7.31e-001	3.01e+001
-3.21e+003	1.00e+000	3.21e+003

It is seen from the results that the system's relative damping ratio is ζ = 0.731, being insignificantly different from the objective ζ = 0.707.

The system's Percentage Maximum Overshoot (PMO) is determined by substituting the determined value of the relative damping ratio ζ = 0.731 in the following equation:

$$PMO = 100e^{-\pi\varsigma/\sqrt{1-\varsigma^2}} = 3.472\% \tag{4.18}$$

The system's settling time (t_S) is defined as the time required for the step response to be brought within a specified percentage of its final value. For a specified limit of ±5% t_S is determined by substituting the obtained values of the relative damping ratio ζ = 0.731 and the natural frequency ω_n = 30.1 rad/sec as follows:

$$t_{S(5\%)} = \frac{4.6}{\varsigma\omega_n} = 0.209 \text{ sec} \tag{4.19}$$

The system's time to maximum overshoot and the time ratio are determined similarly as follows:

$$t_m = \frac{\pi}{\omega_n\sqrt{1-\varsigma^2}} = 0.153 \text{ sec} \tag{4.20}$$

$$t_{S(5\%)} / t_m = 1.366 \tag{4.21}$$

As seen from Table 4.1, all the achieved results are meeting the ITAE criterion, since they have values that match or are lower than the targeted objectives.

Table 4.1

Comparison between Objectives and Real Results (System Type 1)

Specifications	Objectives	Real Results	Consideration
ζ	= 0.707	= 0.731	Close Match
PMO	≤ 4%	= 3.472%	Better
$t_{s(5\%)}/t_m$	≤ 2.5	= 1.366	Better

The performance evaluation results of t_S and t_m are also confirmed by the system step response determined in the time domain.

4.3 Design of a Robust Controller for a System Type 0

4.3.1 Design of the Robust Controller Stages (System Type 0)

As an example for a design of a robust controller, the **armature-controlled dc motor and a type-driving mechanism** system of Type 0 is considered. Taking into account equation (3.28), the open-loop transfer function of the suggested system is considered as the plant transfer function $G_{P0}(s)$ and is presented in equation (4.22). The system is with two variable parameters, that are the system's gain K and time-constant T. Initially, it is suggested that the gain is set to K = 10, while T is variable.

$$G_{PO}(s) = \frac{K}{(1+Ts)(1+0.5s)(1+0.8s)} = \frac{K}{0.4Ts^3 + (1.3T+0.4)s^2 + (1.3+T)s + 1} \quad (4.22)$$

The robust controller consists of a series stage G_{S0}(s), a forward stage G_{F0}(s). An integrating stage G_{I0}(s) is also included in the controller as seen from Figure 4.7.

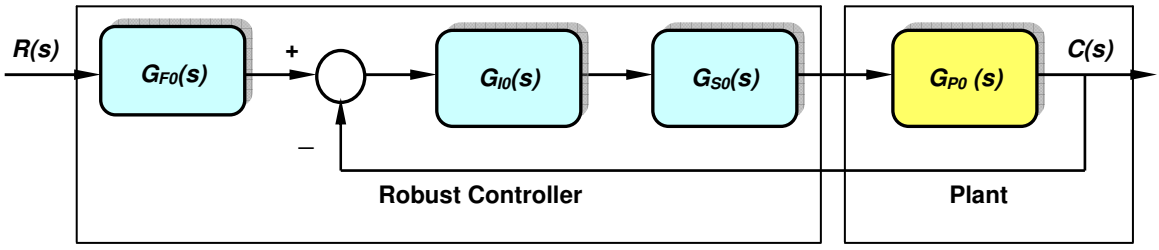

Figure 4.9: *Robust Controller and Integration Incorporated in the Control System*

Similar design steps are considered:

Step 1: A unity feedback system of the G_{P0} (s) as a standalone plant is having a closed-loop transfer function presented as:

$$\left.\begin{aligned} G_{CLO}(s) &= \frac{K}{(1+Ts)(1+0.5s)(1+0.8s)+K} = \\ &= \frac{K}{0.4Ts^3+(1.3T+0.4)s^2+(1.3+T)s+1+K} \end{aligned}\right\} \qquad (4.23)$$

Step 2: A similar to systems Type 1 design strategy for constructing the series stage of the controller is applied. It has the task to place its two zeros near the desired dominant closed-loop poles, that satisfy the condition $\zeta = 0.707$. The reason for this is that **after applying the unity negative feedback to the cascade connection of $G_{S0}(s)$, $G_{I0}(s)$ and $G_{P1}(s)$, these zeros will appear as dominant poles of the closed-loop system** involving the series controller stage, the integrator and the plant. If $K = 10$, the optimal value of the time-constant T corresponding to the relative damping ratio $\zeta = 0{,}707$ of the closed-loop system, is determined by the code:

```
>> T=[20:0.01:35];
>> for n=1:length(T)
G_array(:,:,n)=tf([10],[0.4*T(n) (1.3*T(n)+0.4) (1.3+T(n)) 11]);
end
>> [y,z]=damp(G_array);
>> [y,z]=damp(G_array);
>> plot(T,z(1,:))
```

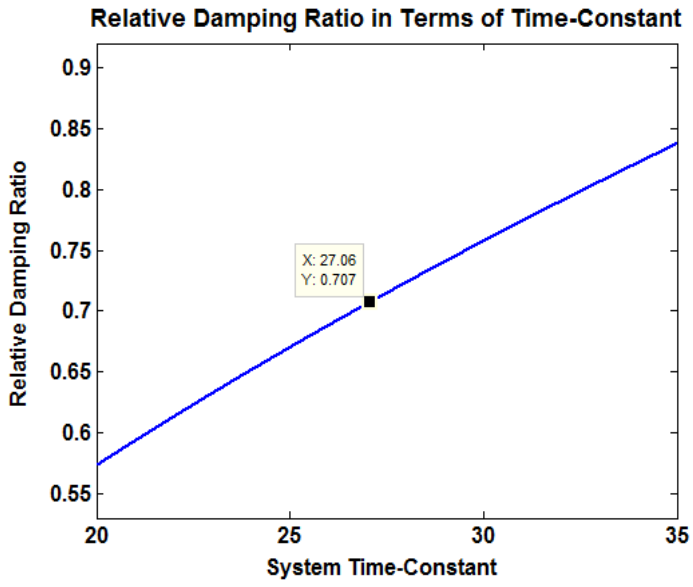

Figure 4.10: *Time-Constant Corresponding to Relative Damping Ratio $\zeta = 0{,}707$*

As seen from Figure 4.8, the relative damping ratio becomes ζ = 0.707 if the time-constant is tuned to T = 27.06 sec.

Step 3: If the value of the time-constant T = 27.06 sec is substituted in equation (4.23), the transfer function of the closed-loop system is modified to:

$$G_{CLO}(s) = \frac{10}{10.824s^3 + 35.578s^2 + 28.36s + 11} \tag{4.24}$$

The assessment of the system proves that the relative damping ratio becomes ζ = 0.707, when the time-constant is T = 27.06 sec, resulting in system's desired closed-loop poles –0.466 ± j0.466. These outcomes are determined from the code:

```
>> GCL0=tf([10],[10.824 35.578 28.36 11])
>> damp(GCL0)
```

Eigenvalue	Damping	Freq. (rad/s)
-4.64e-001 + 4.64e-001i	7.07e-001	6.56e-001
-4.64e-001 - 4.64e-001i	7.07e-001	6.56e-001
-2.36e+000	1.00e+000	2.36e+000

Step 4: Following the design strategy and after approximating of the pole values to –0.5 ± j0.5, the controller zeros can be placed also at –0.5 ± j0.5. Thus, the transfer function of the series robust controller $G_{S0}(s)$ is presented as:

$$G_{S0}(s) = \frac{(s + 0.5 + j0.5)(s + 0.5 - j0.5)}{0.5} = \frac{s^2 + s + 0.5}{0.5} \tag{4.25}$$

Step 5: Further, two poles at $s_{1,2}$ = –1250, j0 can be added to realize physically the $G_{S0}(s)$. They are with negligible effect on the system performance. An integrating stage G_{I0}(s) is added to eliminate the steady-state error of the system. It is connected in cascade with the series controller. To simplify the analysis, the transfer function of the compensated open-loop system will still be the one implementing the equations (4.22) and (4.25) and adding the integrator as follows:

$$G_{OL0}(s) = G_{I0}(s)G_{S0}(s)G_{P0}(s) = \frac{K(s^2 + s + 0.5)}{0.5s(1 + Ts)(1 + 0.5s)(1 + 0.8s)} \tag{4.26}$$

Step 6: When G_{OL0}(s) is involved in a unity feedback system, its closed-loop transfer function is determined as:

$$G_{CL0S}(s) = \frac{K(s^2 + s + 0.5)}{0.5s(1+Ts)(1+0.5s)(1+0.8s) + K(s^2 + s + 0.5)} \tag{4.27}$$

Step 7: It is seen from the equation (4.27) that the closed-loop zeros will attempt to cancel the closed loop poles of the system, since they are in their area. This problem can be avoided if a forward controller G_{F0}(s) is added to the closed-loop system, as shown in Figure 4.7. **The design of the forward controller is such, so that the poles of G_{F0}(s) cancel the zeros of the closed-loop transfer function G_{CL}(s).** For that reason, the transfer function of the forward controller is selected as follows:

$$G_{F0}(s) = \frac{0.5}{s^2 + s + 0.5} \tag{4.28}$$

Step 8: Finally, the transfer function of the total compensated system is derived considering the block diagram in Figure 4.7.

$$\left.\begin{aligned} G_{T0}(s) &= G_{F0}G_{CL0S}(s) = \\ &= \frac{K}{0.5s(1+Ts)(1+0.5s)(1+0.8s) + K(s^2 + s + 0.5)} = \\ &= \frac{K}{0.5s[0.4Ts^3 + (1.3T + 0.4)s^2 + (1.3 + T)s + 1] + K(s^2 + s + 0.5)} \\ &= \frac{K}{0.2Ts^4 + (0.65T + 0.2)s^3 + (0.65 + 0.5T)s^2 + 0.5s + K(s^2 + s + 0.5)} \end{aligned}\right\} \tag{4.29}$$

4.3.2 D-Partitioning Analysis of the Robust Control System Type 0

The D-Partitioning in terms of the variable time-constant T can be determined from the characteristic equation of (4.29) based on the total system. If K = 10, then:

$$T = -\frac{0.4s^3 + 21.3s^2 + 21s + 10}{0.4s^4 + 1.3s^3 + s^2} \tag{4.30}$$

The D-Partitioning obtained after the robust compensation is plotted by the code:

```
>> T = tf([-0.4 -21.3 -21 10],[0.4 1.3 1 0 0])
>> dpartition(T)
```

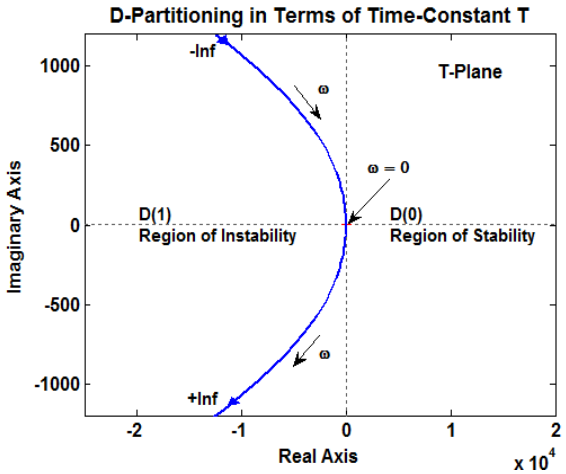

Figure 4.11: *D-Partitioning in Terms of the Time-Constant* ***after the Robust Compensation***

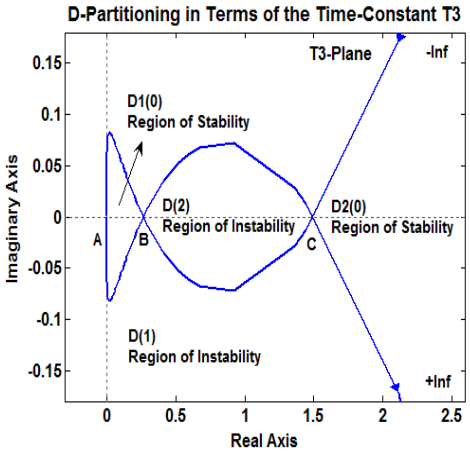

Figure 4.12: *D-Partitioning in Terms of the Time-Constant* ***before the Robust Compensation***

As seen from Figure 4.11, the D-Partitioning determines two regions in the complex *T*-Plane: D(0) and D(1). Only D(0) is a region of stability, since its position is on the left-hand side of the D-partitioning curve for the frequency variation from $-\infty$ to $+\infty$.

By comparing Figure 4.11 and Figure 4.12, it is seen that the robust controller has improved considerably the margin of stability of the compensated system. The original system is unstable between its marginal values T = 0.25sec and T = 1.5sec. **After the robust compensation, the system will be stable for any positive values of the time constant, or $T > 0$,** since then T is entirely within the region of stability D(0).

4.3.3 Robust Performance Assessment of the Compensated System Type 0

The applied robust compensation develops insensitivity of the system's stability with respect to changes of the system's time-constant T and gain K. For comparison of the system's insensitivity to time-constant variation before and after applying the robust compensation, initially at system gain K = 10 the values of the time-constant values of T = 0.1 sec and T = 2 sec are substituting the suggested in equation (4.22). A case of T = 0.8 sec, corresponds to the region of instability D(2) and definitely to an unstable control system. The transient responses of the original system, accordingly illustrated in Figure 4.13 and 4.14, are achieved by the following code:

```
>> Gp001=tf([0 10],[0.04 0.53 1.4 1])
>> Gp008=tf([0 10],[0.32 1.44 2.1 1])
>> Gp02=tf([0 10],[0.8 3 3.3 1])
>> Gp0fb001=feedback(Gp001,1)
>> Gp0fb02=feedback(Gp02,1)
>> step(Gp0fb001,Gp0fb02)
>> step(Gp0fb008)
```

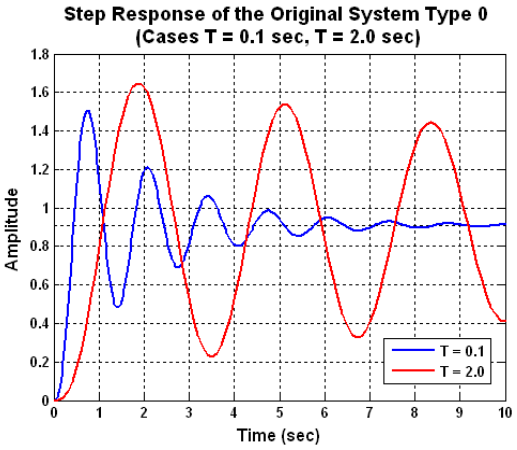

Figure 4.13: *Step Responses of the* ***Original*** *Control System Type 0 (T=0.1sec, T =2sec at K=10)*

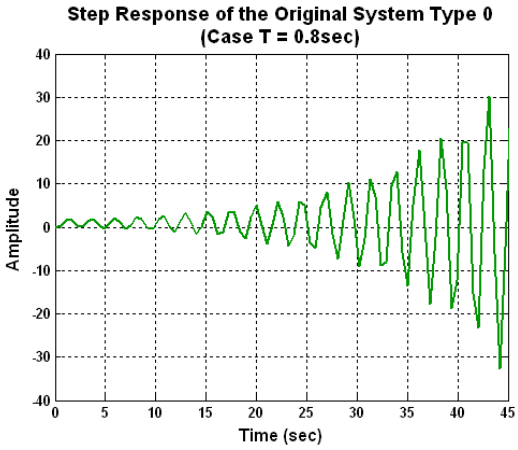

Figure 4.14: *Step Responses of the* ***Original*** *Control System Type 0 (T=0.8sec, at K=10)*

The total compensated system is also examined for robustness in the time-domain. Taking into consideration the same values of the time-constant, as those used for the assessment of the original system, T = 0.1 sec, T = 0.8 sec and T = 2 sec at system gain K = 10 and substituting them in equation (4.29), the following transfer functions are obtained:

$$G_{T0}(s)_{T\,=\,0.1} = \frac{10}{0.04s^4 + 0.53s^3 + 21.4s^2 + 21s + 10} \tag{4.31}$$

$$G_{T0}(s)_{T\,=\,0.8} = \frac{10}{0.32s^4 + 1.44s^3 + 22.1s^2 + 21s + 10} \tag{4.32}$$

$$G_{T0}(s)_{T\,=\,2} = \frac{10}{0.8s^4 + 3s^3 + 23.3s^2 + 21s + 10} \tag{4.33}$$

The step responses, representing the time-constant variation of the robust system Type 0, shown in Figure 4.15, are determined by the code:

```
>> GT01=tf([10],
          [0.04 0.53 21.4 21 10])
>> GT08=tf([10],
          [0.32 1.44 22.1 21 10])
>> GT20=tf([10],
          [0.8 3 23.3 21 10])
>> step(GT01,GT08,GT20)
```

As seen from Figure 4.13, due to the applied robust controller, the control system becomes quite insensitive to variation of the time-constant *T*. The step responses for cases of *T* = 0. 1 sec and *T* = 0. 8 sec and *T* = 2 sec coincide.

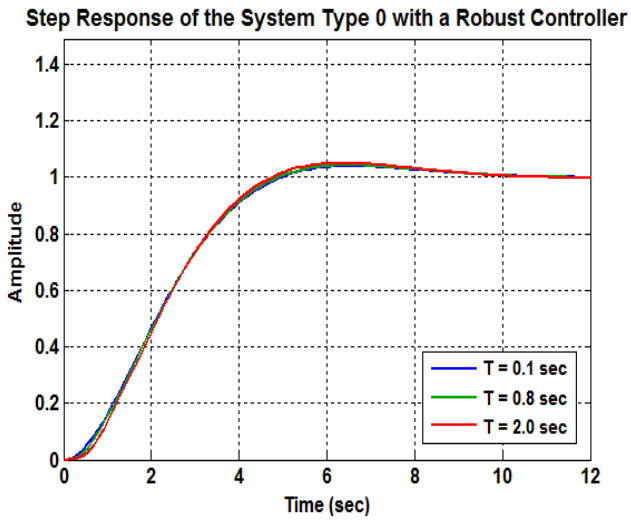

Figure 4.15*: Step Responses of the System Type 0* ***with a Robust Controller*** *(T = 0. 1 sec, T = 0. 8 sec, T = 2 sec at K = 10)*

Experiments with variation of the time constant within the limits $0.1T < T < 10T$, regarding the robust control system, make evident that the system becomes quite insensitive to variations of the time-constant.

Since the discussed system is with two variable parameters, now the gain will be altered, applying: $K = 5$, $K = 10$, $K = 20$, while keeping the system's time-constant at $T = 0.8$ sec. For comparison of the system's insensitivity to the gain variation before and after applying the robust compensation, initially the suggested values as shown above are substituted in equation (4.22). The transient responses of the original system are illustrated in Figure 4.16 and 4.17 and are achieved by the following code:

```
>> Gp05=tf([0 5],[0.32 1.44 2.1 1])
>> Gp010=tf([0 10],[0.32 1.44 2.1 1])
>> Gp020=tf([0 20],[0.32 1.44 2.1 1])
>> Gp0fb5=feedback(Gp05,1)
>> Gp0fb10=feedback(Gp010,1)
>> Gp0fb20=feedback(Gp020,1)
>> step(Gp0fb5,Gp0fb10,Gp0fb20)
>> step(Gp0fb5,Gp0fb10)
>> step(Gp0fb20)
```

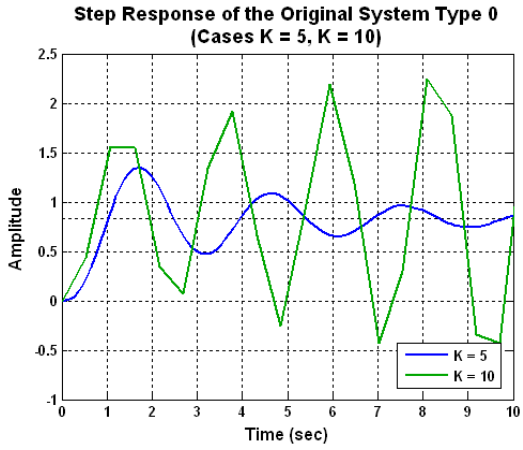

Figure 4.16*: Step Responses of the* ***Original*** *Control System Type 0 (K = 5, K = 10 at T = 0.8sec)*

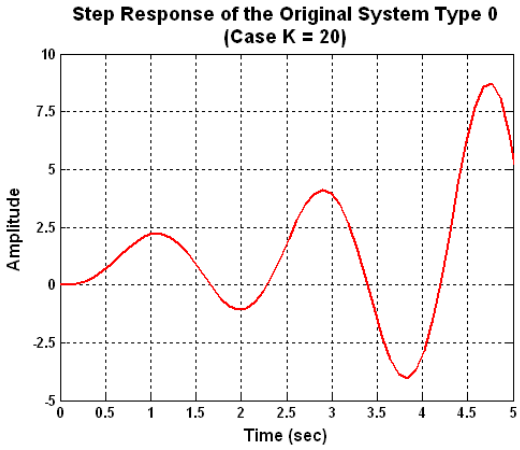

Figure 4.17*: Step Responses of the* ***Original*** *Control System Type 0 (K = 20 at T = 0.8sec)*

From Figures 4.16 and 4.17 it is obvious that the cases of K = 10 and K = 20, correspond to an unstable control system. Also, it is seen that for all transient response cases of the original control system Type 0 the steady-state error is $e_{ss} \neq 0$.

Next, the variable gain K = 5, K = 10, K = 20 will be applying to the robust compensated system, keeping the system's time-constant at T = 0.8 sec. These values are substituted in equation (4.29). As a result, the following outcomes are delivered:

$$G_{T0}(s)_{K=5} = \frac{5}{0.32s^4 + 1.44s^3 + 12.1s^2 + 11s + 5} \tag{4.34}$$

$$G_{T0}(s)_{K=10} = \frac{10}{0.32s^4 + 1.44s^3 + 22.1s^2 + 21s + 10} \tag{4.35}$$

$$G_{T0}(s)_{K=20} = \frac{20}{0.32s^4 + 1.44s^3 + 42.1s^2 + 41s + 20} \tag{4.36}$$

To compare the system robustness before and after the robust compensation, the step responses for the three different cases, representing the gain variation of the robust system Type 0, are plotted in Figure 4.18 with the aid of the code as shown below:

```
>> GTK5=tf([2.5],
        [0.16 0.72 6.05 5.5 2.5])
>> GTK10=tf([5],
        [0.16 0.72 11.05 10.5 5])
>> GTK20=tf([10],
        [0.16 0.72 21.05 20.5 10])
>> step(GTK5,GTK10,GTK20)
```

As a result of the applied robust controller, the control system becomes also quite insensitive to variation of the gain *K*. The step responses for the three cases are almost coinciding. For all transient response cases the steady-state error is $e_{ss} = 0$.

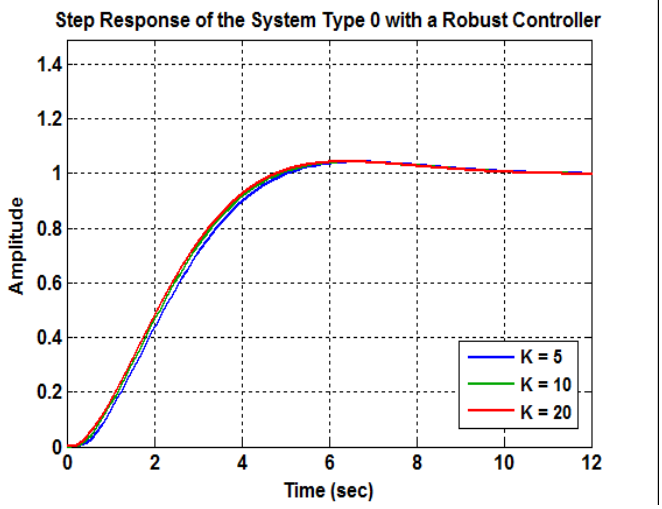

Figure 4.18: *Step Responses of the System Type 0* ***with the Robust Controller*** *(K = 5, K = 10, K = 20 at T = 0.8 sec)*

Testing with the gain variation within the limits $0.5K < K < 5K$, of the system with the robust controller, makes obvious that the system is quite insensitive to variations of the gain *K*. Insignificant step response difference is observed also if the experiment is repeated with the same variation of the gain, but with time-constants, different from T = 0.8 sec. Similarly the strategy of the robust controller design can be applied with the same effect, if initially the time-constant is fixed and the gain considered as a variable.

An average case is chosen with $K = 10$ and $T = 0.8$ sec for the assessment of the system's performance after the application of the robust controller. This case will differ insignificantly from the other cases of the discussed variable *K* and *T*. The performance evaluation is achieved by following code:

```
>> GT10=tf([10],[0.32 1.44 22.1 21 10])
>> damp(GT10)
```

Eigenvalue	Damping	Freq. (rad/s)
-4.91e-001 + 4.89e-001i	7.09e-001	6.93e-001
-4.91e-001 - 4.89e-001i	7.09e-001	6.93e-001
-1.76e+000 + 7.88e+000i	2.18e-001	8.07e+000
-1.76e+000 - 7.88e+000i	2.18e-001	8.07e+000

It is seen that the relative damping ratio enforced by the system's dominant poles is ζ = 0.709, being insignificantly different from the objective ζ = 0.707, due to the rounding of the desired system's poles from –0.466 ± j 0.466 to –0.5 ± j0.5, during the design procedure of the series controller stage.

The Percentage Maximum Overshoot (PMO) is determined by substituting the real value of the relative damping ratio ζ = 0.709 in the following equation:

$$PMO = 100e^{-\pi\varsigma/\sqrt{1-\varsigma^2}} = 3.98\% \tag{4.37}$$

The settling time t_S for specified limit of ±5% is determined by substituting the obtained values of the relative damping ratio ζ = 0.709 and the natural frequency ω_n = 0.693 rad/sec as follows:

$$t_{S(5\%)} = \frac{4.6}{\varsigma\omega_n} = 9.362 \text{ sec} \tag{4.38}$$

The system's time to maximum overshoot t_m is determined similarly as follows:

$$t_m = \frac{\pi}{\omega_n\sqrt{1-\varsigma^2}} = 6.425 \text{ sec} \tag{4.39}$$

The time ratio is determined as one of the objectives as follows:

$$t_{S(5\%)} / t_m = 1.457 \tag{4.40}$$

As seen from Table 4.2, all the achieved results are meeting the ITAE criterion, since they either match or have values lower than the targeted objectives.

Table 4.2

Comparison between Objectives and Real Results (System Type 0)

Specifications	Objectives	Real Results	Consideration
ζ	= 0.707	= 0.709	Close Match
PMO	≤ 4%	= 3.98%	Better
$t_{s(5\%)}/t_m$	≤ 2.5	= 1.457	Better

4.4 Robust System Sensitivity in Cases of Parameter Uncertainties

4.4.1 General Discussion on Sensitivity of a Robust Control System

The sensitivity interpretation of a system with respect to parameter variations can be easily achieved with the aid of the frequency-domain plots. A comparison between the sensitivity of the original and the compensated systems confirm the obtained results established in the time-domain, shown in sections 4.2 and 4.3. Initially, it is assumed that only the plant parameters uncertainties are affecting the system's output signal, while there are no disturbances *D(s)* and the noise *N(s)*, as seen in Figure 4.19. An integrator $G_I(s)$ can be included to eliminate the system's steady state error, in case of a plant of Type 0.

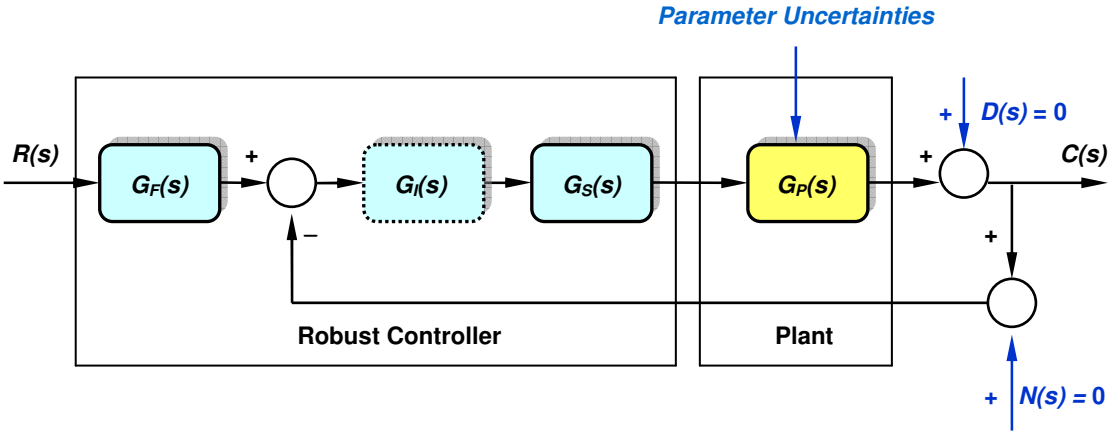

Figure 4.19: *Robust Controller Incorporated in the Control System (Type 0 or Type 1) Subjected to Parameters Uncertainties*

Taking into account that the original control systems of Type 0 and Type 1 with a unity feedback has a general transfer function of the type:

$$W(s) = \frac{G_P(s)}{1 + G_P(s)} \tag{4.41}$$

If taking into consideration **the variations of any of the parameters of the original open-loop system, represented by the plant transfer function $G_P(s)$,** the sensitivity of *W(s)* with respect to any variations of $G_P(s)$ is determined as follows [70], [71], [72], [73]:

$$S_G^W(s) = \frac{dW(s)/W(s)}{dG_P(s)/G_P(s)} = \frac{G_P(s)^{-1}}{1+G_P(s)^{-1}} = \frac{1}{1+G_P(s)} \tag{4.42}$$

The best sensitivity value is considered as $S_G^W(s) = 0$.

Generally, in addition to the regular performance criteria, a design criterion on sensitivity, modified in the frequency format, can be formulated in the following manner:

$$\left|S_G^W(j\omega)\right| = \left|\frac{G_P(j\omega)^{-1}}{1+G_P(j\omega)^{-1}}\right| = \left|\frac{1}{1+G_P(j\omega)}\right| \le k \tag{4.43}$$

where k is a positive real number [70], [71], [72], [73].

If $W_R(s)$ is the unity feedback transfer function involving the total robust compensated control system, the sensitivity of $W_R(s)$ with respect to any variations of any of the plant parameters is determined as follows:

$$S_{GT}^{WR}(s) = \frac{dW_R(s)/W_R(s)}{dG_{T1}(s)/G_{T1}(s)} = \frac{1}{1+G_{T1}(s)} \tag{4.44}$$

4.4.2 Sensitivity of a Robust Control System in Case of Parameter Uncertainties (Original System Type 0)

Initially, the system Type 0 with the transfer function described by equation (4.22) is considered and substituted it into (4.42), where T = 0.8 sec and K is variable. For the three different successive cases K = 5, K = 10 and K = 20, the sensitivities of $W(s)$ with respect to any variations of $G_{\odot}(s)$ of the original system are:

$$S_{G0\ Original\ \ K=5}^{W}(s) = \frac{0.32s^3 + 1.44s^2 + 2.1s + 1}{0.32s^3 + 1.44s^2 + 2.1s + 6} \tag{4.45}$$

$$S_{G0\ Original\ \ K=10}^{W}(s) = \frac{0.32s^3 + 1.44s^2 + 2.1s + 1}{0.32s^3 + 1.44s^2 + 2.1s + 11} \tag{4.46}$$

$$S_{G0\ Original\ \ K=20}^{W}(s) = \frac{0.32s^3 + 1.44s^2 + 2.1s + 1}{0.32s^3 + 1.44s^2 + 2.1s + 21} \tag{4.47}$$

Taking into account the total robust control system Type 0 described by equation (4.29) and substituting it in (4.44), the sensitivities of the robust control system for T = 0.8 sec and the cases K = 5, K = 10 and K = 20 are determined as:

$$S_{GT\,0\ Robust\ \ K=5}^{WR}(s) = \frac{0.32s^4 + 1.44s^3 + 12.1s^2 + 11s + 5}{0.32s^4 + 1.44s^3 + 12.1s^2 + 11s + 10} \tag{4.48}$$

$$S_{GT\,0\ Robust\ \ K=10}^{WR}(s) = \frac{0.32s^4 + 1.44s^3 + 22.1s^2 + 21s + 10}{0.32s^4 + 1.44s^3 + 22.1s^2 + 21s + 20} \tag{4.49}$$

$$S_{GT\,0\ Robust\ \ K=20}^{WR}(s) = \frac{0.32s^4 + 1.44s^3 + 42.1s^2 + 41s + 20}{0.32s^4 + 1.44s^3 + 42.1s^2 + 41s + 40} \tag{4.50}$$

For comparison of the system's sensitivity before and after the robust compensation,, the functions described by the equations (4.45), (4.46), (4.47) and (4.48), (4.49), (4.50) are plotted in the frequency domain as shown in Figure 4.20 with the aid of the following code:

```
>> G0OriginalK5=tf([0.32 1.44 2.1 1],[0.32 1.44 2.1 6])
>> G0OriginalK10=tf([0.32 1.44 2.1 1],[0.32 1.44 2.1 11])
>> G0OriginalK20=tf([0.32 1.44 2.1 1],[0.32 1.44 2.1 21])
>> GT0RobustK5=tf([0.32 1.44 12.1 11 5],[0.32 1.44 12.1 11 10])
>> GT0RobustK10=tf([0.32 1.44 22.1 21 10],[0.32 1.44 22.1 21 20])
>> GT0RobustK20=tf([0.32 1.44 42.1 41 20],[0.32 1.44 42.1 41 40])
>>bode(G0OriginalK5,G0OriginalK10,G0OriginalK20,GT0RobustK5,
GT0RobustK10,GT0RobustK20)
```

As seen from Figure 4.20, the sensitivities of the original system at different gains are $S_G^W(s) \geq 0\,\text{dB}$ in the range 2 rad/sec < ω < 10 rad/sec, reaching $S_G^W(s) = 21.6\,\text{dB}$ for the case K = 10. The sensitivity of the robust control system for the case of K = 5, coincide with the cases of K = 10 and K = 20. The sensitivity of the robust control systems at different gains is $S_{GT}^{WR}(s) \leq 0\,\text{dB}$ for ω < 1 rad/sec and ω > 8 rad/sec, while they are $S_{GT}^{WR}(s) \geq 0\,\text{dB}$, but with a negligible value in the range 1 rad/sec < ω < 8 rad/sec. Figure 4.20 shows that the robust system is with considerably lower sensitivity values compared with the original one, thus proving the system's robustness after applying the compensation.

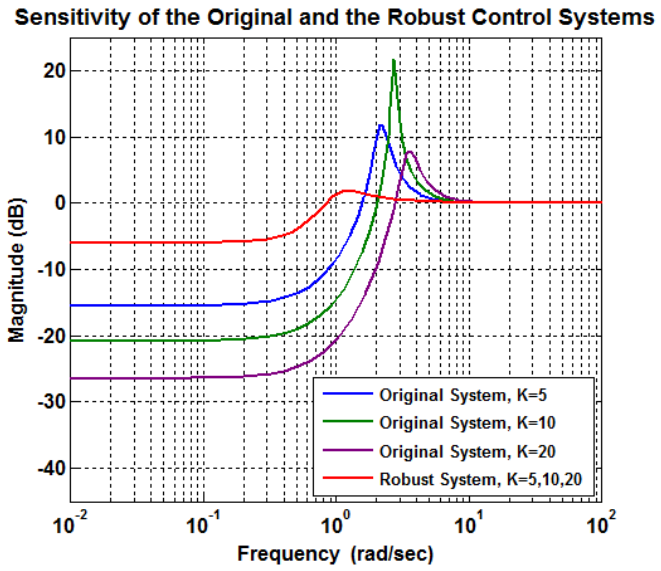

Figure 4.20: *Sensitivity of the Original and the Robust Control Systems Type 0 (Variable Gain K)*

If for the original system of Type 0 equation (4.22) is substituted into (4.42) in case of K = 10, while the time- constant is varied as T = 0.1 sec T = 0.8 sec T = 2 sec, the sensitivities of $W(s)$ with respect to any variations of $G_O(s)$ of the original system are:

$$S^{W}_{G0\ Original\ \ T=0.1}(s) = \frac{0.04s^3 + 1.7s^2 + 1.4s + 1}{0.04s^3 + 1.7s^2 + 1.4s + 11} \tag{4.51}$$

$$S^{W}_{G0\ Original\ \ T=0.8}(s) = \frac{0.32s^3 + 1.44s^2 + 2.1s + 1}{0.32s^3 + 1.44s^2 + 2.1s + 11} \tag{4.52}$$

$$S^{W}_{G0\ Original\ \ T=2}(s) = \frac{0.8s^3 + 3s^2 + 3.3s + 1}{0.8s^3 + 3s^2 + 3.3s + 11} \tag{4.53}$$

Considering the total robust control system Type 0 described by equation (4.29) and substituting it in (4.44), the sensitivities of the robust control system for K = 10, while the time-constant is varied like T = 0.1 sec T = 0.8 sec T = 2 sec are determined as:

$$S^{WR}_{GT\,0\ Robust\ \ T=0.1}(s) = \frac{0.02s^4 + 0.465s^3 + 10.7s^2 + 10.5s + 5}{0.02s^4 + 0.465s^3 + 10.7s^2 + 10.5s + 15} \tag{4.54}$$

$$S^{WR}_{GT0\ Robust\ T=0.8}(s) = \frac{0.16s^4 + 0.92s^3 + 11.05s^2 + 10.5s + 5}{0.16s^4 + 0.92s^3 + 11.05s^2 + 10.5s + 15} \tag{4.55}$$

$$S^{WR}_{GT0\ Robust\ T=2}(s) = \frac{0.4s^4 + 1.7s^3 + 11.65s^2 + 10.5s + 5}{0.4s^4 + 1.7s^3 + 11.65s^2 + 10.5s + 15} \tag{4.56}$$

To compare the functions described by the equations (4.51), (4.52), (4.53) and (4.54), (4.55), (4.56), they are plotted in the frequency domain as shown in Figure 4.21 with the aid of the following code:

```
>> G0OriginalT01=tf([0.04 1.7 1.4 1],[0.04 1.7 1.4 11])
>> G0OriginalT08=tf([0.32 1.44 2.1 1],[0.32 1.44 2.1 11])
>> G0OriginalT2=tf([0.8 3 3.3 1],[0.8 3 3.3 11])
>> GT0RobustT01=tf([0.02 0.465 10.7 10.5 5],[0.02 0.465 10.7 10.5 15])
>> GT0RobustT08=tf([0.16 0.92 11.05 10.5 5],[0.16 0.92 11.05 10.5 15])
>> GT0RobustT2=tf([0.4 1.7 11.65 10.5 5],[0.4 1.7 11.65 10.5 15])
>>bode(G0OriginalT01,G0OriginalT08,G0OriginalT2,GT0RobustT01,
GT0RobustT08,GT0RobustT2)
```

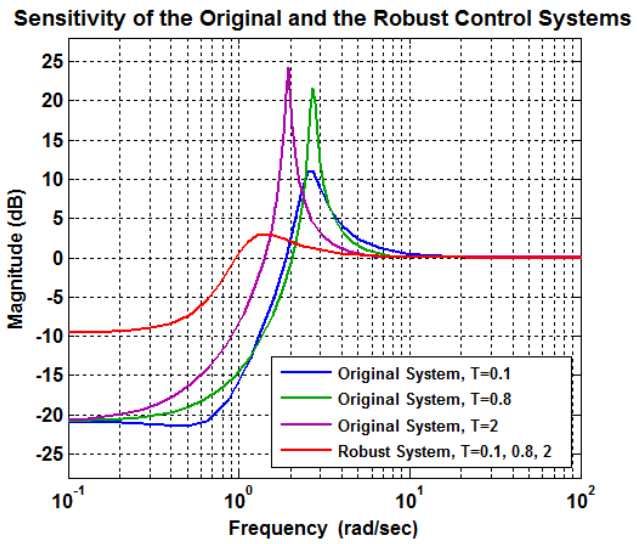

Figure 4.21: *Sensitivity of the Original and the Robust Control Systems Type 0 (Variable Time-Constant T)*

It is seen from Figure 4.21 that the sensitivities of the original system at different time-constants are $S^W_G(s) \geq 0\,\text{dB}$ in the range 0.2 rad/sec < ω < 10 rad/sec, reaching

$S_G^W(s) = 24.2\,\text{dB}$ at 2 rad/sec for the case T = 2. The sensitivity of the robust control system for the case of T = 0.1, coincide with the cases of T = 0.8 and T = 2. The sensitivity of the robust control systems at different gains is $S_{GT}^{WR}(s) \le 0\,\text{dB}$ for ω < 1 rad/sec and ω > 8 rad/sec. Within the range 1 rad/sec < ω < 8 rad/sec, at frequency 1.51 rad/sec they are reaching a maximum of $S_{GT}^{WR}(s) = 2.98\,\text{dB}$, a **sensitivity value that is much lower than the one of the original system.**

4.4.3 Sensitivity of a Robust Control System in Case of Parameter Uncertainties (Original System Type 1)

Taking into account the system Type1 with the transfer function described by equation (4.3) and substituting it into equation (4.42) for T = 0.02 sec and the cases K = 100, K = 200 and K = 500, the sensitivities of the original system are:

$$S_{G1\,Original\;\;K=100}^{W}(s) = \frac{0.0001s^3 + 0.025s^2 + s}{0.0001s^3 + 0.025s^2 + s + 100} \tag{4.57}$$

$$S_{G1\,Original\;\;K=200}^{W}(s) = \frac{0.0001s^3 + 0.025s^2 + s}{0.0001s^3 + 0.025s^2 + s + 200} \tag{4.58}$$

$$S_{G1\,Original\;\;K=500}^{W}(s) = \frac{0.0001s^3 + 0.025s^2 + s}{0.0001s^3 + 0.025s^2 + s + 500} \tag{4.59}$$

Similarly, taking into account the total robust control system Type 1 described by equation (4.13) and substituting it in (4.44), the sensitivities are determined as:

$$S_{GT\,1\,Robust\;\;K=100}^{WR}(s) = \frac{0.0001\,s^3 + 0.125\,s^2 + 5.4s + 96.8}{0.0001\,s^3 + 0.125\,s^2 + 5.4s + 196.8} \tag{4.60}$$

$$S_{GT\,1\,Robust\;\;K=200}^{WR}(s) = \frac{0.0001\,s^3 + 0.225\,s^2 + 9.8s + 193.6}{0.0001\,s^3 + 0.225\,s^2 + 9.8s + 393.6} \tag{4.61}$$

$$S_{GT\,1\,Robust\;\;K=500}^{WR}(s) = \frac{0.0001\,s^3 + 0.525\,s^2 + 23s + 484}{0.0001\,s^3 + 0.525\,s^2 + 23s + 984} \tag{4.62}$$

The sensitivity functions (4.57), (4.58), (4.59) and (4.60), (4.61), (4.62) are plotted in the frequency domain with the aid of the following code and shown in Figure 4.22.

```
>> G1OriginalK100=tf([0.0001 0.025 1 0],[0.0001 0.025 1 100])
>> G1OriginalK200=tf([0.0001 0.025 1 0],[0.0001 0.025 1 200])
>> G1OriginalK500=tf([0.0001 0.025 1 0],[0.0001 0.025 1 500])
>> G1RobustK100=tf([0.0001 0.125 5.4 96.8],[0.0001 0.125 5.4 196.8])
>> G1RobustK200=tf([0.0001 0.225 9.8 193.6],[ 0.0001 0.225 9.8 393.6])
>> G1RobustK500=tf([0.0001 0.525 23 484],[ 0.0001 0.525 23 984])
>>bode(G1OriginalK100,G1OriginalK200,G1OriginalK500,G1RobustK100,
G1RobustK200,G1RobustK200)
```

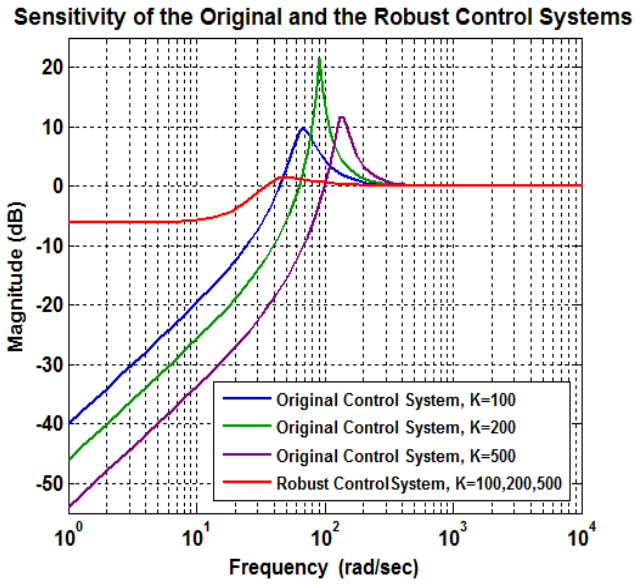

Figure 4.22: *Sensitivity of the Original Type 1 System and the Robust Control System (Variable Gain K)*

As seen from Figure 4.22, the sensitivity of the original control systems are $S_G^W(s) \geq 0\,\text{dB}$ in the frequency range 65 rad/sec < ω < 400 rad/sec, reaching $S_G^W(s) = 21.6\,\text{dB}$ for the case of K = 200. The sensitivity of the robust system for the case of K = 100, coincide with the cases of K = 200 and K = 500. The sensitivity of the robust control system is $S_{GT}^{WR}(s) \leq 0\,\text{dB}$ for ω < 30 rad/sec and for ω > 400 rad/sec, while it is $S_{GT}^{WR}(s) \geq 0\,\text{dB}$, but is with an insignificant value in the frequency range of 30 rad/sec < ω < 200 rad/sec. From Figure 4.22 is seen that the **robust system is again with considerably lower sensitivity compared with the original one.**

Considering the same system of Type1 and substituting equation (4.3) into (4.42) for K = 300 and the cases T = 0.001 sec, T = 0.02 sec and T = 0.08 sec, the sensitivities of the original system are:

$$S^{W}_{G1\,Original\ T=0.001}(s) = \frac{0.000005\,s^3 + 0.006\,s^2 + s}{0.000005\,s^3 + 0.006\,s^2 + s + 300} \tag{4.63}$$

$$S^{W}_{G1\,Original\ T=0.02}(s) = \frac{0.0001\,s^3 + 0.025\,s^2 + s}{0.0001\,s^3 + 0.025\,s^2 + s + 300} \tag{4.64}$$

$$S^{W}_{G1\,Original\ T=0.08}(s) = \frac{0.0004\,s^3 + 0.085\,s^2 + s}{0.0004\,s^3 + 0.085\,s^2 + s + 300} \tag{4.65}$$

Taking into consideration the total robust control system Type 1 described by equation (4.13) and substituting it in (4.44), the sensitivities are determined as:

$$S^{WR}_{GT1\,Robust\ T=0.001}(s) = \frac{0.000005\ s^3 + 0.306\,s^2 + 14.2s + 290.4}{0.000005\ s^3 + 0.306\,s^2 + 14.2s + 590.4} \tag{4.66}$$

$$S^{WR}_{GT1\,Robust\ T=0.02}(s) = \frac{0.0001\,s^3 + 0.325\,s^2 + 14.2s + 290.4}{0.0001\,s^3 + 0.325\,s^2 + 14.2s + 590.4} \tag{4.67}$$

$$S^{WR}_{GT1\,Robust\ T=0.08}(s) = \frac{0.0004\,s^3 + 0.385\,s^2 + 14.2s + 290.4}{0.0004\,s^3 + 0.385\,s^2 + 14.2s + 590.4} \tag{4.68}$$

The sensitivity functions derived from the original system and described by the equations (4.63), (4.64), (4.65) and those derived from the robust system and described by equations (4.66), (4.67), (4.68) are plotted in the frequency domain as shown in Figure 4.23 with the aid of the following code:

```
>> G1OriginalT0001=tf([0.000005 0.006 1 0],[0.000005 0.006 1 300])
>> G1OriginalT002=tf([0.0001 0.025 1 0],[0.0001 0.025 1 300])
>> G1OriginalT008=tf([0.0004 0.085 1 0],[0.0004 0.085 1 300])
>> G1RobustT0001=tf([0.000005 0.306 14.2 290.4],[0.000005 0.306 14.2 590.4])
>> G1RobustT002=tf([0.0001 0.325 14.2 290.4],[0.0001 0.325 14.2 590.4])
>> G1RobustT008=tf([0.0004 0.385 14.2 290.4],[0.0004 0.385 14.2 590.4])
>>bode(G1OriginalT0001,G1OriginalT002,G1OriginalT008,G1RobustT0001,
G1RobustT002,G1RobustT008)
```

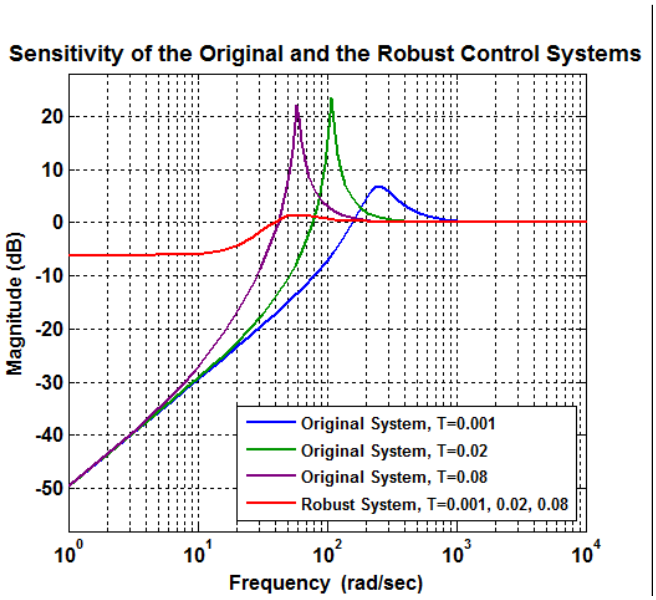

Figure 4.23: *Sensitivity of the Original Type 1 System and the Robust Control System (Variable Time-Constant T)*

As shown in Figure 4.23, the sensitivity of the original control systems are $S_G^W(s) \geq 0\,\text{dB}$ in the frequency range 40 rad/sec < ω < 300 rad/sec, reaching $S_G^W(s) = 23.4\,\text{dB}$ at 108 rad/sec for the case of *T* = 0.02 sec. The sensitivity of the robust system for the case of *T* = 0.001 sec, coincide with the cases of *T* = 0.02 sec and *T* = 0.08 sec. The sensitivity of the robust control system is $S_{GT}^{WR}(s) \leq 0\,\text{dB}$ for ω < 40 rad/sec and for ω > 100 rad/sec, while it is $S_{GT}^{WR}(s) \geq 0\,\text{dB}$, but is with an insignificant value in the frequency range of 40 rad/sec < ω < 100 rad/sec. From Figure 4.23 is seen that **the robust system is with significantly lower sensitivity compared with the one of the original system, again proving the improved robustness** of the system after the compensation.

In this section is discussed the sensitivity of the closed-loop original system *W(s)* with respect to any parameter variations within the open-loop original plant $G_P(s)$. The analysis on sensitivity is performed in case of variations of different uncertain parameters of the original open-loop system $G_P(s)$, like the system gain or time-constant. Systems of Type 0 and Type 1 are examined and discussed in the process. All cases are revealing achieved lower sensitivity to parameter variations and therefore improved robustness of the systems.

4.5 Robust Control in Case of Disturbance and Noise

4.5.1 General Discussion on Sensitivity of Robust Control Systems in Case of External Disturbance and Noise

In many control system applications, the system must yield performance that is robust not only to parameter variations, but also to external disturbances and noise. Although, feedback employing high loop gain in conventional control systems has the ability of reducing the effects of external disturbances and noise, robustness achieved in this way is detrimental to stability. Alternatively, the required robust effect can be accomplished by applying the designed in this research controller. This section is focused on the impact of disturbances and noise on the system, neglecting any parameter uncertainties. It is assumed that the disturbances appear at the system's output. The noise is usually read on the sensor inputs. Considering that both disturbances and noise are additive to the system's output signal, Figure 4.15 can be modified into Figure 4.24 [70], [71], [72], [73].

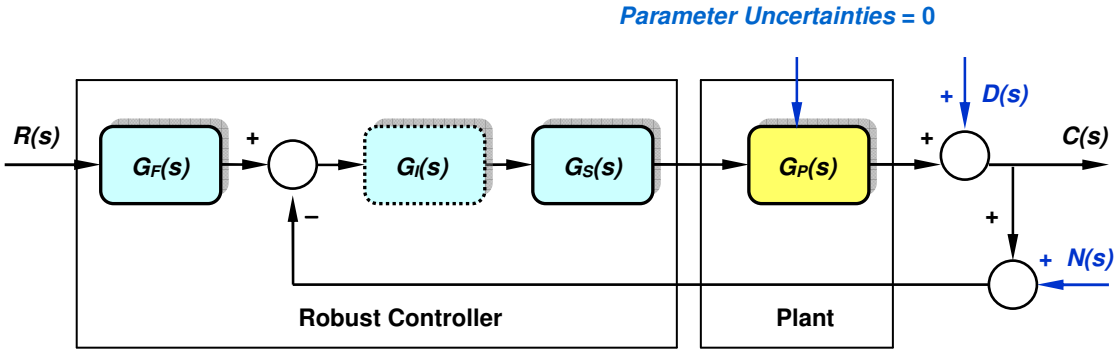

Figure 4.24: *Robust Controller Incorporated in the Control System (Type 0 or Type 1) Subjected to Disturbance and Noise*

4.5.1.1 Discussion on Sensitivity of Robust Control Systems in Case of External Disturbance

If the value of the disturbance is $D(s) = 0$ and the value of the noise is $N(s) = 0$, the input-output transfer function of the system (not considering the integrating stage $G_I(s)$ in the equation) is determined from the block diagram of Figure 4.24 as follows:

$$W_{Robust}(s) = \frac{C(s)}{R(s)} = G_F \times \frac{G_S(s)G_P(s)}{1 + G_S(s)G_P(s)} \tag{4.69}$$

It is suggested that **the series controller $G_S(s)$ is to be designed with the objective, the output signal $C(s)$ to be insensitive to the disturbance $D(s)$ or to the noise $N(s)$ over the frequency range in which the disturbance or the noise are dominant.** At the same time **the forward controller $G_F(s)$ is to be designed to achieve the desired transfer function $W_{Robust}(s)$ between the input $R(s)$ and the output $C(s)$ of the system.** The sensitivity of $W_{Robust}(s)$ with respect to any variations of $G_P(s)$ is:

$$S_{GP}^{WR}(s) = \frac{dW_{Robust}(s)/W_{Robust}(s)}{d[G_P(s)G_S(s)]/[G_P(s)G_S(s)]} = \frac{1}{1 + G_S(s)G_P(s)} \tag{4.70}$$

In the ideal case the sensitivity value should be $S_{GP}^{WR}(s) = 0$.

Taking into account the block diagram at Figure 4.24, if the input is $R(s) = 0$ and the noise is $N(s) = 0$, the disturbance-to-output transfer function is presented as follows:

$$Q_{Robust\ D}(s) = \frac{C(s)}{D(s)} = \frac{1}{1 + G_S(s)G_P(s)} \tag{4.71}$$

The best case of disturbance rejection would be if $Q_{Robust\ D}(s) = 0$

It is seen that the result of equation (4.71) is the same like the results of equation (4.70). ***Therefore the disturbance-to-output transfer function and the sensitivity function are identical.***

4.5.1.2 Discussion on Sensitivity of Robust Control Systems in Case of External Noise

From the block diagram at Figure 4.24, if the input is $R(s) = 0$ and the disturbance is $D(s) = 0$, the noise-to-output transfer function is:

$$Q_{Robust\ N}(s) = \frac{C(s)}{N(s)} = -\frac{G_S(s)G_P(s)}{1 + G_S(s)G_P(s)} \tag{4.72}$$

The ideal case of noise rejection is considered when $Q_{Robust\ N}(s) = 0$

The noise-to-output transfer function, described by equation (4.72) is identical to the input-to-output transfer function of the closed-loop section of the system, seen as a part of equation (4.69), except for the negative sign in the noise-to-output transfer function.

4.5.2 Sensitivity of a Robust Control System in Case of External Disturbance (Original System Type 0)

Taking into account the discussed system of Type 0 and the its related series controller described by equations (4.22) and (4.25) and also considering equations (4.69) and (4.71), the disturbance-to-output transfer function can be represented for the cases before and after the application of the designed robust controller as follows:

$$Q_{Original\ D0}(s) = \frac{C_{Original0}(s)}{D(s)} = \frac{1}{1 + G_{P0}(s)} = \frac{0.32s^3 + 1.44s^2 + 2.1s + 1}{0.32s^3 + 1.44s^2 + 2.1s + 11} \tag{4.73}$$

$$Q_{Robust\ D0}(s) = \frac{C_{Robust0}(s)}{D(s)} = \frac{1}{1 + G_{S0}(s)G_{P0}(s)} = \frac{0.32s^3 + 1.44s^2 + 2.1s + 1}{0.32s^3 + 21.44s^2 + 22.1s + 11} \tag{4.74}$$

In case of parameter uncertainties, as already discussed, the system becomes more robust, with the designed controller. However, the system cannot be evaluated for disturbance rejection in the time domain by applying a unit step function. The true improvement of the disturbance rejection is more appropriately analyzed by comparing the Bode magnitudes of the transfer functions $Q_{OriginalD0}(s)$ and $Q_{RobustD0}(s)$ in the frequency domain.

The functions (4.73) and (4.74) are plotted in the frequency domain with the aid of the following code and shown in Figure 4.25.

```
>> Q0OriginalK10=tf([0.32 1.44 2.1 1],[0.32 1.44 2.1 11])
>> Q0RobustK10=tf([0.32 1.44 2.1 1],[0.32 21.44 22.1 11])
>> bode(Q0OriginalK10,Q0RobustK10)
```

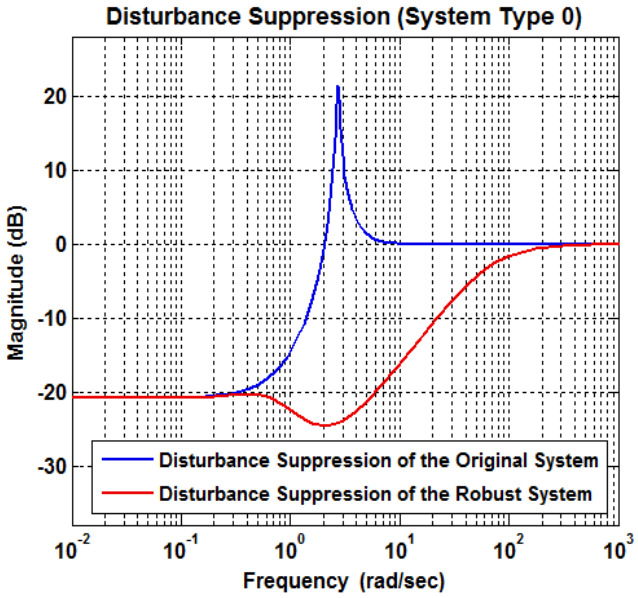

Figure 4.25: *Disturbance Rejection of the Original Control System Type 0 and the Robust Control System*

As seen from the magnitude Bode plot in Figure 4.25, the disturbance rejection of the original control system is $Q_{OriginalD0} \geq 0$ dB in the frequency range 2 rad/sec < ω < 7 rad/sec, reaching $Q_{OriginalD0} = 21.6$ dB at 2.71 rad/sec. **After applying the robust controller, there is a considerable rejection of the disturbance.** The magnitude of disturbance-to-output function is much smaller than the one of the original system and in this case it is $Q_{RobustD0} \leq 0$ in the full frequency range.

4.5.3 Sensitivity of a Robust Control System in Case of External Disturbance (Original System Type 1)

Bearing in mind the system of Type 1 and the related series controller, described by equations (4.3) and (4.6) and also taking into consideration equations (4.71), the disturbance-to-output transfer function for the original and the robust control systems are represented as follows:

$$Q_{Original\ D1}(s) = \frac{C_{Original1}(s)}{D(s)} = \frac{1}{1+G_{P1}(s)} = \frac{0.0001s^3 + 0.025s^2 + s}{0.0001s^3 + 0.025s^2 + s + 200} \qquad (4.75)$$

$$Q_{Robust\ D1}(s) = \frac{1}{1 + G_{S1}(s)G_{P1}(s)} = \frac{0.0001s^3 + 0.025s^2 + s}{0.0001s^3 + 0.2316s^2 + 10.1s + 200} \tag{4.76}$$

Again, the true improvement of the disturbance rejection is analyzed by comparing the transfer functions $Q_{OriginalD1}(s)$ and $Q_{RobustD1}(s)$ in the frequency domain. The functions (4.75) and (4.76) are plotted as Bode magnitudes in the frequency domain with the aid of the following code and shown in Figure 4.26.

```
>> Q1OriginalK200=tf([0.0001 0.025 1 0],[0.0001 0.025 1 200])
>> Q1RobustK200=tf([0.0001 0.025 1 0],[0.0001 0.231 10.1 200])
>> bode(Q1OriginalK200,Q1RobustK200)
```

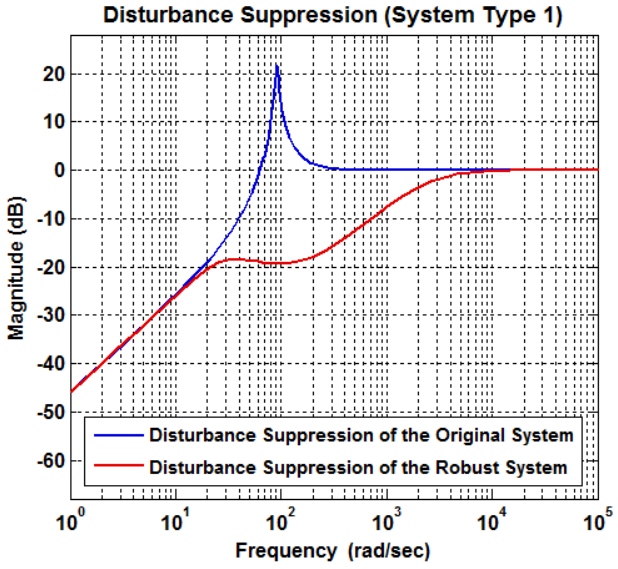

Figure 4.26: *Disturbance Rejection of the Original Control System Type 1 and the Robust Control System*

The magnitude Bode plot shown in Figure 4.26 reveals that the disturbance rejection of the original control system is $Q_{OriginalD1} \geq 0$ dB in the frequency range 60 rad/sec < ω < 300 rad/sec, reaching $Q_{OriginalD1}$ = 21.6 dB at 90.6 rad/sec. **By applying the robust controller, the disturbance rejection is significant.** The magnitude Bode plot of disturbance-to-output function is $\boldsymbol{Q_{RobustD1} \leq 0}$ in the full frequency range.

4.5.4 Sensitivity of a Robust Control System in Case of External Noise (Original System Type 0)

Likewise, the system Type 0 cannot be evaluated for noise rejection in the time domain by applying a unit step function. The true improvement of the noise rejection is more appropriately analyzed by comparing the transfer functions $Q_{OriginalN0}(s)$ and $Q_{RobustN0}(s)$ in the frequency domain [70], [71], [72], [73].

Taking into account equations (4.22) and (4.25) and (4.72), the noise-to-output transfer functions for the case before and after the application of the robust controller are:

$$\left.\begin{aligned} Q_{Original\ N0}(s) &= \frac{C_{Original0}(s)}{N(s)} = \\ &= -\frac{G_{P0}(s)}{1+G_{P0}(s)} = -\frac{10}{0.32s^3+1.44s^2+2.1s+11} \end{aligned}\right\} \quad (4.77)$$

$$\left.\begin{aligned} Q_{Robust\ N0}(s) &= \frac{C_{Robust0}(s)}{N(s)} = \\ &= -\frac{G_{S0}(s)G_{P0}(s)}{1+G_{S0}(s)G_{P0}(s)} = -\frac{20s^2+20s+10}{0.32s^3+21.44s^2+22.1s+11} \end{aligned}\right\} \quad (4.78)$$

The functions (4.77) and (4.78) are plotted in the frequency domain as shown in Figure 4.27 with the aid of the following code:

```
>> Q0OriginalK10N=tf([-10],[0.32 1.44 2.1 11])
>> Q0RobustK10N=tf([-20 -20 -10],[0.32 21.44 22.1 11])
>> bode(Q0OriginalK10N,Q0RobustK10N)
```

As seen from the magnitude Bode plot in Figure 4.21, the noise rejection of the original control system is $Q_{OriginalN0} \geq 0$ dB in the frequency range 0.9 rad/sec < ω < 3.6 rad/sec, reaching $Q_{OriginalN0} = 21.9$ dB at 2.71 rad/sec.

After applying the robust controller, the noise rejection is substantial. The amplitude Bode plot of the noise-to-output functions is $Q_{RobustN0} \leq 0$ in the complete frequency range.

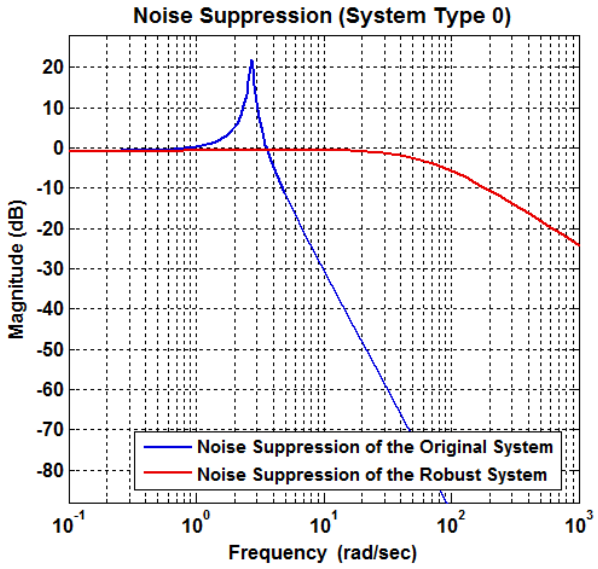

Figure 4.27: *Noise Rejection of the Original Control System Type 0 and the Robust Control System*

4.5.5 Sensitivity of a Robust Control System in Case of External Noise (Original System Type 1)

Taking into consideration the system of Type 1 and the related series controller, described by equations (4.3) and (4.6) and also bearing in mind equations (4.57), (4.69) and (4.72), the noise-to-output transfer functions for the original and the robust control systems are represented as follows:

$$\left.\begin{aligned} Q_{Original\ N1}(s) &= \frac{C_{Original\ 1}(s)}{N(s)} = \\ &= -\frac{G_{P1}(s)}{1+G_{P1}(s)} = -\frac{300}{0.0001s^3+0.025s^2+s+300} \end{aligned}\right\} \quad (4.79)$$

$$\left.\begin{aligned} Q_{RobustN\ 1}(s) &= \frac{C_{Robust\ 1}(s)}{N(s)} = \\ &= -\frac{G_{S1}(s)G_{P1}(s)}{1+G_{S1}(s)G_{P1}(s)} = -\frac{0.031s^2+13.64s+300}{0.0001s^3+0.3356s^2+14.64s+300} \end{aligned}\right\} \quad (4.80)$$

The functions (4.79) and (4.80) are plotted in the frequency domain, as shown in Figure 4.28, with the aid of the following code:

```
>> Q1OriginalK300N=tf([-300],[0.0001 0.025 1 300])
>> Q1RobustK300N=tf([-0.031 -13.64 -300],[0.0001 0.335 14.64 300])
>> bode(Q1OriginalK300N,Q1RobustK300N)
```

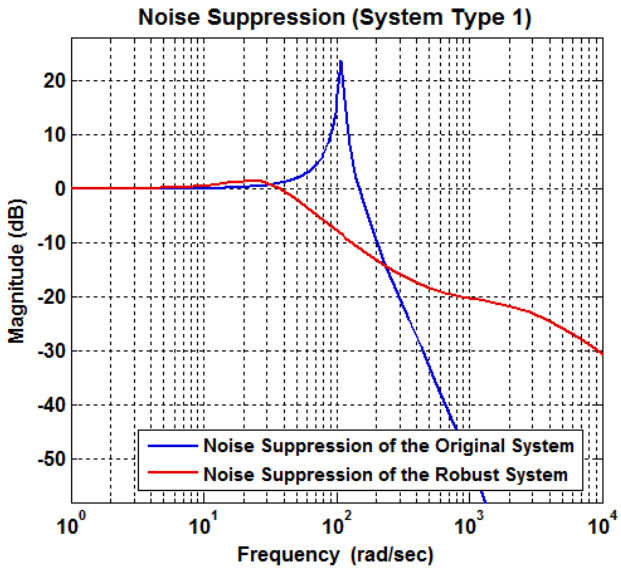

Figure 4.28: *Noise Suppression of the Original Control System Type 1 and the Robust Control System*

The actual improvement of the noise rejection is analyzed by comparing the transfer functions $Q_{OriginalN1}(s)$ and $Q_{RobustN1}(s)$ in the frequency domain. As seen from the magnitude Bode plot of Figure 4.28, the noise suppression of the original control system is $Q_{OriginalN1} \geq 0$ dB in the frequency range 20 rad/sec $< \omega <$ 147 rad/sec and is reaching $Q_{OriginalN1} = 23.6$ dB at 108 rad/sec. **By applying the robust controller, the noise rejection is significant, again proving the efficiency of the robust controller in terms of Noise rejection as well.** The magnitude Bode plot of the noise-to-output function is $Q_{RobustN1} \geq 0$ dB in the frequency range 5 rad/sec $< \omega <$ 38 rad/sec dB is reaching $Q_{RobustN1} = 1.4$ dB at 24 rad/sec and is insignificant, compared with the one of the original system, while $Q_{RobustN1} \leq 0$, for the rest of the frequency range.

4.6 Summary on the Robust Controller Design, System Robustness and Sensitivity Assessment

The design strategy of a robust controller for linear control systems of Type 0 and Type 1 proves that by choosing and implementing desired dominant system poles, the controller enforces the required relative damping ratio and system performance. For systems Type 1, the robust controller consists of a series and a forward stage, while for systems Type 0, an additional integrating stage ensures a steady-state error equal to zero.

The robust controller has an effect of bringing the system to a state of insensitivity to the variation of its parameters within specific limits of the parameter variations. The experiments in the time-domain with variation of different parameters show only insignificant difference in performance for the different system conditions.

Since the design of the robust controller is based on the desired system performance in terms of relative damping, its contribution and its unique property is that it can operate effectively for any of the system's parameter variations or simultaneous variation of a number of parameters. This property is demonstrated by the comparison of the system's performance before and after the application of the robust controller. Tests demonstrate that the system performance in terms of damping, stability and time response remains robust and insensitive in case of any simultaneous variations of the gain and the time-constant within specific limits.

The results from the sensitivity analysis illustrate that the introduction of the designed robust controller considerably reduces the system's sensitivity to multivariable parameter uncertainties and therefore improves the robustness of the system, as.

From the results, it is also seen that **the robust controller has the effect of considerable suppression of the disturbance and noise, bringing their additive components to the system's output signal close to zero. The robust controller also has the effect of eliminating the steady-state error in case of systems of Type0.**

Chapter 5

ADVANCED STABILITY ANALYSIS OF DIGITAL CONTROL SYSTEMS WITH VARIABLE PARAMETERS

This chapter suggests a strategy for analysis of a digital robust control system, with variable or uncertain parameters. The system is analyzed for stability with the aid of the D-partitioning method in the discrete-time domain. The system's performance is also examined for robustness in the discrete-time domain.

5.1 The Concept of Digital Robust Control Systems

5.1.1 General Models of Digital Control systems

A block diagram of digital control system [74], shown in Figure 5.1, illustrates the interaction between its components. The interface at the input of the computer is an analogue-to-digital converter (ADC) converting the continuous-time error signal *E(s)* into its digital format that can be processed by the computer. At the computer output a digital-to-analogue converter (DAC) converts the computer output into continuous-time signal format that is necessary to drive the plant. The computer in combination with its interface, synchronized by a clock, operates as a digital compensator.

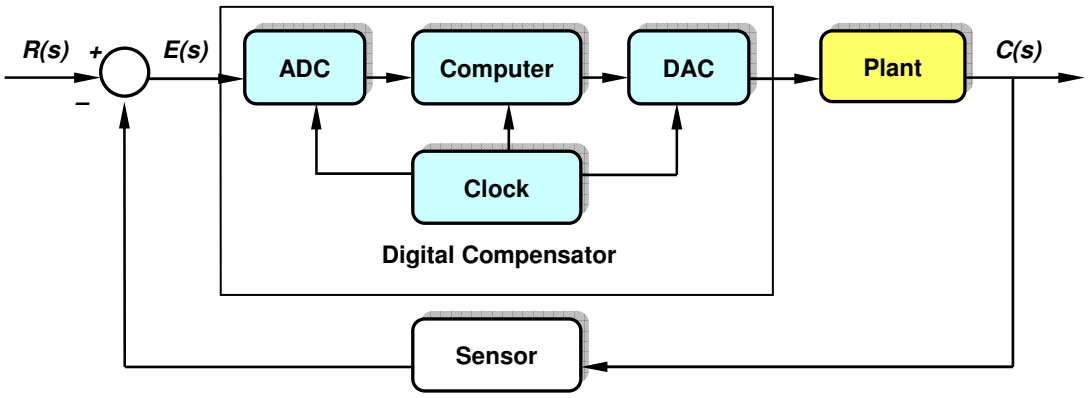

Figure 5.1: *Basic Components of a Digital Control System*

The digital compensator can realize any type of controller equation or algorithm known as the difference equation. A sensor is representing a transducer that converts the variable under control into a signal of a desired format. It can be assumed that the system has unity feedback. As seen in Figure 5.2, the ADC, digital computer and DAC can be accurately represented by the combination of an ideal sampler, a digital filter *D(z)*, that solves the difference equation, and a zero-order hold (ZOH). By applying the Euler's approximation [75], [76], [77], proper value of the sampling period T_S is considered in relation to the minimum time constant of the plant T_{min}.

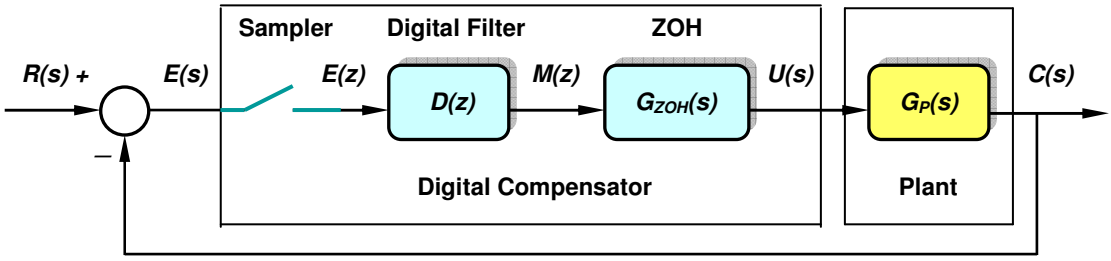

Figure 5.2: *Modified Model of a Digital Control System*

5.1.3 Choice of a Transform Method for Systems Discretization

The transform method specifies the type of algorithms used in the discretization and offers following main options [78]:

5.1.3.1 Zero-Order Hold on the Inputs

Zero-Order Hold (ZOH) devices convert sampled signals to continuous-time signals for analyzing sampled continuous-time systems. The ZOH discretization of a continuous-time LTI model is illustrated in the block diagram of Figure 5.2. The ZOH device creates a continuous signal U(s) by holding each sample value constant over one sampling period T_s. To achieve accuracy of the analysis, it is essential that the Euler's approximation should be observed, or the sampling period T_s should be within the range $T_s \leq (0.1\,T_{min}$ to $0.2\,T_{min})$ [77], [78].

5.1.3.2 Linear Interpolation of Inputs

The Linear interpolation of inputs applies a **First-Order Hold (FOH)** mechanism. The FOH differs from ZOH by the basic hold mechanism. To turn the input samples into a

continuous input, FOH uses linear interpolation between samples. Although, this method is more precise than ZOH, it is only available for continuous-to-digital "*c2d*" conversions, and not for digital-to-continuous "*d2c*" conversions [77], [78].

5.1.3.3 Bilinear (Tustin) Approximation

The **Bilinear Transform** (known as **Tustin's Method**) [77], [78] is used in discrete-time control theory to transform continuous-time system representations to discrete-time and vice versa. The bilinear transform is a special case of a conformal mapping. The bilinear transform is a first-order approximation of the natural logarithm function that is an exact mapping of the z-plane to the s-plane and vice versa. It maps positions from the $j\omega$ axis in the s-plane to the unit circle |z| = 1 in the z-plane. The Tustin or bilinear approximation and its inverse are presented as:

$$z = e^{sT_s} = \frac{e^{sT_s/2}}{e^{-sT_s/2}} \approx \frac{1 + sT_s/2}{1 - sT_s/2} \qquad s = \frac{1}{T_s}\ln(z) \approx \frac{2}{T_s}\frac{z-1}{z+1}$$

To employ the Bilinear Transform, the Tustin MATLAB code *'tustin'* is to be applied, performing the transform of the continuous-time system to discrete-time system representations and vice versa.

5.1.3.4 Tustin Approximation with Frequency Prewarping

Every point of the discrete-time system z-plane is mapped to a point in the continuous-time system s-plane. Every point on the unit circle |z| = 1 in the discrete-time system z-plane, is mapped to a point on the $j\omega_c$ axis in the continuous-time system s-plane, $s = j\omega_c$. The complete continuous frequency range $-\infty < \omega_a < +\infty$ is mapped onto the discrete frequency interval $-\pi/T_s < \omega < +\pi/T_s$ [78], [79], [80]. Then, the discrete-time to continuous-time frequency mapping and the inverse mapping is:

$$\omega_C = \frac{2}{T_s}\tan\left(\omega\frac{T_s}{2}\right) \qquad \omega = \frac{2}{T_s}\arctan\left(\omega_C\frac{T_s}{2}\right)$$

This variation of the Tustin approximation uses the equivalences:

$$H_d(z) = H\left[\frac{\omega}{\tan(\omega T_s/2)}\frac{z-1}{z+1}\right] \quad \text{and} \quad H_d(j\omega) = H_d\left(e^{j\omega T_s}\right)$$

To employ the **Tustin with Frequency Prewarping Transform**, the MATLAB code *'tustin with prewarping'* is to be applied [81].

5.1.3.5 Matched Z-transform Method

The **Matched Z-transform Method**, also called the **Pole–Zero Mapping** or **Pole–Zero Matching Method** [80], [81], [82], is a technique for converting a continuous-time system design to a discrete-time system (digital system) design. This method applies only to SISO systems. The discrete to continuous transformation is:

$$z = e^{sT_s}$$

The method works by mapping all poles and zeros of the s-plane design to z-plane locations, for a sampling period T_s. To employ the **Matched Z-Transform Method,** MATLAB codes "*c2d*" or "*d2c*" are to be applied, performing the transform of the continuous-time system to discrete-time system representations and vice versa. The Euler's approximation should be strictly observed, or the sampling period T_s should be within the range $T_s \leq (0.1\,T_{min}$ to $0.2\,T_{min})$, T_{min} being the minimum time-constant of the continuous system.

The comparison of the transform methods for systems discretization is revealing that the results obtained from the **Bilinear Tustin Transform** and the **Tustin Approximation with Frequency Prewarping** closely match and are more accurate, if evaluated against the **Matched Z-transform Method, the Zero-Order Hold (ZOH) on the Inputs,** or the **Linear interpolation of inputs** methods. For this reason, the **Bilinear Transform,** or the **Tustin Method** is going to be the choice of the method of transform for systems discretization. It is intended to be applied for the D-partitioning analysis in the discrete-time domain.

5.2 Advancement of the D-Partitioning Analysis in the Discrete-Time Domain

5.2.1 D-Partitioning by Variable Gain (System Type 1)

The D-Partitioning analysis can be applied in the discrete-time domain with the aid of the **bilinear transform,** or the **Tustin's method**, exploring the regions of stability of the control system. The analysis can be demonstrated by a **solar tracker control system**, described in section 3.3.2.2. The modified continuous-time system is represented by a transfer function as follows:

$$G_p(s) = \frac{K}{0.0004\,s^3 + 0.085\,s^2 + s} \tag{5.1}$$

The plant's gain K is considered as variable system parameter. For the digital system analysis, the D-Partitioning is applied in terms of the variable parameter employing the bilinear transform to the continuous plant, on condition that the sampling period T_s is taken into account and compared with the plant's minimum time-constant T_{min}. To achieve analysis accuracy, following the Euler's approximation the sampling period T_s should be within the range $T_s \leq (0.1\,T_{min}$ to $0.2\,T_{min})$. For the discussed system, the plant's minimum time constant is T_{min} = 0.005sec and accordingly the sampling period is chosen as T_s = 0.001sec.

Following the steps of the D-Partitioning analysis, the characteristic equation of the continuous independent plant $G_P(s)$ is:

$$G(s) = 0.0004s^3 + 0.085s^2 + s + K = 0 \tag{5.2}$$

The variable parameter K of the original system is determined from equation (5.2) as:

$$K(s) = -0.0004\,s^3 - 0.085\,s^2 - s \tag{5.3}$$

Initially, the variable $K(s)$ is introduced as a continuous function and next converted into its digital equivalent $K(z)$ with the aid of the bilinear transform employing the "*tustin*" code. Further, applying the "*dpartition*" code, the D-Partitioning is achieved in the discrete-time in terms of the variable gain K as follows:

```
>> K=tf([-0.0004 -0.085 -1 0],[0 1])
Transfer function:
-0.0004 s^3 - 0.085 s^2 – s
>> Kd1 = c2d(K,0.001,'tustin')
Transfer function:
-3.542e006 z^3 + 9.938e006 z^2 - 9.258e006 z + 2.862e006
-----------------------------------------------------
            z^3 + 3 z^2 + 3 z + 1
Sampling time: 0.001
>> dpartition(Kd1)
```

where

$$K(z) = \frac{-3542000\,z^3 + 9938000\,z^2 - 9258000\,z + 2862000}{z^3 + 3z^2 + 3z + 1} \tag{5.4}$$

Taking into account that the frequency range applied in the discrete-time domain is $\omega = \pm \omega_s/2 = \pm 2\pi/2T_s = \pm 3141.6$ rad/sec [74], [75] the plotted D-Partitioning curve in the *K*-plane is considered within the range –3141.6 rad/sec ≤ ω ≤ +3141.6 rad/sec.

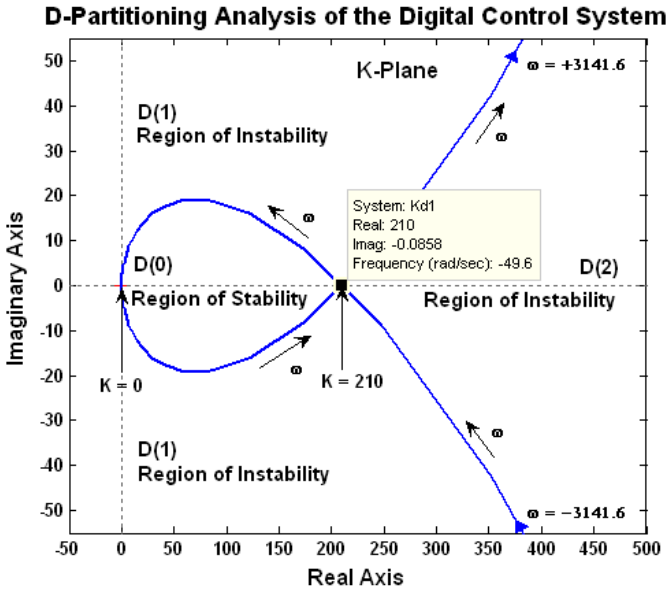

Figure 5.3: *D-Partitioning Analysis of the Digital Control System in Terms of the Variable Gain K (System Type 1)*

The D-Partitioning, as seen in Figure 5.3, determines three regions on the *K*-plane: D(0), D(1) and D(2). Only D(0) is the region of stability, being always on the left-hand side of the curve [24], [77], [78]. This implies that the system is stable only when its gain is within the range 0 ≤ *K* ≤ 210. At *K* = 210 the digital system becomes marginal. The result of the system's marginal value can be confirmed from the following code:

```
>> Gp1=tf([0 210],[0.0004 0.085 1 0])
Transfer function:
   210
-------------------------
0.0004 s^3 + 0.085 s^2 + s

>> Gp1d = c2d(Gp1,0.001,'tustin')
Transfer function:
5.929e-005 z^3 + 0.0001779 z^2 + 0.0001779 z + 5.929e-005
-----------------------------------------------------
    z^3 - 2.806 z^2 + 2.614 z - 0.808
Sampling time: 0.001

>> margin(Gp1d)
GM = 0.103 dB, PM = 0.158 deg
```

As seen from Figure 5.4, after substituting the marginal value of $K = 210$ in equation (5.1) and applying the bilinear transform, the results for the digital control system gain and phase margins are accordingly $GM = 0.103\text{dB} \approx 0\text{dB}$ and $PM = 0.158° \approx 0°$.

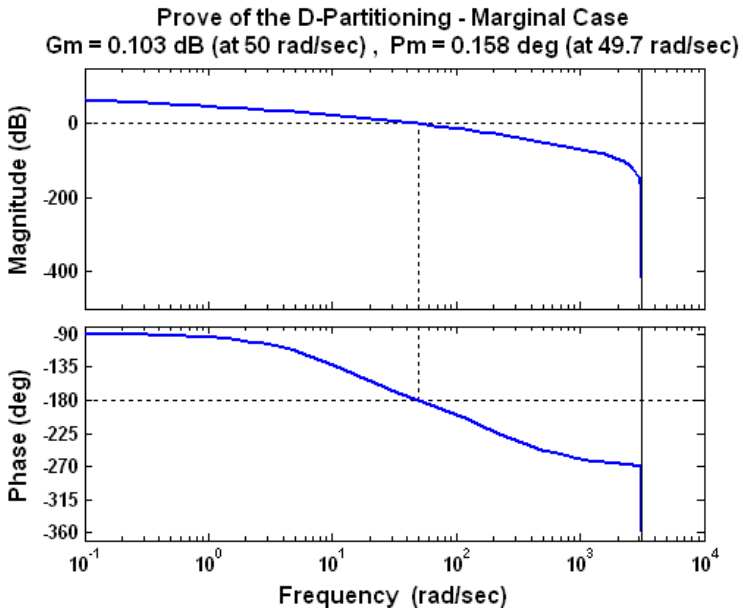

Figure 5.4: *Prove of the D-Partitioning Analysis – Marginal Case of the Digital Control System*

It is also seen from Figure 5.4 that the analysis in the discrete-time domain is restricted within the frequency range $\omega \leq \pm \omega_s/2 = \pm 2\pi/2T_s = +3141.6$ rad/sec.

The system stability within the region D(0) can be explored by allocating a **value for the variable gain K = 20** and applying the following code:

```
>> Gp2=tf([0 20],[0.0004 0.085 1 0])
Transfer function:
     20
-------------------------
0.0004 s^3 + 0.085 s^2 + s
>> Gp2d = c2d(Gp2,0.001,'tustin')
Transfer function:
5.647e-006 z^3 + 1.694e-005 z^2 + 1.694e-005 z + 5.647e-006
-----------------------------------------------------------
   z^3 - 2.806 z^2 + 2.614 z - 0.808
Sampling time: 0.001
>> margin(Gp2d)
GM = 20.5 dB, PM = 38.8 deg
```

The positive values for the gain and phase margins ($GM = 20.5$ dB and $PM = 38.8°$), prove that the digital control system is stable within the region D(0).

The system stability is also explored within the region D(2), by allocating a **value for the variable gain K = 300** and applying the following code:

```
>> Gp3=tf([0 300],[0.0004 0.085 1 0])
Transfer function:
  300
-------------------------
0.0004 s^3 + 0.085 s^2 + s

>> Gp3d = c2d(Gp3,0.001,'tustin')

Transfer function:
8.47e-005 z^3 + 0.0002541 z^2 + 0.0002541 z + 8.47e-005
-------------------------------------------------------
        z^3 - 2.806 z^2 + 2.614 z - 0.808

Sampling time: 0.001
>> margin(Gp3d)

GM= - 3 dB, PM= - 4.63deg
```

The negative values for the gain and phase margins (GM = - 3 dB and PM = - 4.63°), prove that the digital control system is unstable within the region D(2) in this way again confirming the D-Partitioning analysis of this system as shown above.

5.2.2 D-Partitioning by Variable Time-Constant (System Type 0)

The plant discussed in section 3.3.3., consisting of an **armature-controlled dc motor and a type-driving mechanism**, can be modified to a digital control system. In this case the time-constant is the variable. The D-Partitioning analysis can be applied in the discrete-time domain with the aid of the bilinear transform, exploring the regions of stability of the digital control system, taking into consideration the sampling time as $T_s \leq (0.1\,T_{min}$ to $0.2\,T_{min})$ according to the Euler's approximation [76], [77]. The open-loop transfer function of the continuous system is:

$$G_{PO}(s) = \frac{10}{(1+T_1 s)(1+0.5s)(1+0.8s)} = \frac{10}{T_1(0.4s^3+1.3s^2+s)+0.4s^2+1.3s+1} \tag{5.5}$$

The characteristic equation of the continuous stand-alone unity feedback system is:

$$G(s) = T_1(0.4s^3+1.3s^2+s)+0.4s^2+1.3s+11=0 \tag{5.6}$$

To implement the D-Partitioning method, the regions of stability of the system are initially determined in terms of the variable time-constant T_1. From equation (5.6), the variable parameter is presented as follows:

$$T_1(s) = -\frac{0.4s^2 + 1.3s + 11}{0.4s^3 + 1.3s^2 + s} \tag{5.7}$$

The variable $T_1(s)$ is introduced as a continuous-time function and next converted into its digital equivalent $T_1(z)$ with the aid of the bilinear transform. The plant's minimum time-constant is T_{min} = 0.5sec and the sampling period is chosen as T_s = 0.05sec, observing that $T_s \leq (0.1T_{min}$ to $0.2T_{min})$. Further, the D-Partitioning is achieved in the discrete-time domain in terms of the variable time-constant T_1 as follows:

```
>> T1 = tf([-0.4 -1.3 -11],[0.4 1.3 1 0])

Transfer function:
-0.4 s^2 - 1.3 s - 11
---------------------
0.4 s^3 + 1.3 s^2 + s

>> T1d = c2d(T1,0.05,'tustin')

Transfer function:

-0.02536 z^3 + 0.02002 z^2 + 0.02377 z - 0.02161
------------------------------------------------
  z^3 - 2.844 z^2 + 2.694 z - 0.8499

Sampling time: 0.05

>> dpartition(T1d)
```

where

$$T_1(z) = -\frac{-0.02536z^3 + 0.02002z^2 + 0.02377z - 0.02161}{z^3 - 2.844s^2 + 2.694z - 0.8499} \tag{5.8}$$

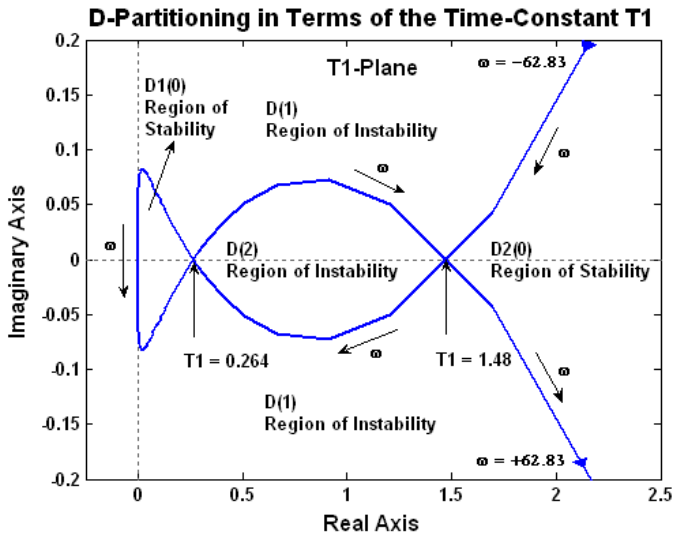

Figure 5.5: *D-Partitioning Analysis of the Digital Control System in Terms of the Variable Time-Constant T_1 (System Type 0)*

As seen from Figure 5.5, the D-partitioning determines four regions in the complex T-Plane: D1(0), D2(0), D(1) and D(2). Only D1(0) and D2(0) are regions of stability, since the position of these regions is always on the left-hand side of the D-Partitioning curve within the frequency range –62.83 rad/sec ≤ ω ≤ +62.83 rad/sec. Only the real values of T_1 are considered, hence the regions of stability are reduced to lines of stability.

If the time-constant is within 0 sec ≤ T_1 ≤ 0.262 sec, corresponding to the region of stability D1(0), the system will be stable. If T_1 is varied within 0.264 sec ≤ T_1 ≤ 1.48 sec, the system will be unstable, being within the region of instability D(2). If T_1 > 1.48 sec, the system is again stable and is operating in the region of stability D2(0). If the time-constant becomes T_1 = 0.264sec or T_1 = 1.48sec, the digital closed-loop control system becomes marginal. The open-loop transfer functions for both marginal cases of the system's continuous part are determined from equation (5.4) accordingly:

$$G_{PO0.264}(s) = \frac{10}{(1+0.264s)(1+0.5s)(1+0.8s)} = \frac{10}{0.1056s^3 + 0.7432s^2 + 1.564s + 1} \quad (5.9)$$

$$G_{PO1.48}(s) = \frac{10}{(1+1.48s)(1+0.5s)(1+0.8s)} = \frac{10}{0.592s^3 + 2.324s^2 + 2.78s + 1} \quad (5.10)$$

The D-Partitioning in the discrete-time domain is confirmed for the two marginal values of T_1, by introducing them into the system's continuous transfer functions and further converting them into their digital equivalent with the bilinear transform:

```
>> Gpo0264=tf([0 10],[0.1056 0.7432 1.564 1])
Transfer function:
     10
-----------------------------------
0.1056 s^3 + 0.7432 s^2 + 1.564 s + 1

>> Gpod1 = c2d(Gpo0264,0.05,'tustin')
Transfer function:
0.001248 z^3 + 0.003745 z^2 + 0.003745 z + 0.001248
-----------------------------------------------------
  z^3 - 2.671 z^2 + 2.375 z - 0.7029
Sampling time: 0.05
>> Gpo148=tf([0 10],[0.592 2.324 2.78 1])
Transfer function:
     10
---------------------------------
0.592 s^3 + 2.324 s^2 + 2.78 s + 1
>> Gpod2 = c2d(Gpo148,0.05,'tustin')
```

Transfer function:
0.0002397 z^3 + 0.0007191 z^2 + 0.0007191 z + 0.0002397
----
z^3 - 2.811 z^2 + 2.633 z - 0.8217

Sampling time: 0.05
>> margin(Gpod1)

GM = 0.00652 dB, PM = 0.0193 deg

>> margin(Gpod2)

GM = - 0.0756 dB, PM = - 0.276 deg

bode(Gpod1,Gpod2)

As seen, after applying the bilinear transform, utilizing the Tustin code, the digital equivalents of equations (5.9) and (5.10) are reflected in equations (5.11) and (5.12).

$$G_{Pod1}(z) = G_{PO0.264}(z) = \frac{0.001248z^3 + 0.003745z^2 + 0.003745z + 0.001248}{z^3 - 2.671z^2 + 2.375z - 0.7029} \quad (5.11)$$

$$G_{Pod2}(z) = G_{PO1.48}(z) = \frac{0.0002397z^3 + 0.0007191z^2 + 0.0007191z + 0.0002397}{z^3 - 2.811z^2 + 2.633z - 0.8217} \quad (5.12)$$

Further, by applying the "*margin*" and "*bode*" codes, the results confirm the outcome of the D-Partitioning analysis, proving the existence of the two marginal conditions.

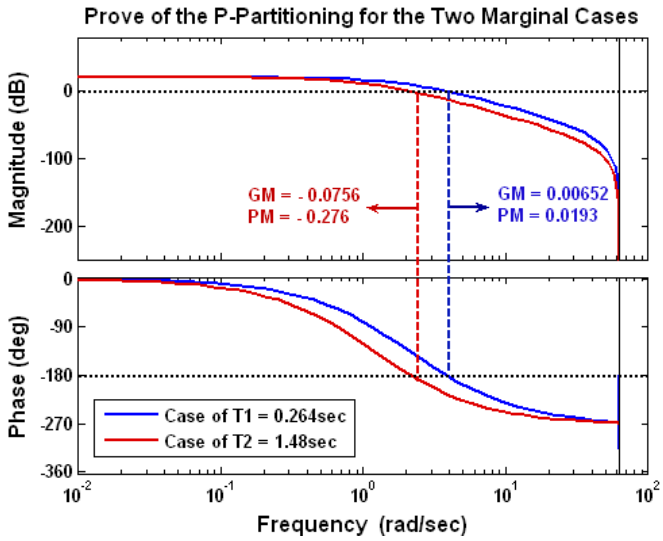

Figure 5.6: *Prove of the D-Partitioning Analysis – Marginal Case of the Digital Control System (Cases T_1 = 0.264sec and T_1 = 1.48sec)*

As seen from Figure 5.6, if the marginal value of the time-constant is T_1 = 0.264 sec, the results for the digital system gain margin is *GM* = 0.00652 dB ≈ 0 dB and the system phase margin is *PM* = 0.0193° ≈ 0°, achieved at frequency 3.84 rad/sec. Also, it is seen the analysis is restricted to $\omega \leq \pm \omega_s/2 = \pm 2\pi/2T_s$ = +62.83 rad/sec.

The results also prove the case of the second marginal value of the time-constant T_1 = 1.48sec, where the gain margin is *GM* = – 0.0756 dB ≈ 0 dB and phase margin is *PM* = – 0.276° ≈ 0°, achieved at frequency 2.17 rad/sec. The analysis is again restricted again to the frequency $\omega \leq \pm \omega_s/2 = \pm 2\pi/2T_s$ = +62.83 rad/sec.
The system stability within the region D1(0) is explored by allocating a value for the variable time-constant T_1 = 0.1 sec and applying the following code:

```
>> Gpo01=tf([0 10],[0.04 0.53 1.4 1])
>> Gpod3 = c2d(Gpo01,0.05,'tustin')
Transfer function:
0.002886 z^3 + 0.008658 z^2 + 0.008658 z + 0.002886
-----------------------------------------------------
   z^3 - 2.444 z^2 + 1.956 z - 0.51
Sampling time: 0.05
>> margin(Gpod3)
GM = 4.89 dB, PM = 15.5 deg
```

The achieved positive values for the gain and phase margins (*GM* = 4.89 dB and *PM* = 15.5 *º*), prove that the digital system is stable within the region D1(0).

Further, the system stability within the region D(2) is explored by allocating a value for the variable time-constant T_1 = 1 sec and applying the following code:

```
>> Gpo1=tf([0 10],[0.4 1.7 2.3 1])
>> Gpod4 = c2d(Gpo1,0.05,'tustin')
Transfer function:
0.000352 z^3 + 0.001056 z^2 + 0.001056 z + 0.000352
---------------------------------------------------
  z^3 - 2.795 z^2 + 2.604 z - 0.8085
Sampling time: 0.05
>> margin(Gpod4)
GM= - 1.14 dB, PM= - 4.11deg
```

The negative values of the system's margins (*GM* = –1.14 dB and *PM* = – 4.11 *º*), prove that the digital system is unstable within the region D(2).

The system stability is also explored within the region D2(0) by allocating a value for the variable time-constant T_1 = 5 sec and applying the following code:

```
>> Gpo5=tf([0 10],[2 6.9 6.3 1])
>> Gpod5 = c2d(Gpo5,0.05,'tustin')
Transfer function:
7.179e-005 z^3 + 0.0002154 z^2 + 0.0002154 z + 7.179e-005
-----------------------------------------------------
    z^3 - 2.834 z^2 + 2.676 z - 0.8415
Sampling time: 0.05
>> margin(Gpod5)
GM = 6.34 dB, PM = 24 deg
```

The positive values for the gain and phase margins (GM = 6.34 dB and $PM = 24^{o}$), prove again that the digital system is stable within the region D2(0).

The analysis above, prove that the results achieved by the D-Partitioning in the discrete-time domain are correct. It confirms that the digital system reaches margin of stability at two different values of the time-constant: T_1 = 0.264sec and T_1 = 1.48sec. Also, it is confirmed that the two regions D1(0) and D2(0), accomplished by the discrete D-Partitioning analysis, correspond to a stable digital control system, while within the region D(2) the digital control system is unstable.

5.3. Summary on the Advancement of the D-Partitioning Analysis in the Discrete-Time Domain

Further advancement of the D-Partitioning method is accomplished in terms of applying the analysis in the discrete-time domain. The control system is considered as a combination of a digital compensator and a plant. For the purpose of the analysis, the bilinear transform is applied to convert continuous-time system representations to their discrete-time equivalents. Further, the **D-Partitioning analysis is applied directly in the discrete-time domain. It is taken into account that the bilinear transform is an exact mapping of the s-plane to the z-plane.** To achieve D-Partitioning analysis accuracy, the Euler's approximation should be observed, or the sampling period T_s should be within the range $T_s \leq (0.1T_{min}$ to $0.2T_{min})$, where T_{min} is the minimum time-constant of the continuous system [76], [77].

Both cases of systems of Type 0 and Type 1 with a variable gain and a variable time-constant are discussed. The achieved results are similar to those of D-Partitioning analysis of linear control systems. The performance and the stability for both system types are significantly dependent on the uncertainty of the variable parameters.

The successful application of the D-Partitioning analysis in the discrete-time domain, by employing the bilinear transform, demonstrates that the basic idea of the advanced D-Partitioning is relevant and valid for digital control systems as well. This part of the research has considerable practical effect. It can be used for analysis of industrial digital control systems that have unstable and variable parameters due to different ambient conditions.

Chapter 6

DESIGN OF A DIGITAL ROBUST CONTROLLER

6.1. Choice of Design Methodology

6.3.4 **Direct Discrete Controller Design**

The direct design of digital controllers is without reference to any original analogue design. The direct design methods are based on the principle of finding a discrete controller that provides a specific closed-loop transfer function of the total compensated system. **Such a controller, achieved by direct discrete controller design, firstly cancels the plant dynamics and then includes additional terms necessary to provide the desired closed-loop transfer function** [76], [77]. Digital controllers are not restricted by realization using physical elements.

The main problem in the direct discrete controller design is finding a suitable target closed-loop transfer function to aim for. This chosen closed-loop transfer function should provide the required performance and yet must be practical and realizable. Another disadvantage of the direct design method is that it treats the controlled plant as a discrete-time system. The plant output is thus only considered at the sample instants and the response between samples is ignored at the design stage. Further disadvantage of the direct discrete controller design is that it may provide good results only if an accurate model of the plant is available. The practical realities of uncertain or time-varying dynamics of the plant mean that controllers achieved by the direct discrete design may perform inadequately and may even cause system instability. It is also acknowledged that with the direct discrete controller design there should be always a compromise between performance and robustness. Finally, the direct discrete controller design approach can lead to very high order transfer functions of the controllers that have to be simplified with care to avoid undesirable performance or system instability [76], [77].

6.3.5 Design of Digital Controllers Based on Analogue Prototypes

The design approach for the majority of digital controllers used in industry is based upon analogue prototypes design that delivers quite adequate performance. Usually the parameters of such controllers can be tuned to achieve the best performance by implementing particular mapping technique. It is acknowledged that the designed digital controllers based on their analogue prototypes will never provide exactly the same performance as the original analogue model. The zero-order hold incorporated in most digital to analogue converters introduces an additional delay of approximately half a sample interval into the process dynamics. **However, by applying the bilinear transform and if the sampling is reasonably fast compared to the plant's dynamics, the digital approximation provides results close to the performance of the original analogue model** [72], [76], [77].

6.3.6 Sample Rate Selection

The selection of sample rate or sampling period T_s is of critical importance to the performance of any digital control system. There are contradictive considerations in the selection of the sampling period. Any sampled-data feedback system is in effect in open loop between samples, therefore larger sampling frequency f_s will result in more accurate control. On the other hand, rapid sample rates lead to problems like accuracy, quantization, noise, stability and cost. There are few different methods for choosing the proper sampling rate.

One of the approaches for sample rate selection is to implement the Shannon's sampling theorem. It suggests a theoretical limit on the sampling rate for band limited signals. If the desired closed-loop frequency bandwidth is f_b and the sampling frequency is presented as $f_s = 1/T_s$, **the Shannon's sampling theorem implies that $f_s \geq$ (5 to 20)f_b** [76], [77].

Another approach can be used in the cases of design of digital controllers based on analogue prototypes. Then by expressing the gain-crossover frequency of the open-loop system as $f_c = \omega_c/2\pi$, the sampling frequency can be chosen as $\boldsymbol{f_s \geq 36 f_c}$ [77].

Taking into account that the intended objective is to achieve a design procedure of a universal robust controller that can be applicable generally, rather than one to be

associated to specific performance limitations, the Euler's approximation method is the most suitable and will be preferred choice for the sample rate selection. According to the **Euler's approximation method the sampling period T_s should be within the range $T_s \leq (0.1T_{min}$ to $0.2T_{min})$,** where T_{min} is the minimum time-constant of the continuous-time system, or the analogue plant model prototype [76], [77].

This part of the research is focusing mainly on the challenges of the digital robust control design. Taking into account some of the advantages of the digital controllers design based on analogue prototypes, **this method will be adopted for the design of the digital robust controller.**

The technique employed is applying digital series compensation with a unity feedback, combined with a cascade digital forward compensation. The practical implementation of the designed discrete controller stages is converting their transfer functions into difference equations, based on which microcontrollers can be programmed [74], [75], [76], [77]. It is expected that the digital robust controller will enforce a desired system damping, margin of stability and time response, suppressing the effects of parameter variations, disturbances and noise.

6.2. Design of a Digital Robust Controller for Systems Type 1

6.2.1 Design of the Robust Controller Stages

The performance criterion ITAE is applied again to achieve an optimal robust control. The digital controller design employs two-step compensation [78], [79], [80], [81]. Similar design steps are followed like those for the realization of the robust controller in the continuous-time domain. As a demonstration of the design procedures in the discrete-time domain, **the modified plant transfer function of the solar tracker system**, described in section 3.3.2.2 is taken into account:

$$G_{p1}(s) = \frac{K}{0.0004\,s^3 + 0.085\,s^2 + s} \tag{6.1}$$

The block diagram of the total compensated system, involving the digital robust compensator is shown in Figure 6.1:

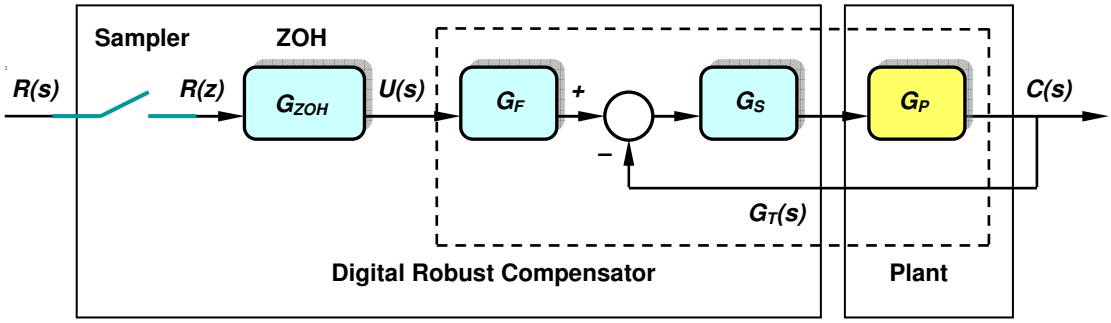

Figure 6.1*: Robust Controller Incorporated into the Discrete-Time Control System Type 1*

The following design procedure is suggested:

Step 1: The digital robust controller is going to be built on basis of the desired performance of the plant's closed-loop system. Initially the plant $G_{P1}(s)$ as a stand-alone block is involved in a unity feedback system. Its closed-loop transfer function $G_{CL1}(s)$ is presented as:

$$G_{CL1}(s) = \frac{G_P(s)}{1 + G_P(s)} = \frac{K}{0.0004s^3 + 0.085s^2 + s + K} \tag{6.2}$$

Step 2: The strategy for constructing the series stage G_S of the digital robust controller is to place its two zeros near the desired dominant closed-loop poles that satisfy the ITAE criterion. **The reason for this step is that after applying the unity negative feedback to the cascade connection of G_S and G_P, these zeros will appear as dominant poles of the closed-loop system**. To apply the ITAE criterion, the optimal gain K at a relative damping ratio ζ = 0.707 is established by plotting the relationship $\zeta = f(K)$ with the aid of the following code:

```
>> K=[0:0.001:10];
>> for n=1:length(K)
Gp_array(:,:,n)=tf([10000*K(n)],[4 850 10000 10000*K(n)]);
 end
>> [y,z]=damp(Gp_array);
>> plot(K,z(1,:))
```

Interacting with the plot of Figure 6.2, **the optimal gain** is determined as ***K* = 5.879**.

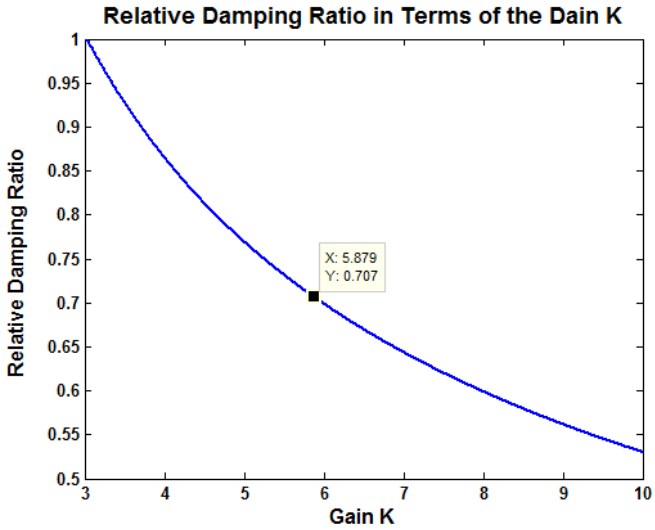

Figure 6.2: *Determination of the Optimal System Gain K*

Step 3: If the optimal gain value ***K* = 5.879** is substituted in equation (6.1), the transfer function is modified to:

$$G_{p1}(s) = \frac{5.879}{0.0004\,s^3 + 0.085\,s^2 + s} \tag{6.3}$$

Initially, the optimal open-loop and closed-loop transfer functions of the system are introduced in the continuous-time domain.

```
>> Gp1=tf([0 5.879],[0.0004 0.085 1 0])
Transfer function:
        5.879
-------------------------
0.0004 s^3 + 0.085 s^2 + s

>> Gp1fb=feedback(Gp1,1)
Transfer function:
          5.879
---------------------------------
0.0004 s^3 + 0.085 s^2 + s + 5.879
```

Considering that the plant's minimum time constant is T_{min} = 0.005sec, to achieve design accuracy by applying the Euler's approximation, sampling period is chosen as T_s = 0.001sec being within the range $T_s \leq (0.1\,T_{min}$ to $0.2\,T_{min})$. Further, by applying the **bilinear transform** employing the **Tustin code,** the optimal open-loop and closed-loop transfer functions of the system are determined in the discrete-time domain:

```
>> Gpd1 = c2d(Gp1,0.001,'tustin')
Transfer function:
1.66e-006 z^3 + 4.979e-006 z^2 + 4.979e-006 z + 1.66e-006
-----------------------------------------------------
        z^3 - 2.806 z^2 + 2.614 z - 0.808
Sampling time: 0.001

>> Gpd1fb=feedback(Gpd1,1)
Transfer function:
1.66e-006 z^3 + 4.979e-006 z^2 + 4.979e-006 z + 1.66e-006
-----------------------------------------------------
        z^3 - 2.806 z^2 + 2.614 z - 0.808
Sampling time: 0.001
```

The results from the procedure above are used for further comparison between the desired closed-loop poles of the optimal plant analogue prototype and its optimal digital equivalent as follows:

For the optimal system analogue prototype:

```
>> damp(Gpfb)
      Eigenvalue              Damping    Freq. (rad/s)
-6.05e+000 + 6.06e+000i    7.07e-001     8.56e+000
-6.05e+000 - 6.06e+000i    7.07e-001     8.56e+000
-2.00e+002                 1.00e+000     2.00e+002
```

For the optimal system digital equivalent:

```
>> damp(Gpdfb)
      Eigenvalue              Magnitude   Equiv. Damping   Equiv. Freq. (rad/s)
 9.94e-001 + 6.02e-003i     9.94e-001     7.07e-001        8.56e+000
 9.94e-001 - 6.02e-003i     9.94e-001     7.07e-001        8.56e+000
 8.18e-001                  8.18e-001     1.00e+000        2.01e+002
```

The results confirm that by implementing the bilinear transform mapping technique there is a match between the corresponding pole location on the s-plane and on the z-plane. **Both the optimal plant analogue prototype and its optimal digital equivalent are having exactly the same relative damping of $\zeta = 0.707$. Based on these results, the controller stages are further designed in the continuous-time domain and then converted into their discrete-time equivalents.**

Step 4: Following the design strategy, and after approximating the system optimal pole values to $-6.1 \pm j6.1$, the two zeros of the series controller stage can be placed at $-6.1 \pm j6.1$. For physical realization of the controller's series stage two remote

controller poles, are added at $s_{1,2}$ = −1000, j0, so that their effect on the system performance is negligible [9], [26], [92]. Thus, the transfer function of the series robust controller stage is presented as:

$$G_{S1}(s) = \frac{(s+6.1+j6.1)(s+6.1-j6.1)}{74.42(s+1000)^2} = \frac{s^2+12.2s+74.42}{74.42(s+1000)^2} \tag{6.4}$$

Step 5: Further, the transfer function of the cascade connection of the series controller stage and the plant is presented as:

$$G_{OL1}(s) = G_S(s)G_P(s) = \frac{0.01344K(s^2+12.2s+74.42)}{0.0004s^3+0.085s^2+s} \tag{6.5}$$

Step 6: When G_{OL1}(s) is involved in a unity feedback system, its closed-loop transfer function is determined as:

$$G_{CL1}(s) = \frac{0.01344K(s^2+12.2s+74.42)}{0.0004s^3+0.085s^2+s+0.01344K(s^2+12.2s+74.42)} \tag{6.6}$$

Step 7: As seen from equation (6.6), the zeros of the closed-loop transfer function are in the vicinity of its poles. As a result, zero-pole cancellation may occur at the closed-loop transfer function. To avoid this problem, a forward controller G_{F1}(s) [23], [83], [92] is added in series to the closed-loop transfer function G_{CL}(s). The strategy for design of the forward stage G_{F1}(s) is such that its poles should cancel the zeros of the closed-loop plant transfer function G_{CL1}(s). **As a result, the total compensated part of the system $G_{T1}(s)$ will be dominated mainly by the two poles –6.1 ± j6.1 that optimizes its performance. To improve on the step response rise time, a zero is added to the transfer function of the forward stage.** Initially, the forward controller section is designed as a linear continuous stage. As a conscience, the transfer function of the forward controller stage is presented as:

$$G_{F1}(s) = \frac{74.42(0.1s+1)}{s(s^2+12.2s+74.42)} \tag{6.7}$$

Step 8: The total transfer function of the compensated system, as seen from the block diagram in Figure 6.1, is presented as:

$$G_{T1}(s) = G_{F1}(s)G_{CL1}(s) = \\ = \frac{K(0.1s+1)}{0.0004\,s^3 + 0.085\,s^2 + s + 0.01344\,K(s^2 + 12.2s + 74.42)} \tag{6.8}$$

Further, the design of digital controller stages based on their analogue prototypes is achieved by applying the bilinear transform. Taking into account equation (6.4), the transfer function of the series robust stage can be determined by:

$$G_{S1}(s) = \frac{s^2 + 12.2s + 74.42}{74.42(s+1000)^2} = \frac{s^2 + 12.2s + 74.42}{74.42s^2 + 148840\,s + 74420000} \tag{6.9}$$

Then the series controller stage is converted into its digital equivalent as follows:

```
>> Gs1=tf([1 12.2 74.42],[74.42 148840 74420000])
Transfer function:
    s^2 + 12.2 s + 74.42
--------------------------------
74.42 s^2 + 148840 s + 7.442e007

>> Gs1d = c2d(Gs1,0.001,'tustin')
Transfer function:
0.006009 z^2 - 0.01194 z + 0.005936
-----------------------------------
    z^2 - 0.6667 z + 0.1111
Sampling time: 0.001
```

From the code outcome the transfer function of the series digital robust stage is presented in the discrete-time domain:

$$G_{S1d}(z) = \frac{0.006009\ \mathrm{z}^2 - 0.01194\ \mathrm{z} + 0.005936}{\mathrm{z}^2 - 0.6667\ \mathrm{z} + 0.1111} = \frac{Y(z)}{X(z)} \tag{6.10}$$

Equation (6.10) can be also presented as:

$$z^2Y(z) - 0.6667\ zY(z) + 0.1111Y(z) = \\ = 0.006009\ z^2X(z) - 0.01194\ zX(z) + 0.005936X(z) \tag{6.11}$$

From equation (6.11), the output of the series controller in the discrete-time domain is finally determined as:

$$Y(z) = 0.006009\ X(z) - 0.01194\ X(z)\mathrm{z}^{-1} + 0.005936\ X(z)\mathrm{z}^{-2} + \\ + 0.6667\ Y(z)\mathrm{z}^{-1} - 0.1111Y(z)\mathrm{z}^{-2} \tag{6.12}$$

To enable the implementation of a microcontroller in the mini-loop of the system, the transfer function of the series digital robust control stage $D_{S1}(z)$, based on equation (6.12), is represented by the following **difference equation** [82], [83], [84], [85]:

$$y(kT) = 0.006009\,x(kT) - 0.01194\,x\left[(k-1)T\right] + 0.005936\,x\left[(k-2)T\right] + \\ + 0.6667\,y\left[(k-1)T\right] - 0.1111\,y\left[(k-2)T\right] \tag{6.13}$$

Similarly, from equation (6.5), the transfer function of the forward robust stage is determined by:

$$G_{F1}(s) = \frac{74.42(0.1s+1)}{s(s^2+12.2s+74.42)} = \frac{7.442\,s+74.42)}{s^2+12.2s+74.42} \tag{6.14}$$

Taking into account equation (6.14), the forward controller stage is converted into its digital equivalent as follows:

```
>> Gf1=tf([7.442 74.42],[1 12.2 74.42])
Transfer function:
  7.442 s + 74.42
--------------------
s^2 + 12.2 s + 74.42
>> Gf1d = c2d(Gf1,0.001,'tustin')
Transfer function:
0.003717 z^2 + 3.698e-005 z - 0.00368
-------------------------------------
  z^2 - 1.988 z + 0.9879
Sampling time: 0.001
```

Considering the outcome of the applied code the transfer function of the forward robust control stage, presented in the discrete-time domain, is as follows:

$$G_{F1d}(z) = \frac{0.003717z^2 + 0.00003698\,z - 0.00368}{z^2 - 1.988\,z + 0.9879} = \frac{M(z)}{E(z)} \tag{6.15}$$

Equation (6.15) can be further expressed as:

$$z^2M(z) - 1.988\;zM(z) + 0.9979\,M(z) = \\ = 0.003717\;z^2E(z) + 0.00003698\;zE(z) - 0.00368\,E(z) \tag{6.16}$$

The output of the series controller in the discrete-time domain is determined from equation (6.16) as follows:

$$M(z) = 0.003717\,(z) + 0.0000\,3698\,zE(z)z^{-1} - 0.00368\,E(z)z^{-2} + \\ + 1.988\;M(z)z^{-1} - 0.9979\,M(z)\,z^{-2} \tag{6.17}$$

To facilitate the implementation of a forward microcontroller, the transfer function of the forward digital robust control stage $D_F(z)$ is expressed, based on equation (6.17), by the following **difference equation** [82], [83], [84], [85]:

$$m(kT) = 0.003717\;e(kT) + 0.00003698\;e\left[(k-1)T\right] - \\ - 0.0007434\;e\left[(k-2)T\right] + 1.988\,m\left[(k-1)T\right] - 0.9979\,m\left[(k-2)T\right] \tag{6.18}$$

6.2.2 D-Partitioning Analysis of the Robust Digital System (Case of Analogue Prototype System Type 1)

To analyze and compare the system stability before and after the compensation, the D-Partitioning in terms of the variable parameter K is determined from the characteristic equation of the analogue prototype of the robust compensated system $G_{T1}(s)$ (6.8) and is reflected in the equation (6.19).

$$K(s) = \frac{-0.0004\,s^3 - 0.085\,s^2 - s}{0.0134\,s^2 + 0.164\,s + 1} \tag{6.19}$$

Its digital equivalent $K(z)$ and the D-Partitioning curve of the digital control system after the application of the robust compensation are determined by the code:

```
>> K = tf([-0.0004 -0.085 -1 0],[0.0134 0.164 1])

Transfer function:
-0.0004 s^3 - 0.085 s^2 - s
---------------------------
 0.0134 s^2 + 0.164 s + 1

>> Kd1 = c2d(K,0.001,'tustin')

Transfer function:
-65.68 z^3 + 184.3 z^2 - 171.7 z + 53.07
----------------------------------------
  z^3 - 0.9878 z^2 - z + 0.9878

Sampling time: 0.001
>> dpartition(K)
```

where

$$K(z) = \frac{-65.68\,z^3 + 184.3s^2 - 171.7\,s + 53.07}{z^3 - 0.9878\,z^2 - z + 0.9878} \tag{6.20}$$

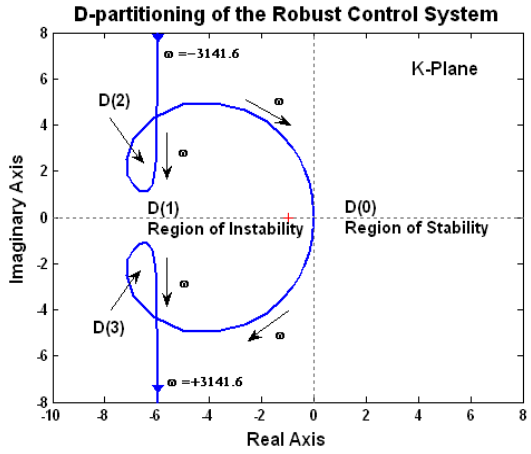

Figure 6.3*: D-Partitioning in the Discrete-Time Domain in Terms of the Variable Gain K* ***after the Robust Compensation*** *(Analogue Prototype System Type 1)*

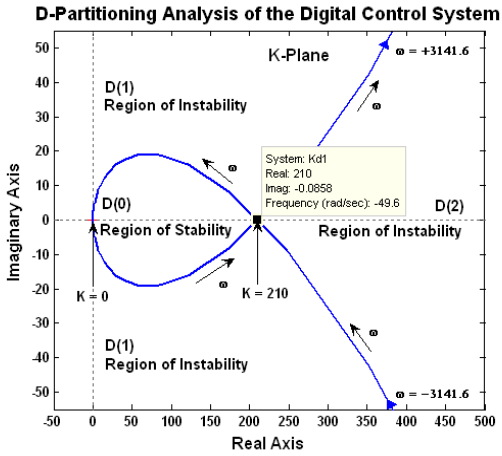

Figure 6.4: D-Partitioning *in the Discrete-Time Domain* in Terms of the Variable Gain K **before the Robust Compensation** *(System Type 1)*

It is seen from Fig. 6.3 that the D-Partitioning curve determines four regions of the *K*-plane: D(0), D(1), D(2) and D(3). Only D(0) is the region of stability, being always on the left-hand side of the curve for a frequency variation from ω = –3141.6 to ω = +3141.6. By comparing Figure 6.3 and Figure 6.4, it is seen that **the robust controller has improved considerably the margin of stability of the digital compensated system.** The analysis in the discrete-time domain confirm that while the original system becomes marginal at *K* = 210, **after implementing the robust compensation, the digital system will be stable for any positive values of the gain, *K* > 0**, since these values are within the region D(0).

6.2.3 Performance Assessment of the Robust Digital System (Case of Analogue Prototype System Type 1)

Reflection on the system's transient responses is used as an approach for the analysis and comparison of the system robustness before and after the compensation. The system's transient responses before the robust compensation for different random values for the gain, *K* = 20, 50 and 200 are determined by considering the characteristic equation of the analogue prototype of the original plant from equation (6.1) and further determining its digital equivalent by applying the bilinear transform employing the Tustin code as follows:

```
>> Gp20=tf([0 20],[0.0004 0.085 1 0])
>> Gp50=tf([0 50],[0.0004 0.085 1 0])
>> Gp200=tf([0 200],[0.0004 0.085 1 0])
>> Hdp20 = c2d(Gp20,0.001,'tustin')
>> Hdp50 = c2d(Gp50,0.001,'tustin')
>> Hdp200 = c2d(Gp200,0.001,'tustin')
>> Hdp20fb = feedback(Hdp20,1)
Transfer function:
5.647e-006 z^3 + 1.694e-005 z^2 + 1.694e-005 z + 5.647e-006
-----------------------------------------------------------
      z^3 - 2.806 z^2 + 2.614 z - 0.808
Sampling time: 0.001
>> Hdp50fb = feedback(Hdp50,1)
Transfer function:
1.412e-005 z^3 + 4.235e-005 z^2 + 4.235e-005 z + 1.412e-005
-----------------------------------------------------------
      z^3 - 2.806 z^2 + 2.614 z - 0.808
Sampling time: 0.001
>> Hdp200fb = feedback(Hdp200,1)
Transfer function:
5.647e-005 z^3 + 0.0001694 z^2 + 0.0001694 z + 5.647e-005
-----------------------------------------------------------
    z^3 - 2.806 z^2 + 2.614 z - 0.808
Sampling time: 0.001
>> step(Hdp20fb,Hdp50fb,Hdp200fb)
```

The compensated system is also examined for robustness in terms if it's transient responses in the discrete-time domain by substituting different random values for the gain, $K = 20$, 50 and 200 in the transfer function, represented by equation (6.8):

$$G_{T1}(s)_{K\,=\,20} = \frac{20(0.1s+1)}{0.0004\,s^3 + 0.35\,s^2 + 4.28\,s + 20} \tag{6.21}$$

$$G_{T2}(s)_{K\,=\,50} = \frac{50(0.1s+1)}{0.0004\,s^3 + 0.76\,s^2 + 9.2\,s + 50} \tag{6.22}$$

$$G_{T3}(s)_{K\,=\,200} = \frac{200(0.1s+1)}{0.0004\,s^3 + 2.77\,s^2 + 33.7\,s + 200} \tag{6.23}$$

Again, it is taken into account that the robust system design and its analysis are based upon the system analogue prototype. Then, the transient responses for the three different cases, representing the gain variation of the robust system, are determined by the following code:

```
>> GT20=tf([2 20],[0.0004 0.35 4.28 20])
Transfer function:
        2 s + 20
-----------------------------------
0.0004 s^3 + 0.35 s^2 + 4.28 s + 20
>> GT50=tf([5 50],[0.0004 0.76 9.2 50])
Transfer function:
      5 s + 50
-----------------------------------
0.0004 s^3 + 0.76 s^2 + 9.2 s + 50
>> GT200=tf([20 200],[0.0004 2.77 33.7 200])
Transfer function:
    20 s + 200
-----------------------------------
0.0004 s^3 + 2.77 s^2 + 33.7 s + 200
>> Gd20 = c2d(GT20,0.001,'tustin')
Transfer function:
0.0008723 z^3 + 0.000881 z^2 - 0.0008549 z - 0.0008636
-------------------------------------------------------
       z^3 - 2.385 z^2 + 1.777 z - 0.3924
Sampling time: 0.001
>> Gd50 = c2d(GT50,0.001,tustin')
Transfer function:
0.001606 z^3 + 0.001622 z^2 - 0.001574 z - 0.00159
--------------------------------------------------
   z^3 - 2.017 z^2 + 1.045 z - 0.0285
Sampling time: 0.001
>> Gd200 = c2d(GT200,0.001,tustin')
Transfer function:
0.002802 z^3 + 0.00283 z^2 - 0.002746 z - 0.002774
---------------------------------------------------
  z^3 - 1.437 z^2 - 0.1078 z + 0.5445
Sampling time: 0.001

>> step(Hd20,Hd50,Hd200)
```

It is obvious that the transfer functions of the digital feedback robust control system for the three different values of the gain, K = 20, 50 and 200 are accordingly:

$$Gdfb(z)_{K=20} = \frac{0.0008723z^3 + 0.000881z^2 - 0.0008549z - 0.0008636}{z^3 - 2.385\,z^2 + 1.777\,z - 0.3924} \quad (6.24)$$

$$Gdfb(z)_{K=50} = \frac{0.001606z^3 + 0.001622z^2 - 0.001574z - 0.00159}{z^3 - 2.017\,z^2 + 1.045\,z - 0.0285} \quad (6.25)$$

$$Gdfb(z)_{K=200} = \frac{0.002802z^3 + 0.00283z^2 - 0.002746z - 0.002774}{z^3 - 1.437z^2 - 0.1078\,z + 0.5445} \quad (6.26)$$

Considering the outcomes of the two codes shown above, the system's transient responses in the discrete-time domain that are achieved after and before the robust compensation are reflected accordingly in Figure 6.5 and 6.6:

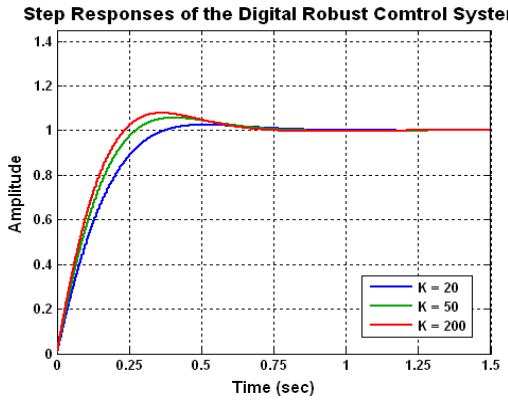

Figure 6.5*: Transient Responses in the Discrete-Time Domain of the* ***Robust Digital Control System*** *of Type 1* ***after the Robust Compensation***

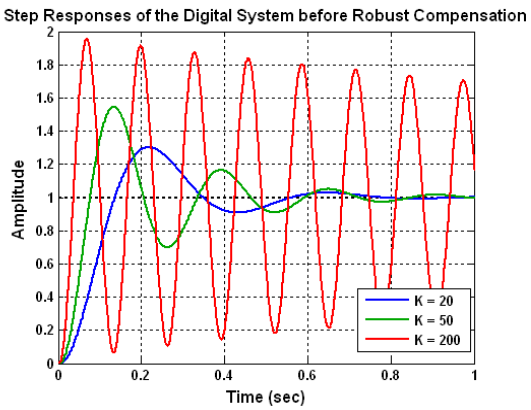

Figure 6.6: *Transient Responses in the Discrete-Time Domain of the* ***Original Digital Control System*** *of Type 1* ***before the Robust Compensation***

It is obvious from Figure 6.5 and Figure 6.6 that as a result of the applied robust controller, the digital control system becomes quite insensitive and robust to variation of the system's gain *K*. The assessment of the robust digital control system in terms of relative damping in the discrete-time domain, reveals that the system performance for the cases of gain $K = 20$, $K = 50$ and $K = 200$ differ insignificantly from each other.

```
>> damp(Hd20)

      Eigenvalue          Magnitude    Equiv. Damping    Equiv. Freq. (rad/s)
9.94e-001 + 4.44e-003i    9.94e-001    8.10e-001          7.61e+000
9.94e-001 - 4.44e-003i    9.94e-001    8.10e-001          7.61e+000
3.97e-001                 3.97e-001    1.00e+000          9.23e+002

>> damp(Hd50)

      Eigenvalue          Magnitude    Equiv. Damping    Equiv. Freq. (rad/s)
9.94e-001 + 5.38e-003i    9.94e-001    7.46e-001          8.14e+000
9.94e-001 - 5.38e-003i    9.94e-001    7.46e-001          8.14e+000
2.88e-002                 2.88e-002    1.00e+000          3.55e+003

>> damp(Hd200)

      Eigenvalue          Magnitude    Equiv. Damping    Equiv. Freq. (rad/s)
9.94e-001 + 5.90e-003i    9.94e-001    7.16e-001          8.50e+000
9.94e-001 - 5.90e-003i    9.94e-001    7.16e-001          8.50e+000
-5.51e-001                5.51e-001    1.86e-001          3.20e+003
```

As seen from the code results, the digital system has become quite robust. In spite of the considerable change of the gain, from $K = 20$, to $K = 50$ and further to $K = 200$,

the system's dominant conjugative poles and the system's relative damping ratio change insignificantly. These results prove once again that the digital control system, after being robust compensated, becomes quite insensitive to variations of the gain within significant limits (increment of 10 times in this case), proving the efficiency of the robust compensation.

An average case of a system gain K = 50 is chosen for the assessment of the system's performance after the application of the robust controller. If the relative damping ratio is ζ = 0.746, the system's (PMO) is determined as:

$$PMO = 100e^{-\pi\varsigma/\sqrt{1-\varsigma^2}} = 2.96\% \tag{6.27}$$

The system's settling time is determined by substituting ζ = 0.746 and the natural frequency ω_n = 8.14 rad/sec as follows:

$$t_{S(5\%)} = \frac{4.6}{\varsigma\omega_n} = 0.757\,\text{sec} \tag{6.28}$$

The system's time to maximum overshoot and the time ratio are as follows:

$$t_m = \frac{\pi}{\omega_n\sqrt{1-\varsigma^2}} = 0.579\ \text{sec} \tag{6.29}$$

$$t_{S(5\%)}/t_m = 1.307 \tag{6.30}$$

As seen from Table 6.1, all the achieved results are meeting the ITAE criterion, since they have values that match or are lower than the targeted objectives.

Table 6.1

Comparison between Objectives and Real Results (Type 1)

Specifications	Objectives	Real Results	Consideration
ζ	= 0.707	= 0.746	Close Match
PMO	≤ 4%	= 2.96%	Better
$t_{s(5\%)}/t_m$	≤ 2.5	= 1.307	Better

The performance evaluation results of t_S and t_m are also confirmed by the system step response determined in the time domain.

6.3 Design of a Digital Robust Controller for Systems Type 0

6.3.1 Design of the Robust Controller Stages

A digital robust controller can be designed for the plant discussed in section 3.3.3.1, considering the time-constant as the variable system parameter. Again, the robust controller is consisting of a series stage G_{S0}(s), a forward stage G_{F0}(s) and an integrating stage G_{I0}(s) as shown in Figure 6.7. In the discussed case, the open-loop transfer function of a complex system is reduced to a third order and is presented as:

$$G_{PO}(s) = \frac{10}{(1+Ts)(1+0.5s)(1+0.8s)} \tag{6.31}$$

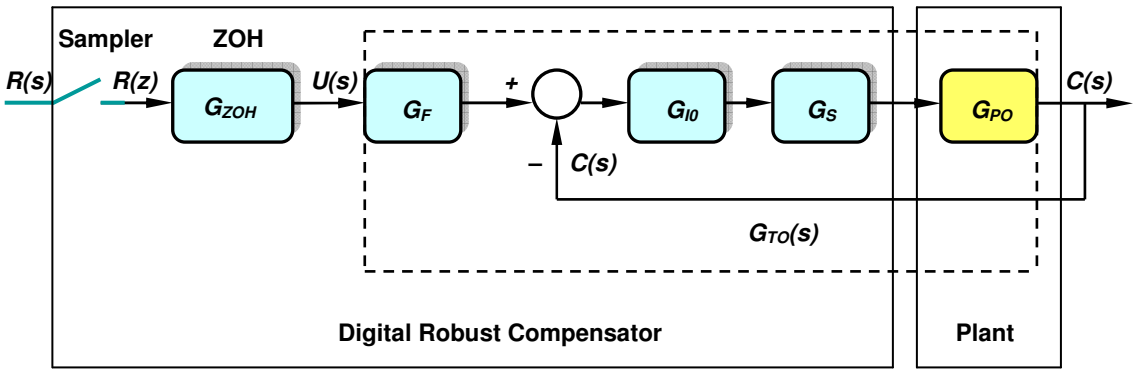

Figure 6.7: *Robust Controller Incorporated into the Discrete -Time Control System Type 0*

The design strategy for constructing the series stage of the controller is similar to the one for systems Type 1.

Step 1: The plant $G_{P0}(s)$ as a stand-alone system is involved in a unity feedback system, having a closed-loop transfer function $G_{CL0}(s)$:

$$G_{CL0}(s) = \frac{G_P(s)}{1+G_P(s)} = \frac{10}{(1+Ts)(1+0.5s)(1+0.8s)+10} \tag{6.32}$$

Step 2: For constructing the series stage G_S of the digital robust controller its two zeros are placed near the desired dominant closed-loop poles that satisfy the ITAE criterion. **These zeros will appear as dominant poles of closed-loop system of**

the cascade connection of G_S and G_P. The optimal time-constant T at a relative damping ratio ζ = 0.707 is established as T = 27.06 sec by plotting and interactive procedure the relationship $\zeta = f(T)$ shown at Figure 4.10.

Step 3: If the optimal value T = 27.06 sec is substituted in equation (6.31), the transfer function is modified to:

$$G_{P0}(s) = \frac{10}{10.824\,s^3 + 35.578\,s^2 + 28.36 + 1} \tag{6.33}$$

From where:

```
>> Gp0=tf([0 10],[10.824 35.578 28.36 1])
Transfer function:
          10
-----------------------------------
10.82 s^3 + 35.58 s^2 + 28.36 s + 1
>> Gp0fb=feedback(Gp0,1)
Transfer function:
          10
-----------------------------------
10.82 s^3 + 35.58 s^2 + 28.36 s + 11
```

The minimum plant time constant established from equation (6.31) is T_{min} = 0.5sec. Following the Euler's approximation, sampling period is chosen as T_s = 0.1sec being within the range $T_s \leq (0.1T_{min}$ to $0.2T_{min})$. By applying the **bilinear transform,** the optimal open-loop and closed-loop transfer functions of the system are determined in the discrete-time domain:

```
>> Gpd0 = c2d(Gp0,0.1,'tustin')
Transfer function:
9.863e-005 z^3 + 0.0002959 z^2 + 0.0002959 z + 9.863e-005
-----------------------------------------------------
  z^3 - 2.697 z^2 + 2.416 z - 0.7193
Sampling time: 0.1
>> Gpd0fb=feedback(Gpd0,1)
Transfer function:
9.863e-005 z^3 + 0.0002959 z^2 + 0.0002959 z + 9.863e-005
-----------------------------------------------------
  z^3 - 2.697 z^2 + 2.416 z - 0.7192
Sampling time: 0.1
```

Comparison between the desired closed-loop poles of the optimal analogue prototype system and its optimal digital equivalent is achieved as follows:

For the optimal system analogue prototype:

```
>> damp(Gp0fb)
      Eigenvalue          Damping     Freq. (rad/s)
-4.64e-001 + 4.64e-001i    7.07e-001     6.56e-001
-4.64e-001 - 4.64e-001i    7.07e-001     6.56e-001
-2.36e+000                 1.00e+000     2.36e+000
```

For the optimal system digital equivalent:

```
>> damp(Gpd0fb)

    Eigenvalue            Magnitude   Equiv. Damping   Equiv. Freq. (rad/s)
9.54e-001 + 4.43e-002i    9.55e-001    7.07e-001        6.56e-001
9.54e-001 - 4.43e-002i    9.55e-001    7.07e-001        6.56e-001
7.89e-001                 7.89e-001    1.00e+000        2.37e+000
```

Both the analogue prototype and its digital equivalent are having the same relative damping of ζ = 0.707. Also, there is a match between the related pole location on the s-plane and on the z-plane.

Based on the close math of the results from the system's analogue prototype and its digital equivalent, the controller stages are further designed in the continuous-time domain and then converted into their discrete-time equivalents.

Step 4: The system optimal poles are −0.464 ± j0.464. After approximating of the pole values to −0.5 ± j0.5, the two series controller zeros are placed also at −0.5 ± j0.5. Two poles at $s_{1,2}$ = −1000, j0 are added for physical realization of the serried controller. The complete transfer function of the series robust controller $G_{S0}(s)$ is presented as:

$$G_{S0}(s) = \frac{(s+0.5+j0.5)(s+0.5-j0.5)}{0.5s(s+1000)^2} = \frac{s^2+s+0.5}{0.5s(s+1000)^2} \tag{6.34}$$

Step 5: An integrating stage, connected in cascade with the series controller, is added to eliminate the steady-state error of the system. The transfer function of the cascade connection of the integrating stage, the series controller stage and the plant is presented as:

$$G_{OL0}(s) = G_I(s)G_{S0}(s)G_{P0}(s) = \frac{20(s^2+s+0.5)}{s(1+Ts)(1+0.5s)(1+0.8s)(s+1000)^2} \tag{6.35}$$

Step 6: By applying a unity feedback the transfer function becomes:

$$G_{CL0}(s) = \frac{20(s^2 + s + 0.5)}{s(1+Ts)(1+0.5s)(1+0.8s) + 20(s^2 + s + 0.5)} \tag{6.36}$$

Step 7: The poles of a forward stage G_{F0}(s) should cancel the zeros of the closed-loop plant transfer function G_{CL0}(s). A zero improves the rise-time of the system:

$$G_{F0}(s) = \frac{0.5(0.1s+1)}{s^2 + s + 0.5} \tag{6.37}$$

Step 8: As a result, the total compensated system $G_{T0}(s)$ will be dominated by the two poles $-0.5 \pm j0.5$, optimizing its performance. Its transfer function is presented as:

$$\left.\begin{aligned} G_{T0}(s) &= G_{F0}G_{CL0S}(s) = \\ &= \frac{10(0.1s+1)}{s(1+Ts)(1+0.5s)(1+0.8s)(s+1000)^2 + 20(s^2 + s + 0.5)} \end{aligned}\right\} \tag{6.38}$$

The design of the series and the forward digital controller stages founded on their analogue prototypes is realized by applying the bilinear transform. Taking into account equation (6.34), the transfer function of the series robust stage can be determined by:

$$G_{S0}(s) = \frac{(s+0.5+j0.5)(s+0.5-j0.5)}{0.5s(s+1000)^2} = \frac{s^2 + s + 0.5}{0.5s^3 + 1000s^2 500000s} \tag{6.39}$$

The digital equivalent of the series controller stage is accomplished as follows:

```
>> Gs0=tf([1 1 0.5],[0.5 1000 500000])
Transfer function:
    s^2 + s + 0.5
------------------------
0.5 s^2 + 1000 s + 500000
>> Gs0d = c2d(Gs0,0.1,'tustin')
Transfer function:
0.0008083 z^2 - 0.001536 z + 0.0007314
-------------------------------------
     z^2 + 1.922 z + 0.9231

Sampling time: 0.1
```

It is seen from the code that the transfer function of the series digital robust stage in the discrete-time domain is as follows:

$$G_{sod}(z) = \frac{0.0008083\mathrm{z}^{2} - 0.001536\mathrm{z} + 0.0007314}{\mathrm{z}^{2} + 1.922\mathrm{z} + 0.9231} = \frac{Y(z)}{X(z)} \tag{6.40}$$

Equation (6.40) can be also presented as:

$$\begin{aligned} & z^{2}Y(z) + 1.922\ zY(z) + 0.9231\ Y(z) = \\ & = 0.0008083\ z^{2}X(z) - 0.00153\ zX(z) + 0.0007314\ X(z) \end{aligned} \tag{6.41}$$

The output of the series controller in the discrete-time domain is determined as:

$$\begin{aligned} Y(z) = {} & 0.0008083X(z) - 0.00153X(z)\mathrm{z}^{-1} + 0.0007314X(z)\mathrm{z}^{-2} \\ & - 1.922Y(z)\mathrm{z}^{-1} - 0.9231Y(z)\mathrm{z}^{-2} \end{aligned} \tag{6.42}$$

To enable the implementation of a microcontroller, the transfer function of the series digital robust control stage $D_{S0}(z)$, based on equation (6.42), is represented by the following **difference equation** [82], [83], [84], [85]:

$$\begin{aligned} y(kT) = {} & 0.0008083\,x(kT) - 0.00153\,x\left[(k-1)T\right] + 0.0007314\,x\left[(k-2)T\right] + \\ & - 1.922\,y\left[(k-1)T\right] - 0.9231\,y\left[(k-2)T\right] \end{aligned} \tag{6.42}$$

From equation (6.37), the transfer function of the forward robust stage can be presented as:

$$G_{F0}(s) = \frac{0.05s + 0.5}{s^{2} + s + 0.5} \tag{6.43}$$

The digital equivalent of the forward controller stage is realized as follows:

```
>> Gf0=tf([0.05 0.5],[1 1 0,5])
Transfer function:
0.05 s + 0.5
------------
s^3 + s^2 + 5
>> Gf0d = c2d(Gf0,0.1,'tustin')
Transfer function:
0.0001785 z^3 + 0.0002974 z^2 + 5.949e-005 z - 5.949e-005
---------------------------------------------------------
        z^3 - 2.901 z^2 + 2.81 z - 0.9036
Sampling time: 0.1
```

Considering the outcome of the applied code the transfer function of the forward robust control stage, presented in the discrete-time domain, is as follows:

$$G_{F0d}(z)=\frac{1.785\times10^{-4}z^3+2.974\times10^{-4}z^2+5.949\times10^{-5}z-5.949\times10^{-5}}{z^3-2.901z^2+2.81z-0.9036}=\frac{M(z)}{E(z)} \quad (6.44)$$

Equation (6.44) can be further expressed as follows:

$$\begin{aligned} z^3M(z)-2.901\,z^2M(z)+2.81zM(z)-0.9036\,M(z)= \\ =1.785\times10^{-4}\,z^3E(z)+2.974\times10^{-4}z^2E(z) \\ +5.949\times10^{-5}zE(z)-5.949\times10^{-5} \end{aligned} \quad (6.45)$$

The series controller output in the discrete-time domain is determined from equation (6.45) as follows:

$$\begin{aligned} M(z)=2.901\,z^{-1}M(z)-2.81z^{-2}M(z)+0.9036z^{-3}M(z) \\ +1.785\times10^{-4}\,E(z)+2.974\times10^{-4}z^{-1}E(z) \\ +5.949\times10^{-5}z^{-2}E(z)-5.949\times10^{-5}z^{-3}E(z) \end{aligned} \quad (6.46)$$

To facilitate the implementation of a forward microcontroller, the transfer function of the forward digital robust control stage $D_F(z)$ is expressed, based on equation (6.46), by the following **difference equation** [82], [83], [84], [85]:

$$\begin{aligned} m(kT)=2.901\,m\left[(k-1)T\right]-2.81\,m\left[(k-2)T\right] \\ +0.9036\,m\left[(k-3)T\right]+ \\ +1.785\times10^{-4}e(kT)+2.974\times10^{-4}e\left[(k-1)T\right] \\ +5.949\times10^{-5}e\left[(k-2)T\right]-5.949\times10^{-5}e\left[(k-3)T\right] \end{aligned} \quad (6.47)$$

The discrete-time control systems described in Figure 6.1 and Figure 6.7 are modified by incorporating the two-stage digital robust controller and are presented in the block diagram shown in Figure 6.10. The design of two robust control stages can be further upgraded to digital filters based on microcontrollers. The combination of

the samplers, the digital filters $D_F(z)$ *and* $D_S(z)$, solving their related difference equations, plus the zero-order hold (ZOH) components, can be represented by microcontrollers incorporating the corresponding ADC, CPU and DAC.

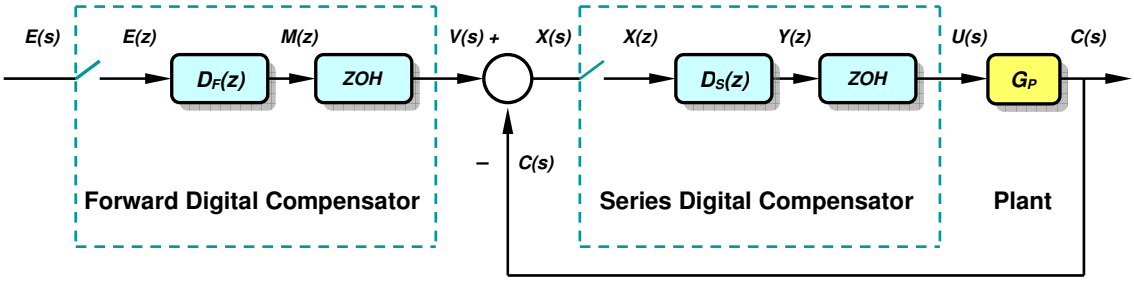

Figure 6.8: *Two-Stage Digital Robust Controller Incorporated into the Control System*

The two-stage digital robust controller, as shown in Figure 6.8, is finally modified to a two-stage robust microcontroller incorporated into the control system as revealed in Figure 6.9. A multiple-input multiple-output MIMO microcontroller is incorporated to perform this task. One of its sections is operating as a forward microcontroller, while a second section, as a series microcontroller. The operation of the systems presented in Figure 6.1 and Figure 6.7 is a complete match of the one shown in Figure 6.9. Microcontrollers offer up to 200 MHz operating frequency. At sampling period T_s = 0.001sec, for the case of system of Type 1, the sampling frequency is f_s = 1 kHz, while at T_s = 0.1sec, or T_s = 0.05 sec for the case of system of Type 0, the sampling frequency is f_s = 10 Hz, or f_s = 20 Hz. All these cases can be managed successfully by a microcontroller having 200 MHz operating frequency.

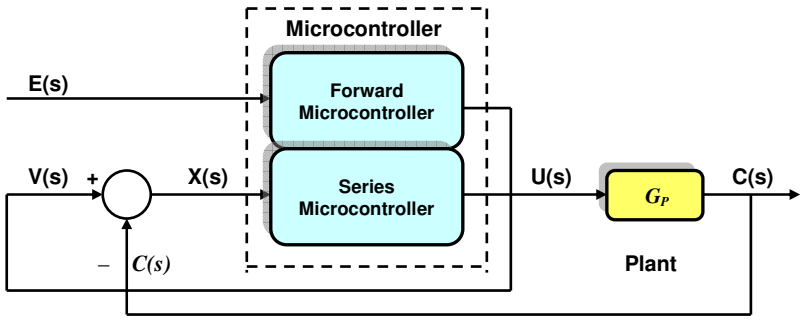

Figure 6.9: *Two-Stage MIMO Microcontroller Incorporated into the Robust Control System*

6.3.2 D-Partitioning Analysis of the Robust Digital System (Case of Analogue Prototype System Type 0)

Based on the total system and taking into consideration the Euler's approximation, the D-Partitioning in terms of the variable time-constant T_1 can be determined from the characteristic equation of (6.20).

$$T_1 = -\frac{0.4\,s^5 + 800.5\,s^4 + 402601.8\,s^3 + 1302000\,s^2 + 1000000\,s + 10}{0.4\,s^6 + 400.8\,s^5 + 1201\,s^4 + 802000\,s^3 + 1000000\,s^2} \qquad (6.48)$$

The D-Partitioning curve shown in Figure 6.10, reflecting the stability of the digital robust control system is plotted by the code:

```
>> T10 = tf([-0.4 -800.5 -402601.8 -1302020 -1000020 -10],[0.4 400.8 1201 802000 1000000 0 0])

Transfer function:
-0.4 s^5 - 800.5 s^4 - 4.026e005 s^3 - 1.302e006 s^2 - 1e006 s - 10
-------------------------------------------------------------------
   0.4 s^6 + 400.8 s^5 + 1201 s^4 + 802000 s^3 + 1e006 s^2

>> T1d0 = c2d(T0,0.05,'tustin')

Transfer function:
-0.4679 z^6 - 0.1035 z^5 + 1.227 z^4 + 0.1889 z^3 - 1.071 z^2 - 0.08544 z + 0.3118
-----------------------------------------------------------------------------------
  z^6 - 0.5854 z^5 - 1.568 z^4 - 0.1615 z^3 + 1.518 z^2 + 0.6484 z - 0.8514

Sampling time: 0.05
>> dpartition(Td0)
```

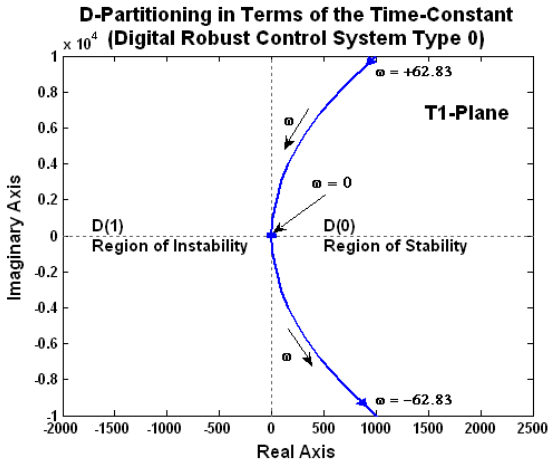

Figure 6.10: *D-Partitioning in the Discrete-Time Domain in Terms of the Variable Time-Constant T_1* ***after the Robust Compensation*** *(Analogue Prototype System Type 0)*

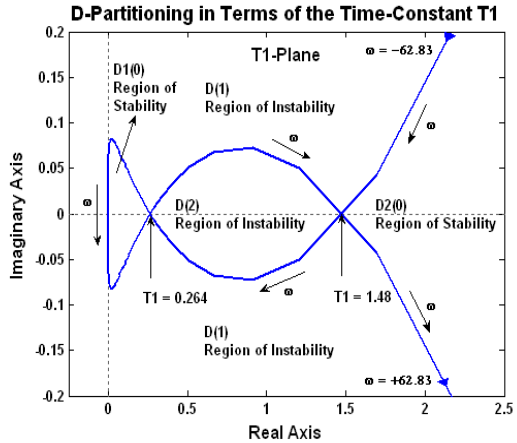

Figure 6.11: *D-Partitioning in the Discrete-Time Domain in Terms of the Variable Time-Constant T_1* ***before the Robust Compensation*** *(Analogue Prototype System Type 0)*

where

$$T_1(z) = \frac{\left[\begin{array}{l} -0.4679\,z^6 - 0.1035\,s^5 + 1.227\,s^4 + \\ +0.1889\,s^3 - 1.071\,s^2 - 0.08544\,z + 0.3118 \end{array}\right]}{\left[\begin{array}{l} z^6 - 0.5854\,z^5 - 1.568\,z^4 - 0.1615\,z^3 + \\ +1.518\,z^2 + 0.6484\,z - 0.8514 \end{array}\right]} \tag{6.49}$$

As seen from Figure 6.10, the D-Partitioning determines two regions in the *T*-Plane that are D(0) and D(1). Only D(0) is a region of stability, since its position is on the left-hand side of the D-Partitioning curve for the frequency variation from $\omega = -62.83$ rad/sec to $\omega = +62.83$ rad/sec. When comparing Figure 6.10 and Figure 6.11, it is evident that the robust controller has improved considerably the margin of stability of the digital compensated system. The analysis in the discrete-time domain confirm that while the original system becomes unstable within the range at 0.264 sec < T_1 < 1.48sec , **after implementing the robust compensation, the digital system will be stable for any positive values of the time-constant,** $T_1 > 0$, since these values are within the region D(0).

6.3.3 Performance Assessment of the Robust Digital System (Case of Analogue Prototype System Type 0)

Again the system's transient responses are used as methodology for the analysis and comparison of the system robustness before and after the compensation. The system's transient responses for different time-constants T_1 = 0.1 sec, T_1 = 0.8 sec and T_1 = 2 sec are determined before the robust compensation by taking into account the equation (6.31) of the original plant analogue prototype and further determining its digital equivalent by applying the bilinear transform as follows:

```
>> Gp01=tf([0 10],[0.04 0.53 1.4 1])
Transfer function:
          10
------------------------------
0.04 s^3 + 0.53 s^2 + 1.4 s + 1
>> Gp08=tf([0 10],[0.32 1.44 2.1 1])
Transfer function:
          10
------------------------------
0.32 s^3 + 1.44 s^2 + 2.1 s + 1

>> Gp20=tf([0 10],[0.8 3 3.3 1])
```

```
Transfer function:
          10
--------------------------
0.8 s^3 + 3 s^2 + 3.3 s + 1

>> Hdp01 = c2d(Gp01,0.1,'tustin')

>> Hdp08 = c2d(Gp08,0.1,'tustin')

>> Hdp20 = c2d(Gp20,0.1,'tustin')

>> Hdp01fb = feedback(Hdp01,1)

Transfer function:
0.002886 z^3 + 0.008658 z^2 + 0.008658 z + 0.002886
-----------------------------------------------------
  1.003 z^3 - 2.435 z^2 + 1.965 z - 0.5071

Sampling time: 0.1
>> Hdp08fb = feedback(Hdp08,1)

Transfer function:
0.0004373 z^3 + 0.001312 z^2 + 0.001312 z + 0.0004373
-----------------------------------------------------
 z^3 - 2.782 z^2 + 2.584 z - 0.798

Sampling time: 0.1
>> Hdp20fb = feedback(Hdp20,1)

Transfer function:
0.0001781 z^3 + 0.0005344 z^2 + 0.0005344 z + 0.0001781
-----------------------------------------------------
 z^3 - 2.819 z^2 + 2.649 z - 0.8288

Sampling time: 0.1
>> step(Hdp01fb,Hdp20fb)
>> step(Hdp08fb)
```

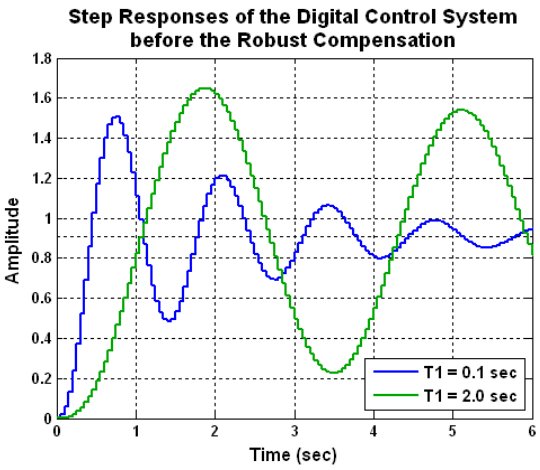

Figure 6.12: *Transient Responses in the Discrete-Time Domain of the Original Control System (Type 0 Prototype, T_1=0.1sec, T_1 =2sec at K=10)*

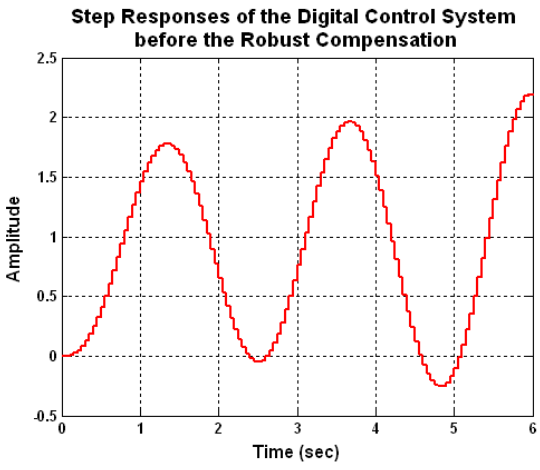

Figure 6.13: *Transient Responses in the Discrete-Time Domain of the Original Control System (Type 0 Prototype, T_1=0.8sec at K=10)*

It is acknowledged that the transient responses of the digital control system, presented in the discrete-time domain, as seen from Figure 6.12 and Figure 6.13,

have a close match with the transient responses of the linear analogue prototype system, presented in Figure 4.13 and Figure 4.14. While the digital control system is stable at T_1 = 0.1 sec and T_1 = 2 sec, it is unstable if T_1 = 0.8 sec. Also it is evident that the performance of the digital control system is quite sensitive to variations of the time-constant T_1.

Further, the digital compensated system is also examined for robustness in the discrete-time domain, considering its transient responses. Initially different random values for the time-constants, T_1 = 0.1 sec, T_1 = 0.8 sec and T_1 = 2 sec are substituted in the transfer function of the analogue prototype system, represented by equation (6.38). The two remote poles $s_{1,2}$ = −1000, j0, added for the physical realization of the serried controller are not considered, since they would have negligible effect on this part of the analysis. Therefore, the results are as follows:

$$G_{T0}(s)_{T_1=0.1} = \frac{s+10}{0.04s^4 + 0.53s^3 + 21.4s^2 + 21s + 10} \tag{6.50}$$

$$G_{T0}(s)_{T_1=0.8} = \frac{s+10}{0.32s^4 + 1.44s^3 + 22.1s^2 + 21s + 10} \tag{6.51}$$

$$G_{T0}(s)_{T_1=2.0} = \frac{s+10}{0.8s^4 + 3s^3 + 23.3s^2 + 21s + 10} \tag{6.52}$$

Since the digital robust control design and analysis are based upon its analogue prototype, t**he transient responses of the robust control system in the discrete-time domain**, representing the time-constant variation, are determined by the code:

```
>> GT001=tf([1 10],[0.04 0.53 21.4 21 10])

Transfer function:
     s + 10
-----------------------------------------
0.04 s^4 + 0.53 s^3 + 21.4 s^2 + 21 s + 10

>> GdT001 = c2d(GT001,0.1,'tustin')

Transfer function:
0.001528 z^4 + 0.004075 z^3 + 0.003057 z^2 + 1.697e-019 z - 0.0005094
-----------------------------------------------------------------------
    z^4 - 1.691 z^3 + 1.087 z^2 - 0.9129 z + 0.5252

Sampling time: 0.1
```

```
>> GT008=tf([1 10],[0.32 1.44 22.1 21 10])

Transfer function:
          s + 10
-----------------------------------------
0.32 s^4 + 1.44 s^3 + 22.1 s^2 + 21 s + 10

>> GdT008 = c2d(GT008,0.1,'tustin')

Transfer function:
0.0004167 z^4 + 0.001111 z^3 + 0.0008334 z^2 + 4.627e-020 z - 0.0001389
-----------------------------------------------------------------------
 z^4 - 3.153 z^3 + 4.023 z^2 - 2.536 z + 0.6683

Sampling time: 0.1
>> GT020=tf([1 10],[0.8 3 23.3 21 10])

Transfer function:
     s + 10
-------------------------------------
0.8 s^4 + 3 s^3 + 23.3 s^2 + 21 s + 10

>> GdT020 = c2d(GT020,0.1,'tustin')

Transfer function:
0.0001855 z^4 + 0.0004946 z^3 + 0.0003709 z^2 + 2.059e-020 z - 6.182e-005
-------------------------------------------------------------------------
 z^4 - 3.457 z^3 + 4.633 z^2 - 2.874 z + 0.6981

Sampling time: 0.1
>> step(GdT001,GdT008,GdT020)
```

It is seen from the code above that the corresponding transfer functions of the robust control system, at T_1 = 0.1 sec, T_1 = 0.8 sec and T_1 = 2 sec, presented in the discrete-time domain are as follows:

$$GdT(z)_{T_1=0.1} = \frac{\left[\begin{array}{c} 0.001528z^4 + 0.004075z^3 + 0.003057z^2 + \\ +1.697\times10^{-19}z - 0.0005094 \end{array}\right]}{z^4 - 1.691z^3 + 1.087z^2 - 0.9129z + 0.5252} \tag{6.53}$$

$$GdT(z)_{T_1=0.8} = \frac{\left[\begin{array}{c} 0.0004167z^4 + 0.001111z^3 + 0.0008334z^2 + \\ +4.627\times10^{-20}z - 0.0001389 \end{array}\right]}{z^4 - 3.153z^3 + 4.023z^2 - 2.536z + 0.6683} \tag{6.54}$$

$$GdT(z)_{T_1=2.0} = \frac{\left[\begin{array}{c} 0.0001855z^4 + 0.0004946z^3 + 0.0003709z^2 + \\ +2.059\times10^{-20}z - 6.182\times10^{-5} \end{array}\right]}{z^4 - 3.457z^3 + 4.633z^2 - 2.874z + 0.6981} \tag{6.55}$$

As seen from Figure 6.14, the coinciding transient responses have insignificant differences, proving the robustness of the compensated digital control system.

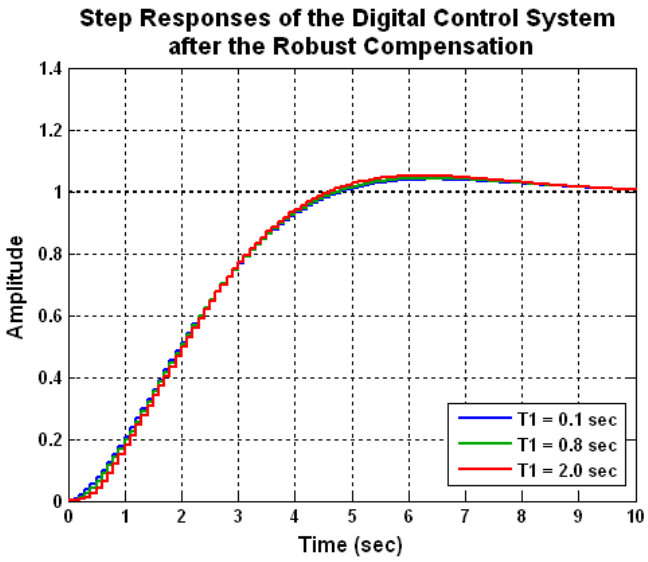

Figure 6.14: *Transient Responses in the Discrete-Time Domain of the Compensated Robust Control System (Type 0 Prototype, T_1=0.1sec, T_1=0.8sec, T_1 =2sec at K=10)*

The system assessment in the discrete-time domain, for cases of T_1 = 0.1 sec, T_1 = 0.8 sec and T_1 = 2 sec is revealed from the following code:

```
>> damp(GdT001)
      Eigenvalue          Magnitude    Equiv. Damping    Equiv. Freq. (rad/s)
 9.50e-001 + 4.58e-002i   9.52e-001     7.18e-001          6.92e-001
 9.50e-001 - 4.58e-002i   9.52e-001     7.18e-001          6.92e-001
-1.05e-001 + 7.54e-001i   7.62e-001     1.57e-001          1.73e+001
-1.05e-001 - 7.54e-001i   7.62e-001     1.57e-001          1.73e+001

>> damp(GdT008)
      Eigenvalue          Magnitude    Equiv. Damping    Equiv. Freq. (rad/s)
 9.51e-001 + 4.65e-002i   9.52e-001     7.08e-001          6.93e-001
 9.51e-001 - 4.65e-002i   9.52e-001     7.08e-001          6.93e-001
 6.25e-001 + 5.88e-001i   8.59e-001     1.98e-001          7.70e+000
 6.25e-001 - 5.88e-001i   8.59e-001     1.98e-001          7.70e+000

>> damp(GdT020)
      Eigenvalue          Magnitude    Equiv. Damping    Equiv. Freq. (rad/s)
 9.52e-001 + 4.78e-002i   9.53e-001     6.91e-001          6.94e-001
 9.52e-001 - 4.78e-002i   9.53e-001     6.91e-001          6.94e-001
 7.76e-001 + 4.07e-001i   8.77e-001     2.63e-001          5.00e+000
 7.76e-001 - 4.07e-001i   8.77e-001     2.63e-001          5.00e+000
```

The evaluation results demonstrate that the digital control system has become quite robust. In spite of the considerable change of the time-constant, from T_1 = 0.1 sec, to

T_1 = 0.08 sec and further to T_1 = 2.0 sec, the system's dominant conjugative poles and the system's relative damping ratio change insignificantly.

For the assessment of the digital robust control system, the case of T_1 = 0.08 sec is taken into account. Its corresponding relative damping ratio is ζ = 0.708, being insignificantly different from the objective ζ = 0.707.

The Percentage Maximum Overshoot (PMO) is determined as:

$$PMO = 100e^{-\pi\zeta/\sqrt{1-\zeta^2}} = 4.1\% \tag{6.56}$$

The settling time t_S is determined considering ζ = 0.708 and ω_n = 0.693 rad/sec:

$$t_{S(5\%)} = \frac{4.6}{\zeta\omega_n} = 9.375 \text{ sec} \tag{6.67}$$

The system's time to maximum overshoot t_m is:

$$t_m = \frac{\pi}{\omega_n\sqrt{1-\zeta^2}} = 6.419 \text{ sec} \tag{6.58}$$

The time ratio is determined as one of the objectives as follows:

$$t_{S(5\%)} / t_m = 1.461 \tag{6.59}$$

As seen from Table 6.2, all the achieved results are meeting the ITAE criterion, since they either match or have values lower than the targeted objectives.

Table 6.2

Comparison between Objectives and Real Results (Type 0)

Specifications	Objectives	Real Results	Consideration
ζ	= 0.707	= 0.708	Close Match
PMO	≤ 4%	= 4.1%	Close Match
$t_{s(5\%)}/t_m$	≤ 2.5	= 1.461	Better

6.4 Summary on Digital Robust Controller Design and Compensated System Analysis in Terms of Robustness

The main contribution of this part of the research is further advancement of the D-partitioning method in its application for analysis of digital control systems. Another contribution is the modified methodology for digital robust control design. **The results of the research clearly demonstrate that the D-Partitioning analysis can be applied to the digital control systems, based on their analogue prototypes, considering the Euler's approximation and implementing the bilinear transform.**

With the aid of the D-Partitioning analysis, **the marginal conditions of the digital system are determined and further the results are confirmed by the system's transient response in the discrete-time domain.**

The original digital control system is examined for robustness. It is established that the system is quite sensitive to any changes of the plant's gain. Based on the ITAE criterion, **a modified strategy for the design of a digital robust controller is suggested, similar to the one for continuous linear control systems.** An optimal digital robust controller is achieved by applying forward-series digital compensation with two degrees of freedom, enforcing a desired system damping and therefore a desired margin of stability.

The compensated digital robust control system is analyzed in the discrete-time domain and the results prove that it becomes quite insensitive to its parameter variations.

For the practical realisation of the digital robust controller, the transfer functions of its two stages are presented by their related difference equations. **A MIMO microcontroller is incorporated into the control system. Its sections can operate accordingly as forward and series robust control stages and can be programmed to solve their corresponding difference equations.** Due to the advantages associated with the digital systems in comparison with analogue systems, the microcontroller robust design strategy is the better option and can be applied for any control system.

Chapter 7

ADVANCED STABILITY ANALYSIS OF NONLINEAR CONTROL SYSTEMS WITH VARIABLE PARAMETERS

This part of the research proposes a strategy for analysis of nonlinear robust control systems with variable parameters. The system's stability and robust assessment is based on the interaction between its nonlinear and linear sections. D-Partitioning, time-response and Describing Function analyses are implemented before and after the robust compensation. The lack of a comprehensive and user friendly analysis tool for nonlinear control systems is the motivating factors for this part of the research.

The D-Partitioning assessment of the linear section of the nonlinear system is a significant part in the overall analysis. It verifies the precondition of a stable linear section, to achieve the overall stability of the system. The interaction assessment between the linear and nonlinear stages of the system with the aid of the Goldfarb stability criterion is based on the Describing Function analysis and examines the stability and the robustness of the resulting limit cycles [89], [90], [91], [92]. **The describing function approach, although being an approximate tool**, enables the application of frequency-response methods to reshape the locus of the plant's linear section and as found in this part of the research to improve system's performance.

7.1 The Concept of the Describing Function Analysis

The concept of the Goldfarb stability criterion also known as the Describing Function analysis can be explained with the aid of the block diagram of a basic nonlinear system. It consists of a nonlinear and a linear component as shown in Figure 7.1.

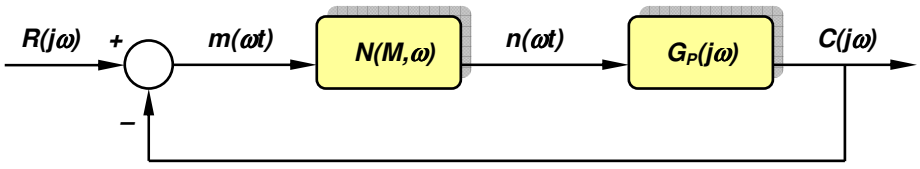

Figure 7.1: Basic Block Diagram of a Closed-loop Nonlinear System

According to the Goldfarb stability criterion, the input signal to the nonlinear element is considered as:

$$m(\omega t) = M \sin \omega t \tag{7.1}$$

The Describing Function analysis assumes that the output of a nonlinear element is a periodic signal having the same fundamental frequency as that of the input where all harmonics and any dc component are neglected.

$$n(\omega t) = N_1 \sin(\omega t + \varphi_1) + N_2 \sin(2\omega t + \varphi_2) + N_3 \sin(3\omega t + \varphi_3) + \ldots \tag{7.2}$$

In most of the cases, the fundamental term is the only significant component of the output of the nonlinear element. **Following the conception of the describing function analysis** [89], [90], [91], [92], **the transfer function of the nonlinear element can be presented as**:

$$N(M, \omega) = \frac{n(\omega t)}{m(\omega t)} \approx \frac{N_1 \sin(\omega t + \varphi_1)}{M \sin \omega t} = \frac{N_1}{M} e^{j\varphi_1} \tag{7.3}$$

Then, the transfer function of the closed-loop system shown in Figure 7.1 becomes:

$$\frac{C(j\omega)}{R(j\omega)} = \frac{N(M,\omega)G_P(j\omega)}{1 + N(M,\omega)G_P(j\omega)} \tag{7.4}$$

Accordingly, the characteristic equation of the closed-loop system is [90], [91], [92]:

$$1 + N(M,\omega)G_P(j\omega) = 0 \tag{7.5}$$

or

$$G_P(j\omega) = -\frac{1}{N(M,\omega)} = Z(M,\omega) \tag{7.6}$$

The characteristic equation (7.5) is also known as the **harmonic balance equation.** The harmonic balance equation is a **necessary condition** for the existence of limit cycles in the nonlinear system [89], [90], [91], [92]. The **approximate** analysis gives good estimates if the low-pass filter hypothesis is strongly verified. The Describing Function analysis can be considered as a linear approximation of a static nonlinearity limited to the first harmonic [89], [90], [91], [92]. The accuracy of the analysis is even better for higher-order systems since they have better low-pass filter characteristics. The harmonic balance equation is similar to the characteristic polynomial function that leads to the Nyquist condition for closed-loop stability.

If equation (7.6) is satisfied, then the system output will be experiencing a limit cycle. This corresponds to the case where the $G_P(j\omega)$ locus passes through a critical point. While in the conventional frequency-response analysis of linear control systems, the critical point is (-1, j0), **in the describing function analysis, the critical point is modified so that the entire $Z(M) = -1/N(M,\omega)$ locus becomes a locus of critical points.** Therefore, the relative location and intersection of the $Z(M) = -1/N(M,\omega)$ locus and the $G_P(j\omega)$ locus will provide the stability information [89], [90], [91], [92].

The stability of a nonlinear system is determined by plotting the $Z(M) = -1/N(M,\omega)$ locus and the $G_P(j\omega)$ locus on a common plane. **There is an important precondition that $G_P(j\omega)$ should correspond to a stable stand-alone system.**

Taking into account **the concept of the Goldfarb stability criterion**, based on the Describing Function analysis, **the criterion for stability of the closed-loop nonlinear system** [89], [90], [91], [92] **is stated as follows:**

1. If the **$Z(M) = -1/N(M,\omega)$ locus is not enclosed by the $G_P(j\omega)$ locus**, the **closed-loop system is stable**. There is no limit cycle at its steady state.
2. If the **$Z(M) = -1/N(M,\omega)$ locus and the $G_P(j\omega)$ locus intersect**, the system output may exhibit a sustained oscillation, or a limit cycle. Such a sustained oscillation is not sinusoidal, but it can be approximated by a sinusoidal one. **This sustained oscillation is characterized by the magnitude M of the $Z(M) = -1/N(M,\omega)$ locus and the value of the frequency ω of the $G_P(j\omega)$ locus at the intersection.** A limit cycle may be stable or unstable.
    a. **If the $G_P(j\omega)$ locus is not enclosing the points of $Z(M) = -1/N(M,\omega)$ locus corresponding to increment of M, the closed-loop system is stable.**
    b. **If the $G_P(j\omega)$ locus is encloses the points of $Z(M) = -1/N(M,\omega)$ locus corresponding to increment of M, the closed-loop system is unstable.**
3. **If the $Z(M) = -1/N(M,\omega)$ locus is completely enclosed by the $G_P(j\omega)$ locus, then the closed-loop system is unstable.**

7.2 Analysis of Nonlinear Control System: A Case of ON-OFF Element with Hysteresis and Saturation

7.2.1 D-Partitioning Applied to the Original Linear Section of the System (Case of Variable Linear Section Prototype Gain *K*)

To achieve a **tight-speed control of a DC motor**, the armature of the separately excited dc motor is connected as one of the ratio arms of a Wheatstone bridge. The interaction of the dc motor and the Wheatstone bridge is a unique arrangement that can be specified as an Active Wheatstone Bridge (AWB) [93], [94]. The bridge is originally balanced at static armature conditions when only the motor armature resistance participates in the bridge ratio arm. Under running conditions, the bridge becomes unbalanced and its output voltage, depending directly to the motor speed, is continuously compared with a preset reference voltage. **The comparator may be a nonlinear element of saturation type or an on-off element with hysteresis.** The system is a combination of a linear and a nonlinear part, as shown in Figure 7.2.

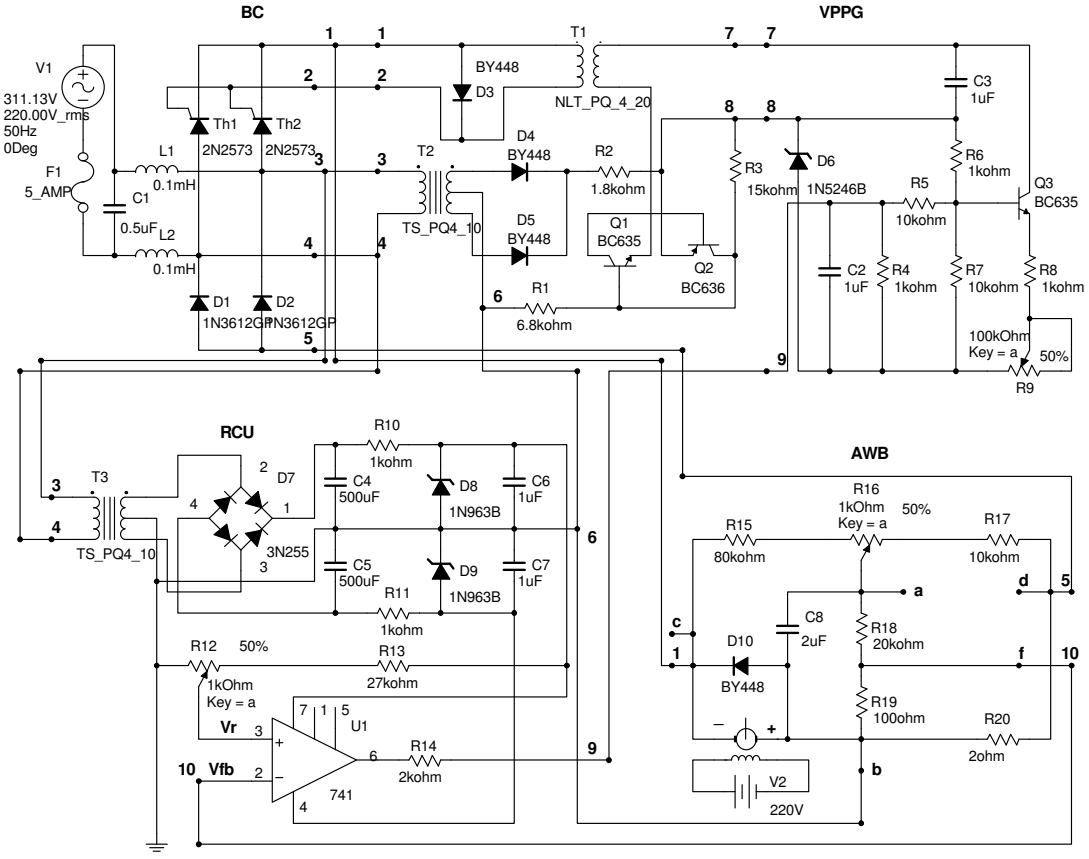

Figure 7.2: *Precise Speed Control System of a DC Motor*

The feedback signal V_{fb} obtained from the (AWB) is applied to a Reference and Comparison Unit (RCU), where it is compared with a reference voltage V_r. The output of the comparator Φ controls a Variable-Phase Pulse Generator (VPPG). Its output signal is controlling the Bridge Converter (BC) thyristor-firing angles. The block diagram of the dc motor control system is presented in Figure 7.3 [87], [88].

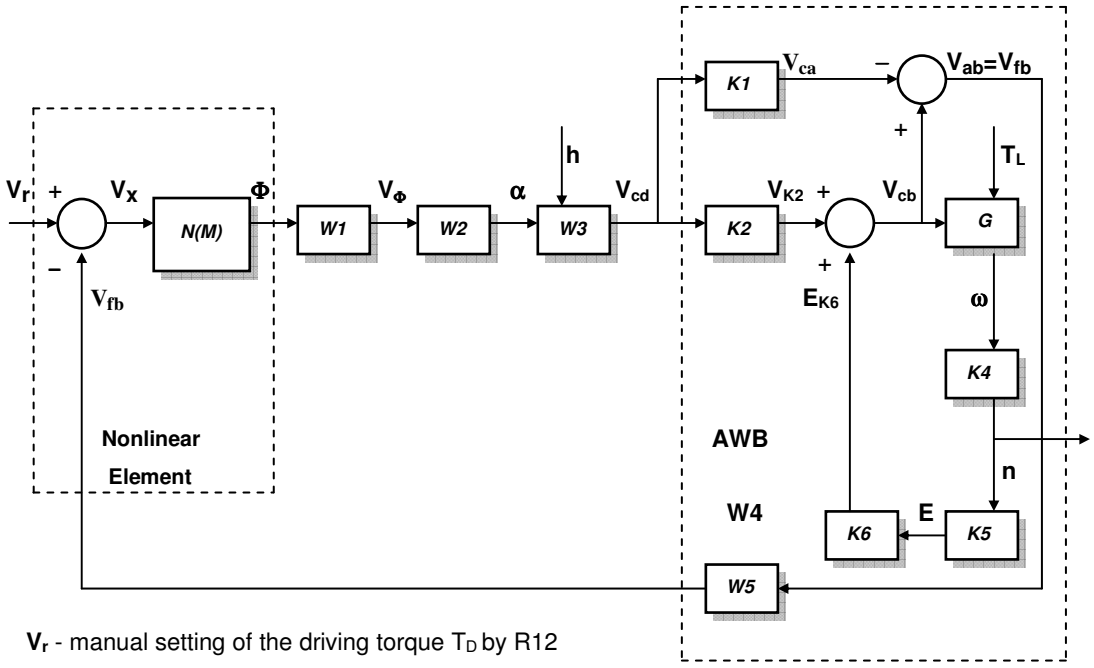

V_r - manual setting of the driving torque T_D by R12

h - manual setting of the firing angle α by R9

T_L - load torque applied to the dc motor

Figure 7.3: *Block Diagram of the DC Motor Speed Control System*

Taking into account the electronic circuit diagram of Figure 7.2 and the block diagram of Figure 7.3, the stages of the linear part of the system are described as follows:

$$W_1(s) = \frac{V_\Phi(s)}{\Phi(x)};\ W_2(s) \times W_3(s) = \frac{V_{cd}(s)}{V_\Phi(s)};\ W_4 = \frac{V_{fb}(s)}{V_{cd}(s)};\ W_5 = \frac{V_{fb}(s)}{V_{ab}(s)}$$

Then the transfer function of the total open loop linear section, as a stand alone system, obtained from the product of W_1, W_2, W_3, and W_4 is presented as:

$$G_P(s) = \frac{21.6K}{(1+0.01s)(1+0.03s)(1+0.042s)} = \frac{21600K}{0.0126s^3 + 1.98s^2 + 72s + 1000} \quad (7.7)$$

where K is a variable parameter

The comparator is represented in the block diagram of Figure 7.3 and Figure 7.4 as a summing point. The nonlinearity shown in the electronic diagram is of saturation type. It can be also designed as an on-off element with hysteresis, represented by a Schmitt trigger. Both nonlinearity types produce similar effect on the system, usually a stable limit cycle with a specific magnitude and frequency of operation. Initially, the nonlinear part is considered as an ON-OFF element with hysteresis, having a describing function *N(M).* It combines a number of nonlinear element properties. A control system of such nature operates in a limit cycle of specific amplitude and frequency that is permissible in particular applications. The block diagram of Figure 7.4, introduces digital robust control to the nonlinear control system.

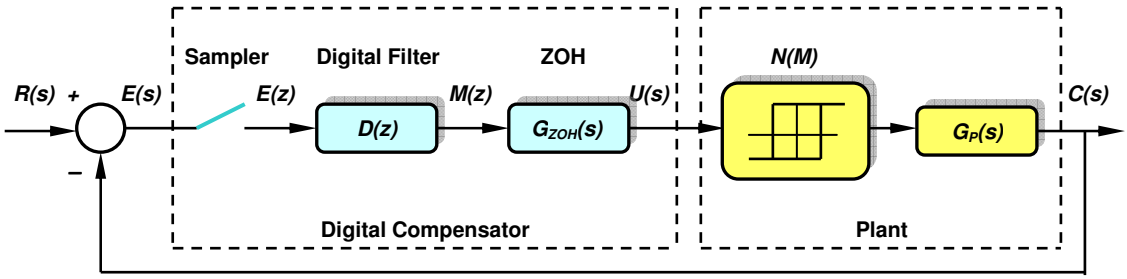

Figure 7.4: *Modified Model of the Control System Including a Digital Compensator*

Considering digital robust control, by implementing the Euler's approximation, the D-partitioning analysis is applied only to the continuous linear section of the plant. The sampling period T_s should be within the range $T_s \leq (0.1\,T_{min}$ to $0.2\,T_{min})$, where T_{min} is the minimum time-constant of the continuous-time system or the analogue plant model prototype [71], [87], [88] as already discussed. The plant's minimum time constant is T_{min} = 0.01sec. Then the sampling period of the system is chosen as T_s = 0.001 sec which satisfies the condition $T_s \leq 0.1\,T_{min}$. Again, the D-Partitioning analysis is applied in the discrete-time domain with the aid of the **bilinear transform** [73], [88]. Initially, the plant's gain K is considered as variable system parameter. Following the steps of the D-Partitioning analysis, the characteristic equation of the continuous independent plant $G_P(s)$ is:

$$G(s) = 0.0126s^3 + 1.98s^2 + 72s + 1000 + 21600K = 0 \qquad (7.8)$$

The variable parameter K of the linear section of the system is determined from equation (7.8) as:

$$K(s) = -\frac{0.0126s^3 + 1.98s^2 + 72s + 1000}{21600} \tag{7.9}$$

Initially, the variable *K(s)* is introduced as a continuous function and next converted into its digital equivalent *K(z)* with the aid of the bilinear transform. Further, the D-Partitioning is achieved in the discrete-time in terms of the variable gain *K* as follows:

```
>> K=tf([-0.0126 -1.98 -72 -1000],[0 21600])
Transfer function:
-0.0126 s^3 - 1.98 s^2 - 72 s - 1000
-----------------------------------
          21600
>> Kd1 = c2d(K,0.001,'tustin')
Transfer function:
-5040 z^3 + 1.436e004 z^2 - 1.363e004 z + 4307
---------------------------------------------
        z^3 + 3 z^2 + 3 z + 1
Sampling time: 0.001
>> dpartition(Kd1)
```

where

$$K(z) = \frac{-5040z^3 + 14360z^2 - 13630z + 4307}{z^3 + 3z^2 + 3z + 1} \tag{7.10}$$

The D-Partitioning curve, plotted in the *K*-plane, is considered within the frequency range $\omega = \pm \omega_s/2 = \pm 2\pi/2T_s = \pm 3141.6$ rad/sec.

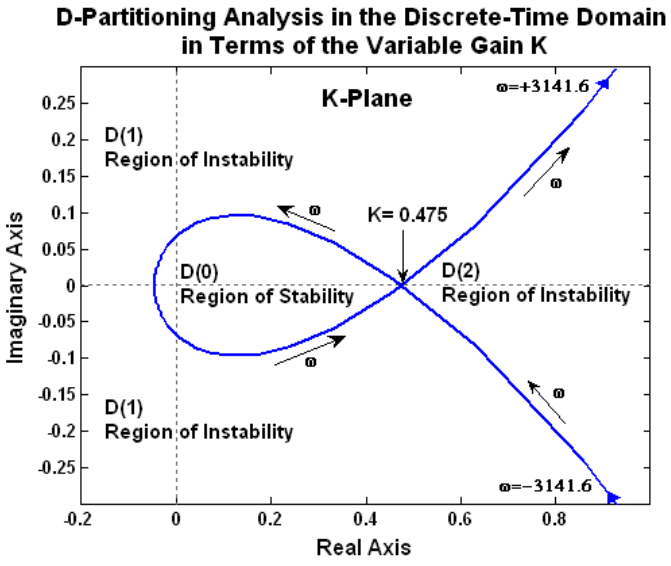

Figure 7.5: *D-Partitioning Analysis in the Discrete-Time Domain of the Linear Section Prototype in Terms of the Variable Gain K*

The D-Partitioning, as seen in Figure 7.5, determines three regions on the *K*-plane: D(0), D(1) and D(2). Only D(0) is the region of stability, being always on the left-hand side of the curve. Therefore, the system will be stable only when its gain is within the range $0 \leq K \leq 0.475$. The negative part of the stability region D(0) is ignored, since the gain *K* may obtain only positive values. The performance of the entire system depends on the stability of the continuous linear section prototype as a stand alone system. The overall system may become even instable if $K \geq 0.475$. There is a need of a robust control to make the system insensitive to parameter uncertainties.

7.2.2 Describing Function Analysis Applied to the Original System in Case of ON-OFF Element with Hysteresis and Variable Linear Gain *K*

The nonlinear section of the discussed plant is an ON-OFF nonlinearity with hysteresis. Its transfer characteristic and its properties are shown in Figure 7.6.

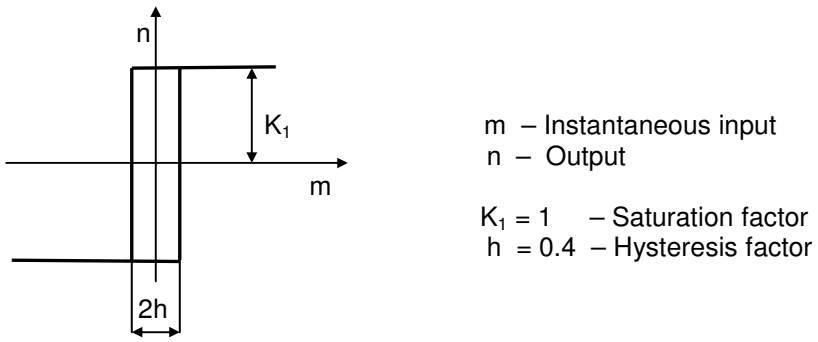

Figure 7.6: *Characteristic and Properties of the ON-OFF Nonlinearity with Hysteresis*

The describing function of the ON-OFF nonlinearity with hysteresis is presented as follows [15], [87], [88], [89]:

$$N(M) = \frac{4K_1}{\pi M} \angle -\sin^{-1}\left(\frac{h}{M}\right) \tag{7.11}$$

where M is the amplitude of the input variations

In this part of the analysis, it is assumed that the parameters of the nonlinearity ($K_1 = 1$ and $h = 0.4$) are constant. The function *Z(M)* is obtained by applying equation (7.11). The results for different amplitudes *M* are shown in Table 7.1.

Table 7.1

N(M) and *Z(M) = −1/N(M)* at Different Input Amplitudes *M*

(Case of ON-OFF Nonlinearity with Hysteresis; $K_1 = 1$ and $h = 0.4$)

M	**0.4**	**0.8**	**1.2**	**1.6**	**2.0**	**2.4**
N(M)	**3.18∠–90°**	**1.59∠–30°**	**1.06∠–20°**	**0.8∠–30°**	**0.63∠–12°**	**0.53∠–10°**
Z(M)	**–0.31∠+90°**	**–0.63∠+30°**	**–0.94∠+20°**	**–1.25∠+14°**	**–1.59∠+12°**	**–1.9∠+10°**

The results from the D-partitioning analysis demonstrate that if $K < 0.475$ the linear prototype section of the system $G_P(s)$ is stable. Under this condition, $G_P(j\omega)$ prototype equivalent in the discrete-time domain, at different gains ($K = 0.1$, 0.25 and 0.4) and $Z(M) = -1/N(M)$ are plotted in the complex plane as shown in Fig. 7.7.

```
>> Gp01=tf([0 2160],[0.0126 1.98 72 1000])

Transfer function:
          2160
-----------------------------------
0.0126 s^3 + 1.98 s^2 + 72 s + 1000

>> Gp025=tf([0 5400],[0.0126 1.98 72 1000])

Transfer function:
          5400
-----------------------------------
0.0126 s^3 + 1.98 s^2 + 72 s + 1000

>> Gp04=tf([0 8640],[0.0126 1.98 72 1000])

Transfer function:
          8640
-----------------------------------
0.0126 s^3 + 1.98 s^2 + 72 s + 1000

>> Gp1d=c2d(Gp01,0.001,'tustin')

Transfer function:
1.984e-005 z^3 + 5.952e-005 z^2 + 5.952e-005 z + 1.984e-005
-----------------------------------------------------------
        z^3 - 2.849 z^2 + 2.704 z - 0.8545

Sampling time: 0.001
>> Gp2d=c2d(Gp025,0.001,'tustin')

Transfer function:
4.96e-005 z^3 + 0.0001488 z^2 + 0.0001488 z + 4.96e-005
-------------------------------------------------------
        z^3 - 2.849 z^2 + 2.704 z - 0.8545

Sampling time: 0.001
>> Gp3d=c2d(Gp04,0.001,'tustin')

Transfer function:
7.936e-005 z^3 + 0.0002381 z^2 + 0.0002381 z + 7.936e-005
---------------------------------------------------------
        z^3 - 2.849 z^2 + 2.704 z - 0.8545

Sampling time: 0.001
>> nyquist(Gp1d,Gp2d,Gp3d)
```

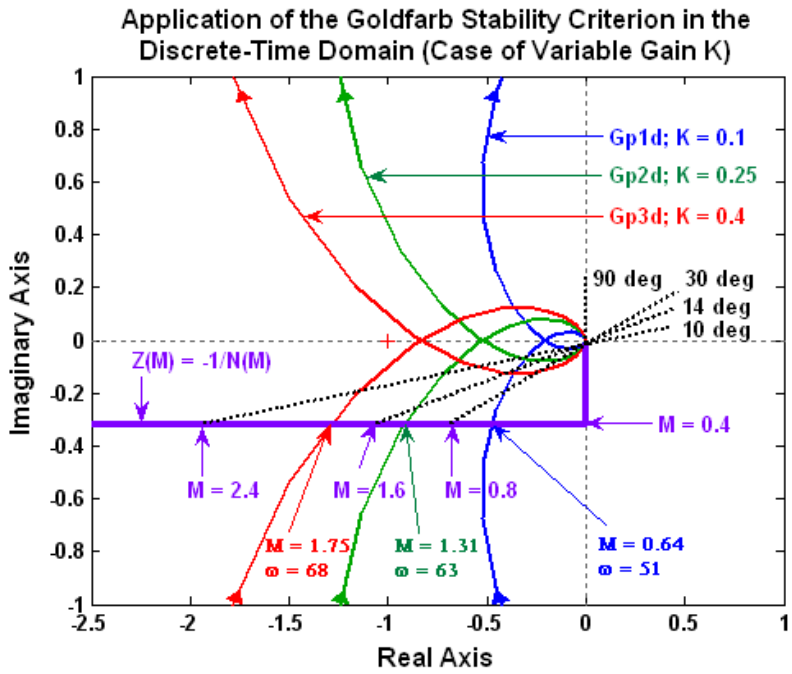

Figure 7.7: *Goldfarb Stability Criterion in the Discrete-Time Domain at Linear Section Prototype Gains: K = 0.1, 0.25, and 0.4 (ON-OFF Nonlinearity with Hysteresis)*

According to the Goldfarb stability criterion, **the control system is stable for any one of the cases**, since as seen from the Figure 7.7, each locus G_{P1d}, G_{P2d} or G_{P3d} is not enclosing the point (-1, j0) of the complex plane and also is not enclosing this part of the characteristic *Z(M)*, corresponding to the increment of *M* after a crossing point *(M,ω),* related to a limit cycle [86], [87], [88], [89]:

Due to the sensitivity to the variation of the linear section gain *K,* the limit cycles are with different amplitude *M* and frequency of oscillation ω as shown in Table 7.2.

Table 7.2

Frequency and Amplitude of Oscillations of the Stable limit Cycles at Different Values of the Gain *K* (Case of ON-OFF Nonlinearity with Hysteresis)

Linear System Gain	*K*	0.1	0.25	0.4
Limit Cycles Properties	*M*	0.64	1.31	1.75
	ω, rad/sec	51	63	68

7.2.3 D-Partitioning Applied to the Original Linear Section Prototype of the System in Case of Variable Time-Constant *T*

If the system's gain has a constant value of $K = 0.25$, while the time-constant related to the AWB stage is variable, equation (7.7) can be modified to:

$$G_P(s) = \frac{21.6K}{(1+0.01s)(1+0.03s)(1+Ts)} = \\ = \frac{5400}{T(0.3s^3 + 40s^2 + 1000s) + 0.3s^2 + 40s + 1000} \tag{7.12}$$

The characteristic equation of the linear stand-alone unity feedback prototype system is:

$$G(s) = T(0.3s^3 + 40s^2 + 1000s) + 0.3s^2 + 40s + 6400 = 0 \tag{7.13}$$

The variable time-constant T is determined from equation (7.13) as follows:

$$T(s) = -\frac{0.3s^2 + 40s + 6400}{0.3s^3 + 40s^2 + 1000s} \tag{7.14}$$

The D-Partitioning is achieved in the discrete-time domain in terms of the variable gain T as follows:

```
>> T = tf([-0.3 -40 -6400],[0.3 40 1000 0])
Transfer function:
 -0.3 s^2 - 40 s - 6400
------------------------
0.3 s^3 + 40 s^2 + 1000 s
>> Td = c2d(T,0.001,'tustin')
Transfer function:
-0.0005021 z^3 + 0.0004297 z^2 + 0.0004921 z - 0.0004397
---------------------------------------------------------
 z^3 - 2.872 z^2 + 2.747 z - 0.8751
Sampling time: 0.001
>> dpartition(Td)
```

where

$$T(z) = -\frac{-0.0005021z^3 + 0.0004297z^2 + 0.0004921z - 0.0004397}{z^3 - 2.872s^2 + 2.747z - 0.8751} \tag{7.15}$$

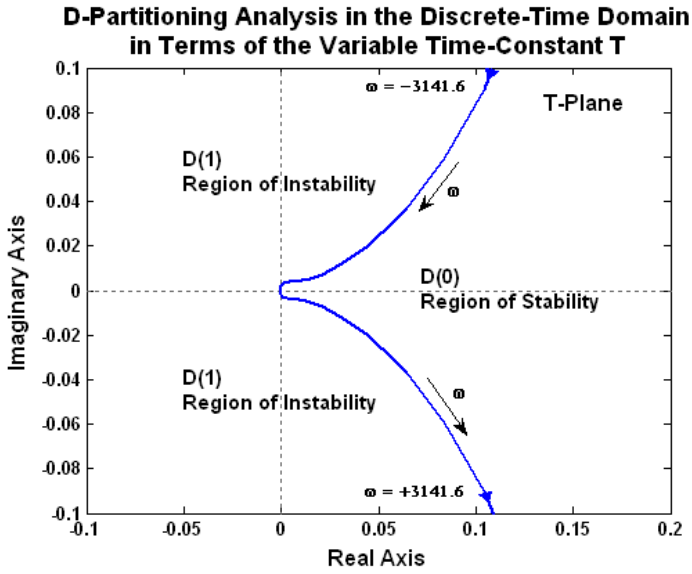

Figure 7.8: *D-Partitioning Analysis in the Discrete-Time Domain of the Linear Section Prototype in Terms of the Variable Time-Constant T*

As seen from Figure 7.8, the D-Partitioning determines two regions in the complex T-Plane: D(0) and D(1). D(0) is the region of stability, being on the left-hand side of the D-Partitioning curve within the frequency range ±3141.6 rad/sec. The linear prototype section will be stable for any positive value of the time-constant $T > 0$.

7.2.4 Describing Function Analysis in Case of ON-OFF Element with Hysteresis in Case of Variable Linear Section Prototype Time-Constant *T*

The linear section prototype $G_P(j\omega)$ equivalent in the discrete-time domain, at a gain value of $K = 0.25$ and different time-constants ($T = 0.01$ sec, 0.05 sec, and 0.1 sec) together with $Z(M) = -1/N(M)$, resulting from Table 7.1, are plotted in the complex plane as shown in Fig. 7.7. Considering equation (7.12), the following results are obtained:

$$G_{P0.01}(s) = \frac{5400}{0.003s^3 + 0.7s^2 + 50s + 1000} \tag{7.16}$$

$$G_{P0.05}(s) = \frac{5400}{0.015s^3 + 2.3s^2 + 90s + 1000} \tag{7.17}$$

$$G_{P0.1}(s) = \frac{5400}{0.03s^3 + 4.3s^2 + 140s + 1000} \tag{7.18}$$

```
>> Gp001=tf([0 5400],[0.003 0.7 50 1000])
Transfer function:
          5400
-------------------------------
0.003 s^3 + 0.7 s^2 + 50 s + 1000
>> Gp005=tf([0 5400],[0.015 2.3 90 1000])
Transfer function:
          5400
-------------------------------
0.015 s^3 + 2.3 s^2 + 90 s + 1000
>> Gp01=tf([0 5400],[0.03 4.3 140 1000])
Transfer function:
          5400
-------------------------------
0.03 s^3 + 4.3 s^2 + 140 s + 1000
>> Gp001d=c2d(Gp001,0.001,'tustin')
Transfer function:
0.0002007 z^3 + 0.0006022 z^2 + 0.0006022 z + 0.0002007
-------------------------------------------------------
        z^3 - 2.777 z^2 + 2.569 z - 0.7918
Sampling time: 0.001
>> Gp005d=c2d(Gp005,0.001,'tustin')
Transfer function:
4.174e-005 z^3 + 0.0001252 z^2 + 0.0001252 z + 4.174e-005
---------------------------------------------------------
          z^3 - 2.852 z^2 + 2.71 z - 0.8578
Sampling time: 0.001
>> Gp01d=c2d(Gp01,0.001,'tustin')
Transfer function:
2.097e-005 z^3 + 6.292e-005 z^2 + 6.292e-005 z + 2.097e-005
-----------------------------------------------------------
          z^3 - 2.862 z^2 + 2.728 z - 0.8664
Sampling time: 0.001
>> nyquist(Gp001d,Gp005d,Gp01d)
```

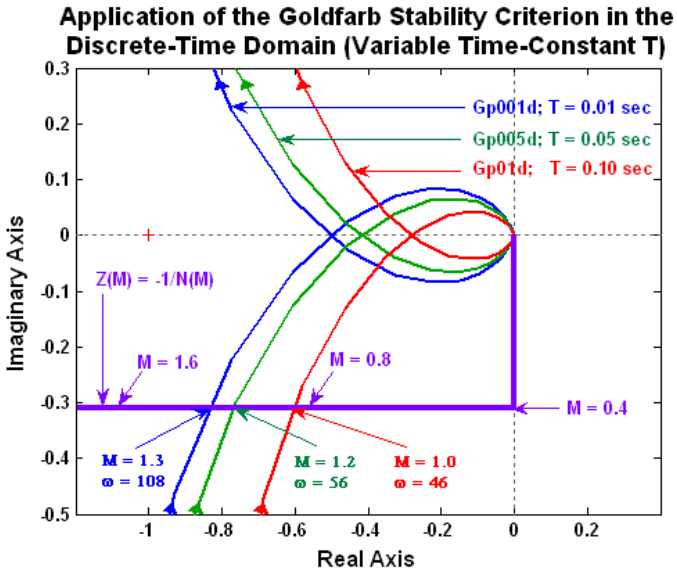

Figure 7.9: *Goldfarb Stability Criterion in the Discrete-Time Domain at Variable Time-Constant: T = 0.01, 0.05, and 0.1sec (ON-OFF Nonlinearity with Hysteresis)*

Again, the control system is stable for any one of the cases, since the linear prototype section is stable for any positive value of the time-constant *T* and also each linear locus is not enclosing this part of the characteristic *Z(M)*, corresponding to the increment of *M* after a crossing point *(M,ω),* related to a limit cycle [87], [88], [89].

It is also seen from Figure 7.9 that the system is sensitive to the variation of the linear section time-constant *T.* The limit cycles of the three cases have different amplitude *M* and frequency of oscillation ω as shown in Table 7.3.

Table 7.3

Frequency and Amplitude of Oscillations of the Stable limit Cycles at Different Values of the Time-Constant *T* (ON-OFF Nonlinearity with Hysteresis)

Linear System Gain	*T*	0.01	0.05	0.1
Limit Cycles Properties	*M*	1.3	1.2	1.0
	ω, rad/sec	108	56	46

7.2.5 Describing Function Analysis in Case of a Saturation Nonlinearity in Case of Variable Linear Section Prototype Gain *K*

Another option of system is the nonlinear section of the plant to be of a saturation type. Then its transfer characteristic and its properties are shown in Figure 7.10.

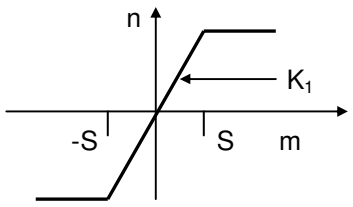

m – Instantaneous input
n – Output

K_1 = 1.57 – Slope
S = 1 – Saturation factor

Figure 7.10: *Characteristic and Properties of the Saturation Nonlinearity*

The describing function of the saturation nonlinearity is presented as follows [89]:

$$N(M) = \frac{2K_1}{\pi}\left[\sin^{-1}\left(\frac{S}{M}\right) + \left(\frac{S}{M}\right)\sqrt{1-\left(\frac{S}{M}\right)^2}\right] \tag{7.19}$$

where *M* is the amplitude of the input variations

Again, the same condition for stability is valid and if $K < 0.475$, the linear section of the system $G_P(s)$ is stable. Under this condition, the digital equivalent of $G_P(j\omega)$ at different gains ($K = 0.1$, 0.25 and 0.4) and $Z(M) = -1/N(M)$ are plotted in the complex plane as shown in Fig. 7.11. For this part of the analysis again it is assumed that the parameters of the nonlinearity $K_1 = 1.57$ and $S = 1$ are constant or change insignificantly. The nonlinear function $Z(M)$ is plotted from the relationship shown in equation (7.19). The results for different values of M are shown in Table 7.4.

Table 7.4

N(M) and *Z(M) = –1/N(M)* at Different Input Amplitudes *M*

(Case of Saturation Nonlinearity; $K_1 = 1.57$ and $S = 1$)

M	1	2	4	10
N(M), rad	1.57	0.95	0.5	0.195
Z(M), 1/rad	–0.63	–1.05	–2.0	–5.1

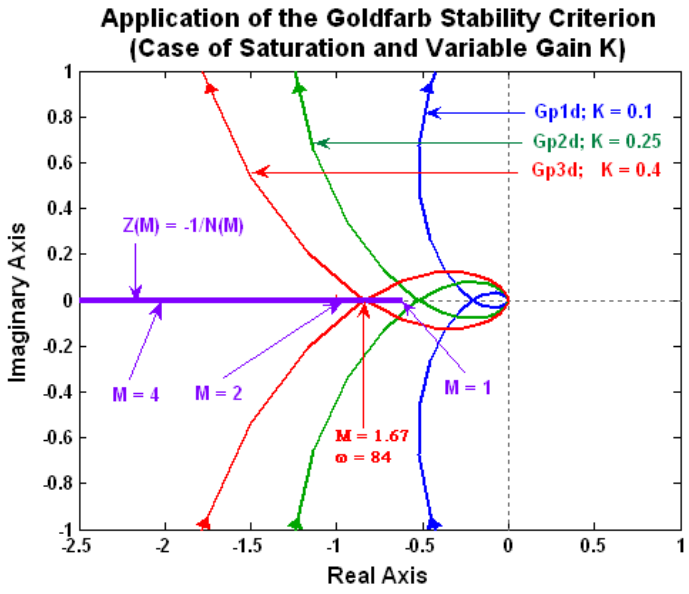

Figure 7.11: *Goldfarb Stability Criterion at Different Linear Section Gains* $K = 0.1$, 0.25 and 0.4 *(Case of Saturation Nonlinearity)*

By applying the Goldpharb stability criterion, the conclusion is that the control system is stable for each of the cases, since the digital equivalents of the linear prototype section $G_{P1d}(j\omega)$, $G_{P2d}(j\omega)$ or $G_{P3d}(j\omega)$ are not enclosing this part of $Z(M)$ corresponding to the increment of M after crossing a point (M,ω) of a limit cycle [15], [87], [88], [89].

It is seen in the Figure 7.11 that the intercept point between *Z(M)* and $G_{P3d}(j\omega)$ corresponds to a stable limit cycle with properties (M = 0.84, ω = 84 *rad/sec)*, while *Z(M)* is not crossing $G_{P1d}(j\omega)$ and $G_{Pd2}(j\omega)$, cases for which the system is still stable. The analysis results are shown in Table 7.5 and are obtained by calculation and confirmed by the interaction with the MATLAB graph.

Table 7.5
Frequency and Amplitude of Oscillations of the Stable limit Cycles at Different Values of the Gain *K* (Case of Saturation Nonlinearity)

Linear System Gain	*K*	0.1	0.25	0.4
Limit Cycles Properties	M	-	-	1.67
	ω, rad/sec	-	-	84

7.3 Analysis of Nonlinear Control System: Case of a Backlash

7.3.1 D-Partitioning Applied to the Original Linear Section Prototype

Backlash is one of the most important non-linearities that limit the performance of speed and position control in industrial, robotics, automotive, automation and other applications. The control of systems with backlash has been the subject of study since the 1940s. Surprisingly few control innovations have been presented since the early path breaking papers that introduced the describing function analysis of systems with backlash.

Figure 7.12 represents a nonlinear servo system consisting of an amplifier, dc motor, a gear train mechanism and a load. Its lineal part that is preliminary reduced and approximated to a second order system with a transfer function $G_P(s)$. Its nonlinear part is a backlash element, having a describing function *N(M)* [95], [96].

The position of the output is fed back to the input, to generate the error signal. A control system of such type may create a limit cycle of specific amplitude and frequency, which in this case is an undesirable effect and should be avoided.

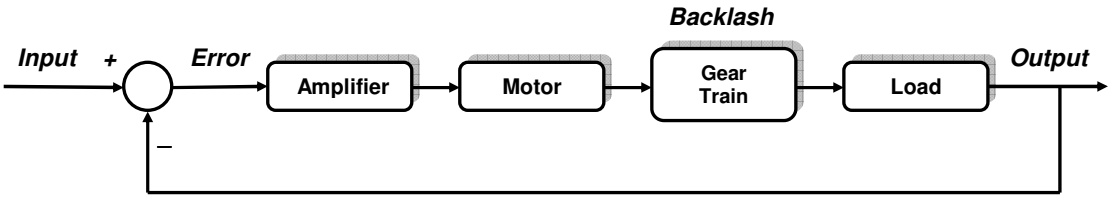

Figure 7.12: *Block Diagram of a Servo System with Backlash*

The gear train consists of two gears. It is assumed that the inertia of the gears and load element is negligible compared with that of the motor. It is also assumed that there is no backlash between the motor shaft and the first gear. Backlash exists only between the first and the second gear. Also it is assumed that the gear ratio between the two gears is unity. The amplifier-motor combination transfer function and the backlash nonlinearity are presented as follows:

$$G_P(s) = \frac{K}{s(1+s)}; \qquad N(M); \tag{7.20}$$

The block diagram of the system can be modified as seen in Figure 7.13. In addition It includes a digital compensator.

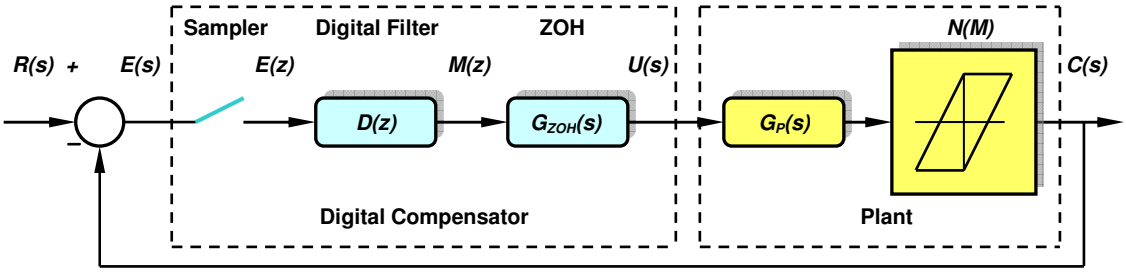

Figure 7.13: *Modified Model of the Backlash Control System with the Digital Compensator*

The D-partitioning analysis is applied in the discrete-time domain with the aid of the **bilinear transform**. It is applied to the continuous linear section prototype of the plant by implementing the Euler's approximation. The plant's minimum time constant is T_{min} = 1sec. Then the sampling period is chosen as T_s = 0. 1 sec which satisfies the condition $T_s \leq 0.1\,T_{min}$.

The plant's gain *K* is the variable parameter due to some temperature effects on the system. To determine the gain marginal limits, the method of the D-Partitioning is applied similarly to the cases of continuous systems [89], [90]. If the continuous linear section prototype of the plant $G_p(s)$ is involved in a unity feedback as a stand-alone stage, its characteristic equation becomes:

$$G(s) = s^2 + s + K = 0 \tag{7.21}$$

Then, the variable parameter *K* is determined as:

$$K(s) = -s^2 - s \tag{7.22}$$

The D-Partitioning in terms of *K*, as seen from Figure 7.14, is achieved from equation (7.22) by applying the following code:

```
>> K=tf([-1 -1 0],[0 1])
Transfer function:
-s^2 - s
>> Kd=c2d(K,0.1,'tustin')
Transfer function:
-420 z^2 + 800 z - 380
----------------------
  z^2 + 2 z + 1
Sampling time: 0.1
>> nyquist(Kd)
```

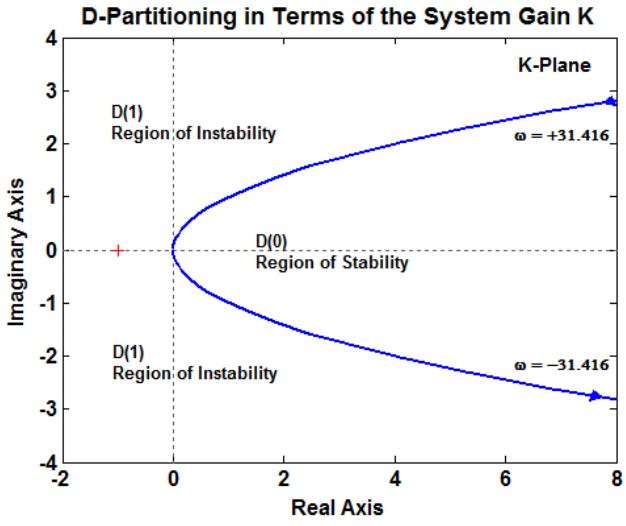

Figure 7.14: *D-Partitioning Analysis in the Discrete-Time Domain of the Linear Section Prototype in Terms of the Variable Gain K (Case of the Nonlinear Backlash System)*

The D-Partitioning curve is achieved within the range –31.416 rad/sec ≤ ω ≤ +31.416 rad/sec. As seen from Figure 7.14, the D-Partitioning determines only two regions on the *K*-plane: D(0) and D(1). D(0) is the region of stability, being always on the left-hand side of the D-Partitioning curve. This implies that the system is stable for any positive gain value or within the range 0 < *K*. However, it will be seen that the interaction between the linear and the nonlinear sections of the system will cause problems of the system operation for high values of the gain *K* if the system is not compensated and made robust.

7.3.3 Describing Function Analysis in Case of a Backlash Nonlinear Element and Variable Linear Section Prototype Gain *K*

The nonlinear section of the servo system plant is backlash nonlinearity [95], [96]. Its transfer characteristic and properties are shown in Figure 7.15.

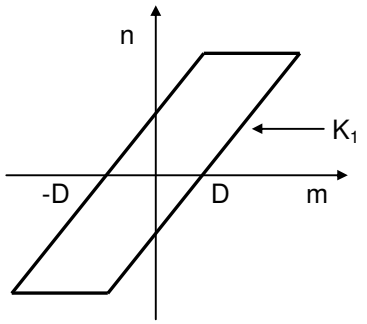

m – Instantaneous input
n – Output
D – Dead Zone

K_1 = 1 – Slope

Figure 7.15: *Characteristic and Properties of the Backlash*

The describing function of the backlash is presented as follows [15], [89], [90]:

$$N(M) = \frac{1}{M}\sqrt{A^2 + B^2}\ \angle \tan^{-1}\left(\frac{A}{B}\right) \tag{7.23}$$

$$A = \frac{2D}{\pi}\left(\frac{2D}{M} - 2\right) \tag{7.24}$$

$$B = \frac{M}{\pi}\left[\frac{\pi}{2} - \sin^{-1}\left(\frac{2D}{M} - 1\right) - \left(\frac{2D}{M} - 1\right)\cos\sin^{-1}\left(\frac{2D}{M} - 1\right)\right] \tag{7.25}$$

where *M* is the amplitude of the input variations

It was established that the linear section of the system $G_P(s)$ is stable for any value of the gain K. Under this condition, $G_P(j\omega)$ at different gains ($K = 4$, and $K = 5$), together with $Z(M) = -1/N(M)$ are plotted in the complex plane as shown in Fig. 7.16. It is assumed that the parameters of the nonlinearity are constant $K_1 = 1$ and $D = 1$ are constant or change insignificantly.

The function $Z(M)$ is plotted by applying equation (7.23). The results for different amplitudes M are shown in Table 7.6.

Table 7.6

$N(M)$ and $Z(M) = -1/N(M)$ at Different Input Amplitudes M

(Case of a Backlash; $K_1 = 1$ and $D = 1$)

M	4	3	2	1.5	1.25	1.1
$N(M)$	0.85∠–15°	0.75∠–25°	0.6∠–36°	0.4∠–45°	0.2∠–55°	0.1∠–65°
$Z(M)$	–1.18∠+15°	–1.3∠+25°	–1.67∠+35°	–2.5∠+45°	–5∠+55°	–10∠+65°

```
>> Gp1=tf([0 4],[1 1 0])
Transfer function:
  4
-------
s^2 + s
>>  Gp2=tf([0 5],[1 1 0])
Transfer function:
  5
-------
s^2 + s
>> G1d=c2d(Gp1,0.1,'tustin')
Transfer function:
0.009524 z^2 + 0.01905 z + 0.009524
-----------------------------------
  z^2 - 1.905 z + 0.9048
Sampling time: 0.1
>> G2d=c2d(Gp2,0.1,'tustin')
Transfer function:
0.0119 z^2 + 0.02381 z + 0.0119
-------------------------------
 z^2 - 1.905 z + 0.9048
Sampling time: 0.1
>> nyquist(G1d,G2d)
```

As seen from Figure 7.16, there are two intersections between the loci of $Z(M)$ with each one of the loci $G_{P1}(s)$ and $G_{P2}(s)$. Applying the Goldfarb stability criterion reveals

that the point on the $G_{P1}(s)$ loci (M = 2, ω = 1.6) and the point on the $G_{P2}(s)$ loci (M = 1.5, ω = 1.2) correspond to stable limit cycles.

The other two intersections between the *N(M)* loci with each one of the loci $G_{P1}(s)$ and $G_{P2}(s)$, correspond to unstable limit cycles, since $G_{P1}(s)$ and $G_{P2}(s)$ enclose this part of *Z(M)*, related to increment of *M*. Although, in this case, the unstable limit cycles can still be described theoretically with their amplitude and frequency of oscillation, they cannot physically occur.

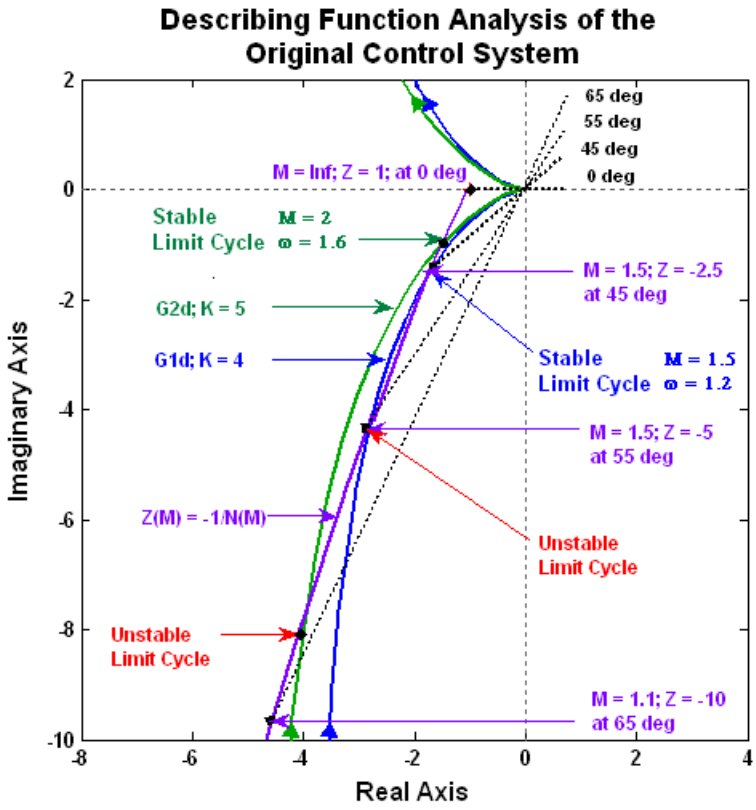

Figure 7.16: *Application of the Describing Function Analysis in the Discrete-Time Domain at Linear Section Prototype Gains: K = 4 and K = 5 (Case of a Backlash)*

Further, the stable limit cycles are undesirable effect for this system. Also, if the two loci are tangent, or almost tangent, a limit cycle or a slowly damped oscillation may occur. To avoid the limit-cycle behavior, the gain of the amplifier must be decreased sufficiently so that the $G_P(s)$ locus is placed well apart the *Z(M)* locus. Alternatively, the application of a robust controller will put apart the $G_P(s)$ and the *Z(M)* loci, still keeping the desirable system gain and maintaining the system robust.

7.4 Summary on the Advancement of the Stability Analysis for Nonlinear Systems with Variable Parameters

Stability analysis of nonlinear control systems is achieved by examining their linear sections with the aid of the D-Partitioning and further assessing the interaction between their linear prototype sections and nonlinear sections. The advanced D-Partitioning method is applied again in discrete-time domain.

The stability assessment of the overall nonlinear systems is achieved by applying the Goldfarb stability criterion, based on the Describing Function analysis. Although it is considered as an approximate tool, it is apparent that by applying it, useful results with practical accuracy are achieved.

Systems of three different most common types of nonlinear elements are examined: cases of on-off element with hysteresis, saturation and backlash. The performances of all of them show that they are quite sensitive to the variation of the gain K of the plant's linear prototype. The performance of one of them, the DC Motor Speed Control System, is also examined in case of variation of one of its time-constants T. This demonstrates that the original system is also quite sensitive to the variation of the time-constant T.

For all of the discussed control systems in this chapter, it is assumed that the parameters of the nonlinearities are constant or change insignificantly. The reasons for this assumption are mainly two. First, in most of the real-life systems and especially in the systems demonstrated for this research, the practice is proving that the nonlinear properties like saturation factor, hysteresis factor, dead zone, slope, etc. remain almost constant or vary insignificantly. As a second point, after the application of the designed in the next chapter digital robust controller, it will influence directly and mainly the linear section of the system, reshaping its locus and in this way improving the stability, the performance and the robustness of the overall nonlinear control system. The robust controller also improves the system's robustness in case of variation of some of the nonlinear properties within specific limits. This is demonstrated in the next chapter.

Chapter 8

DESIGN OF A DIGITAL ROBUST CONTROLLER FOR NONLINEAR CONTROL SYSTEMS WITH VARIABLE PARAMETERS

Like in the previously discussed chapters, a digital robust controller design employs a two-step compensation operating in two degrees of freedom. To achieve an optimal robust control, the ITAE criterion is considered. **The design is based on the linear section prototype of the system and again is considered as a general robust control design, not restricted to some specific limits.** Nevertheless, practice shows that it affects the robustness of the total nonlinear control system within some quite reasonable bounds in respect to the original values of the variable parameters.

8.1 Robust Controller Design: System Nonlinearity: Case of ON-OFF Element with Hysteresis and Case of Saturation

8.1.1 Design of the Robust Controller Stages

A similar procedure, like in Chapter 6 is implemented. Initially, the DC Motor Speed Control System is considered, described in Chapter 7. The objective is that the robust control system should become a system with two dominant poles, enforced to the linear section prototype, satisfying specific performance criteria. To achieve this objective, the following design steps are considered:

Step 1: The closed-loop transfer function of the linear section of the plant as a stand alone system is determined from equation (7.7) as follows:

$$G_{CL_O}(s) = \frac{21600K}{0.0126s^3 + 1.89s^2 + 72s + 1000 + 21600K} \tag{8.1}$$

Step 2: The optimal value of the gain K corresponding to the closed-loop relative damping ratio $\zeta=0.707$ is determined by the following code and interactive procedure:

```
>>  K=[0:0.0001:0.11];
>> for n=1:length(K)
 G_array(:,:,n)=tf([21600*K(n)],[0.0126 1.89 72 1000+21600*K(n)]);
end
>> [y,z]=damp(G_array);
>>  plot(K,z(1,:))
```

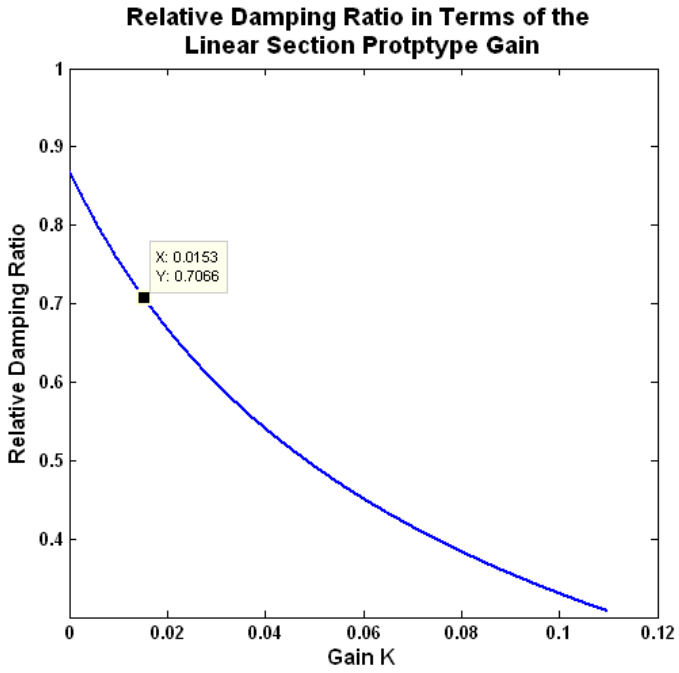

Figure 8.1: *Determination of the Optimal Gain K (Case of DC Motor System)*

As seen from Figure 8.1, if the relative damping ration is ζ = 0.7066 ≈ 0.707 the related gain is K = 0.0153.

Step 3: By substituting K = 0.0153 in equation (8.1) the transfer function of the closed-loop system is modified to:

$$G_{CL_O}(s)=\frac{330.48}{0.0126s^3+1.89s^2+72s+1000+21600K} \tag{8.2}$$

This condition corresponds to the relative damping of ζ = 0.707 and to the desired closed-loop poles –22.4 ± j22.4 that are determined by the code:

```
>> GCL =tf([330.48],[0.0126 1.89 72 1330.48])
Transfer function:
          330.5
-----------------------------------
0.0126 s^3 + 1.89 s^2 + 72 s + 1330

>> damp(GCL)
  Eigenvalue                 Damping    Freq. (rad/s)
-2.24e+001 + 2.24e+001i      7.07e-001  3.17e+001
-2.24e+001 - 2.24e+001i      7.07e-001  3.17e+001
-1.05e+002                   1.00e+000  1.05e+002
```

Taking into account that for this system T_s = 0.001 sec, by applying the **bilinear transform** the optimal open-loop and closed-loop transfer functions of the system are determined in the discrete-time domain:

```
>> GdCL = c2d(GCL,0.001,'tustin')
Transfer function:
3.046e-006 z^3 + 9.137e-006 z^2 + 9.137e-006 z + 3.046e-006
-----------------------------------------------------------
 z^3 - 2.855 z^2 + 2.716 z - 0.8606
Sampling time: 0.001

>> damp(GdCL)
  Eigenvalue                 Magnitude  Equiv. Damping  Equiv. Freq. (rad/s)
9.78e-001 + 2.19e-002i       9.78e-001  7.07e-001       3.17e+001
9.78e-001 - 2.19e-002i       9.78e-001  7.07e-001       3.17e+001
9.00e-001                    9.00e-001  1.00e+000       1.05e+002
```

It is apparent that there is a complete match between the corresponding pole location on the s-plane and on the z-plane. Both, the optimal plant analogue prototype and its optimal digital equivalent are having exactly the same relative damping of ζ = 0.707. Due to this conclusion, the controller stages are designed in the continuous-time domain and further converted into their discrete-time equivalents.

Step 4: The two controller zeros can be placed at –22 ± j22. Then, the transfer function of the series controller stage is:

$$G_S(s) = \frac{(s+22+j22)(s+22-j22)}{968(s+1000)^2} = \frac{s^2+44s+968}{968(s+1000)^2} \tag{8.3}$$

Usually, for the physical realization of the series controller stage two remote poles, can be added. However, for straightforwardness of the analysis, they are not included in the further robust controller design procedure, since they will cause insignificant effect on the final system performance.

Step 5: The series connection of the series robust controller $G_S(s)$ and the continuous linear prototype section of the plant as a stand alone system $G_P(s)$ results in the product of their transfer functions:

$$G_{OL}(s) = G_S(s)G_P(s) = \frac{22.314K(s^2 + 44s + 968)}{0.0126s^3 + 1.98s^2 + 72s + 1000} \tag{8.4}$$

Step 6: Further, $G_{OL}(s)$ is involved in a unity feedback and the closed-loop transfer function is determined as:

$$G_{CL}(s) = \frac{22.314K(s^2 + 44s + 968)}{0.0126s^3 + 1.98s^2 + 72s + 1000 + 22.314K(s^2 + 44s + 968)} \tag{8.5}$$

Step 7: As seen in the equation (8.5), in order to avoid the closed-loop zero - pole cancelation, a forward controller G_F(s), as presented in equation (8.6), is added to the closed-loop system. It cancels the zeros of the closed-loop transfer function G_{CL}(s).

$$G_F(s) = \frac{968}{s^2 + 44s + 968} \tag{8.6}$$

Step 8: The transfer function of the total compensated robust control system is:

$$G_T(s) = G_F(s)G_{CL}(s) =$$

$$= \frac{21.6K}{0.0000126s^3 + 0.00198s^2 + 0.072s + 1 + 0.022314K(s^2 + 44s + 968)} \tag{8.7}$$

Realizing the series and forward robust controller stages is similar to the approach already used in Chapter 6 by implementing digital filters based on microcontrollers [95], [96], [102], [103]. Taking into account equation (8.3), the series robust control stage can be presented in the discrete-time domain by the following code:

```
>> Gs=tf([1 44 968],[968 1936000 968000000])
Transfer function:
  s^2 + 44 s + 968
-------------------------------
968 s^2 + 1.936e006 s + 9.68e008
>>  Gds=c2d(Gs,0.001,'tustin')
Transfer function:
0.0004693 z^2 - 0.0009181 z + 0.0004491
---------------------------------------
 z^2 - 0.6667 z + 0.1111
Sampling time: 0.001
```

From the code, the transfer function of the series digital robust stage is presented in the discrete-time domain as follows:

$$G_{ds}(z) = \frac{0.0004693\ \mathrm{z}^2 - 0.0009181\ \mathrm{z} + 0.0004491}{\mathrm{z}^2 - 0.6667\ \mathrm{z} + 0.1111} = \frac{Y(z)}{X(z)} \tag{8.8}$$

The output of the series controller in the discrete-time domain is determined from equation (8.8) as follows:

$$\begin{aligned} Y(z) = {} & 0.0004693\ X(z) - 0.0009181\ z^{-1}X(z) + 0.0004491 z^{-2}X(z) + \\ & + 0.6667\ z^{-1}Y(z) - 0.1111 z^{-2}Y(z) \end{aligned} \tag{8.9}$$

To enable the implementation of a microcontroller in the mini-loop of the system, the transfer function of the series digital robust control stage $D_S(z)$, based on equation (8.9), is represented by the following **difference equation** [77], [78], [89], [90]:

$$\begin{aligned} y(kT) = {} & 0.0004693\, x(kT) - 0.0009181\, x\left[(k-1)T\right] + \\ & + 0.0004491\, x\left[(k-2)T\right] + 0.6667\, y\left[(k-1)T\right] - 0.1111\, y\left[(k-2)T\right] \end{aligned} \tag{8.10}$$

Similarly, from equation (8.6), the transfer function of the forward robust stage can be modified by adding a zero to improve the speed of system response:

$$G_F(s) = \frac{96.8s + 968}{s^2 + 44s + 968} \tag{8.11}$$

The forward robust control stage can be presented in the discrete-time domain by the following code:

```
>> Gf=tf([96.8 968],[1 44 968])
Transfer function:
 96.8 s + 968
----------------
s^2 + 44 s + 968
>> Gdf=c2d(Gf,0.001,'tustin')
Transfer function:
0.04758 z^2 + 0.0004735 z - 0.04711
-----------------------------------
 z^2 - 1.956 z + 0.957
Sampling time: 0.001
```

From the outcome of the applied code, the transfer function of the forward robust control stage presented in the discrete-time domain is as follows:

$$G_{dF}(z) = \frac{0.04758\ z^2 + 0.0004735 z - 0.04711}{z^2 - 1.956\ z + 0.957} = \frac{M(z)}{E(z)} \tag{8.12}$$

The output of the forward controller in the discrete-time domain is determined from equation (8.12) as follows:

$$\begin{aligned} M(z) = 0.04758\ E(z) + 0.0004735\, E(z)z^{-1} - 0.04711\, E(z)z^{-2} + \\ + 1.956\ M(z)z^{-1} - 0.957\, M(z)\, z^{-2} \end{aligned} \tag{8.13}$$

Based on equation (8.13), to facilitate the implementation of a forward microcontroller, the transfer function of the forward digital robust control stage $D_F(z)$ is expressed by the following **difference equation** [77], [78], [89], [90]:

$$\begin{aligned} m(kT) = 0.04758\, e(kT) + 0.0004735\ e\left[(k-1)T\right] - 0.04711\, e\left[(k-2)T\right] \\ + 1.956\, m\left[(k-1)T\right] - 0.957\, m\left[(k-2)T\right] \end{aligned} \tag{8.14}$$

8.1.2 D-Partitioning Analysis of the Robust Compensated Linear Prototype Section of the System

Based on the characteristic equation of the total system, the variable parameter K is determined as:

$$K(s) = -\frac{0.0126s^3 + 1.98s^2 + 72s + 1000}{22.314s^2 + 981.818s + 21599.95} \tag{8.15}$$

The D-Partitioning curve related to the linear section prototype of the system after the robust compensation is plotted in the discrete-time domain, as shown in Figure 8.2 with the aid of the following code:

```
>> K=tf([-0.0126 -1.98 -72 -1000],[22.314 981.818 21599.95])
Transfer function:
-0.0126 s^3 - 1.98 s^2 - 72 s - 1000
-----------------------------------
22.31 s^2 + 981.8 s + 2.16e004
>> Kd = c2d(K,0.001,'tustin')
Transfer function:
-1.193 z^3 + 3.399 z^2 - 3.226 z + 1.02
--------------------------------------
  z^3 - 0.956 z^2 - 0.9991 z + 0.957
Sampling time: 0.001
>> dpartition(Kd)
```

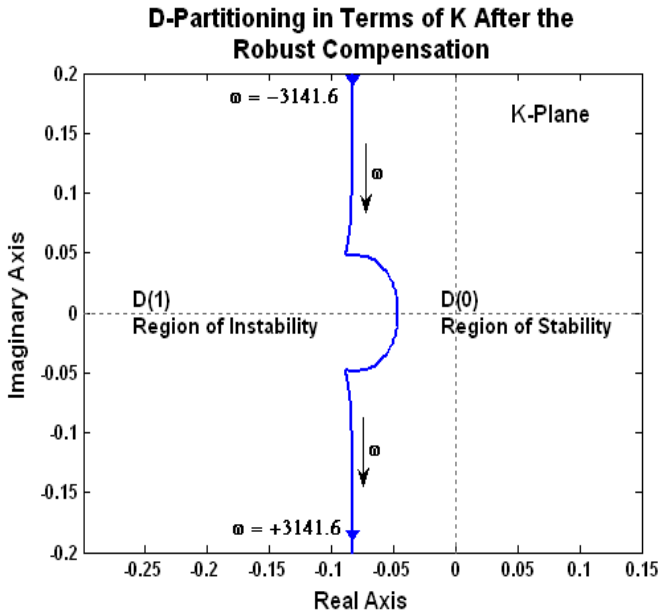

Figure 8.2: *D-Partitioning after the Robust Compensation (Case of DC Motor Control System)*

The D-Partitioning determines two regions of the *K*-plane: D(0) and D(1). As seen from Figure 8.2, D(0) is the region of stability, being on the left-hand side of the curve for a frequency variation within the range –3141.6 rad/sec ≤ ω ≤ +3141.6 rad/sec. The system is stable for any positive values of the gain, $K > 0$.

8.2.3 System Performance after Robust Compensation

8.2.3.1 Describing Function Analysis after Robust Compensation in Case of ON-OFF Nonlinearity with Hysteresis and Variable Linear Gain *K*

The compensated system will be examined for robustness by applying the Describing Function analysis in the discrete-time domain for two gain values $K = 0.5$ and $K = 10$. Both gain values are even larger compared with case of the assessment before the robust compensation.

The Goldpharb stability criterion is implemented by submitting the gain values $K = 0.5$ and $K = 10$ in equation (8.7) and considering the data from Table 7.1. The system performance can be assessed from Figure 8.3 after applying the following code:

```
>> GT05=tf([0 10.8],[0.0000126 0.013 0.56 10.65])
Transfer function:
      10.8
-----------------------------------------
1.26e-005 s^3 + 0.013 s^2 + 0.56 s + 10.65
>> GdT05 = c2d(GT05,0.001,'tustin')
Transfer function:
7.016e-005 z^3 + 0.0002105 z^2 + 0.0002105 z + 7.016e-005
-----------------------------------------------------------
 z^3 - 2.295 z^2 + 1.62 z - 0.3242
Sampling time: 0.001
>> GT10=tf([0 216],[0.0000126 0.222 9.75 212.96])
Transfer function:
       216
---------------------------------------
1.26e-005 s^3 + 0.222 s^2 + 9.75 s + 213
>> GdT10 = c2d(GT10,0.001,'tustin')
Transfer function:
0.0002142 z^3 + 0.0006425 z^2 + 0.0006425 z + 0.0002142
-------------------------------------------------------
 z^3 - 1.16 z^2 - 0.5994 z + 0.7614
Sampling time: 0.001
>> nyquist(GdT05,GdT10)
```

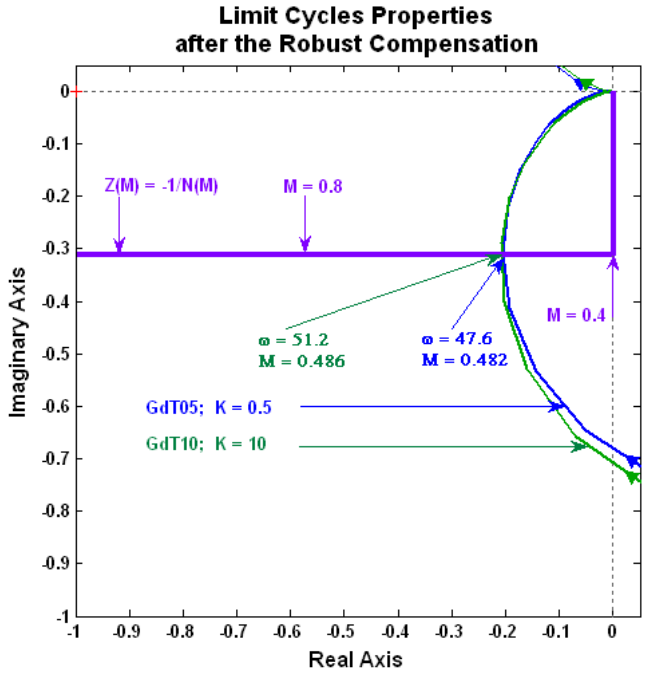

Figure 8.3: *Interaction with the Nonlinearity after the Robust Compensation (Case of ON-OFF Element with Hysteresis and Variable Gains: K = 0.5 and K = 10)*

The stable limit cycles properties, corresponding to the intercept points between *Z(M)* and the compensated G_{dT05}, G_{dT10}, are presented in Table 8.1.

Table 8.1

Properties of the Stable Limit Cycles at Different Values of the Gain *K*

Linear Section Gain	*K*	0.5	10
Limit Cycles Properties	M	0.482	0.486
	ω, *rad/sec*	47.6	51.2

By comparing Figure 8.3 with Figure 7.7 and Table 8.1 with Table 7.2, it is seen that after the application of the robust controller the properties of the limit cycles differ insignificantly, regardless the substantial variation of the linear section gain *K*. This outcome demonstrates the achieved robustness of the system after the application of the robust controller. The system will still be robust if the points of the limit cycles are located at the horizontal part of Z(M).

8.2.3.2 Describing Function Analysis after Robust Compensation in Case of ON-OFF Nonlinearity with Hysteresis and Variable Time-Constant *T*

The total nonlinear compensated system will be examined for robustness by applying the Describing Function analysis in the discrete-time domain for two time-constant values T = 0.05 sec and T = 0.1 sec, in case of K = 0.25. If equation 7.12 is incorporated into equation 8.7, the transfer functions of the compensated linear section prototypes are accordingly:

$$G_T(s)_{T=0.05} = \frac{5.4}{0.000015s^3 + 0.00788s^2 + 0.3345s + 6.4} \tag{8.16}$$

$$G_T(s)_{T=0.1} = \frac{5.4}{0.00003s^3 + 0.00988s^2 + 0.3845s + 6.4} \tag{8.17}$$

Taking into account equations (8.16) and (8.17) and considering the data from Table 7.1, the system performance can be assessed from Figure 8.4 after applying the following code:

```
>> GT005=tf([0 5.4],[0.000015 0.00788 0.3345 6.4])

Transfer function:
          5.4
-------------------------------------------
1.5e-005 s^3 + 0.00788 s^2 + 0.3345 s + 6.4

>> GdT005 = c2d(GT005,0.001,'tustin')

Transfer function:
3.548e-005 z^3 + 0.0001064 z^2 + 0.0001064 z + 3.548e-005
-----------------------------------------------------
 z^3 - 2.568 z^2 + 2.154 z - 0.5857

Sampling time: 0.001
>> GT01=tf([0 5.4],[0.00003 0.00988 0.3845 6.4])

Transfer function:
          5.4
-----------------------------------------
3e-005 s^3 + 0.00988 s^2 + 0.3845 s + 6.4
>> GdT01 = c2d(GT01,0.001,'tustin')

Transfer function:
1.927e-005 z^3 + 5.78e-005 z^2 + 5.78e-005 z + 1.927e-005
-----------------------------------------------------
    z^3 - 2.707 z^2 + 2.425 z - 0.718

Sampling time: 0.001
>> nyquist(GdT005,GdT01)
```

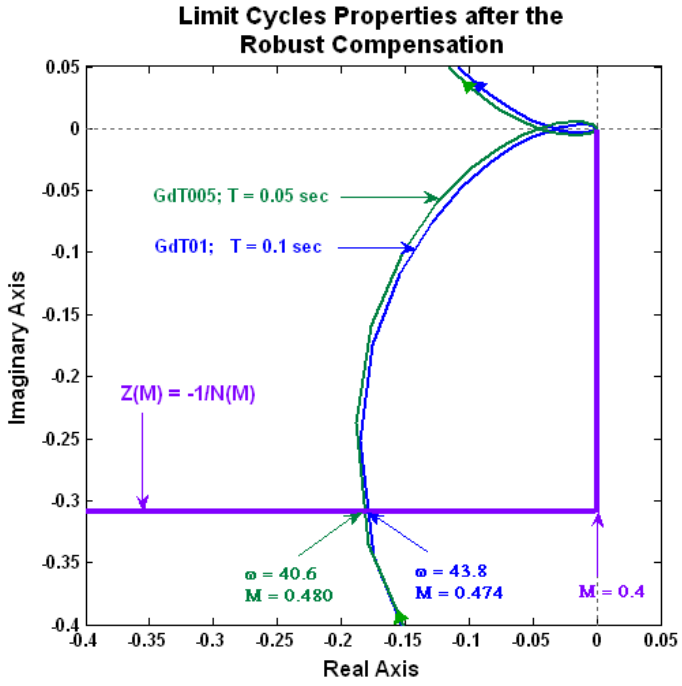

Figure 8.4: *Interaction with the Nonlinearity after the Robust Compensation (Case of ON-OFF Element with Hysteresis and Variable Time-Constants: T = 0.05 sec and T = 0.1 sec)*

The limit cycles properties, corresponding to the intercept points between *Z(M)* and the compensated G_{dT005}, G_{dT01}, are presented in Table 8.2.

Table 8.2

Properties of the Stable Limit Cycles at Different Values of the Time-Constant *T*

Linear Section Gain	*T*	0.1	0.05
Limit Cycles Properties	*M*	0.474	0.480
	ω, rad/sec	43.8	40.6

When comparing the results shown in Figure 8.4 and Figure 7.9, as well as the results presented in Table 8.2 and Table 7.3, it is evident that the properties of the limit cycles differ insignificantly after the application of the robust controller, despite the variation of the linear section prototype time-constant *T*. This validates the accomplished robustness of the system after the application of the robust controller.

8.2.3.3 Describing Function Analysis after Robust Compensation in Case of ON-OFF Nonlinearity with Hysteresis and Variable Hysteresis Factor

The properties of the limit cycles are considered also in case of the variation of the hysteresis factor *h* within specific limits (h ≥ 0.75), as shown in Figure 8.5. By applying equations (7.11), (8.16) and (8.17), the compensated system is examined for robustness by applying the Describing Function analysis in the discrete-time domain for $T = 0.05$ sec and $T = 0.1$ sec, $K = 0.25$ and saturation factor $K_1 = 1$.

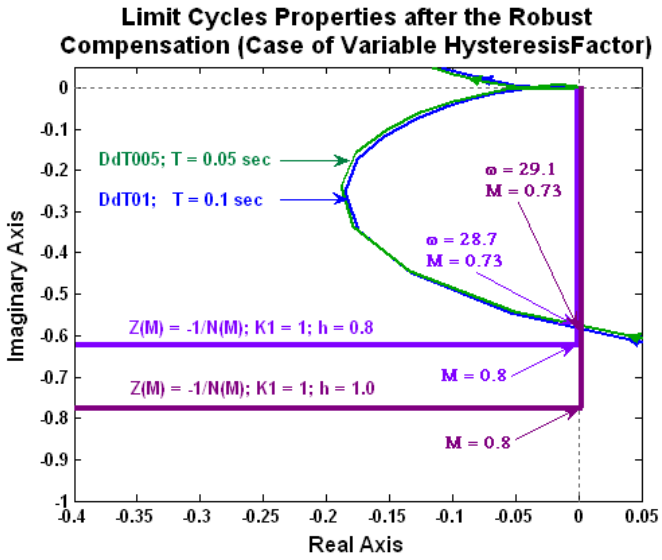

Figure 8.5*: Describing Function Analysis of the Robust System (Case of Variable Hysteresis Factor h)*

The limit cycles properties, corresponding to the intercept points between *Z(M)* and the compensated G_{dT005}, G_{dT01}, are presented in Table 8.3.

Table 8.3

Properties of the Stable Limit Cycles at Different Values of the Hysteresis Factor *h*

Linear Section Gain	*h*	0.8	1.0
Limit Cycles Properties	M	0.73	0.73
	ω, *rad/sec*	28.7	29.1

It is obvious that the properties of the limit cycles differ insignificantly after the application of the robust controller, despite the variation of the hysteresis factor *h*. This confirms the achieved robustness of the system in terms of the variation of the hysteresis factor *h* within specific limits after the application of the robust controller.

8.2.3.4 Describing Function Analysis after Robust Compensation in Case of ON-OFF Nonlinearity with Hysteresis and Variable Saturation Factor

The properties of the limit cycles are examined also in case of the variation of the saturation factor K_1 within specific limits ($K_1 \leq 1.1$), as shown in Figure 8.6.

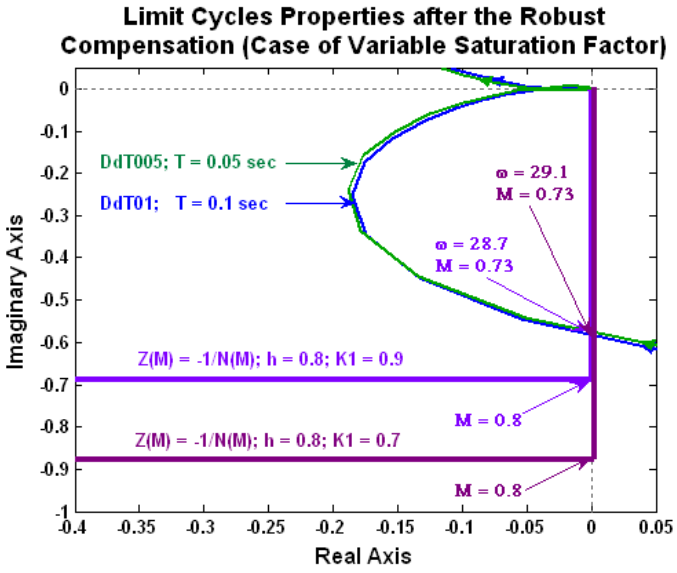

Figure 8.6: *Describing Function Analysis of the Robust System (Case of Variable Saturation Factor K_1)*

The compensated system is assessed for robustness by applying the Describing Function analysis in the discrete-time domain for the case K_1 = variable, T = 0.05 sec T = 0.1 sec, K = 0.25 and hysteresis factor h = 0.8. The limit cycles properties are presented in Table 8.4.

Table 8.4

Properties of the Stable Limit Cycles at Different Values of the Saturation Factor K_1

Linear Section Gain	K_1	0.9	0.7
Limit Cycles Properties	M	0.73	0.73
	ω, *rad/sec*	28.7	29.1

Again the properties of the limit cycles differ insignificantly after the application of the robust controller, regardless of the variation of the saturation factor K_1. This proves the insensitivity of the system in terms of the variation of the saturation factor K_1 within specific limits after the application of the robust compensation.

8.1.3.5 Describing Function Analysis after Robust Compensation in Case of Saturation Type of Nonlinearity and Linear Section Variable Gain *K*

In case of a saturation type of nonlinearity, in a similar way, by applying the Goldpharb stability criterion, the system performance can be assessed after the introduction of the robust controller. If $K < 0.475$, the original linear section prototype $G_P(s)$ is stable. Under this condition, $G_{dT}(j\omega)$ in the discrete-time domain, at different gains (K = 0.5 and K = 10) and $Z(M) = -1/N(M)$ are plotted in the complex plane as shown in Fig. 8.7.

The function $Z(M)$ is plotted with the aid of the data shown in Table 7.4. The parameters of the nonlinearity (K_1 = 1.57 and S = 1) are constant or change insignificantly. The system performance is assessed from Figure 8.7 that is achieved, based on the same code like the one used for plotting Figure 8.3.

According to the Goldpharb stability criterion, the control system is stable for each of the cases, since $G_{dT05}(j\omega)$ *and* $G_{dT10}(j\omega)$ are not enclosing any part of $Z(M)$ [88], [89]. The system is not operating in a limit cycle mode, since there is no intersect between any of the investigated $G_{dT}(j\omega)$ loci and $Z(M)$.

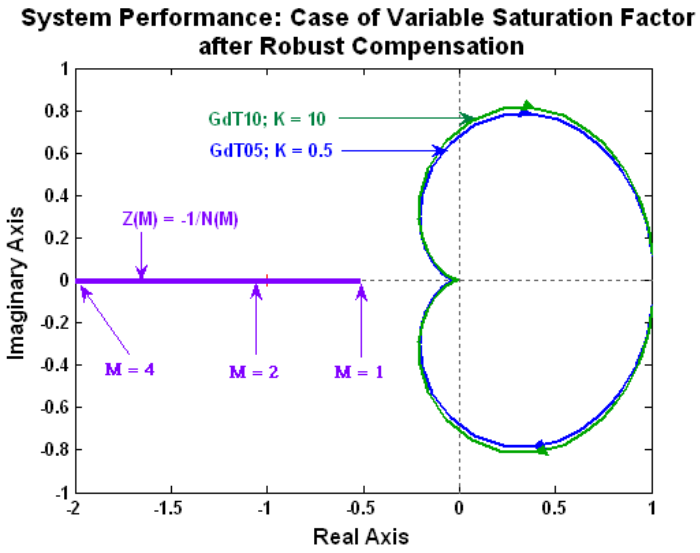

Figure 8.7: *Describing Function Analysis after the Robust Compensation (Case of Saturation Element and Variable Linear Section Gains: K* = 0.5 and *K* = 10*)*

While variation of the slope K_1 and the saturation factor S before the application of the robust compensation may cause an additional stable limit cycle, experiments with variation of the K_1 and S of the robust compensated system are showing that they are causing insignificant effect on the system's performance due to the remote position of the $G_{dT}(j\omega)$ loci and $Z(M)$.

8.3 Robust Controller Design: Backlash System Nonlinearity

8.2.1 Design of the Robust Controller Stages

The nonlinear servo system is considered, as described in Section 7.2.1. Yet again the design strategy for constructing the series stage $G_S(s)$ of the controller is to place its two zeros near the desired closed-loop poles satisfying the optimal system condition. The following design steps are considered:

Step 1: The closed-loop transfer function of the linear section of the plant as a stand alone system is determined by applying a unity feed back to the original plant described by equation (7.20):

$$G_{CL_O}(s) = \frac{K}{s^2 + s + K} \tag{8.18}$$

Step 2: The optimal gain K of the continuous linear plant at a relative damping ratio $\zeta = 0.707$ can be determined by an interactive procedure with the plot of the $\zeta = f(K)$, shown in Fig 8.8.

```
>> K=[0:0.1:10];
>> for n=1:length(K)
G_array(:,:,n)=tf([K(n)],[1 1 K(n)]);
end
>> [y,z]=damp(G_array);
>> plot(K,z(1,:))
```

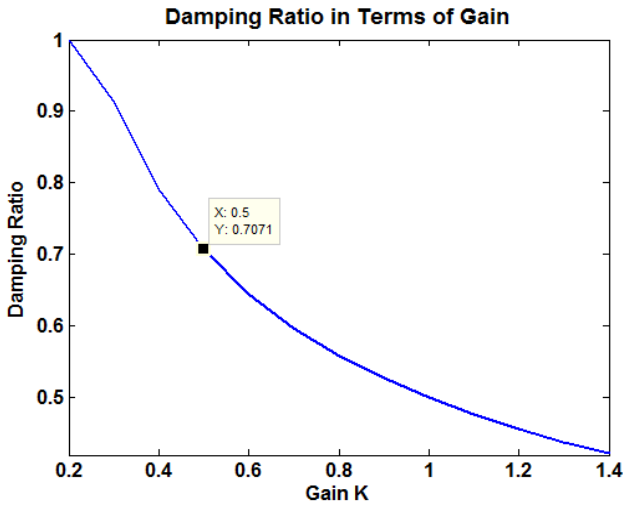

Figure 8.8: *Determination of the Optimal Gain K*

The relative damping ration is $\zeta = 0.7071$ if the gain is $K = 0.5$, seen from Figure 8.8.

Step 3: By substituting $K = 0.5$ in equation (8.11) the transfer function of the closed-loop system becomes:

$$G_{CL_O}(s) = \frac{0.5}{s^2 + s + 0.5} \tag{8.19}$$

Further, the system is evaluated at optimal conditions by applying the code:

```
>> GCLO =tf([0 0.5],[1 1 0.5])
>> damp(GCLO)
```

Eigenvalue	Damping	Freq. (rad/s)
-5.00e-001 + 5.00e-001i	7.07e-001	7.07e-001
-5.00e-001 - 5.00e-001i	7.07e-001	7.07e-001

It is seen that at damping of $\zeta = 0.707$ the desired closed-loop poles are $-0.5 \pm j0.5$.

By applying the **bilinear transform,** considering that for this system the sampling period was established as T_s = 0. 1 sec, the optimal open-loop and closed-loop transfer functions of the system are determined in the discrete-time domain:

```
>> GdCLO = c2d(GCLO,0.1,'tustin')

Transfer function:
0.001189 z^2 + 0.002378 z + 0.001189
-----------------------------------
 z^2 - 1.9 z + 0.9049

Sampling time: 0.1
>> damp(GdCLO)

 Eigenvalue                Magnitude   Equiv. Damping   Equiv. Freq. (rad/s)

 9.50e-001 + 4.76e-002i    9.51e-001   7.07e-001        7.07e-001
 9.50e-001 - 4.76e-002i    9.51e-001   7.07e-001        7.07e-001
```

There is a complete match between the related pole mapping on the s-plane and on the z-plane. The optimal plant analogue prototype and its digital equivalent are having the same relative damping of ζ = 0.707. Then, the robust controller stages are designed in continuous-time and after that transferred into their discrete-time equivalents. The

Step 4: The series controller zeros are placed at –0.5 ± j0.5 as follows:

$$G_S(s) = \frac{(s+0.5+j0.5)(s+0.5-j0.5)}{0.5} = \frac{s^2+s+0.5}{0.5} \tag{8.20}$$

Step 5: The series robust controller $G_S(s)$ is connected in cascade to the linear section of the plant considered as a stand alone system $G_P(s)$:

$$G_{OL}(s) = G_S(s)G_{CL_O}(s) = \frac{K(s^2+s+0.5)}{0.5(s^2+s)} \tag{8.21}$$

Step 6: Further, the unity feedback closed-loop transfer function is determined as:

$$G_{CL}(s) = \frac{K(s^2+s+0.5)}{0.5(s^2+s)+K(s^2+s+0.5)} \tag{8.22}$$

Step 7: The poles of G_F(s) have the objective to cancel the zeros of the closed-loop transfer function G_{CL}(s). As a result the transfer function of the forward controller is:

$$G_F(s) = \frac{0.5}{s^2 + s + 0.5} \tag{8.23}$$

Step 8: The transfer function of the total compensated robust control system is:

$$G_T(s) = G_F(s)G_{CL}(s) = \frac{0.5K}{0.5(s^2 + s) + K(s^2 + s + 0.5)} \tag{8.24}$$

The design of the series and the forward digital controller stages founded on their analogue prototypes is realized again by applying the bilinear transform. Taking into account equation (8.20), the transfer function of the modified series robust controller stage can be presented as:

$$G_{s0}(s) = \frac{(s + 0.5 + j0.5)(s + 0.5 - j0.5)}{0.5s(s + 1000)^2} = \frac{s^2 + s + 0.5}{0.5s^3 + 1000s^2 500000s} \tag{8.25}$$

Its digital equivalent is realized by the code:

```
>> Gs0=tf([1 1 0.5],[0.5 1000 500000])
Transfer function:
    s^2 + s + 0.5
------------------------
0.5 s^2 + 1000 s + 500000
>> Gs0d = c2d(Gs0,0.1,'tustin')
Transfer function:
0.0008083 z^2 - 0.001536 z + 0.0007314
---------------------------------------
      z^2 + 1.922 z + 0.9231
Sampling time: 0.1
```

Following the code result, the transfer function of the series robust controller stage in the discrete-time domain is as follows:

$$G_{sod}(z) = \frac{0.0008083z^2 - 0.001536z + 0.0007314}{z^2 + 1.922z + 0.9231} = \frac{Y(z)}{X(z)} \tag{8.26}$$

To enable the implementation of a microcontroller, the transfer function of the series digital robust control stage is represented by the following **difference equation**:

$$\begin{aligned} y(kT) = {} & 0.0008083\,x(kT) - 0.00153\,x\left[(k-1)T\right] + 0.0007314\,x\left[(k-2)T\right] + \\ & - 1.922\,y\left[(k-1)T\right] - 0.9231\,y\left[(k-2)T\right] \end{aligned} \tag{8.27}$$

From equation (8.23), the modified transfer function of the forward robust stage can be presented as:

$$G_{F0}(s) = \frac{0.05s + 0.5}{s^2 + s + 0.5} \tag{8.28}$$

Its digital equivalent is realized as follows:

```
>> Gf0=tf([0.05 0.5],[1 1 0,5])
Transfer function:
0.05 s + 0.5
-------------
s^3 + s^2 + 5
>> Gf0d = c2d(Gf0,0.1,'tustin')
Transfer function:
0.0001785 z^3 + 0.0002974 z^2 + 5.949e-005 z - 5.949e-005
---------------------------------------------------------
        z^3 - 2.901 z^2 + 2.81 z - 0.9036
Sampling time: 0.1
```

From the code the transfer function of the forward robust control stage, in the discrete-time domain is:

$$G_{F0d}(z) = \frac{1.785\times10^{-4}z^3 + 2.974\times10^{-4}z^2 + 5.949\times10^{-5}z - 5.949\times10^{-5}}{z^3 - 2.901z^2 + 2.81z - 0.9036} = \frac{M(z)}{E(z)} \tag{8.29}$$

To facilitate the implementation of a forward microcontroller, the transfer function of the forward robust control stage is expressed, by the following **difference equation**:

$$\begin{aligned} m(kT) &= 2.901\, m\left[(k-1)T\right] - 2.81\, m\left[(k-2)T\right] \\ &+ 0.9036\, m\left[(k-3)T\right] + \\ &+ 1.785\times10^{-4} e(kT) + 2.974\times10^{-4} e\left[(k-1)T\right] \\ &+ 5.949\times10^{-5} e\left[(k-2)T\right] - 5.949\times10^{-5} e\left[(k-3)T\right] \end{aligned} \tag{8.30}$$

Taking into account all the discussed in this research nonlinear control systems, the design of two robust control stages is upgraded to digital filters based on microcontrollers. The combination of the samplers, the digital filters $D_F(z)$ and $D_S(z)$, shown in Figure 8.9, solving their related difference equations, plus the zero-order

hold (ZOH) components, can be represented by microcontrollers incorporating the corresponding ADC, CPU and DAC.

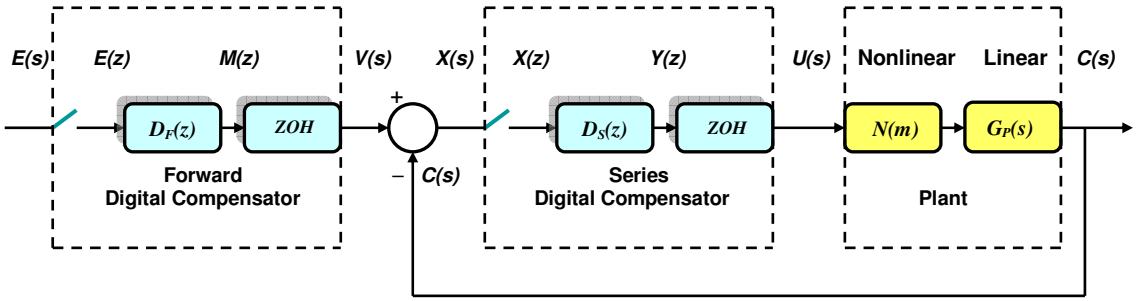

Figure 8.9: *Two-Stage Digital Robust Controller Incorporated into the Control System*

The two-stage digital robust controller, as shown in Figure 8.9, is finally modified to a two-stage robust microcontroller incorporated into the control system as revealed in Figure 8.10.

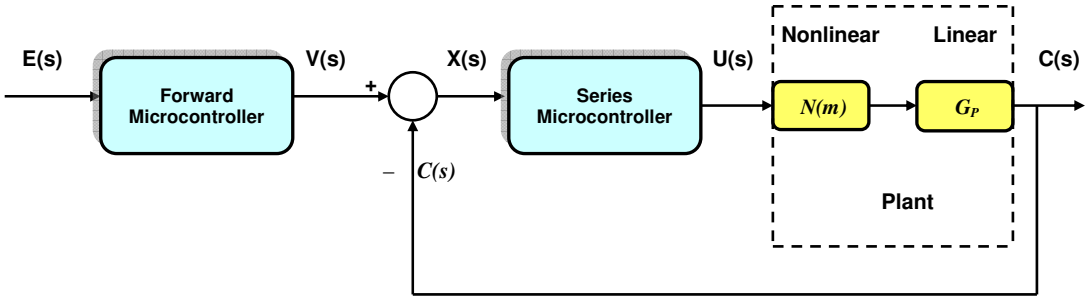

Figure 8.10: *Two-Stage Robust Microcontroller Incorporated into the Control System*

The two-stage digital robust controller, as shown in Figure 8.9, is finally modified to a two-stage robust microcontroller incorporated into the control system as revealed in Figure 8.10. The two microcontrollers are usually combined in a single chip of a multiple-input multiple-output MIMO microcontroller. Some of the latest produced microcontrollers can offer up to 200 MHz operating frequency. All discussed cases operate at sampling frequencies easily managed by such a microcontroller.

8.2.2 Describing Function Analysis after Robust Compensation in Case of Backlash Nonlinearity and Variable Linear Gain *K*

The system performance after robust compensation is assessed with the aid of the Goldpharb stability criterion, taking into account equation (8.17) representing the transfer function of the total robust compensated linear section prototype. As a precondition, both loci G_{dT1} and G_{dT2}, at the two different gains (K = 4, and K = 10), correspond to stable linear prototype sections, seen from Figure 8.11. The function *Z(M)* is plotted by applying equation (7.15) and the data for different amplitudes *M* are shown in Table 7.6. Both G_{dT} loci and *Z(M) = −1/N (M)* loci are plotted in the complex plane following the code:

```
>> GT1=tf([0 2],[4.5 4.5 2])
Transfer function:
   2
-------------------
4.5 s^2 + 4.5 s + 2
>> GdT1 = c2d(GT1,0.1,'tustin')
Transfer function:
0.001057 z^2 + 0.002114 z + 0.001057
-----------------------------------
   z^2 - 1.901 z + 0.9049
Sampling time: 0.1
>> GT2=tf([0 5],[10.5 10.5 5])
Transfer function:
    5
--------------------
10.5 s^2 + 10.5 s + 5
>> GdT2 = c2d(GT2,0.1,'tustin')
Transfer function:
0.001133 z^2 + 0.002265 z + 0.001133
-----------------------------------
 z^2 - 1.9 z + 0.9049
Sampling time: 0.1
>> nyquist(GdT1,GdT2)
```

As already discussed, limit cycles should be completely avoided in systems with a backlash type of nonlinearity. As seen from Figure 8.11, this main objective is achieved after the application of the robust compensation. The locus *Z(M) = −1/N(M)* became quite apart from the two loci G_{dT1} and G_{dT2}, in this way **preventing any undesirable limit cycles** to occur during the system operation. Further, from the comparison between Figure 8.11 and Figure 7.16, it is seen that the linear prototype section of the system becomes quite insensitive to uncertainties. After robust compensation, the two loci G_{dT1} and G_{dT2}, almost coincide.

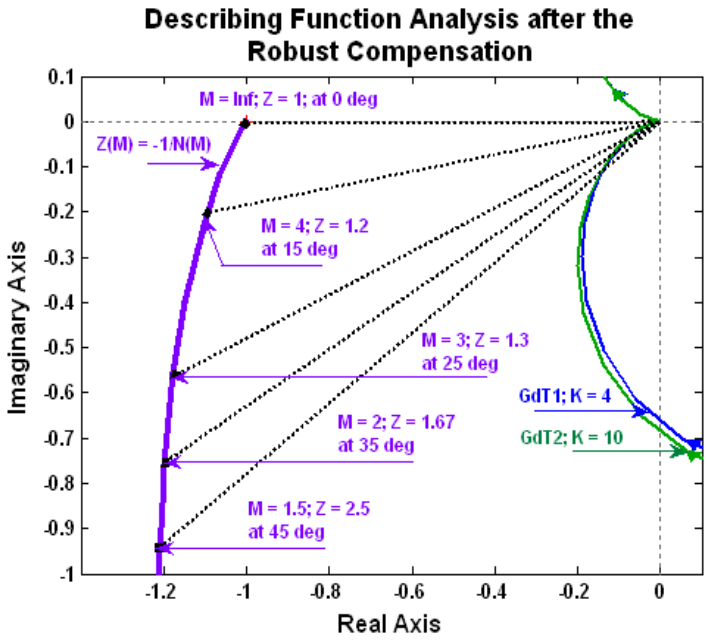

Figure 8.11: *Describing Function Analysis after Robust Compensation at Different Linear Prototype Section Gains K = 4 and K = 10 (Case of a Backlash)*

Although, the system is examined only for variation of the linear section prototype gain *K*, very similar results are achieved in case of a time-constant *T* variation, as already described in section 8.1.3.2.

Experiments prove that for the case of a system with a backlash type of nonlinearity, the parameters of the nonlinearity (the slope K_1 and the dead zone *D*) may change insignificantly and are no challenge for the system performance. Hence, there is no need for assessment of the system sensitivity in terms of variation of these parameters.

8.3 Summary on the Digital Robust Control of Nonlinear Systems

Contribution of this part of the research is the advancement of the D-partitioning method in its application for analysis and design of a digital robust control for a nonlinear control system with a low degree of nonlinearity. The results of the research demonstrate that **the D-Partitioning analysis can be applied independently to the continuous linear prototype section of the system** if the sampling period is at least 5 to 10 times smaller than the plant's minimum time constant. The outcome

from the **D-Partitioning analysis by considering only the stability of the linear prototype part of the system is an important precondition** for further discussion on the interaction between the linear and nonlinear sections.

The system is assessed in terms of the interaction between the linear and the nonlinear sections with the aid of the Goldfarb stability criterion, based on the Describing Function analysis. The outcome proves that **after implementation of the robust controller, the properties of resulting desirable limit cycles (case of on-off control with hysteresis) differ insignificantly, regardless of the variation of the linear prototype section gain. For other type of systems (case of backlash), the undesirable limit cycles can be completely avoided.** A major advantage of the Describing Function analysis is again **the graphical display and the simplicity of its application** for systems with complex dynamics in their linear parts. Even though the types of the nonlinear stages used in this research are a case of an on-off control with hysteresis, a case of saturation and a case with a backlash, any other cases of low degree of nonlinearities could be considered. Further research demonstrates that after compensation **the system remains robust with nonlinearity parameters variation within some limits**, although the nonlinearity parameters change insignificantly and do not affect the system performance.

For nonlinear control systems, an optimal robust controller is achieved again by applying forward-series compensation with two degrees of freedom. The controller enforces the desired system performance. Analysis in the discrete-time domain before and after the application of the robust controller proves that the system becomes quite insensitive to its parameter variations. To achieve digital robust control, **the transfer functions of the two controller stages are presented by their difference equations. Microcontrollers are incorporated into the control system** as forward and series robust control stages and can be programmed to solve their related difference equations.

Even if the Describing Function analysis is considered as an approximate method, **the accuracy of the analysis is very practical and useful** and it is even better for higher-order systems since they have better low-pass filter characteristics.

Chapter 9

INTERACTIVE PROCEDURE FOR ANALYSIS AND DESIGN OF ROBUST CONTROL SYSTEMS

This chapter describes the interactive procedure sequence for the analysis and design of a robust control system, subjected to parameter uncertainties, disturbances and noise. The procedure can be achieved in two parts. In the first component, the control system is analyzed before the robust compensation. The second component represents a procedure sequence of a robust controller design and system analysis after the robust compensation. Both combined components reflect the developed advanced interactive tools for analysis and design of robust control systems.

9.1 Analysis Procedure Sequence before Robust Compensation

The first phase of the procedure sequence is demonstrated in the flowchart diagram shown in Figure 9.1. **The system identification** is an important element of any process of analysis. **The dynamics of the linear section of a plant is described by a differential equation and further its transfer function *G(s)* can be derived.**

The properties of the nonlinear section can be identified by the nonlinearity type and its transfer characteristic, from where the describing function *N(M)* of the nonlinearity can be determined. Even if the developed plant model is not a complete match to the exact plant model, this affects insignificantly the final analysis results.

As seen from Figure 9.1, **the characteristic equation of the linear section is determined** from the linear transfer function *G(s)*. Depending on the number of variable or uncertain parameters of this section, there are two possible approaches.

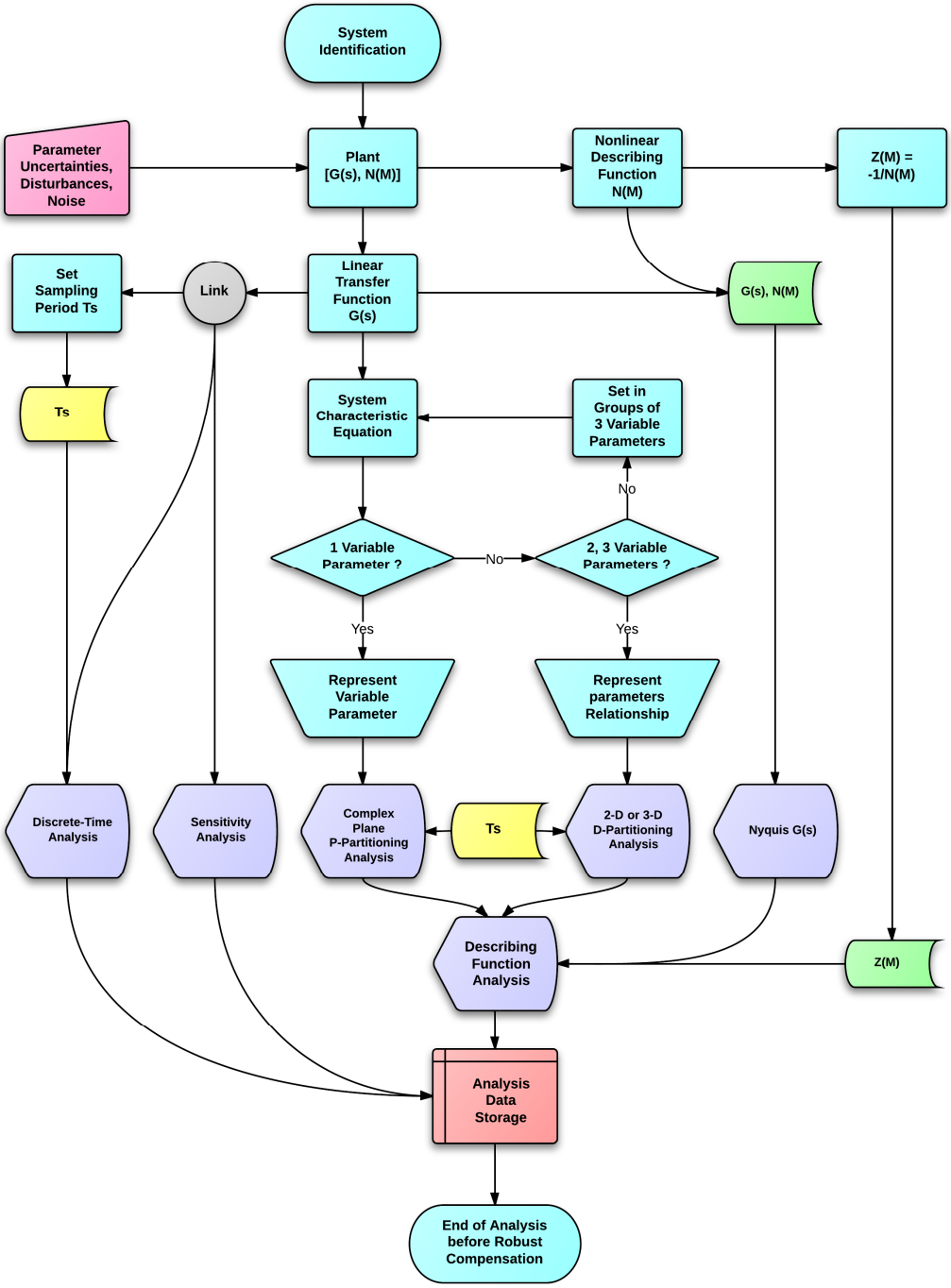

Figure 9.1: *First Phase: Flowchart Diagram of the Analysis Procedure Sequence before Robust Compensation*

If the system is going to be **analysed in terms of only one variable parameter,** this parameter is exposed from the characteristic equation and represented as a complex

number. Accordingly, the D-Partitioning stability analysis of the linear section is applied in the variable parameter complex plane.

If the system is to be **analysed by two or three variable parameters,** the characteristic equation is transformed into an equation describing the relationship between the uncertain parameters. This relationship is used for a **2-D D-Partitioning stability analysis in the plane of any two variable parameters.**

Alternatively, it may be used for a **3-D D-Partitioning stability analysis in the space of any three variable parameters.** In case the number of the variable parameters is larger than three, they are preliminary set in priority groups and the D-partitioning is applied to each group.

Since the intention is to apply digital robust control, the original control system is analyzed in the discrete-time domain. **The D-Partitioning analysis is performed in the discrete-time domain by applying the bilinear transform within the frequency range $\omega = \pm 2\pi/2T_s$.** To achieve accuracy in the D-partitioning analysis, the Euler's approximation is observed, or **the sampling period T_s is within the range $T_s \leq (0.1T_{min}$ to $0.2T_{min})$, where T_{min} is the minimum time-constant of the continuous prototype of the system.**

The system is also analyzed for sensitivity in terms of parameter uncertainties, disturbance and noise before the robust compensation. The sensitivity analysis is applied to the linear section of the plant, reflecting the real systems performance, where the parameters of the nonlinearities may change only insignificantly.

For nonlinear control systems, the D-Partitioning stability analysis, applied to their linear sections, **is a precondition** for the application of the Describing Function analysis. **The Describing Function analysis is the final important part of the nonlinear system assessment, representing the interaction between the linear and nonlinear loci of the system.** It may demonstrate the existence of stable and/or unstable limit cycles, depending on the nature of the system.

Finally, all data obtained from this first component of the advanced interactive procedure for analysis and design of robust control systems are stored to be used for comparison with the data accomplished after the robust compensation.

9.2 Procedure Sequence for Robust Control Design and Analysis after Robust Compensation

The second phase is demonstrated in the flowchart diagram shown in Figure 9.2. There are a number of sequential steps displaying the design of a robust controller with the objective the original system to become insensitive to parameters uncertainties, disturbance and noise. The obtained from the first flowchart, of Figure 9.1, linear transfer function *G(s)*, the functions N(M) and Z(M), the system sampling period T_s and the stored analysis data are used as already known information.

The suggested design of the robust controller is following a number of chronological steps. As seen from Figure 9.2, **initially a unity feedback transfer function is created from the original linear stand-alone transfer function *G(s)*.** Next, the related **gain-damping relationship is established.** Further, **the system gain and dominating poles, satisfying the ITAE criterion are determined.** Considering the desired dominating poles, the **transfer function of the series controller stage $G_S(s)$ is established.** Subsequently, the original stage *G(s)* is connected in series to $G_S(s)$ and both stages are involved in a closed-loop unity-feedback, resulting in transfer function $G_{CL}(s)$. Finally, a **forward controller stage $G_F(s)$**, with a reciprocal transfer function of $G_S(s)$, is connected in series to $G_{CL}(s)$ to obtain the transfer function $G_T(s)$ of totally robust compensated system.

The compensated system $G_T(s)$ is subjected to D-Partitioning analysis in the discrete-time domain. Transient response analysis in the discrete-time domain and analysis for sensitivity in terms of parameter uncertainties, disturbance and noise are also applied. As seen from the flowchart of Figure 9.2, the **D-Partitioning stability analysis applied to $G_T(s)$,** is again a precondition for the application of the Describing Function analysis representing the interaction between $G_T(s)$ and Z(M) loci. **All analysis results are compared with those from the database, obtained before robust compensation.**

In the final step of the flowchart of Figure 9.2, the series and the forward stage transfer functions of the robust controller are presented in discrete-time domain. Accordingly, a **series and forward microcontrollers are programmed reflecting their difference equations.** Finally, the digital robust control system is accomplished by incorporating the microcontroller based controller in the plant system.

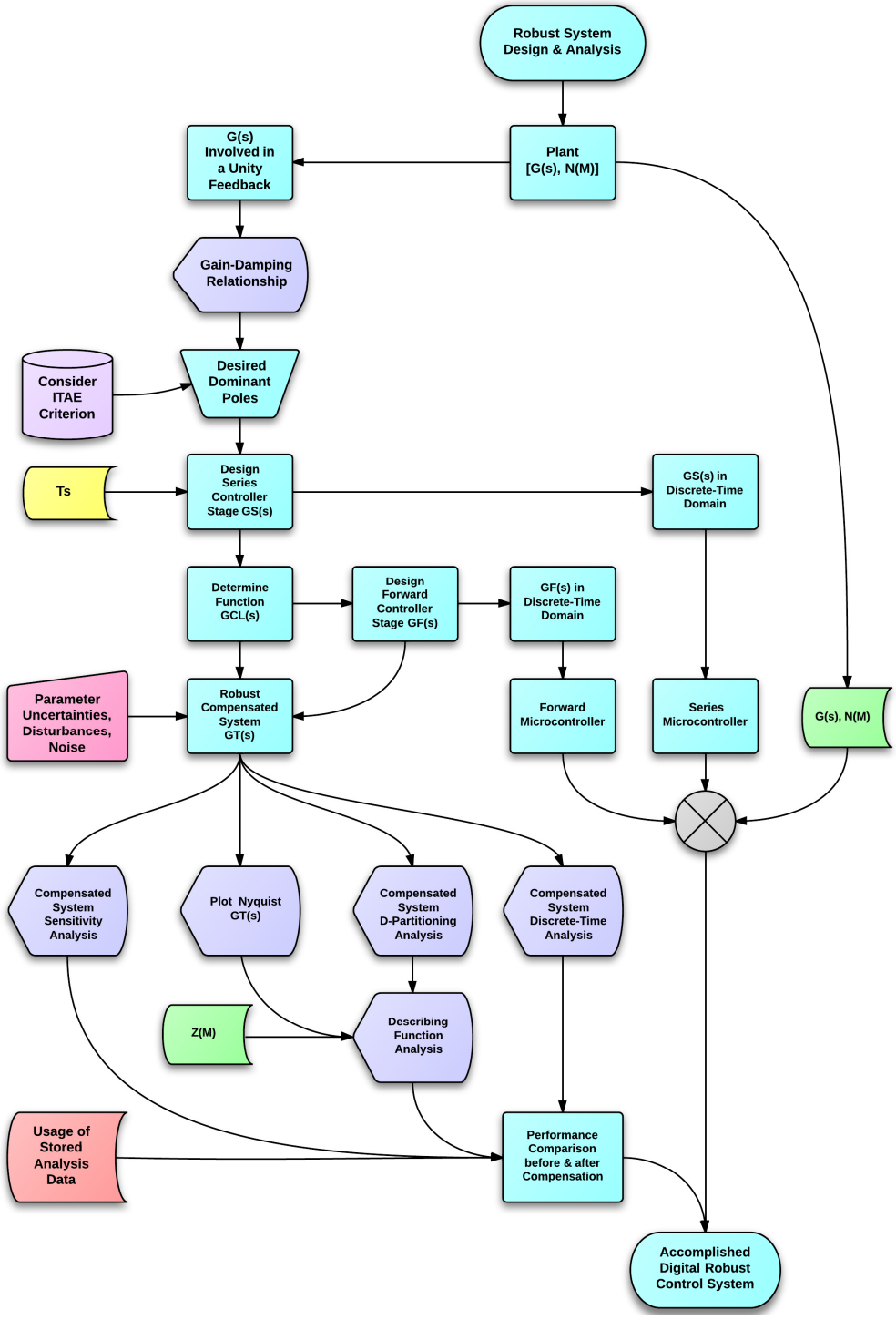

Figure 9.2: *Second Phase: Flowchart Diagram of the Robust Design and Analysis Procedure Sequence after Robust Compensation*

The implementation of the developed tool for analysis and design of variable parameter robust control systems is demonstrated in all parts of this research.

Chapter 10

DISCUSSION AND CONCLUSION

A number of innovative approaches in the field of stability analysis of systems with variable parameters and robust controller design have been proposed and tested in the course of this research. This chapter summarises the novelties of the findings and the techniques employed. Suggestions for prospective future work that will bring further improvement in the line of the research are also presented.

10.1 Discussion

Chapter 1 was discussing the motivation for this research and its objectives. It emphasized that the research methodology will be based on interactive MATLAB procedures. It was stated that the expected contributions would be in terms of achievement of further advancement of the method of the D-Partitioning and to develop an analysis tool that can examine in great detail the effects of multi-parameters variation on system's stability. Also, it was stated that there would be an expectation in terms of the unique property of the designed robust controller that can operate effectively for any of the system's parameter variations or simultaneous variation of a number of parameters, external disturbances and noise and can be applied successfully for linear, digital and nonlinear control systems.

The literature review, performed **in chapter 2** was focusing on the different sources describing stability analysis of systems with variable parameters, robust control design and adaptive control. **The shortage of a generalized stability analysis tool and robust control design method applicable for different type of control systems with variable parameters motivated the research presented in this thesis.** A number of limitations and delimitations were highlighted. **A research choice was made for development of a broad-spectrum analysis tool that can determine the regions of stability, defined by variation of the system's parameters and their interaction in the n-dimensional parameter space.**

Advantages and disadvantages of the D-Partitioning, Routh-Hurwitz stability test, the Kharitonov's Theorem assessment and the Quantitative feedback theory were discussed. Compared to adaptive control, **preference was given to a robust controller design, because it is applicable in cases of unstructured uncertainties and it is expected to function within specified limits of random variations of the system parameters, disturbances and noise.** The robust control can be also implemented at much lower cost.

In chapter 3, further advancement of the method of the D-Partitioning was achieved in terms of applying this analysis in cases of one variable system parameter, as well as in cases of systems with multivariable parameters. Interaction between the variable parameters, influencing the systems stability, was demonstrated in the 2-D and 3-D parameters environment. Advanced D-Partitioning analysis of a higher order minimum phase system with zeros proves that the method is universally applicable. The results from the achieved advanced D-Partitioning analysis were compared with results obtained by applying the Routh-Hurwitz stability criterion and the Kharitonov's Theorem assessment showing the considerable advantages of the D-Partitioning.

Suggested strategy for robust controller design in cases of linear control systems was presented in chapter 4. By implementing desired dominant system poles, the controller enforces the required system performance. The simulations uncertainties of various parameters were demonstrating insignificant difference in the system performance in the presence of the robust controller. **System analysis and sensitivity assessment disclosed the unique property of the designed robust controller that operates properly for any of the parameters simultaneous variation and also having the effect of considerable suppression of the disturbances and noise.**

Further advancement of the D-Partitioning analysis was achieved in terms of applying it in the discrete-time domain. In chapter 5, the control system was reflected as a combination of a digital compensator and a plant by applying the bilinear transform within the frequency range $\omega = \pm 2\pi/2T_s$. The analysis was taking into account the introduced system sampling period, $T_s \leq (0.1T_{min}$ **to** $0.2T_{min})$, based on its comparison with the minimum time-constant of the plant.

Another enhancement of the D-Partitioning method in its application for analysis of digital control systems and **digital robust control design was demonstrated in chapter 6.** The results clearly reveal that the D-partitioning analysis can be applied to the continuous plant of a digital control system, observing a proper value of the sampling period. **By applying the D-Partitioning, the marginal conditions of digital control systems were determined and the results were confirmed by the systems' transient responses in the discrete-time domain.** The research was focusing on the realisation of the digital robust controller. **The transfer functions of its stages were presented by their related difference equations.**

Stability analysis of nonlinear control systems was discussed in chapter 7. It was achieved by **examining their linear section prototypes with the aid of the D-Partitioning and further assessing the interaction between their linear and nonlinear parts by applying the Describing Function analysis.** The D-partitioning was again employed in the discrete-time domain by applying the bilinear transform, considering the system as a combination of a digital compensator and a plant consisting of linear and nonlinear sections.

The results achieved in chapter 8 demonstrate the design and analysis of a digital robust control for nonlinear control systems. D-Partitioning analysis of the robust control system can be applied independently to the continuous linear section of the plant and its outcome was considered as an important precondition for the next design and analysis phase. Further, the system was assessed in terms of the interaction between the linear and the nonlinear sections with the aid of the Describing Function analysis. **The results proved that after introduction of the robust controller, the properties of the resulting desirable limit cycles differ insignificantly, regardless of the variation of system parameters, while the undesirable limit cycles can be completely avoided.** To achieve digital robust control, the transfer functions of the controller's stages are presented again by their difference equations.

The procedures, reflecting the advanced interactive tools for analysis and design of robust control systems subjected to parameter uncertainties, disturbances and noise was demonstrated in chapter 9. It was depicted as a **flowchart diagram presented in two parts.** The aim of the first flowchart section

was to analyze a system before the robust compensation. The second flowchart component demonstrated the steps of the robust controller design and system analysis after the robust compensation.

10.2 Conclusions on the Innovative Results and Contributions to Knowledge

- **The main contribution of this research is further advancement of the method of the D-Partitioning as a broad-spectrum stability analysis tool** that can explore in details the effects of multi-parameters variation on system's stability and robustness.

- **It contributes to knowledge,** since it is the only method of stability analysis that in terms of its results **illustrates graphically and simultaneously:**
  - **The transparent images of regions of stability and instability in case of system's multivariable parameters**
  - **The system's margins of stability in the n-dimensional parameter space**
  - **The interaction of the system's variable parameters in the n-dimensional parameter space**
  - The method of analysis represents a universal **interactive procedure that can be applied to linear, digital or nonlinear control systems with multivariable parameters and is** contributing further to the theory of control systems stability.

- **The second major contribution of the research is the suggested strategy for design of a specialized optimal robust controller.**

- **This contributes to knowledge**, since **the designed robust controller has the unique properties of being:**
  - **efficient in cases of variations of any of the system's parameters**
  - **efficient in cases of simultaneous parameter variations**
  - **efficient in cases of external disturbances and noise**
  - **efficient in terms of improving system's margin of stability**
  - **Applicable to linear, digital and nonlinear control systems**

- **Unique achieved properties compared with the properties of any other known methods**

    - **There is no other known stability analysis method in control theory that can illustrate graphically the system's regions of stability and instability in case of multivariable parameters and to demonstrate the simultaneous marginal values of a number of variable parameters. Only the developed in this research advanced D-Partitioning analysis has these unique properties.**

    - **There is no other known universal strategy for robust controller design. Only the proposed in this research 8-step strategy for robust controller design is developing a controller with unique properties, being effective for simultaneous multiple parameter variations and suppressing the effects of external disturbances and noise.**

    - Further, both the developed by me advanced D-Partitioning analysis and robust controller **can be uniquely applied and be effective for linear, discrete and nonlinear systems.**

10.3 Intended Future Research

Although recognized and appreciated by a significant number of reviewers, the achieved research presented in this Thesis is opening the door for considerable new areas of related research in the future. The following research routes are intended further to be explored:

- The D-Partitioning analysis and robust control can be further applied to MIMO systems with uncertain parameters, subjected to disturbances and noise.

- The D-Partitioning analysis and robust control can be further applied to systems with time delays.

- The D-Partitioning analysis can be applied in the discrete-time domain with the aid of the of the Tustin approximation for systems with time delays.

- The Describing Function analysis can be further upgraded into the 3-D environment.

- Further improvement of system's transient response rise time can be achieved by incorporating a PID controller into the microcontroller based robust controller.

- The designed robust control systems can be further upgraded to adaptive control systems, where the output index performance (IP) can be constantly monitored and compared with a reference IP. Any difference can continuously reprogram the microcontroller stages of the robust controller, enforcing system's adaptive control.

- Cases of systems with non-minimum phase behavior and especially systems with a dead time element will be considered in future research.

- Innovative design procedures for feedback and feedforward robust controllers are considered to be explored in a future research work.

References

[1] Chandrasekharan P., C., *Robust Control of Linear Dynamical Systems*, Academic Press, pp.125-256, 2006.

[2] Tian G., Gao Z., *Benchmark Tests of Active Disturbance Rejection Control on an Industrial Motion Control Platform*, 2009 American Control Conference Hyatt Regency Riverfront, St. Louis, MO, USA, pp.5552-5557, 2009.

[3] Tsumura K., Kitamura M., *Structural Analysis of Robust Control Systems*, IEEE Transections on Automatic Control, Vol. 47, (1), pp.125-132, 2002.

[4] Joseph V., *Robust Parameter Design with Feed-Forward Control*, Technometrics, Vol.5(2), pp.121-126, 2009.

[5] Netushil R., *Theory of Control Engineering,* Moscow, Russia, Vishaia Shkola, pp.179-293, 2004.

[6] Naplatanov N., *Control Theory,* Sofia, Bulgaria, Technika, pp.278-307, 2010.

[7] Bilinear transform. In Wikipedia. Retrieved October 17, 2014, from http://en.wikipedia.org/wiki/Bilinear_transform

[8] Bilinear. MathWorks R2014b Documentation. Retrieved October 17, 2014, from http://www.mathworks.com/help/signal/ref/bilinear.html

[9] Gunchev L.A., *Control Systems Engineering*, Sofia, Bulgaria, Technika, pp.165-169, 2005.

[10] Dorf R.C., *Modern Control Systems*, New York, USA, Addison-Wesley, pp.578-583, 2009.

[11] Kuo B.C., *Automatic Control Systems*, New York, USA, McGraw-Hill, pp.521-530, 2010.

[12] Soltanpour M., Shafiei S., *Robust Adaptive Control of Manipulators in the Task Space by Dynamical Partitioning Approach*, Electronics and Electrical Engineering – Kaunas: Technologija, Vol. 5(101), pp.73–78, 2010.

[13] Besekersky B.A., *Control Engineering Manual*, Moscow, Russia, Nauka, pp.321-326, 2006

[14] Neimark Y., *Determination of the values of parameters for which an automatic system is stable*, Automatic, and Tele-mechanic, pp.190-203, 1978.

[15] Neimark Y., *Robust stability and D-partition*, Automation and Remote Control 53(7), pp. 957–965, 1992.

[16] Neimark Y., *D-partition and Robust Stability*, Computational Mathematics and Modeling, 9(2), pp. 160-166, 2006.

[17] Gryazina E. Polyak B., “Stability Regions in the Parameter Space: D-Decomposition Revisited”, Moscow, Russia, *Automatica*, 13–26, 2006

[18] E. N. Gryazina, B. T. Polyak, A. A. Tremba, “D -decomposition technique state-of-the-art”, Moscow, Russia, *Automatic Remote Control*,1 991–2026, 2008.

[19] Ogata K., *Modern Control Engineering,* London, Prentice-Hall international, Inc., pp. 662-675, 2000.

[20] Jakub O., Vojtech V., *Modification of Neimark D-Partition Method for Desired Phase Margin*, International Conference on Cybernetics and Informatics, VYŠNÁ BOCA, Slovak Republic, pp. 497-502, 2010.

[21] Liu J., Xue Y., *Calculation of PI Controller Stable Region Based on D-Partition Method*, International Conference on Control, Automation and Systems, Gyeonggi-do, Korea, pp.2185-2189, 2010.

[22] Lanzkron R., Higgins T., *D-decomposition Analysis of Automatic Control Systems*, Journal of Automatic Control, IRE Transactions, pp. 150-171, 2003.

[23] Mikhailov U., Aizerman M., *Control Theory*, New York, USA, Addison-Wesley, pp.775-783, 2003.

[24] Yanev K. M., *Application of the Method of D-Partitioning for Stability of Control Systems with Variable Parameters*, BJT, Vol.16, Number 1, pp.51-58, 2007.

[25] Yanev K. M., *Analysis of Systems with Variable Parameters and Robust Controller Design*, Proceedings of the Sixth IASTED International Conference on Modeling, Simulation And Optimization, MSO 2006, ISBN 088986-618-X, pp.75-83, 2006.

[26] Yanev K. M., *Stability of Control Systems with Two Variable Parameters*, Proceedings of the Second IASTED Africa Conference on Modeling and Simulation, ISBN 978-0-88986-763-5, pp.106-111, 2008.

[27] Yanev K. M, Anderson G. O., ObokOpok A., *Achieving Robustness in Control Systems with Variable Time-Constants*, International Journal of Energy Systems, Computers and Control, Vol. 1, Number 1, pp.1-14, 2010.

[28] Glover K., Doyle J., *A State Space Approach to H-Infinity Optimal Control*, Springer-Verlag, New York, Inc, ISBN: 0-387-51605-0, 1989.

[29] Guan X., Liu Y., Chen C., Shi P., *Observer-Based Robust H-Infinity Control for Uncertain Time-Delay Systems*, ANZIAM J., 44, pp.625–634, 2003.

[30] Juma W., Werner H., *Robust H∞ Output Feedback Sliding Mode Control With Applications*, VCC Proceedings – Aalborg University, pp.1-6, 2010.

[31] Evans W.R., *Control System dynamics*, McGraw-Hill, pp.125-286, 1954.

[32] Ackermann J.E., The Root Locus Method, *Robotics and Mechatronics*, 5(2), pp. 47-54, 2004.

[33] Kostov K., Karlova V., *Robust Root Locus Application*, Cybernetics and Information Technologies, 8(1), pp.25-33, 2008.

[34] Merrikh F., Afshar M., *Extending the Root-Locus Method to Fractional-Order Systems*, Journal of Applied Mathematics Volume 2008, pp.1155-1168, 2008.

[35] Cywiak M., *Simple technique for Root-Locus Plotting*, Revista Mexicana De Fisica, 48 (6), pp.556-564, 2002.

[36] Routh–Hurwitz stability criterion. Retrieved October 10, 2014, http://en.wikipedia.org/wiki/Routh%E2%80%93Hurwitz_stability_criterion

[37] Kharitonov's theorem. Retrieved October 10, 2014, http://en.wikipedia.org/wiki/Kharitonov's_theorem

[38] Nakanishi H., Inoue K., *Order Formation in Learning Nonlinear Robust Control Systems by Use of Neural Networks*, International Joint Conference on Neural Networks, Vancouver, BC, Canada, pp.4463-4467, 2006.

[39] Rohr E., Pereira L., Coutinho D., *Robustness analysis of nonlinear systems subject to state feedback linearization*, Control & Automation, Vol.20(4), pp.785-791, 2009.

[40] Saengdeejing A., Qu Z., *Simplified robust control for nonlinear uncertain systems: a method of projection and online estimation*, Automatica 41, pp.1079-1084, 2005.

[41] Egupov D., Ivanov V.,"*Analysis of Discrete Automatic Control Systems with Varying Parameters Using the Method of Orthogonal Expansions*", Journal of Radio-physics and Quantum Electronics, Volume 15, pp.320-328, 2007.

[42] Kevin M., Passino K., Yurkovich S., *Fuzzy Control*, New York, Addison-Wesley, pp.138-152, 2004.

[43] Zadeh M., Yazdian A., Mohamadian M., *Robust Position Control in DC Motor by Fuzzy Sliding Mode Control*, 2006 International Symposium on Power Electronics, Electrical Drives, Automation and Motion, pp.14-47, 2006.

[44] Theodoridis D., Christodoulou M., Boutalis Y., *Direct Adaptive Control of Unknown Multi-variable Nonlinear Systems with Robustness Analysis using a new Neuro-Fuzzy Representation and a Novel Approach of Parameter Hopping*, 17th Mediterranean Conference on Control, pp.558-563, 2009.

[45] Geromel J., Korogui R., *Analysis and Synthesis of Robust Control Systems Using Linear Parameter Dependent Lyapunov Functions*, IEEE Transactions on Automatic Control, Vol. 51, (12), pp.1984-1989, 2006.

[46] Guo S., Zhang L., *Robust Reliability Method for Quadratic Stability Analysis and Stabilization of Dynamic Interval Systems*, International Conference on Control and Automation, pp.789-793, 2005.

[47] Halikias G., Zolotas A., Nandakumar R., *Design of Optimal Robust Fixed-Structure Controllers using the Quantitative Feedback Theory Approach*, Proc. Systems and Control Engineering Vol. 221 Part I, pp.697-716, 2007.

[48] Shafiei S., Soltanpour M., *Robust Adaptive Control of Manipulators in the Task Space by Dynamical Partitioning Approach*, Electronics and Electrical Engineering – Kaunas: Technologija, Vol. 5(101), pp.52–57, 2010.

[49] Blizorukova M., Kappel F., Maksimov V., *A problem of Robust Control of a System with Time Delay*, International Journal of Applied Mathematical Science, Vol.11(4), pp.821-834, 2001.

[50] Joseph V., *Robust Parameter Design with Feed-Forward Control*, Technometrics, Vol.5(2), pp.121-126, 2009.

[51] Megretski A., *Multivariable Control systems*, Proceedings of Massachusetts Institute of Technology, Vol.7(4), 2010, pp.182-189, 2010.

[52] Landau I.D., *Adaptive Control Algorithms and Applications*, Springer, ISBN: 978-0-85729-663-4, 2011, pp.1-587, 2011.

[53] Ioannou, P.A., *Robust Adaptive Control,* PTR Prentice-Hall, Upper Saddle River NJ, pp.1-825, 2007.

[54] Adaptive control. In Wikipedia. Retrieved September 7, 2014, from http://en.wikipedia.org/wiki/Adaptive_control

[55] Horowitz, I., "Synthesis of Feedback Systems", Academic Press, New York, 1963.

[56] Horowitz, I., and Sidi, M., "Synthesis of Feedback Systems with Large Plant Ignorance for Prescribed Time-Domain Tolerances," International Journal of Control, 16(2), pp. 287–309, 1972.

[57] Horowitz, I., "Survey of Quantitative Feedback Theory (QFT)," International Journal of Control, 53(2), pp. 255–291, 1991.

[58] Houpis, C., Rasmussen, S., Garcia-Sanz, M., "Quantitative Feedback Theory Fundamentals and Applications", Taylor & Francis Group, CRC Press, United States, 10:0-8493-3370-9, 2006.

[59] Sorensen D., Lehoucq R., Yang C., Maschhoff K., *MATLAB: Robust Control Toolbox*, MathWorks, 2009.

[60] Dlapa M., Prokop R., *Evolutionary μ-Synthesis: A Simple Controller for Feedback Loop*, Proceedings of the 10th Mediterranean Conference on Control and Automation – MED2002 Lisbon, Portugal, pp.321-330, 2002.

[61] Balas G., Doyle J., Glover K., *μ -Analysis and Synthesis Toolbox for Use with MATLAB,* MathWorks, 2009.

[62] Shinners S.M., *Modern Control System Theory*, Addison-Wesley Publishing Company, pp.369-472, 2004.

[63] Driels M., *Linear control System Engineering*, McGraw-Hill International Inc., pp.145-222, 2006.

[64] James G., *Advanced Modern Engineering Mathematics,* Prentice-Hall, Pearson Education, pp. 2-97, 2000

[65] Yanev, K.M., Anderson G.O., Masupe S., *Application of the D-partitioning for Analysis and Design of a Robust Photovoltaic Solar Tracker System*, IJESCC, Volume 2, No. 1, pp. 43–54, 2011.

[66] Yanev, K.M., Anderson G.O., Masupe S., *D-partitioning Analysis and Design of a Robust Photovoltaic Light Tracker System*, BIE 12th Annual Conference, 6001, ISBN: 97899912-0-731-5, 2011.

[67] Yanev K.M, Anderson G.O., Masupe S., *Multivariable System's Parameters Interaction and Robust Control Design*, Journal of International Review of Automatic Control, Vol. 4, N.2 pp.180-190, 2011.

[68] Yanev K.M., *Advanced D-Partitioning Stability Analysis in the 3-Dimensional Parameter Space,* International Review of Automatic Control, ISSN: 1974-6059, Vol. 6, N. 3, pp. 236-240, 2013.

[69] Kiravu C., Yanev K.M., M.T. Oladiran M.T., *Visualizing Power Frequency Dynamics Using D-Partitioning,* International Review of Automatic Control, ISSN: 1974-6059, Vol. 6, N. 5, pp. 626-630, Index Copernicus: Impact Factor 6.78, September 2013.

[70] Yanev K.M., Masupe S., *Robust Design and Efficiency in Case of Parameters Uncertainties, Disturbances and Noise,* International Review of Automatic Control, Vol. 5, N. 6, ISSN: 1974-6059, pp. 860-867, 2012.

[71] Shinners S., *Modern Control System Theory and Application*, Addison Wesley Publishing Company, London, pp. 43-46, 2008.

[72] Nise N., *Control System Engineering*, Benjamin/Cummings publishing Company, Inc., pp. 333-336, 2002.

[73] D'Azzo J.J., *Linear Control System Analysis and Design*, McGraw-Hill, pp.743-757, 2002.

[74] Takaya K., *Digital Control Systems,* Electrical and Computer Engineering, University of Saskatchewan, 2008.

[75] Millman J., Halkias C., *Integrated Electronics: Analogue and Digital Circuits and Systems*, McGraw-Hill Inc., pp.458-485, 2002.

[76] Discrete Systems**.**Retrieved October 17, 2014, http://www.eng.ox.ac.uk/~conmrc/dcs/dcs1.pdf

[77] Euler Method, In Wikipedia. Retrieved March 27, 2014, from http://en.wikipedia.org/wiki/Euler_method

[78] Continuous-Discrete Conversion Methods. MathWorks R2014b Documentation. Retrieved October 17, 2014, http://www.mathworks.com/help/control/ug/continuous-discrete-conversion-methods.html#bs78nig-1

[79] Tustin with Frequency Prewarping. MathWorks R2014b Documentation. Retrieved October 17, 2014, http://radio.feld.cvut.cz/matlab/toolbox/control/manipmod/ltiops20.html

[80] Phillips C.L., *Digital Control System*, Prentice-Hall International Inc., pp.125-403, 2005.

[81] Matched Z-transform method. In Wikipedia. Retrieved October 17, 2014, from http://en.wikipedia.org/wiki/Matched_Z-transform_method

[82] Yanev K. M., Anderson G. O., Masupe S., *Strategy for Analysis and Design of Digital Robust Control Systems*, ICGST-ACSE Journal, Volume 12, Issue 1, pp. 37-44, 2012.

[83] Golten J., Verwer A., *Control System Design and Simulation,* McGraw-Hill International Inc., pp. 278-335, 2001.

[84] Behera L., Kar I., *Intelligent Systems and Control Principles and Applications*, Oxford University Press, pp. 20-83, 2009.

[85] Bhanot S., Process Control Principles and Applications, Oxford University Press, pp. 170-187, 2010.

[86] Yanev K.M, Anderson G.O., Masupe S., *Strategy for Analysis and Design of a Digital Robust Controller for Nonlinear Control Systems,* 4th IASTED Africa Conference on Modeling and Simulation, Gaborone, ISBN 978-0-88986-929-5, pp. 213-220, 2012.

[87] Yanev K.M., *Advanced Interactive Tools for Analysis and Design of Nonlinear Robust Control Systems,* International Review of Automatic Control, ISSN: 1974-6059, Vol. 6, N. 6, pp. 720-727, 2013.

[88] Bhattacharyya S., *The Parametric Approach* (Englewood Cliffs, NJ, Prentice Hall, pp.325-387, 2005.

[89] Atherton D. P., *Nonlinear Control Engineering – Describing Function Analysis and Design*, Van Nostrand Reinhold Company, New York, pp. 113-237, 2005.

[90] Shinners S.M., *Modern Control System Theory*, Addison-Wesley Publishing Company, pp.369-472, 2004.

[91] Describing function. In Wikipedia. Retrieved November 26, 2014, from http://en.wikipedia.org/wiki/Describing_function

[92] Usai E., *Describing Function Analysis of Nonlinear Systems,* Retrieved November 26, 2014, from http://www.diee.unica.it/~eusai/didattica/Analisi Sistemi2/Describing_Function_Analysis.pdf

[93] Yanev K.M, Anderson G.O., Masupe S., *Stability and Robustness of a Control System for Precise Speed Control*, International Journal of Energy Systems, Computers and Control, Volume 2, No. 1, ISSN: 0976-6782, pp. 11–24, 2011.

[94] Yanev, K.M., Litchev A.I., Rakgati E., *Accurate Speed Control of a dc Motor*, Botswana Institution of Engineers (BIE) 11th Annual Conference, B204, ISBN: 97899912-0-731-5, B204, 2009.

[95] Yanev K.M., *Advanced Interactive Tools for Analysis and Design of Nonlinear Robust Control Systems,* International Review of Automatic Control, ISSN: 1974-6059, Vol. 6, N. 6, pp. 720-727, 2013.

[96] Yanev K.M., *Analysis and Design of a Servo Robust Control System,* International Review of Automatic Control, ISSN: 1974-6059, Vol. 7, N. 2, pp. 217-224, 2014.